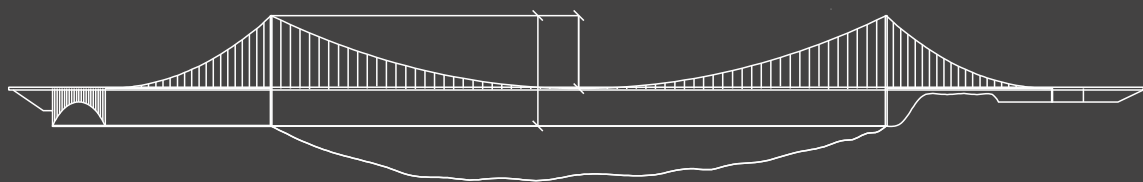
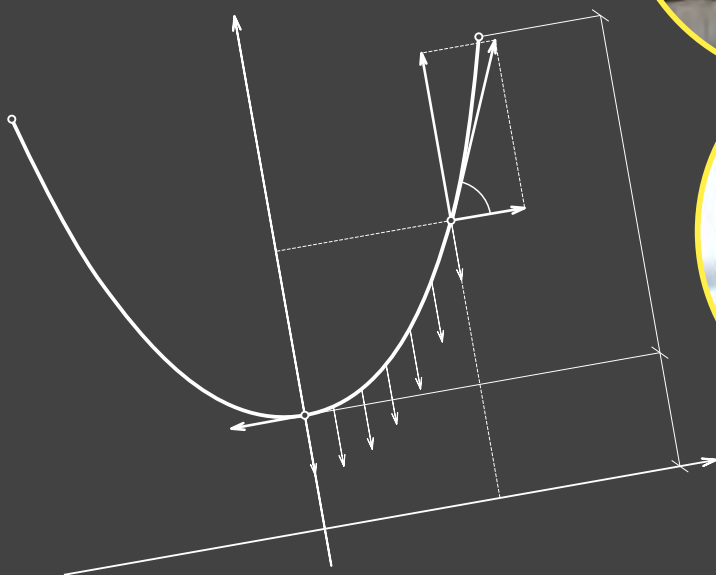


# MATHEMATICS IN EXAMPLES FROM CIVIL ENGINEERING AND ARCHITECTURE

Edwin Koźniewski

Agnieszka Tereszkievicz



Edwin Koźniewski • Agnieszka Tereszkievicz

# **MATHEMATICS IN EXAMPLES FROM CIVIL ENGINEERING AND ARCHITECTURE**



OFICyna WYDAWNICZA POLITECHNIKI BIAŁOSTOCKIEJ  
BIAŁYSTOK 2024

Reviewer:  
Assoc. Prof. Krystyna Romaniak, DSc, PhD

Science editor in the discipline of civil engineering, geodesy and transport:  
Prof. Katarzyna Zabielska-Adamska, DSc, PhD, Eng

Copy editor:  
Aniela Staszewska, Edyta Chrzanowska

Cover of a book:  
Marcin Dominów

Cover photo:  
F. Sadowski, D. Gawryluk

© Copyright by Białystok University of Technology, Białystok 2024

ISBN 978-83-68077-42-1  
ISBN 978-83-68077-43-8 (e-Book)  
DOI: 10.24427/978-83-68077-43-8



The publication is available on license Creative Commons Recognition of authorship  
– Non-commercial use – Without dependent works 4.0 (CC BY-NC-ND 4.0)

Full license content available

on the site [creativecommons.org/licenses/by-nc-nd/4.0/legalcode.pl](https://creativecommons.org/licenses/by-nc-nd/4.0/legalcode.pl).

The publication is available on the Internet  
on the site of the Publishing House of Białystok University of Technology.

Print: Print Profit sp. z o.o.

---

Publishing House of Białystok University of Technology  
Wiejska 45C, 15-351 Białystok  
e-mail: [oficyna.wydawnicza@pb.edu.pl](mailto:oficyna.wydawnicza@pb.edu.pl)  
[www.pb.edu.pl](http://www.pb.edu.pl)

# Contents

<b>Introduction</b> . . . . .	7
<b>Chapter 1. Geometric compactness of the building</b> . . . . .	11
1.1. Optimization problems leading to the concept of compactness of a figure and geometric solid . . . . .	11
1.2. Geometric efficiency and compactness of the building . . . . .	14
1.2.1. Measure of compactness for 3D shapes . . . . .	16
1.2.2. The compactness indicators of 2D . . . . .	18
1.3. Rectangular polygons . . . . .	21
1.3.1. Perimeter defect and area defect . . . . .	23
1.3.2. Span of rectangular polygon . . . . .	25
1.4. Summary . . . . .	27
1.5. Problems . . . . .	27
<b>Chapter 2. Isometries in design</b> . . . . .	29
2.1. Isometries in $E^2$ . . . . .	29
2.2. Tessellation . . . . .	31
2.2.1. Tessellation in $E^2$ – some examples . . . . .	32
2.2.2. Isometries in $E^3$ . . . . .	36
2.3. Between tessellation & polyhedral regular and semi-formal polyhedra . . . . .	39
2.4. Problems . . . . .	44
<b>Chapter 3. Ruled (scroll) surfaces in civil engineering</b> . . . . .	47
3.1. Surfaces resulting from a line rotation . . . . .	47
3.2. Description of hyperboloid surfaces – cooling tower volume . . .	51
3.3. About curves and revolving surfaces . . . . .	56
3.3.1. Equation of the rotational surface . . . . .	57
3.4. Problems . . . . .	62
<b>Chapter 4. Cubature</b> . . . . .	65
4.1. Cubature Ochota Railway Station Warszawa Ochota in Warsaw	65
4.2. The construction of the saddle surface panel as a ruled surface .	66

4.3.	Cavalieri's Theorem . . . . .	69
4.4.	Slice-based transformations . . . . .	69
4.5.	Problems . . . . .	74
<b>Chapter 5.</b>	<b>Curves and offset surfaces in civil engineering . . .</b>	<b>77</b>
5.1.	Offset curves . . . . .	78
5.1.1.	Definition of the offset curve . . . . .	78
5.1.2.	Analytical form of the offset curve . . . . .	83
5.1.3.	About the thickness of the cooling tower in the aspect of offset curves . . . . .	85
5.2.	Offset surfaces . . . . .	86
5.2.1.	Analytical description . . . . .	86
5.2.2.	Thickness of the saddle surface . . . . .	88
5.3.	Problems . . . . .	88
<b>Chapter 6.</b>	<b>Chain curve in civil engineering and architecture .</b>	<b>91</b>
6.1.	Chain curve (catenary curve) . . . . .	91
6.2.	Problems . . . . .	97
<b>Chapter 7.</b>	<b>Surfaces with fast run-up – brachistochrone in skateparks, aquaparks and ski jumps . . . . .</b>	<b>101</b>
7.1.	The problem of brachistochrone – an example of an extremum of a function . . . . .	101
7.2.	Problems . . . . .	106
<b>Chapter 8.</b>	<b>Vibrations in structural mechanics . . . . .</b>	<b>109</b>
8.1.	Eigenvalues and eigenvectors of the operator and diagonalization of the matrix . . . . .	109
8.2.	Second-order ordinary differential equation . . . . .	113
8.3.	Linear differential equations of order two with constant coefficients	114
8.4.	The problem of vibrations in structural mechanics issues . . . . .	117
8.5.	Banachiewicz – Cholesky decomposition . . . . .	119
8.6.	Problems . . . . .	122
<b>Chapter 9.</b>	<b>Moisture field and membrane shape description – the boundary value problem solved by Ritz method . . . . .</b>	<b>125</b>
9.1.	About approximate methods for solving partial differential equations . . . . .	125
9.1.1.	Ritz method . . . . .	125
9.2.	Difference method . . . . .	133
9.3.	Problems . . . . .	138
<b>Chapter 10.</b>	<b>Demand for ready-mix concrete – attempt to describe the problem in the form of a linear model . . . . .</b>	<b>139</b>

10.1. Econometric model . . . . .	139
10.1.1. Selection of explanatory variables . . . . .	140
10.2. Estimating parameters of linear models by the method of least squares . . . . .	146
10.2.1. Estimation of parameters of a model with one explanatory variable . . . . .	147
10.2.2. Estimation of parameters of a model with multiple explanatory variables . . . . .	149
10.2.3. Verification of linear models . . . . .	150
10.3. Problems . . . . .	156
<b>Chapter 11. Optimization of earthmoving in road construction – linear programming . . . . .</b>	<b>157</b>
11.1. Linear programming . . . . .	157
11.2. General problem of linear programming . . . . .	161
11.3. Fundamental theorem of linear programming . . . . .	162
11.4. Transport problem . . . . .	162
11.5. Optimization of transportation of earth masses using various means of transport . . . . .	168
11.6. Problems . . . . .	171
<b>Chapter 12. Mathematical methods of multi-criteria benchmarking analysis on the example of design solutions of selected roof coverings . . . . .</b>	<b>173</b>
12.1. Mathematical methods . . . . .	173
12.2. Method assumptions . . . . .	173
12.3. Coding types . . . . .	174
12.3.1. Standardization . . . . .	174
12.3.2. Normalization . . . . .	175
12.3.3. Coding by Neumann – Morgenstern . . . . .	175
12.3.4. Coding by Pattern method . . . . .	176
12.4. Algorithm for applying mathematical methods . . . . .	176
12.5. Synthetic evaluation formulas . . . . .	177
12.6. Hasse diagrams . . . . .	177
12.7. Ordering set rules . . . . .	179
12.8. Criteria for evaluation of features of selected roofing covers . . . . .	180
12.8.1. Total costs . . . . .	180
12.8.2. Weight of coverage . . . . .	180
12.8.3. Coverage durability . . . . .	181
12.8.4. Coverage aesthetics . . . . .	181
12.8.5. Simplicity of exploitation . . . . .	185
12.9. Proposals of weights for synthetic evaluation . . . . .	187

12.10. Multi-criteria analysis of selected variants . . . . .	188
12.11. Summary . . . . .	192
12.12. Problems . . . . .	192
<b>Bibliography</b> . . . . .	193
<b>Index</b> . . . . .	199
<b>List of Tables</b> . . . . .	201
<b>List of Figures</b> . . . . .	203

# Introduction

The script is an extended version of [62] and supplemented with tasks in some chapters.

This study covers the subject matter of the applied mathematics course taught by the authors in the master's degree program in Civil Engineering at the Faculty of Civil Engineering and Environmental Sciences at Białystok University of Technology. Due to the thematic breadth of the discipline, which is mathematics, determining the content of teaching applied mathematics was not a simple matter. The presented topics of lectures and classes come from different branches of mathematics show techniques for solving previously formulated problems related to the problems of civil engineering and architecture.

There are problems that are solved in a way that does not require advanced techniques. While the statement that the length of the perimeter of a circular area is smaller than the perimeter of a square area of the same area seems intuitively obvious, judging how much the length of the perimeter of a square is larger than the perimeter of a circle requires solving an appropriate ratio. However, the proof that, among figures of the same area, the circle has the smallest perimeter leads to the more difficult so-called isoperimetric problem of variational calculus. By the way, it is somewhat surprising that the isoperimetric issue appears in Wojski's story included in Adam Mickiewicz's *Pan Tadeusz*.

It is unexpected that the curve shape assumed by a freely hanging chain hooked on two poles can inspire the construction of arches and vaults. The shape itself is obtained by solving an ordinary differential equation of order two. But for an engineer, it is important (and perhaps more crucial than the solution itself) to mathematize the problem. Experience in formulating the problem shows how to simplify a complex task and which quantities can and should be omitted.

Variation tasks appear several times in the study. The issue of brachistochrony is again a variational task, the result of which is ob-



tained by solving a second-order ordinary differential equation. It is worth noting here that the types of differential equations leading to the chain curve formula and the brachistochrony formulas are discussed in academic textbooks as two special cases of the general form of the second-order equation. It is further shown that variational methods can work in reverse. Namely, to solve the boundary problem of a partial differential equation, one formulates a suitable functional for which the equation is an Euler necessary condition. This is how we proceed in the Ritz method of describing and solving the problems of the form of the humidity function and the form of the function describing the shape of the membrane.

Differential equations of oscillatory motion are generalized in terms of describing the vibration of structures, and in this context there are references to eigenvectors and eigenvalues of matrices and selected methods for solving systems of equations (matrix triangulation).

From the optimization methods, the authors discuss linear programming, including the transportation issue with application to the transportation of earth masses in road construction.

From the field of statistical data analysis, the publication presents a linear econometric model in the context of analyzing the demand for ready-mix concrete in the construction of buildings.

In project design and construction – due to many criteria – the problem of selecting a project solution, materials or technology arises. Hence one of the chapters is devoted to mathematical methods of multi-criteria comparative analysis.

Because of the introduction of the BIM concept, the study will find many references to geometric models of architectural objects or building elements using CAD tools. After all, in the BIM approach, the building object is already mapped in three-dimensional space in the initial planning phase. Then the resulting model is linked to the entire project process (including the calculation model) and execution process (including materials, technology). Therefore, AutoCAD, as a programming environment familiar to students, is often referred to through the use of its functions. There are numerous references to applications readily available in the virtual space, such as GeoGebra or WolframAlpha. The latter is used for symbolic transformations (determining the solution using the Ritz method). The proposal to use the mentioned applications is intended to inspire the use of other programs, according to the capabilities and interests of students.

References to non-standard geometric objects (surfaces and curves) are expressed through geometric analyses of models of cooling towers, saddle cross-sections and other works (winding columns), which were discussed in the framework of engineering mapping geometry (engineering geometry and graphics, descriptive geometry). Classical isometric, similarity, affine and projective transformations are relevant here, as well as transformations based on cross sections or offset transformations of curves and surfaces.

The study is not a complete lecture on selected mathematical methods, but rather a journey through the more or less familiar facts of mathematics for engineers in a basic lecture. Hence the large number of references to the literature, where a comprehensive study of the subject can be found.

To the readers using this study, the authors will be grateful for any faults noted, as well as for suggestions concerning both content and form.



## Chapter 1

# Geometric compactness of the building

### 1.1. Optimization problems leading to the concept of compactness of a figure and geometric solid

**Problem 1.1.** Pipes are produced with various cross-sectional shapes: circular, square, hexagonal (regular hexagon), but with the same cross-sectional area (Fig.1.1). Which pipe will need more material to be produced? We assume that the amount of material used to produce a circular pipe is 100%.



Figure 1.1: Steel profiles at SEMEX in Czestochowa [13]

**Solution.** To solve this problem, assume the following model: if  $F$  is a cross-sectional figure, then the amount of material (neglecting thickness) will be given by the circumference  $P$  of the figure  $F$ , and the cross-section itself will be given by field  $A$  figures  $F$ .

Let's compare the cross-sections: circular and square. We then have

for circular cross section ( $c$ ):  $P_c = 2\pi r$ ,  $A_c = \pi r^2$ ;

for square cross section ( $s$ ):  $P_s = 4a$ ,  $A_s = a^2$ ,

where  $r$  is the radius of the circle and  $a$  is the length of the side of the square.

By assumption  $A_c = A_s$ . Hence  $\pi r^2 = a^2$ , i.e  $a = r\sqrt{\pi}$ . We express the circuits using the same parameter, i.e.  $r$  or  $a$ . Given that  $P_c = 2\pi r$ ,  $P_s = 4r\sqrt{\pi}$ , we can create a diagram (proportion)

$$\begin{array}{ccc} 2\pi r & \xrightarrow{\quad} & 100\% \\ & \nwarrow \quad \nearrow & \\ 4r\sqrt{\pi} & \xrightarrow{\quad} & x\% \end{array} \quad . \quad (1.1)$$

We will use 12.84% more material to produce square pipes than to produce circular pipes. In this situation, we can call the shape of a circular pipe *reference shape* and refer the material consumption to this shape in the case of other shapes. We can conclude that a circle is a more compact figure than a square. It can be proven that a circle is the most compact figure in a plane. This is the so-called *isoperimetric problem* (it involves determining the figure that has the largest area for a given perimeter). Let us add that the proof of the theorem is not easy. It is worth taking a look at the items [61], [8]. It will also be an interesting experience to read the end of *IV* of the book "Pan Tadeusz" including the footnotes [47].



(a)



(b)

Figure 1.2: Example tanks: (a) spherical tanks at Zakłady Azotowe "PUŁAWY" S.A. [14] (b) cubic tank [15];




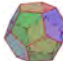


**Problem 1.2.** There are two tanks: one spherical and one cubic (closed), both with the same volume  $V$ . How much more % of material was used to make the cubic tank (Fig. 1.2a, 1.2b)? Assuming that the

amount of material used to make the spherical tank is 100% then the sphere is the reference solid.

**Solution.** Here, after getting the right model and designations ( $r$ -radius of the sphere,  $a$ -length of the cube edge), we formulate the diagram

$$\begin{array}{ccc}
 4\pi r^2 & \xrightarrow{\quad} & 100\% \\
 & \swarrow \quad \searrow & \\
 6r^2 \left( \sqrt[3]{\frac{4}{3}\pi} \right)^2 & \xrightarrow{\quad} & x\%
 \end{array} \quad . \quad (1.2)$$

Table 1.1: Measures of compactness of  $\frac{A_t}{V}$  platonic solids and spheres calculated under the assumption that  $V=1$  (prep. by A.Tereszkiewicz)

Name of solid	Figure	$\alpha$	Formulas			$\frac{A_t}{V}$ for $V=1$
			Area of the solid $A_t$	Volume $V$	Compact. $\frac{A_t}{V}$	
Tetrahedron		edge	$\sqrt{3}a^2$	$\frac{\sqrt{2}a^3}{12}$	$\frac{12\sqrt{3}}{\sqrt{2}a}$	7.21
Cube		edge	$6a^2$	$a^3$	$\frac{6}{a}$	6
Octahedron		edge	$2\sqrt{3}a^2$	$\frac{\sqrt{2}a^3}{3}$	$\frac{6\sqrt{3}}{\sqrt{2}a}$	5.72
Dodecahedron		edge	$3\sqrt{25+10\sqrt{5}}a^2$	$\frac{(15+7\sqrt{5})a^3}{4}$	$\frac{12\sqrt{25+10\sqrt{5}}}{(15+7\sqrt{5})a}$	5.31
Icosahedron		edge	$5\sqrt{3}a^2$	$\frac{5(3+\sqrt{5})a^3}{12}$	$\frac{12\sqrt{3}}{(3+\sqrt{5})a}$	5.15
Sphere		radius	$4\pi a^2$	$\frac{4\pi a^3}{3}$	$\frac{3}{a}$	4.84

After calculating, we get  $x = 124.07\%$ . We can conclude that the sphere is a more compact solid than the cube. How can we measure this compactness? Specifically, the compactness of platonic solids can be determined by the ratio  $\frac{A}{V}$  at  $V = 1$ , as illustrated in the table 1.1. The

smaller the value of the ratio  $\frac{A}{V}$ , the more compact the solid is. Optimization solutions to the above problems concern only the consumption of materials; they do not take into account such properties of constructed objects as strength, statics, functionality, aesthetics,....

This brings us to geometric efficiency and compactness of the building body.

## 1.2. Geometric efficiency and compactness of the building

*Geometric efficiency* of a building that meets the assumed size parameters (usable area, cubature) is a set of geometric features that make the building functional, economical (with low energy demand) in construction and maintenance, safe to use and aesthetic.



Figure 1.3: (a) Fragment of a poster - "information board" of the new SONATA estate being built in Druskininkai, Lithuania. Buildings in the shape of cylinders with an oval base; (b) buildings (cylindrical, oval-shaped) of the new SONATA housing estate in Druskininkai, Lithuania, photo by Ľ. Kolendo

An important geometric feature of a building is its *compactness*. By *compactness of a building*, we mean the compactness of a solid, which is an isometric geometric model of the partitions of a building or part of a building. The *geometric compactness of a rigid solid* (S) is the *ratio between the area of the solid and the volume*. The *classical measure of compactness* is determined by the dimensionless ratio  $\frac{A_t^3}{V^2}$  ( $A_t$  - area of the total surface of the solid S,  $V$  - volume of the solid S) [5]. Then the

classical measures of compactness of a sphere, octahedron, and cube are equal to  $36\pi (\approx 113.09734)$ ,  $108\sqrt{3} (\approx 187.06149)$ , 216, respectively. We can adopt a similar classical definition of compactness with respect to a figure (F); it will be the ratio  $\frac{P^2}{A}$  ( $A$  - area of the figure F,  $P$  - perimeter of the figure F). Then the classical compactnesses of a circle, a regular hexagon, and a square are equal to  $4\pi (\approx 12.56637)$ ,  $\frac{24\sqrt{3}}{3} (\approx 13.85641)$ , 16, respectively. However, such numbers are not very readable in applications to building shape analysis.

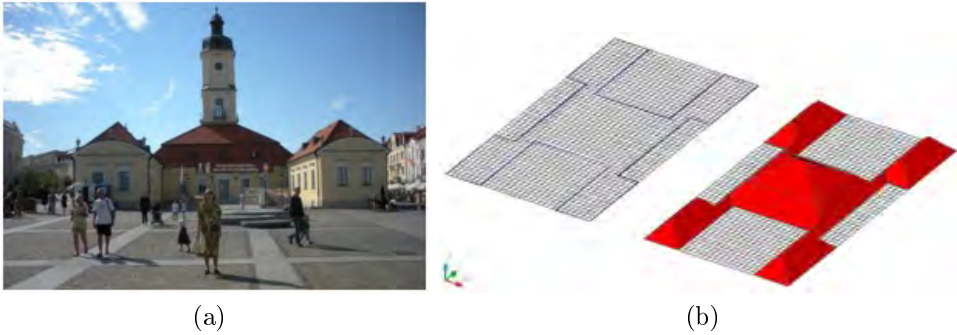


Figure 1.4: (a) The Town Hall in Białystok - an example of a building on the plan of a rectangular polygon, photo by E. Koźniewski; (b) The Town Hall in Białystok – study of the solution of the roof shape, prep. E. Koźniewski

The simplest and most commonly used measure, but dependent on units, is the index  $\frac{A}{V}$ . This index is completely sufficient to characterize the compactness of a one-story house. The method of characterization of geometric compactness proposed for Platonic solids is not transferable to any solid. For example, for a cuboid with edges:  $a, b, c$  the compactness thus understood (i.e., assuming  $V = 1$ ) is expressed by the formula

$$\frac{A}{V} = \frac{2(a^2b^2 + a + b)}{ab} \left( = 2ab + 2 \left( \frac{1}{a} + \frac{1}{b} \right) \right). \quad (1.3)$$

This is because it depends on the units ( $u$ ) and at the same time is not expressed in one unit; namely, it can be divided into two components, where one component has the unit  $[u^2]$ , the other  $[1/u]$ . Thus, it is necessary to formulate measures of compactness of figures (F) and solids (S) in such a way that they are universal; at least for a sufficiently broad class of objects capable of being implemented as models of buildings or their parts.







### 1.2.1. Measure of compactness for 3D shapes

The compactness indicator of a given solid  $S$  (figure F) reasonably relates it to the established *model solid(reference)*  $S_{pat}$  (figure  $F_{pat}$ ) [31, 35, 37, 40, 41]. Then, using the quotient of  $\frac{A_t}{V}$ , we can determine the *relative compactness indicator* as follows

$$RC_{S_{pat}}(S) = \frac{\frac{A_t(S)}{V(S)}}{\frac{A_t(S_{pat})}{V(S_{pat})}} \left( = \frac{A_t(S)}{A_t(S_{pat})} \right). \quad (1.4)$$

Table 1.2: Ideological illustration of the indicator  $RC_{S_{pat}}(S)$ , prep. E. Koźniewski based on [41]

	S		$S_{pat}$
$A_t(S)$		$A_t(S_{pat})$	
$V(S)$		$V(S_{pat})$	

If  $S_{pat}$  is a cube with edge  $a$ , then  $V(S_{pat}) = a^3$ , i.e.  $a = \sqrt[3]{V(S_{pat})}$ . Then for the solid  $S$  under the assumption  $V(S_{pat}) = V(S)$  is  $a = \sqrt[3]{V(S)}$ . So  $A_t(S_{pat}) = 6a^2$ , which means  $A_t(S_{pat}) = 6 \left( \sqrt[3]{V(S)} \right)^2$ , and hence

$$RC_{cube} = \frac{A_t(S)}{A_t(S_{pat})} \left( = \frac{A_t(S)}{6 \left( \sqrt[3]{V(S)} \right)^2} \right).$$

Thus, we have *relative compactness indicator of the solid relative to the cube*

$$RC_{cube} = \frac{A_t(S)}{6 \left( \sqrt[3]{V(S)} \right)^2}.$$

In what follows, we will simplify the notation and instead of  $A_t(S)$  we will write  $A_t$  and instead of  $V(S)$  we will write  $V$ , understanding that  $A_t$  and  $V$  denote the total area and volume of the solid  $S$

$$RC_{cube} = \frac{A_t}{6\sqrt[3]{V^2}} . \quad (1.5)$$

Carrying out analogous reasoning for the sphere, we get the relative indicator of the compactness of the solid relative to the sphere

$$RC_{sphere} = \frac{A_t}{4.84\sqrt[3]{V^2}} . \quad (1.6)$$

Let's pay attention to the numbers 4.84 and 6, which appear in the last column of the array 1.1.

When discussing the indicators of (1.5) and (1.6), it is worth noting the existing indicators-inverse of the expressions (1.5), (1.6) in the literature [45], which are given here in the form "with star".

$$RC_{cube}^* = \frac{6\sqrt[3]{V^2}}{A_t} , \quad (1.7)$$

$$RC_{sphere}^* = \frac{4.84\sqrt[3]{V^2}}{A_t} . \quad (1.8)$$

However, neither the cube nor, even more so, the sphere is a good model of a reference solid for a building, which, as a rule, must have a certain height dictated, among other things, by functional considerations. In a cube, on the other hand, the height is equal to the other dimensions and a kind of unnecessary "stiffness" is created when comparing.

For a smaller class of solids, namely prisms and cylinders in general, we will introduce a new type of indicator. For such a class of solids, the natural model of the reference solid  $S_{pat}$  will be a *regular cuboid* with a given edge  $a$  and height  $h$  or a *circular cylinder* with a given radius  $r$  and height  $h$ . Let's denote by  $A$  the area of the base of the prism  $S$  (the cylinder  $h$ ), by  $P$  the perimeter of the base of the prism  $S$  (the base of the cylinder  $S$ ), and by  $V$  the volume of the prism  $S$  (the cylinder  $S$ ).

Table 1.3: Determination of the indicators  $RC_{cd}$  and  $RC_{cyl}$ , prep. E. Koźniewski

For prism		For cylinder	
$V(S_{pat}) = a^2h$	$V(S) = A(S)h$	$V(S_{pat}) = \pi r^2h$	$V(S) = A(S)h$
$a^2h = A(S)h$		$\pi r^2h = A(S)h$	
$a = \sqrt{A(S)}$		$r = \sqrt{\frac{A(S)}{\pi}}$	
$A_t(S_{pat}) =$ $= 2a^2 + 4ah$	$A_t(S) =$ $= A(S) + P(S)h$	$A_t(S_{pat}) =$ $= 2\pi r^2 + 2\pi rh$	$A_t(S) =$ $= 2A(S) + P(S)h$
$RC_{cd} = \frac{\frac{A_t(S)}{V(S)}}{\frac{A_t(S_{pat})}{V(S_{pat})}} = \frac{A_t(S)}{A_t(S_{pat})} =$ $= \frac{2A(S)+P(S)h}{2A(S)+4\sqrt{A(S)h}}$		$RC_{cyl} = \frac{\frac{A_t(S)}{V(S)}}{\frac{A_t(S_{pat})}{V(S_{pat})}} = \frac{A_t(S)}{A_t(S_{pat})} =$ $= \frac{2A(S)+P(S)h}{2A(S)+2\sqrt{\pi A(S)h}}$	
After omitting the solid S			
$RC_{cd} = \frac{2A+Ph}{2A+4\sqrt{Ah}}$		$RC_{cyl} = \frac{2A+Ph}{2A+2\sqrt{\pi Ah}}$	

Reasoning in the table 1.3 leads us to the definition of indicators

$$RC_{cd} = \frac{2A + Ph}{2A + 4\sqrt{Ah}}, \quad (1.9)$$

$$RC_{cyl} = \frac{2A + Ph}{2A + 2\sqrt{\pi Ah}}. \quad (1.10)$$

### 1.2.2. The compactness indicators of 2D

The counterparts of  $RC_{cd}$  and  $RC_{cyl}$  on the plane are the indicators  $RC_{sq}$  i  $RC_{circle}$  (table 1.4).

Table 1.4: Definition of indicators  $RC_{cd}$  i  $RC_{cyl}$ , prep. E. Koźniewski

For a polygon with respect to the regular cuboid	For a region with an edge in the form of a closed curve relative to the circle
$A(F_{pat}) = a^2$   $A(F)$	$A(F_{pat}) = \pi r^2$   $A(F)$
$a^2 = A(F)$	$\pi r^2 = A(F)$
$a = \sqrt{A(F)}$	$r = \sqrt{\frac{A(F)}{\pi}}$
$A(F) = A(F_{pat})$	
$RC_{sq} = \frac{\frac{P(F)}{A(F)}}{\frac{P(F_{pat})}{A(F_{pat})}} = \frac{P(F)}{P(F_{pat})} = \frac{P(F)}{4\sqrt{A(F)}}$	$RC_{circle} = \frac{\frac{P(F)}{A(F)}}{\frac{P(F_{pat})}{A(F_{pat})}} = \frac{P(F)}{P(F_{pat})} = \frac{P(F)}{2\sqrt{\pi A(F)}}$
After omitting the figure label F	
$RC_{sq} = \frac{P}{4\sqrt{A}}$	$RC_{circle} = \frac{P}{2\sqrt{\pi A}}$

The table 1.4 shows the definition of indicators

$$RC_{sq} = \frac{P}{4\sqrt{A}}, \quad (1.11)$$

$$RC_{cyl} = \frac{P}{2\sqrt{\pi A}}. \quad (1.12)$$

The indicator  $RC_{sq}$  is strictly related to the indicator  $\frac{W}{F}$  (*Wall/Floor ratio*) given by J. Cooke [29], which is defined by the quotient

$$JC = \frac{P - P_s}{P_s}, \quad (1.13)$$

where  $P$  is the perimeter of a figure  $F$  with area  $A$ ,  $P_s$  is the perimeter of a square with the same area  $A$ , i.e.,  $JC = \frac{P-4\sqrt{A}}{4\sqrt{A}}$ . Hence,  $JC = \frac{P}{4\sqrt{A}} - 1$ , i.e.  $JC = RC_{sq} - 1$ . The indicator  $RC_{sq}$  is described by the relationship of the size of the area  $A$  and the perimeter  $P$  of a given figure. Another compactness indicator described by the size of the area  $A$  and the perimeter  $P$  of a given figure is the indicator  $LBI$  (*Length/Breadth Index*) described by D. Banks defined by the formula, [29].

$$LBI = \frac{P + \sqrt{P^2 - 16A}}{P - \sqrt{P^2 - 16A}}. \quad (1.14)$$

What is the origin of the formula (1.14)? Suppose a given figure has area  $A$  and perimeter  $P$ . Let us construct a rectangle with area  $A$  and perimeter  $P$ . Then let  $a, b$  be the lengths of the sides of the rectangle ( $a > 0, b > 0$ ). Then, we get two equations  $P = 2a + 2b$  and  $A = a \cdot b$ . From the second equation, we determine  $a = \frac{A}{b}$  and after substitution in the first equation, we get  $P = 2\frac{A}{b} + 2b$ . After the conversion, we get a quadratic equation  $2b^2 - Pb + 2A = 0$  with solutions  $b_1 = \frac{P + \sqrt{P^2 - 16A}}{4}$ ,  $b_2 = \frac{P - \sqrt{P^2 - 16A}}{4}$ . A rectangle with area  $A$  and perimeter  $P$  has sides of lengths  $b_1, b_2$ . The numbers  $b_1, b_2$  thus define the shape of such a rectangle, which can be expressed just by the number  $LBI \left( = \frac{b_1}{b_2} \right) = \frac{P + \sqrt{P^2 - 16A}}{P - \sqrt{P^2 - 16A}}$ . To describe a multi-story building with varying perimeters of individual floors, the  $LBI$  index is generalized to the form

$$PSI = \frac{G + \sqrt{G^2 - 16R}}{G - \sqrt{G^2 - 16R}} \quad (\text{Plan/Shape Index}), \quad (1.15)$$

where  $G$  denotes the sum of the perimeters of each floor divided by the number of floors (average perimeter),  $R$  denotes the sum of the areas of each floor divided by the number of floors (average area) [29]. For a building with the same area of each floor, the indexes  $LBI$  and  $PSI$  are identical. Note also that  $\lim_{h \rightarrow \infty} RC_{cd} = \lim_{h \rightarrow \infty} \frac{2A+Ph}{2A+4\sqrt{Ah}} = \lim_{h \rightarrow \infty} \frac{\frac{2A}{h}+P}{\frac{2A}{h}+4\sqrt{A}} = \frac{P}{4\sqrt{A}} = RC_{sq}$ . This means that in a tall building, a good measure of compactness is the index  $RC_{sq}$ .

In the literature, there is also an indicator

$$EWA/FA = \frac{Ph}{A} \quad (\text{External Wall Area/Floor Area}) \quad (1.16)$$

expressing the ratio of the area of the building's exterior walls to the area of the building's exterior [37], [11]. We have the following relationships between the indicator  $EWA/FA$  and the indicators  $RC_{cd}$  and  $RC_{sq}$ .

$$RC_{sq} = \frac{P}{4\sqrt{A}} = \frac{\frac{Ph}{A}}{\frac{4h}{\sqrt{A}}} = \frac{EWA/FA}{\frac{4h}{\sqrt{A}}}, \quad (1.17)$$

$$RC_{cd} = \frac{2A + Ph}{2A + 4\sqrt{Ah}} = \frac{2 + EWA/FA}{2 + \frac{4h}{\sqrt{A}}}. \quad (1.18)$$

Under the assumption that  $A$  (area of the building projection) and  $h$  (height) are constant quantities, the relationships (simple and inverse) between the indices  $RC_{cd}$  and  $EWA/FA$  are linear. After all, the magnitudes of  $\frac{4h}{\sqrt{A}}$  and  $2 + \frac{4h}{\sqrt{A}}$  are constant. Note, moreover, that the popular ratio  $\frac{A}{V}$ , with the accepted notations described by the quotient  $\frac{A_t}{V}$  expressed in the form

$$\frac{A}{V} = \left( \frac{2A + Ph}{Ah} = \frac{1}{h} \cdot \frac{Ph}{A} + \frac{2}{h} \right) = \frac{1}{h}(EWA/FA) + \frac{2}{h}. \quad (1.19)$$

depends linearly on the ratio  $EWA/FA$ . As a result of the superposition of the inverse of the linear function, we get  $RC_{cd} = \frac{2\sqrt{A}}{2\sqrt{A}+4h}(A/V)$ . Finally, with constant values of  $A, h$ , the relationships  $(RC_{cd} \leftrightarrow EWA/FA)$ ,  $(A/V \leftrightarrow EWA/FA)$ ,  $(RC_{cd} \leftrightarrow A/V)$  are linear. As shown in the work of [37] and [40], the  $A/V, EWA/FA, RC_{cd}$  indicators are in close correlation with the construction cost and energy demand over the lifetime of a single-family home. The  $RC_{cd}$  index represents the best measure:  $RC_{cd} = 1$  is the ideal shape, a deviation of the  $RC_{cd}$  value from 1 indicates a deviation from the ideal compactness of the reference building. When multiplied by 100%, the deviation can be expressed in percentage points.

### 1.3. Rectangular polygons

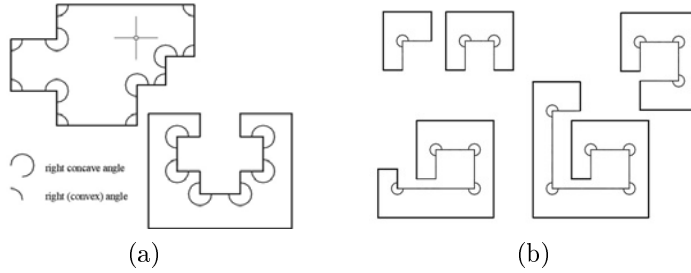


Figure 1.5: (a) rectangular polygons; (b) rectangular polygons: hexagon, octagon, decagon, dodecagon, tetradecagon, prep. E. Koźniewski

Most buildings, especially single-family houses, are built on the plan of a *rectangular polygon* (Fig. 1.5). It is a polygon that has only right angles: convex ( $90^\circ$ ) or concave ( $270^\circ$ ) [31], [35]. Rectangular polygons have, among other things, the property that the number of sides must be even, and the difference between the number of convex and concave angles is equal to 4. Indeed, denoting by  $m$  the number of convex right angles and by  $k$  the number of concave right angles of any  $n$ -angle, we get the following system of equations

$$\begin{cases} m \cdot 90^\circ + k \cdot 270^\circ = (n - 2) \cdot 180^\circ, \\ m + k = n, \end{cases} \quad (1.20)$$

where  $m, k$  and  $n$  are integers. The solution to the system (1.20) is a pair of numbers

$$m = \frac{n}{2} + 2, \quad k = \frac{n}{2} - 2. \quad (1.21)$$

For the solution (1.20) of the system (1.21) to exist the number  $n$  must be even. As you can see, the difference between  $m$  and  $k$  equals 4. Every rectangle has no concave angles, a rectangular hexagon has one reflex angle, rectangular octagon has two concave corners, decagon - three, etc. (Fig. 1.5a, 1.5b).



Figure 1.6: (a) patio [11]; (b) atrial buildings in Białystok on Warszawska street [31], photo by W. Wolkow

Sometimes a building has an inner courtyard (i.e. *patio*, (Fig. 1.6a), [11]) or *atrium* (Fig. 1.6b). We will assume that the rectangular polygons described here are connected areas and may have "holes" (Fig. 1.7c). Connectivity of a polygon (defined generally for a plane set) means that any two points of the polygon can be connected by a broken line contained in the interior of the polygon. If we consider a  $l$ -connected rectangular polygon (i.e., with  $l-1$  holes)  $RP^l$  with  $n$  vertices, then each  $i$ th hole is a simple connected rectangular polygon with  $h_i$  vertices ( $i = 1, 2, \dots, l-1$ ). The sides of an  $l$ -connected rectangular polygon are mutually perpendicular or parallel. We then have  $n = n_0 + \sum_{i=1}^{l-1} h_i$ , where  $n_0$  is the number of vertices of the polygon containing holes, treated as a simple connected polygon. Then every convex angle  $i$  of the  $h_i$ -angled polygon is concave and vice versa. Using the solution of (1.21), in the case of a  $l$ -connected rectangular polygon with  $l-1$   $h_i$ -angled holes ( $i = 1, 2, \dots, l-1$ ), the number of concave angles is equal to

$$k = \frac{n_0}{2} - 2 + \sum_{i=1}^{l-1} \left( \frac{h_i}{2} + 2 \right), \quad (1.22)$$

and the number of convex angles is expressed by the formula

$$m = \frac{n_0}{2} + 2 + \sum_{i=1}^{l-1} \left( \frac{h_i}{2} - 2 \right). \quad (1.23)$$

It can be seen that  $m + k = n$  [35].

### 1.3.1. Perimeter defect and area defect

We will now introduce two parameters that characterize the shape of a rectangular polygon inscribed in a rectangle (figs. 1.7, 1.8), which figure we will consider to be reference for both area  $A$  and perimeter  $P$ . The sides of a  $l$ -connected rectangular polygon  $RP^l$  are mutually perpendicular or parallel. This can be characterized as follows: walking on the edge of a rectangular polygon, we go in four directions: forward (fd), left (lt), right (rt) and backward (bk). Thus, we can associate the polygon  $RP^l$  unambiguously with the rectangle  $R$  described on it. We will say that the rectangular polygon  $RP^l$  is *inscribed in the rectangle* of  $R$  if and only if  $RP^l \subset R$  and each side of the rectangle  $R$  contains at least one side of the rectangular polygon  $RP^l$ . Rectangle  $R$  can be thought of as *described on* polygon  $RP^l$ . We can agree that the sides of the rectangle  $R$  are parallel to the axes of some rectangular coordinate system  $OXY$ , with the  $OX$  axis being horizontal, the  $OY$  axis vertical. Then each edge point of the rectangle  $R$  is the projection of at least two edge points of the polygon  $RP^l$ . Thus, it is possible with the sides of the polygon  $RP^l$  (after moving parallel to the axes  $OX, OY$  to the edge of the rectangle  $R$ , respectively), "wallpaper" the edge of the rectangle  $R$ . Denoting by  $P(F)$  the perimeter of the area  $F$  with respect to the polygon  $RP^l$  inscribed in the rectangle  $R$ , we can write the following formula

$$P(RP^l) = P(R) + \Delta P(RP^l). \quad (1.24)$$

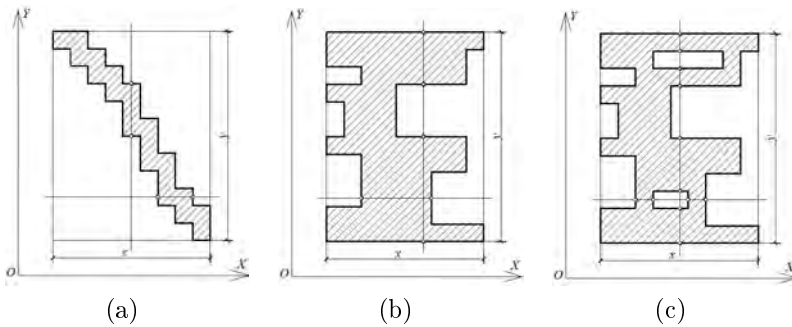


Figure 1.7: Rectangular polygons inscribed in a rectangle: (a) simple connected polygon monotonic (any line parallel to the axis but not containing a side intersects the edge at two points) with respect to both axes, i.e., normal; (b) simple connected polygon monotonic with respect to the  $OY$  axis but non-monotonic with respect to the  $OX$  axis; (c) 3-connected polygon non-monotonic with respect to both axes [35]



The quantity  $\Delta P(RP^l)$ , defined by the formula (1.24), will be called the *perimeter defect* of the polygon  $RP^l$ . The perimeter defect of a rectangular polygon is always positive.

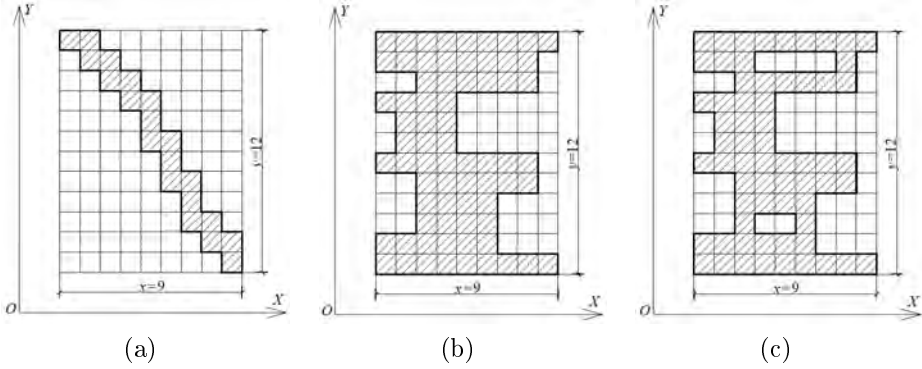


Figure 1.8: Rectangular polygons inscribed in a rectangle of  $x \times y$ ,  $x = 9u$ ,  $y = 12u$ : (a) with large field defect ( $\Delta A = 88u^2$ ,  $RDA = 0.81(81\%)$  and zero perimeter defect,  $RDP = 0(0\%)$ ); (b) with positive perimeter defect ( $\Delta P = 24u$ ,  $RDP = 0.57(57\%)$ ), with area defect ( $\Delta A = 38u^2$ ,  $RDA = 0.35(35\%)$ ); (c) with a positive perimeter defect ( $\Delta P = 40u$ ,  $RDP = 0.95(95\%)$ ), with a area defect ( $\Delta A = 44u^2$ ,  $RDA = 0.41(41\%)$ ) [35]

The second parameter characterizing the geometry of a rectangular polygon  $RP^l$  is its area  $A(RP^l)$  (generally the area  $A(F)$  of the area  $F$ ). The area of a rectangular polygon  $A(RP^l)$  is expressed as follows

$$A(RP^l) = A(R) - \Delta A(RP^l), \quad (1.25)$$

where  $\Delta A(RP^l)$  we will call the *area defect of the rectangular polygon*. The perimeter defect and area defect of a rectangular polygon, defined in an absolute way, do not reflect the magnitude of the deviation measures from the perimeter and area of the rectangle. Besides, in practical applications, they will depend on the adopted units of measure of length and area. Hence, it is useful to describe these measures of deviation (from the ideal figure - a rectangle) in relative terms. Thus, we will introduce two more concepts: the *relative perimeter defect of a rectangular polygon*

$$RDP(RP^l) = \frac{\Delta P}{P(R)} \quad (1.26)$$

and the *relative area defect of a rectangular polygon*

$$RDA(RP^l) = \frac{\Delta A}{A(R)}. \quad (1.27)$$

The relative area defect, with a perimeter defect equal to zero, shows the degree of "imperfection" of the border line. The same length of perimeter takes up roughly  $\frac{\Delta A}{A(R)} \cdot 100\%$  smaller area; so there is loss in the area at the same perimeter. Because the larger the perimeter defect the larger the perimeter, area defect with increased perimeter results in even greater losses of the area. Denoting by  $A$  the area and by  $P$  the perimeter of a rectangular polygon, and by  $A_R$  the area and by  $P_R$  the perimeter of a rectangle described by a rectangular polygon, the formulas (1.26) and (1.27) can be written in a more readable form

$$RDP = \frac{P - P_R}{P_R}, \quad (1.28)$$

$$RDA = \frac{A_R - A}{A_R}. \quad (1.29)$$

### 1.3.2. Span of rectangular polygon

An important parameter of the building structure is its span.

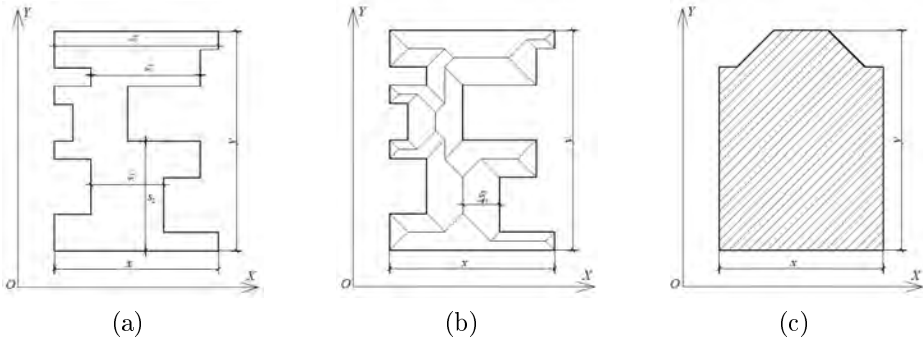


Figure 1.9: Determining the span of a rectangular polygon: (a) after the first overview the span value of a polygon is not directly visible:  $s_2$  or  $s_3$ , or perhaps  $s_4$ ?; (b) after constructing a simple skeleton the algorithm for determining the span is easy to formulate; c) a shape close to a rectangular polygon [35]

It turns out that in the case of a building it is good to use the slopes of the roof, but before that the roof must be resolved. In the case of a rectangular polygon, we will do the same by constructing a simple

skeleton (explicitly defined for this polygon) [31,35]. Treating the border of the rectangular polygon as the eaves line, we construct the skeleton of the roof (Fig. 1.8b). By the *span*  $s(RP^l)$  of a rectangular polygon, we will mean the greatest of the heights of the projections of all slopes measured relative to the eaves (Fig. 1.8). For a given projection of a rectangular roof skeleton spanning the edge of a rectangular polygon, we can calculate the span according to the following procedure (Fig. 1.9).

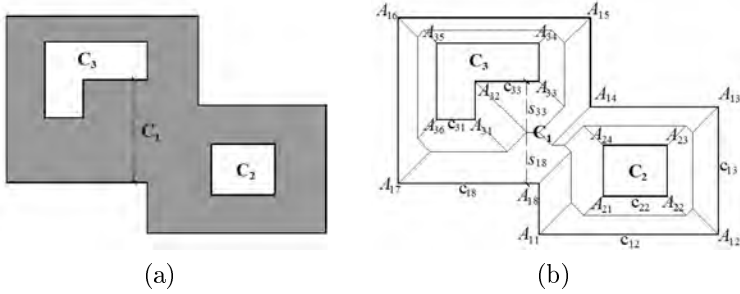


Figure 1.10: Determining the span of a 3-connected rectangular polygon  $RP^3$ : (a) a 3-connected rectangular polygon indicating the polygon  $C_1$  and sub-polygons (holes)  $C_2$ ,  $C_3$  of the line segment defined in figure (b) defining the span; (b) the process of determining the span  $s(RP^3)$  by the roof solution:  $s(RP^3) = 2 \cdot s_{18}$ ,  $s(RP^3) = 2 \cdot s_{33}$ , as well as the sum of  $s(RP^3) = s_{18} + s_{33}$  heights of hipped roof end adjacent to each other along the ridge [35]

1. From the corner points of the skeleton of the roof we construct line segments  $s_{ij}$  of  $s_{ij}$ -lengths descended into the eaves  $(i, j)$  (the base of the corresponding polygon of  $(i, j)$ -th hipped roof end) [47]. The two-index hipped roof end indicators are derived from [30], where for the generalized  $l$ -connected polygons:  $i$  represents the number of a polygon ( $i = 1$ ) or sub-polygon-hole ( $i = 2, 3, \dots, l$ ),  $j$ -eaves number (hipped roof end number) of the polygon (sub-polygon) ( $i = 1, 2, 3, \dots, l$ ) (Fig. 1.3a).
2. The length of the maximum hipped roof end height multiplied by 2 is the span of a polygon, ie.

$$s(RP^l) = 2 \cdot \max_{ij} \{s_{ij}\}.$$

This is another interesting application of geometry of the roof (straight skeletons), this time to facilitate the formulation and determination of the rectangular polygon span, as a result of a fairly simple geometric

process involving viewing the height of slope following the eaves. The span of a polygon indicates its "slender" qualities. Note that the span of a rectangle is equal to the length of its shorter side. It is worth to add that the concept of span can be generalized to any polygon, not necessarily rectangular, and that then, for example, the span of a triangle is equal to double the distance of the point of intersection of the angle bisectors from any side. The concept of span can be generalized to any planar region into which a polygon can be inscribed.

## 1.4. Summary

The presented properties of rectangular polygons and their parameters can be used to describe and analyze the shape of buildings (especially single-family houses) and their optimization. These properties, in practice, for example, in practice, applied to the optimization of building shape, can also be used for many shapes similar to rectangular polygons (Fig. 1.9c). This naturally requires additional analysis and discussion verifying the possibility of overlooking the lack of complete shape (degree of accuracy) of a rectangular polygon.

## 1.5. Problems

1. For which pipe will we use the least amount of material, if the cross-sections of the considered pipes, are: circle, square, regular hexagon, regular octagon?

**Hint.** Without focusing on the thickness of the pipe, count the areas of the cross-sections and the lengths of the perimeters of these cross-sections.

2. Consider the following containers: spherical, cubic, cylindrical with a ratio of height to diameter of 1 : 1. For which of them will we use less material?

**Hint.** Not focusing on the thickness of the walls, that is, assuming a thickness of zero.

3. Calculate: classical, geometric measure of compactness of solids and  $RC_{cube}$ ,  $RC_{cd}$ ,  $RC_{cyl}$  for: cube, cylinder and solid from the figure 1.11.

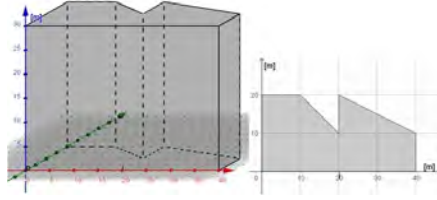


Figure 1.11: Solid and projection of the base of the solid, prep. A. Tereszkievicz

4. Design a rectangular tank with a volume of 144 cubic meters so as to use as little material as possible.
5. There is a forest adjacent to the straight section of the road, which is fenced due to the animals along the road. One of the co-owners of the forest intends to start a rectangular-shaped forest crop on part of the forest area adjacent (on one side) to the road. For its fence, 1000 m of forest netting has been reserved. What dimensions should the forest planting have in order to make the fenced area as large as possible?
6. A cylindrical open tank with a volume of 10 cubic meters is to be made of sheet steel. Find the dimensions of the tank that will require the least amount of material to make it.
7. The material for the bottom costs 60% more than the strength glass for the four walls of an open aquarium. Find the shape of the cheapest aquarium of a given volume  $V = 1 \text{ m}^3$ .
8. Calculate all the linear interrelationships between the indicators  $A/V$ ,  $EWA/FA$ ,  $RC_{cd}$ .
9. For selected ten single-family houses, study the relationship between the indices  $LBI$  and  $RC_{cd}$ .
10. Derive the formulas for the relative compactness indicator if the reference figure is a rectangle in which the ratio of the lengths of the sides is equal to  $k$ . For what values of  $k$  is the reference figure a "golden", "silver" rectangle (compare [41])?

## Chapter 2

# Isometries in design

Important transformations implemented in CAD systems are the *isometries*. These are transformations of Euclidean space ( $E^n$ ) that preserve the distance of points. Isometries form a *transformation group*, i.e., the set of all isometries has the property: (sup) the superposition of two isometries is an isometry, (inv) the inverse transformation of an isometry is an isometry, (id) the identity transformation is an isometry. The basic isometry is the *symmetry with respect to a straight line* in  $E^2$ , the *symmetry of a plane* in  $E^3$  and in general the *symmetry of a hyperplane* in  $E^n$ . We say that symmetry is the *generator* of the isometry group. We can consider any of the transformations of a group as a generator of some subgroup of that group.

### 2.1. Isometries in $E^2$

In the plane, every isometry is:

- 1) an axial symmetry  $S_p$  about the  $p$  axis or
- 2) a superposition of two axial symmetries  $S_a, S_b$ , whereby it is:
  - A) *translation*  $T_{2AB} = S_b S_a$ , when the axes  $a, b$  are parallel ( $a \parallel b$ , Fig. 2.1a) or
  - B) *rotation*  $R_{O,2\varphi} = S_b S_a$ , when the axes  $a, b$  intersect ( $a \cap b = \{O\}$ , Fig. 2.1b)or
- 3) a superposition of three axial symmetries  $S_a, S_b, S_c$  (Fig. 2.2b). The superposition of the three symmetries is either an *axial symmetry* or a *glide symmetry*.

If  $a \perp b$ , the superposition  $S_b S_a$  is rotation  $R_{O,2,90^\circ}$  by an angle of  $180^\circ$ , i.e. *central symmetry (half-rotation)*  $S_O$  (Fig. 2.2a).

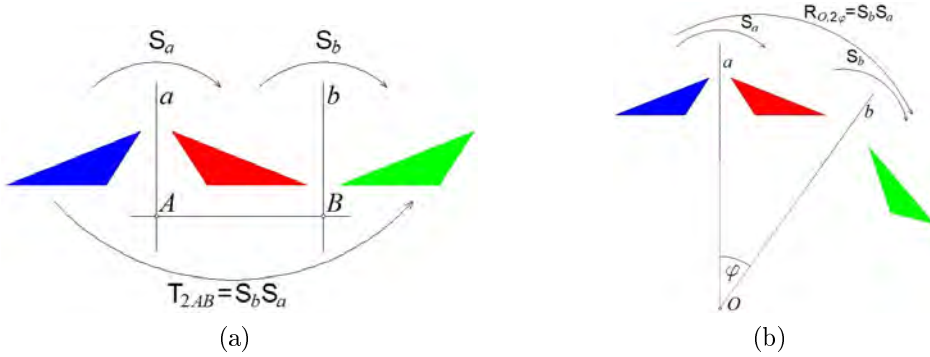


Figure 2.1: (a) the superposition  $S_b S_a$  of axial symmetries  $S_a, S_b$  with  $a|b$ -parallel axes is a translation  $T_{2AB}$  ( $AB$  – a vector defined by the points  $A, B$  lying on the lines  $a$  and  $b$ , respectively, with  $AB \perp a$  and  $AB \perp b$ ); (b) the superposition  $S_b S_a$  of the axial symmetries  $S_a, S_b$  with axes  $a, b$  intersecting  $a \cap b = \{O\}$  is a rotation of  $R_{O, 2\varphi}$  by an angle of  $2\varphi$ , prep. E. Koźniewski

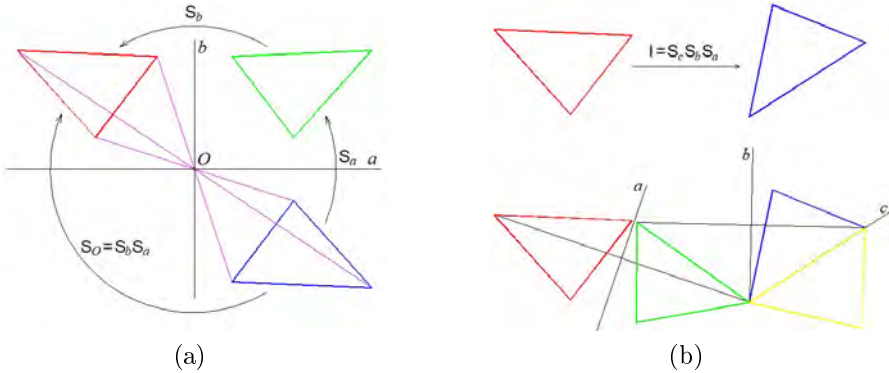


Figure 2.2: (a) the superposition  $S_b S_a$  of axial symmetries  $S_a, S_b$  with perpendicular axes  $a, b$  is point symmetry  $S_O$ , with point  $O$ ; (b) the superposition  $S_c S_b S_a$  of the three symmetries  $S_a, S_b, S_c$  with respect to the straight lines  $a, b, c$  transforms the triangle into a pre-given triangle congruent to it, prep. E. Koźniewski

Two triangles are congruent if they have respectively equal sides. Then there is an isometry that transforms the first triangle into the second (fig. 2.2b). To realize this isometry, it is enough to superposition at most three axial symmetries (Fig. 2.2b). Each figure (geometric object) has its group of *self isometries*, i.e. those that transform the figure into itself. For example, the letter  $A$  (as a figure – a set of points) has a group of self isometries  $Id, S_p$ , where  $Id$  is an identity transformation,  $S_p$  is an axial symmetry.

## 2.2. Tessellation

We will use isometries to design tessellation. *Tessellation/tiling* on a plane is the covering of the plane with figures adjacent to each other, but not overlapping (the sum of the figures forms a plane, any two figures share only edge points). We deal with tiling, for example, when designing and laying floors, sidewalks, etc.

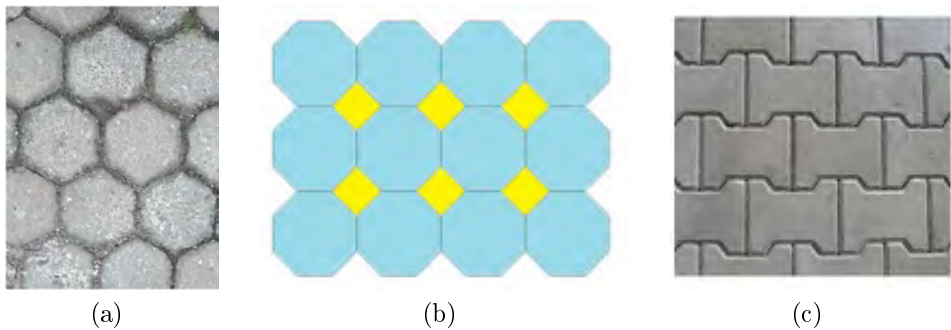


Figure 2.3: (a) regular tilings (from regular polygons of one kind), photo by E. Koźniewski; (b) semi-regular tilings (from regular polygons of different types), prep. E. Koźniewski; (c) monohedral tessellation of any shape, photo by E. Koźniewski

A relatively simple class of tessellations to shape are polygonal regular and semi-regular tessellations (figs. 2.3a – 2.3c). In the creation of such tessellations, it is important how many and what kind of regular figures can meet at a single point. It is not difficult to see that the sum of the angles should be equal to  $360^\circ$ . The tessellation in the figure 2.3a has the characteristic  $6 - 6 - 6$ , that is, the polygons meet at a point: hexagon-hexagon-hexagon ( $120^\circ + 120^\circ + 120^\circ = 360^\circ$ ); the tiling in the figure 2.3b has the characteristic  $8 - 8 - 4$ , that is, the polygons meet at a point: octagon-octagon-quadrilateral ( $135^\circ + 135^\circ + 90^\circ = 360^\circ$ ). The program to create them can be found on the website [12]. The tessellation in the figure 2.3c is neither regular nor semi-regular. We write about creating such parquets below.



### 2.2.1. Tessellation in $E^2$ – some examples

**Example 2.1.** Transformations on a parallelogram (pigeons). We consider two different curves (2.4a) and move them in two directions (Fig. 2.4a1). We obtain the elementary object "pigeon" (Fig. 2.4a2).

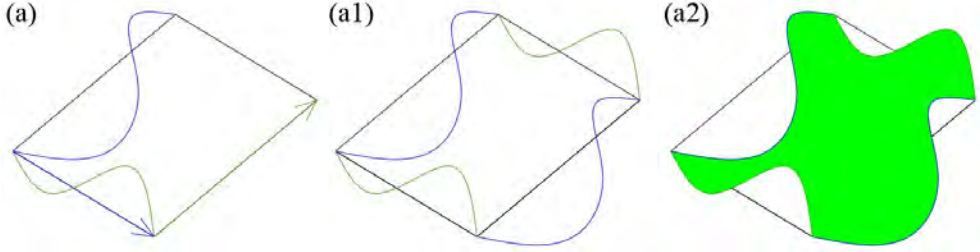


Figure 2.4: Transformations on a parallelogram: (a) any two curves with ends at the vertices of the polygon; (a1) shift the curves by the vectors induced by the parallelogram; (a2) the resulting shape ("pigeon"), prepared by E. Koźniewski based on [51]

The displacements of the resulting object by the vectors defined by the parallelogram define the tiling (Fig. 2.5).

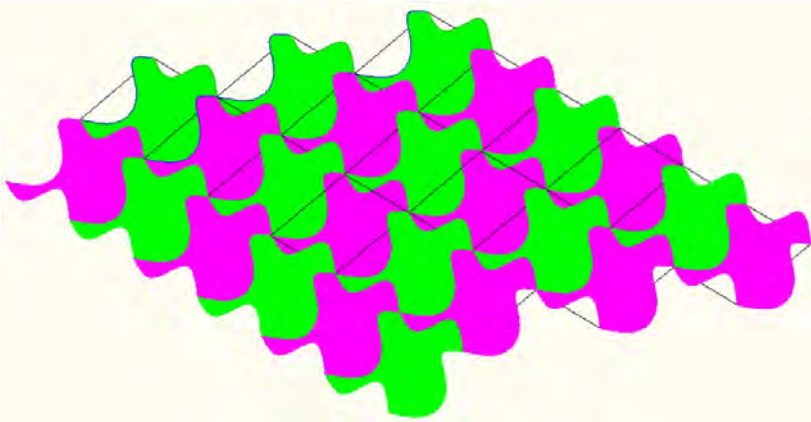


Figure 2.5: Tessellations with two curves spanning a parallelogram ("pigeons"), prepared by E. Koźniewski based on [51]

**Example 2.2.** Transformations on an equilateral triangle (variations on Escher's three butterflies). Take any curve that connects the vertex of an equilateral triangle to the center of a side about that vertex (Fig. 2.6a). We then transform this curve by a central symmetry (Fig. 2.6a1), further by two rotations (Fig. 2.6a2) and by five rotations (Fig. 2.6a3).

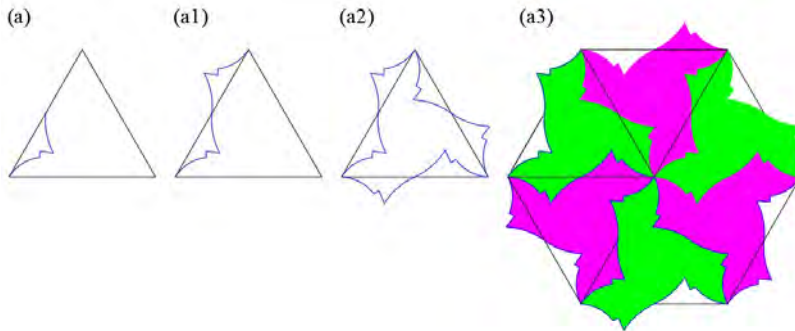


Figure 2.6: Transformations on an equilateral triangle - variations on Escher's three butterflies: (a) any curve; (a1) its central image of symmetry; (a2) two rotations; (a3) six (five) rotations, prepared by E. Koźniewski based on [51]

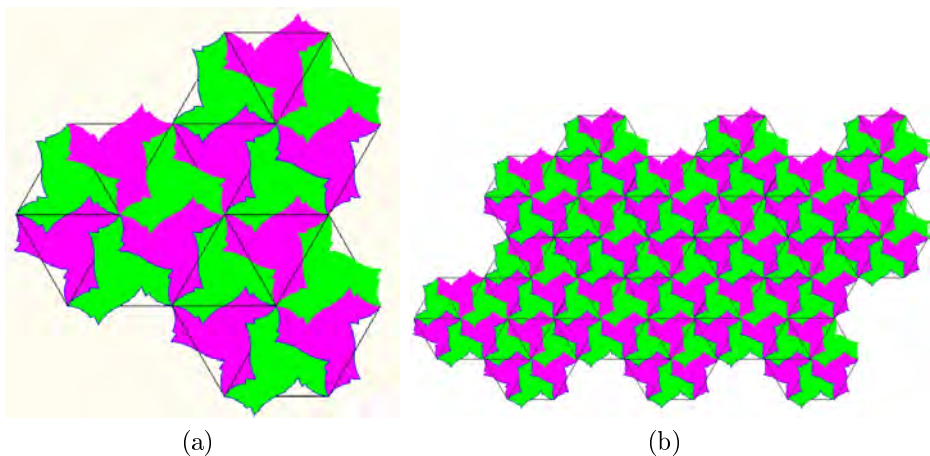


Figure 2.7: (a) two rotations of the shape from the figure 2.6 [36]; (b) a few corresponding shifts of the shape from figure 2.7a in directions parallel to the sides of the triangles (hexagons), prepared by E. Koźniewski based on [51]

**Example 2.3.** Transformations on a square ("lizards"): two arbitrary (but appropriately chosen) curves with a start at a vertex and an end point at the other vertex of the side of a given square (Fig. 2.8a). Then such curves are rotated around their respective vertices by a rotation angle of  $90^\circ$  (Fig. 2.8a1) and the shape of the lizard is obtained (Fig. 2.8a2).

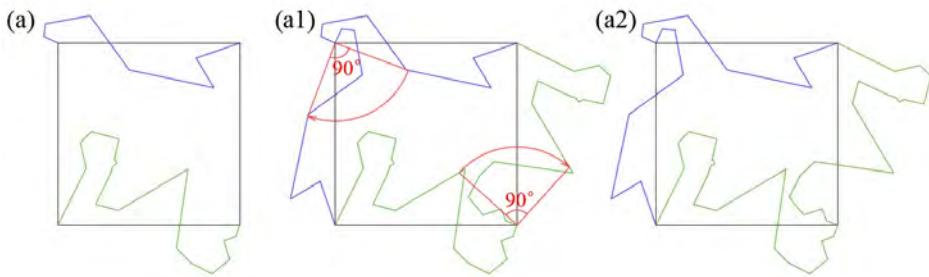


Figure 2.8: Transformations on a square: (a) two curves; (a1) two rotations around the vertices by an angle of  $90^\circ$ ; (a2) received elementary shape, prepared by E. Koźniewski based on [51]

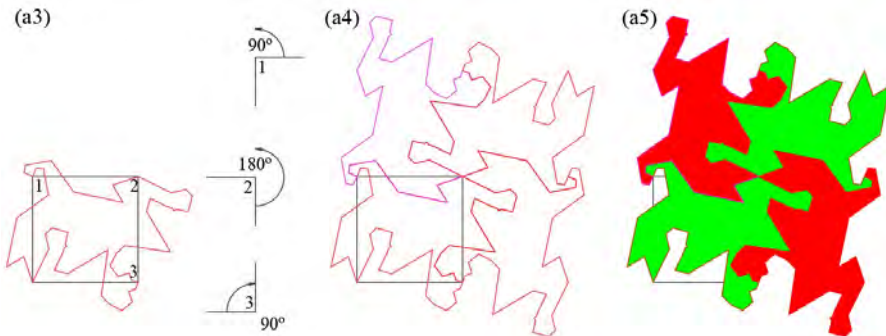


Figure 2.9: Transformations on a square: (a3) three selected vertices; (a4) configuration obtained by three rotations around the vertices with corresponding rotation angles  $90^\circ$ ,  $180^\circ$ ,  $90^\circ$ ; (a5) obtained compound shape (prepared by E. Koźniewski based on [51])

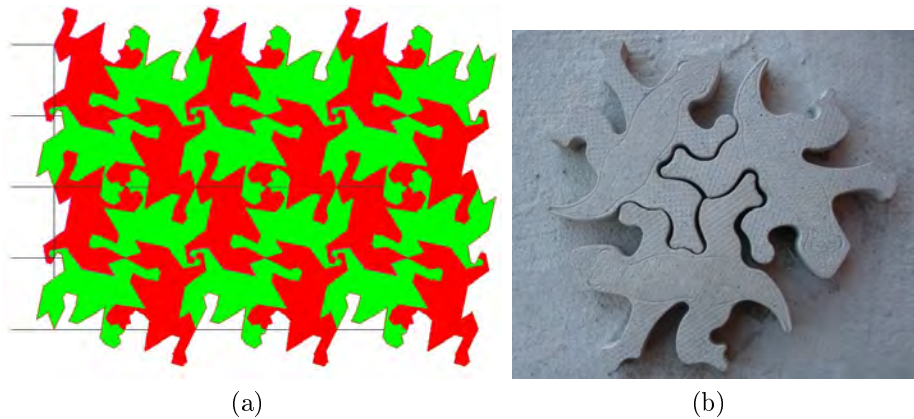


Figure 2.10: (a) transformations on a square: – the obtained tessellations, prepared by E. Koźniewski based on [51]; (b) concrete paving texture designed on the basis of an equilateral triangle, photo by E. Koźniewski

Table 2.1: Seventeen crystallographic two-dimensional space groups according to Coxeter [7] (\*half-turn = rotation by  $180^\circ$  or central symmetry, \*\*reflection with glide = superposition of axial symmetry and translation with respect to the same straight line, \*\*\*quarter-turn = rotation by  $90^\circ$ )

Symbol	Generatrns
$p1$	two independent translations
$p2$	three half-turns *
$pm$	two reflection and a translations
$pg$	two parallel glide reflection **
$cm$	a reflection and a parallel glide reflection
$pmm$	reflections in the four sides of a rectangle
$pmg$	a reflectionand two half-turns
$pgg$	two perpendicular glide reflections
$cmm$	two perpendicular reflections and a hulf-turn
$p4$	a half-turn and a quarter-turn ***
$p4m$	reflections in the three sides of a $(45^\circ, 45^\circ, 90^\circ)$ triangle
$p4g$	a reflection and quarter-turn
$p3$	two rotations throught $120^\circ$
$p3m1$	a reflection and a rotation trougt $120^\circ$
$p31m$	reflections in the three sides of an equilateral triangle
$p6$	a half-turn and a rotation trougt $120^\circ$
$p6m$	reflections in the three sides of a $(30^\circ, 60^\circ, 90^\circ)$ triangle

Interesting information about tessellations can be found in a number of publications, including [7], [51], which describes seventeen discrete isometry groups involving two independent tessellations. It is noteworthy that six of these groups arise as symmetry groups of known rectangular patterns, which we can consider as bricks or tiles [7]. These groups are listed in 2.1.

### 2.2.2. Isometries in $E^3$

As mentioned reflection, translation and rotation in the (two-dimensional) plane can be generalized to three dimensions. One generalization of two-dimensional reflection is the three-dimensional reflection of  $S_p$  with respect to a straight line  $p$ , called axial symmetry. We can also consider another reflection of  $S_\omega$  with respect to the  $\omega$  plane, called plane symmetry. Isometries on the  $E^3$  plane have as a set of generators a set of plane symmetries. Each isometry is:

- 1) *symmetry* relative to the plane  $S_\alpha$   
or
- 2) superposition of two plane symmetries  $S_\alpha, S_\beta$ , whereby it is:
  - A) *translation*  $T_{2AB} = S_\beta S_\alpha$ , if the planes  $\alpha, \beta$  are parallel ( $\alpha \parallel \beta$ ) or
  - B) *rotation*  $R_{c,2\varphi} = S_\beta S_\alpha$ , if the planes  $\alpha, \beta$  intersect  $\alpha \cap \beta = c$ ; for  $\varphi = 90^\circ$  we have axial symmetry of  $S_c$  with respect to the straight line  $c$   
or
- 3) superposition of three plane symmetries  $S_\alpha, S_\beta, S_\gamma$ , which is:
  - A) a *glide symmetry* (a glide symmetry is the superposition of a plane symmetry and a translation by a vector parallel to that plane)  
or
  - B) *rotation* with perpendicular reflection relative to the plane  
or
- 4) superposition of four axial symmetries  $S_\alpha, S_\beta, S_\gamma, S_\delta$ , which is a twist move [7].

Isometries 2 and 4 are even (do not change orientation), isometries 1 and 3 are odd (change orientation to the opposite). Isometries are an important tool for modeling three-dimensional objects.

**Example 2.4.** Make virtual models of two Platonic polyhedra: the dodecahedron and the icosahedron.

**Solution.** We construct an icosahedron using the wall method (each wall in CAD terms is a solid here). First, we make the (horizontal) wall of the icosahedron, then, using the Monge method, we determine the angle of inclination of the five walls [32] and rotate the horizontal wall to get the first inclined wall (Fig. 2.11a), then rotate the sloped wall four times (Fig. 2.11a1), reflect symmetrically about the plane (Fig. 2.11a2), rotate and move to the position in figure 2.11a3.

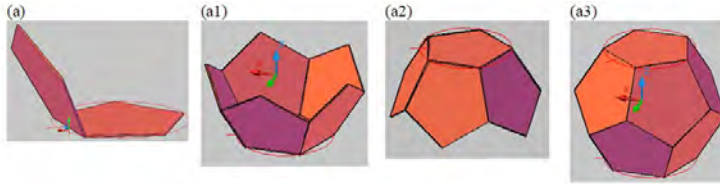


Figure 2.11: Modeling of the icosahedron: (a) finding (using Monge's method) the appropriate angle; (a1) five rotations (four rotations) of one wall; (a2) plane symmetry; (a3) one rotation and one translation, prep. E. Koźniewski based on [32]

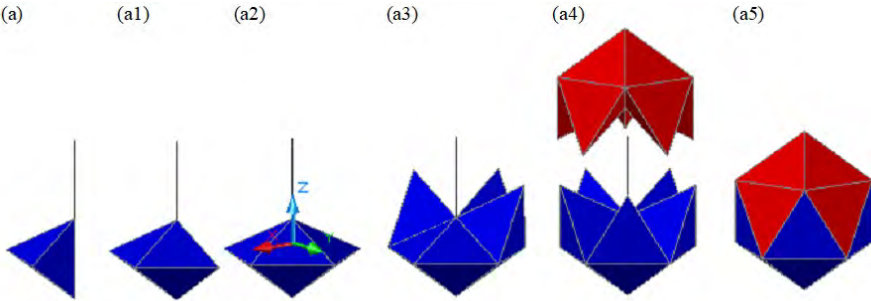


Figure 2.12: Creating an icosahedron model: (a) determining (by Monge method) the corresponding triangular pyramid with the edge in the vertical position; (a1) one reflection relative to the pyramid wall; (a2) three reflections about the corresponding planes or three rotations; (a3) three reflections about the corresponding walls; (a4) two consecutive reflections and one reflection about the plane determined by the five top vertices of the bottom solid and one corresponding rotation about the vertical line; (a5) one translation, prep. E. Koźniewski based on [32]

**Example 2.5.** Make a virtual model of the *rhombic dodecahedron*.

**Solution.** The rhombic dodecahedron can be generated by adding a congruent pyramid to the six faces of the cube (Fig. 2.13). First, we construct a tetrahedral pyramid with a height equal to half the edge of the cube. The next construction is shown in figure 2.13. The rhombic icosahedron has an interesting property, because it completely fills the space (Fig. 2.14). This spatial space-filling operation reminds us of tessellation on the plane. Using translation in two directions, we can fill the entire three-dimensional Euclidean space with the rhombic dodecahedron. The rhombic dodecahedron can be treated as a refined shape of bricks for making a wall.

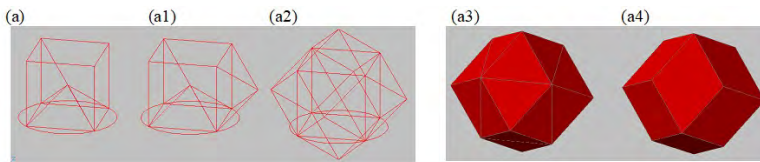


Figure 2.13: Creating a model of the rhombic dodecahedron: (a) building a tetrahedral pyramid with a height equal to half the edge of the cube; (a1) one rotation; (a2) one reflection, three rotations and one translation; (a3) whole solid with visual decomposition; (a4) a solid obtained by a (Boolean) sum, prep. E. Koźniewski based on [36]

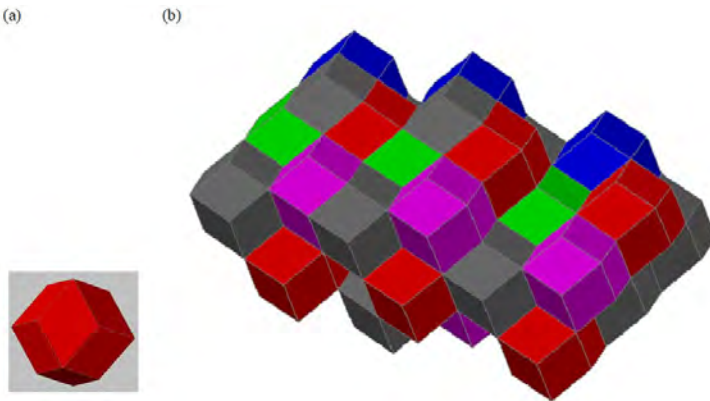


Figure 2.14: The rhombic dodecahedron can be treated as a refined brick shape: (a) brick; (b) wall made of rhombic dodecahedrons, prep. E. Koźniewski

**Example 2.6.** Make a virtual model of the Art Tower by Arata Isozaki [51].

**Solution.** The model is obtained by skillfully duplicating a previously built regular tetrahedron using plane symmetry.

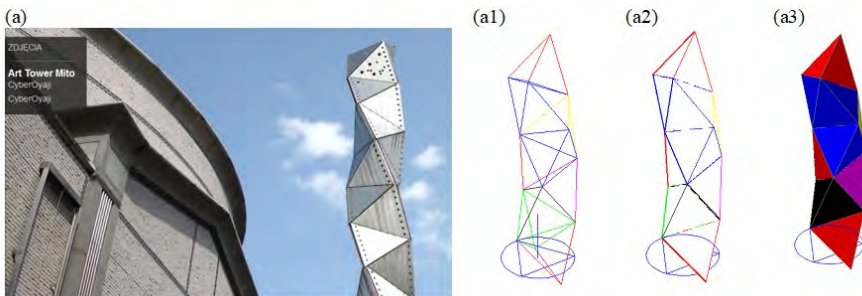


Figure 2.15: Art Tower model creation: (a) Art Tower in Mito, designed by Arata Isozaki [51], [16]; (a1)–(a3) sequence of reflected tetrahedrons in different visualization styles [36], prep. E. Koźniewski

## 2.3. Between tessellation & polyhedral regular and semi-formal polyhedra

The icosahedron and the dodecahedron (Fig. 2.17a) belong to the group of five *form polyhedrons* often called Platonic solids (Table 1.1). In a regular polyhedron, all walls are congruent regular polygons and all polyhedral angles (corners) are congruent (isometric). The regular polyhedron is a special case of the polyhedra *semi-regular polyhedron* (*Archimedean polyhedron*), in which the (regular) walls need not be congruent. A regular polyhedron is characterized by a pair of numbers  $(p, q)$  (symbol Schläfli), which means that the polyhedron has  $q$  faces at each vertex, and each face is a  $p$ -angle. If we denote the number of vertices, edges and faces by  $V$ ,  $E$ ,  $F$ , respectively, the equality (Euler's formula)  $V - E + F = 2$  holds. Note that the pairs (tetrahedron, tetrahedron), (cube, octahedron), (dodecahedron, icosahedron) equal to  $((3, 3), (3, 3))$ ,  $((4, 3), (3, 4))$ ,  $((5, 3), (3, 5))$ , respectively, have mutually rearranged pairs in Schläfli symbols. We say that the tetrahedron is *self-dual*, while a cube and an octahedron as well as a dodecahedron and an icosahedron are mutually *dual*. Geometrically, this is expressed in



such a way that by connecting the centers of the faces of any regular polyhedron with segments, we get another regular polyhedron dual to it.

A *semi-regular polyhedron* (*Archimedean polyhedron*) is called a polyhedron in which all faces are regular polygons and all polyhedral angles (corners) are congruent. There are 13 semi-regular polyhedrons (15 if you count mirror images of two of them) and two infinite series (regular prisms, i.e., with a  $n$ -gon base and square faces, e.g. concrete paving, and so-called *anti-prisms*, in which the bases are rotated relative to each other by an angle  $\frac{\pi}{n}$  and the faces are equilateral triangles). Archimedean polyhedra can be obtained by properly "cutting off" regular pyramids at the vertices of a regular polyhedron (Fig. 2.17b, 2.17c).

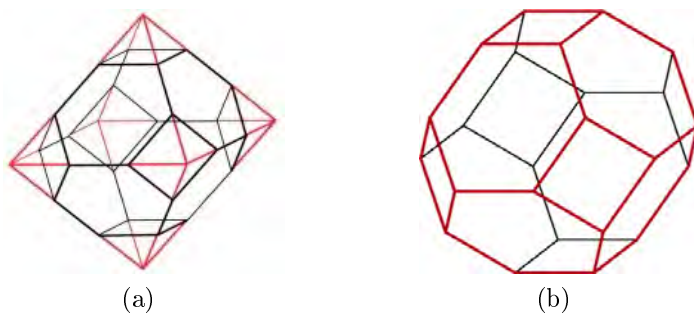


Figure 2.16: (a) Construction of the Archimedean tetrahedron on the basis of an octahedron; (b) The Archimedean tetrahedron constructed on the basis of a regular octahedron, prep. E.Koźniewski

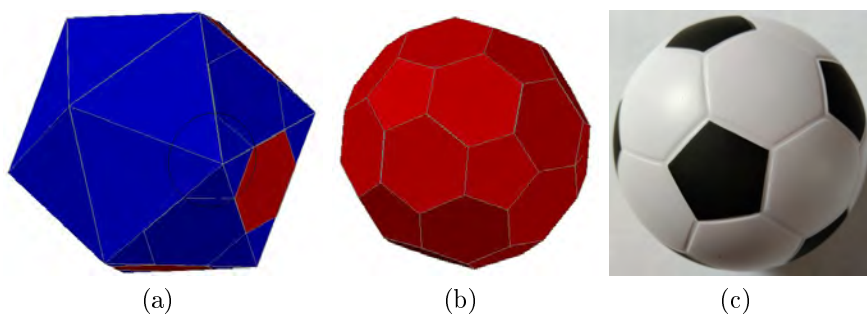


Figure 2.17: (a) icosahedron regular, by E. Koźniewski; (b) construction of a truncated icosahedron, by E. Koźniewski; (c) the way of stitching the soccer ball (football) according to the structure of the truncated icosahedron, photo by E. Koźniewski

A classic example of the use of a truncated icosahedron shape is the way a soccer ball is stitched (Fig. 2.17c).



Figure 2.18: Orthodox Church of the Resurrection in Białystok, designed by Jerzy Uścińowicz, 1991 – 1994. Shape of dome fragment resembling flat  $8 - 4 - 8$  semi-formal tessellation (dome from left), shape of other domes resembling fragment of Archimedean tetrahedron (Fig. 2.16) – square bordered by four regular hexagons (four domes from right), photo by M. Koźniewski

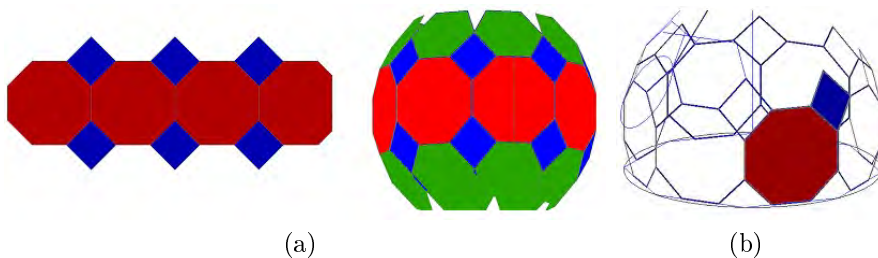


Figure 2.19: (a) fragment of tessellation  $8 - 8 - 4$  arranged over a ferny octagon (eight octagons), the squares "become" rhomboids with little deformation relative to the square and unexpectedly the possibility of completing a regular hexagon (AutoCAD) appears; (b) Space structure of tessellation  $8 - 8 - 4$  on octagon (AutoCAD), prep. E. Koźniewski

Regular polyhedra can be thought of as an analogue of tessellation, i.e. a structure in which (in three-dimensional space) we arrange equal (i.e. congruent) regular polygons (platonic solids) so as to "close" a certain area. If we allow various regular polyhedra, we get semi-regular polyhedra, otherwise known as Archimedean polyhedra. In both cases, these areas will have a rather rich group of self isometries. But space can also be "closed" in a mixed way. An excellent example of this approach is the geometric structure of the domes of the Orthodox Church of the Resurrection in Białystok, designed by Prof. Jerzy Uścińowicz.

Let's analyze the geometric structure of the solutions in the domes of the orthodox church in question. Analogon of the dome model we start by constructing a regular octagon - an octagonal base, whose faces are squares (Fig. 2.19). In these squares we inscribe regular octagons. The adjacent edges of the common sides of the inscribed octagons generate rhombuses (Fig. 2.19). It turns out that the sides of two rhombuses and the side of an octagon are consecutive sides of a regular hexagon (Fig. 2.19b). Indeed, in a rectangular projection, the projections of rhombuses are rhombuses – this is because one of the diagonals of each rhombus is parallel to the horizontal (horizontal projecting plane). Then, based on the invariant of the characteristic rectangular projection, the projection of the perpendicular diagonals are perpendicular diagonals. At the same time, it follows from the construction of the model that the sides of the rhombus are parallel to the sides of the initial octagon (Fig. 2.19a, 2.19b), that is, the projection angles of each rhombus have measures of  $45^\circ$  i  $135^\circ$  (Fig. 2.20a, 2.20b). So we have the configuration of an isosceles trapezoid, from which it follows that the diagonal of the hexagon parallel to the projection plane is twice as long as the side. This proves that the hexagon is regular.

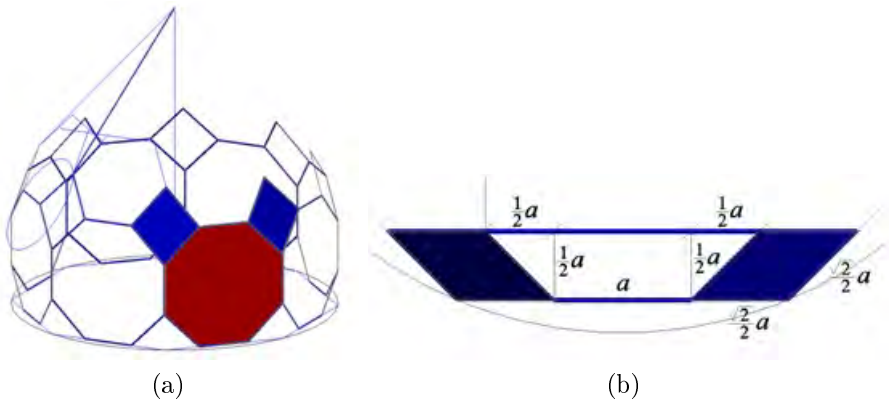


Figure 2.20: (a) modeling of the dome based on 8–8–4 tessellation, construction of a regular hexagon as a complement to the space tessellation (AutoCAD); (b) rectangular projection of two rhombuses whose edges together with the edge of the regular octagon generate a regular hexagon (AutoCAD), prep. E. Koźniewski

Since the domes of Orthodox churches have an elongated shape similar to the flame of a burning candle (although this is not the rule and usually depends on the cultural area), the hexagons were elongated and enclosed as pentagons (non-regular, of course).

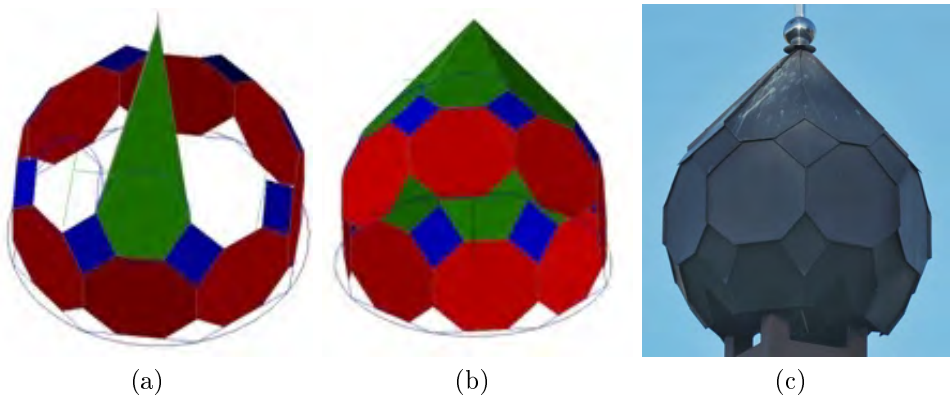


Figure 2.21: (a) modeling of the geometric structure of the dome – addition of the hexagon to the pentagon constituting the upper slope of the dome, prep. E. Koźniewski; (b) the space structure of the 8–8–4 tessellation (without the lower part) topologically equivalent to the solid of the orthodox church dome, prep. E. Koźniewski; (c) the dome over the chapel of the Orthodox Church of the Resurrection in Białystok, designed by Jerzy Uścińowicz, photo by M. Koźniewski

The geometric structure of the domes of the second type resembles a fragment of the Archimedean tetrahedron (Fig. 2.16) – involving a square bordered by four regular hexagons.

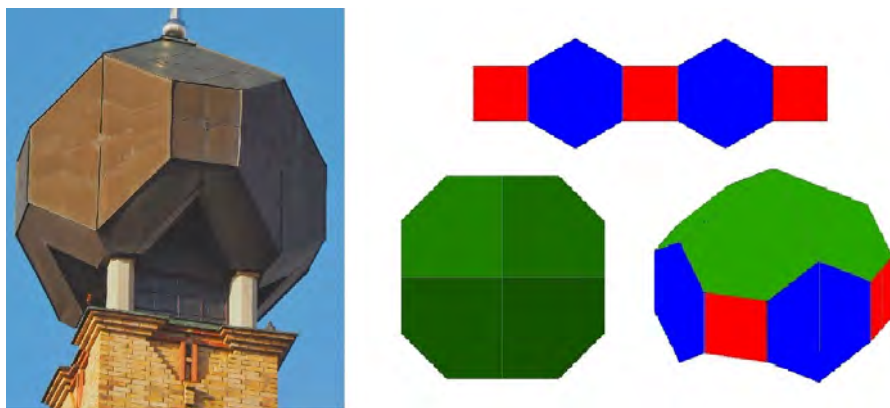


Figure 2.22: Left: the main dome of the Orthodox Church of the Resurrection in Białystok, designed by Jerzy Uścińowicz, photo by M. Koźniewski; right: geometric model topologically equivalent to the structure of the main dome of the Orthodox Church, prep. E. Koźniewski

## 2.4. Problems

1. List the self isometries (indicate the group of self isometries) of:

- |                             |              |
|-----------------------------|--------------|
| a) a square;                | f) letter E; |
| b) an equilateral triangle; | g) letter H; |
| c) an isosceles triangle;   | h) letter G; |
| d) a semicircle             | i) letter Z; |
| e) a circle                 | j) letter N. |

Which pairs of letters have the same groups of self isometries?

2. Draw semi-regular tessellations:

- |                       |                   |
|-----------------------|-------------------|
| a) 6 – 3 – 3 – 3;     | c) 3 – 4 – 6 – 4; |
| b) 4 – 4 – 3 – 3 – 3; | d) 3 – 12 – 12.   |

3. Which semi-regular tessellations exist:

- a) 8 – 6 – ...; b) 8 – 4 – ...; c) 8 – 3 – ... ?

4. Build a wall of rhombic dodecahedrons.

5. Design the tessellations, following the examples of 2.1 – 2.3.
6. Describe and draw a semi-regular tessellation – the prototype of the flooring (Fig. 2.23a).
7. Describe and draw a semi-regular tessellation – prototype of the parking lot pavement (Fig. 2.23b).
8. Design (e.g., in the AutoCAD environment) a paving (Fig. 2.23c) based on the diagrams of examples 2.2, 2.3.
9. With respect to regular tessellations, formulate the principle of duality and identify dual and self-dual regular tessellations.
10. Describe the isometry groups of Platonic solids:
  - a) a tetrahedron; b) a cube c) an octahedron.
11. In a suitably friendly coordinate system, determine the coordinates of the tetrahedral regular octahedron (Fig. 2.17b).

**Hint.** We divide the edges of the octahedron into three equal parts and compare the coordinates of the three vectors.

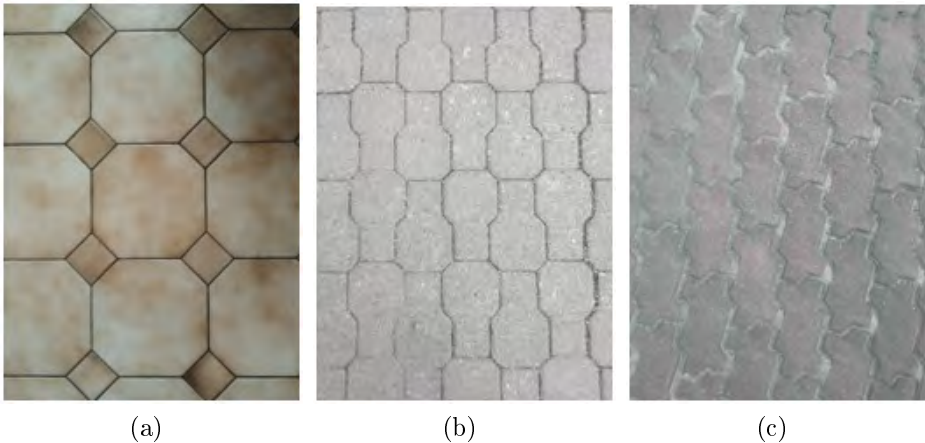


Figure 2.23: Examples of practical solutions in floor and pavement design, photo by E. Koźniewski: (a) floor tiles—styling of semi-regular tessellation  $x-y-z$ ; (b) parking lot paving –paver blocks "mirror", sidewalk designed according to  $p-q-r$  semi-regular tessellation; (c) sidewalk paving – paver blocks designed according to tessellation based on transformations on the square (combining the schemes from examples 2.2, 2.3 and gluing the two patterns)



## Chapter 3

# Ruled (scroll) surfaces in civil engineering

### 3.1. Surfaces resulting from a line rotation

As a result of rotation of a straight line around another line, we get three surfaces: *ruled conical surface (cone)*, *cylindrical surface (cylinder)* and *hyperboloid of one sheet* (Fig. 3.1 – 3.2).

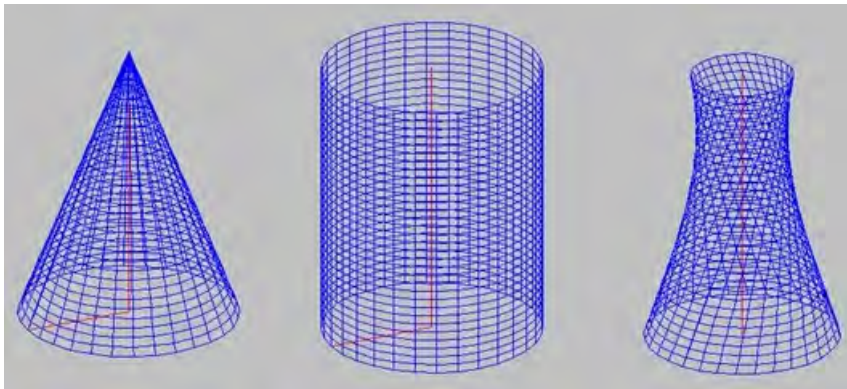


Figure 3.1: Three surfaces resulting from the rotation of the straight line around a given straight line (axis) (three variants: the straight line intersects the axis, is parallel to it, is skew to it ), prep. E. Koźniewski



Figure 3.2: Three surfaces resulting from the rotation of the straight line around a given straight line (top view), prep. E. Koźniewski



The first two surfaces in Fig. 3.1, 3.2 are used in the realization of silos (Fig. 3.3), while the third one is often found as the supporting structure of expansion tank tower, or so-called "water towers" (Fig. 3.4b, 3.6a), bracing structure of tower buildings (Fig. 3.6b) and usually as the shape structure of cooling towers in steel mills and power plants (Fig. 3.8). The world's first hyperboloid building, as a water tower, was built in 1896 in Nizhny Novgorod (Russia) according to the design of Vladimir Shukhov [50]. Also noteworthy are the 1963-built Port Tower in Kobe, Japan, the 1970-built cathedral in Brazil designed by Oscar Niemeyer, or the record-breaking (318 m) Aspire Tower, built between 2005 and 2007 in Doha, Qatar, to a design by Hadi Siman [50].

In Poland, a unique structure is the water tower in Ciechanów (Fig. 3.4a), which in 1972 was designed as a tower surge tank. The author of the project was Warsaw architect Jerzy Michał Boguslawski, with whom the designers Dr. Jerzy Wiblik, Stanisław Gajowniczek and Bohdan Szczeszek collaborated. The construction technology was developed by engineer Stanisław Majkowski. The project was carried out at the Design and Research Office of Construction *Miastoprojekt Mazowsze* in Warsaw with the cooperation of the Warsaw University of Technology. In 1977 the structure received a prize from the Minister of Construction and Building Materials Industry, and the creator was congratulated by the Governor of Ciechanów for outstanding creative achievement in the field of architecture and civil engineering. The tank has the shape of a torus set on a one sheet hyperboloid represented by two bands of formers. The tank, with a volume of  $1560 \text{ m}^3$ , is located on a 22-meter tower with the shape of a rotating hyperboloid – its bottom base diameter is 11.25 m and upper one is 17.70 m, and its narrowing diameter is about 7 m. Other data are as follows: the diameter of the support tube is 20 cm, the diameter of the torus is 17.70 m (the same as the top base), the diameter of the torus tube is 6 m, and the diameter of the ring (axial) is 6.20 m; in turn, the railing posts are 1.20 m high and 0.04 m in diameter (Fig. 3.7, 3.14, 3.15). The structure is a towering expansion tank, not a water tower, but the residents of Ciechanów call it that and it operates there under such a circulated name. Since the 1980s, the tower has stood abandoned. Plans to install an observation deck here (the tower stands at one of the highest points in the city, 143 meters above sea level) and an altitude restaurant failed. In recent years, however, it has been revitalized and an Exploratorium of Mathematics and Technology has been built nearby. The tower functions

under the name the Torus Science Park in Ciechanów (Fig. 3.5).

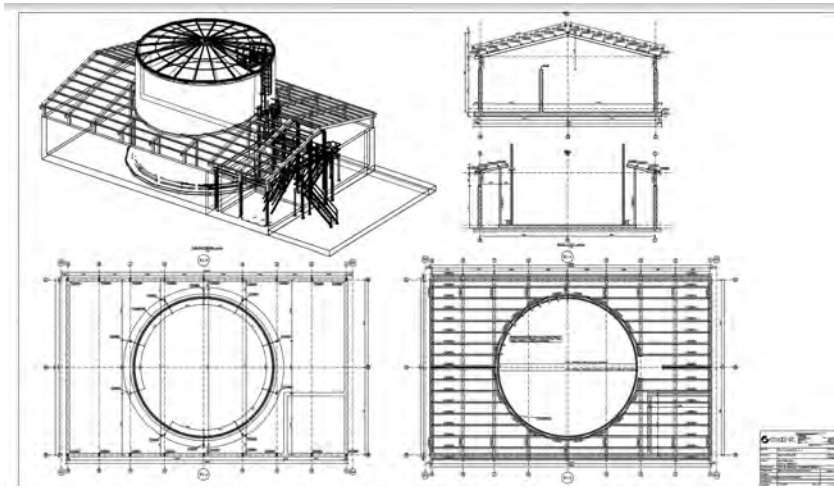


Figure 3.3: Design of fuel tank canopy (cylindrical and conical surface structure). Design collaboration B. Koźniewski

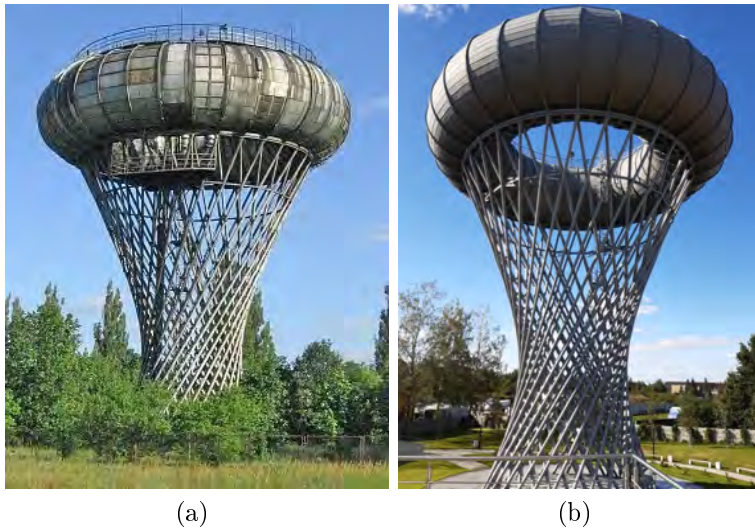


Figure 3.4: Hyperboloid-shaped structures: (a) water tower in Ciechanów – single-shell hyperboloid-shaped support structure and torus-shaped tank – condition before renovation; (b) The Ciechanów water tower after renovation as the main element of the science park, photo by B. Koźniewski



Figure 3.5: Torus Science Park in Ciechanów, photo by B. Koźniewski



(a)



(b)

Figure 3.6: (a) Kaszubskie Oko in Gniewino – geometry of construction solutions (cylinder, helical surface, single-shell hyperboloid); (b) Kaszubskie Oko in Gniewino has socio-cultural and tourist functions, photo by W. Reglińska

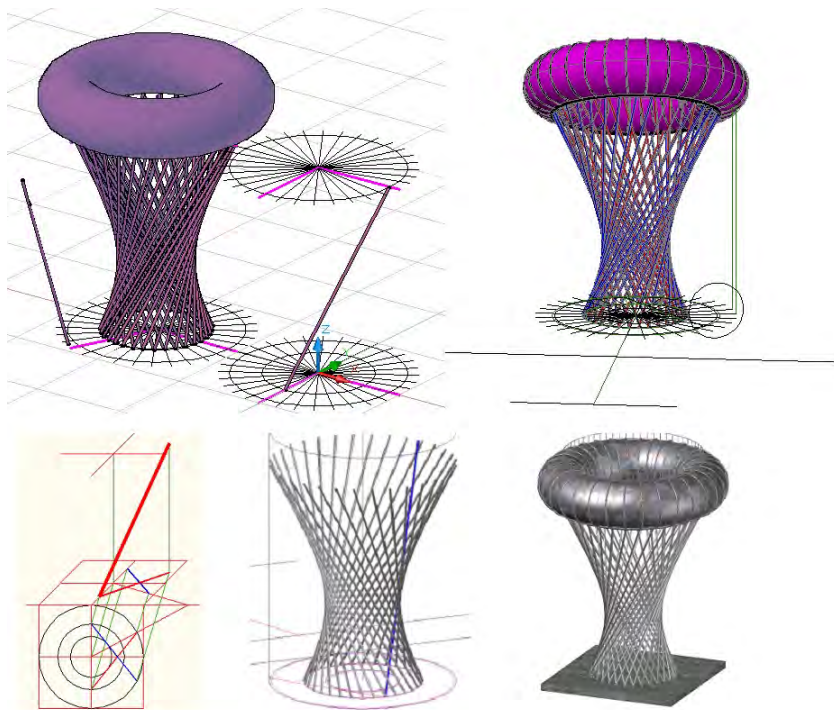


Figure 3.7: 3D model of Ciechanów water tower realized in AutoCAD environment; in the second line on the left is given an illustration of 2D structure forming hyperboloids in axonometry using axial affinity, made by E. Koźniewski

### 3.2. Description of hyperboloid surfaces – cooling tower volume

We will begin the geometric analysis of the hyperboloid structure by solving the problem of the cooling tower, whose geometric data we have on the basis of [50].

**Problem 3.1.** Calculate:

- A) the volume (cubic capacity) of the cooling tower (dimensions in Fig. 3.8),
- B) the amount of a material ( $\text{m}^3$ ) used to build the cooling tower,
- C) the area of the cooling tower.

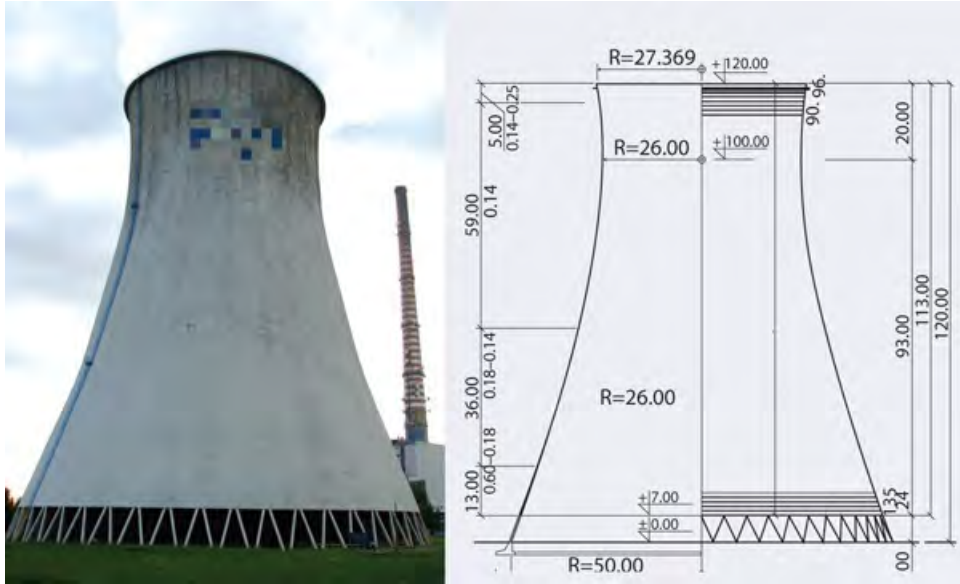


Figure 3.8: Schema of cooling tower [50, 54]

**Solution.** We will describe the procedure for calculating the volume of the cooling tower, the volume of the material used for construction (the volume of the shell wall), and the area of the outer surface of the shell, using the example of the Jaworzno III, Rybnik II type cooling tower, using information from literature [50, 54].

- A) "Cooling towers are a construction consisting of a very thin shell, flaccid columns supporting the shell, and a foundation, usually ring-shaped, founded on a soil substrate that varies due to its dimensions. The shell of a cooling tower is usually constructed as a single-shell rotating hyperboloid with a height that already reaches more than 160 m, a minimum thickness of 16 cm and a ratio of it to the smallest radius of 1/200. The problem of the static work of these shells, which are ruled surfaces with negative Gaussian curvature, is not yet completely investigated, and the intensive development of their applications in energy construction has not been without disasters." "The cooling tower at Kozienice Power Plant has reached its target height of 185.1 m and is thus the largest cooling tower in Europe. Construction of the facility began last March. The cold storage facility is part of a new unit under construction at Kozienice Power Plant" [26].

From the hyperbola formula

$$\frac{x^2}{a^2} - \frac{y^2}{b^2} = 1 \quad (3.1)$$

we calculate the second half-axis of the hyperbola

$$b = |y| \cdot \left( \sqrt{\frac{x^2}{a^2} - 1} \right)^{-1}. \quad (3.2)$$

Taking the coordinate system accordingly, we can read from the figure (3.8), that  $a = 26$ ,  $x = 50$ ,  $y = -100$ , and inserting into the (3.2), we get  $b = 60.88$ . Consequently, the equation (3.1) takes the form

$$\frac{x^2}{26^2} - \frac{y^2}{60.88^2} = 1 \quad (3.3)$$

in  $OXY$ . To calculate the cubic volume, we rotate the obtained hyperbola (3.3) around the point  $(0,0)$  by an angle  $-\frac{\pi}{2}$  (Fig. 3.9).

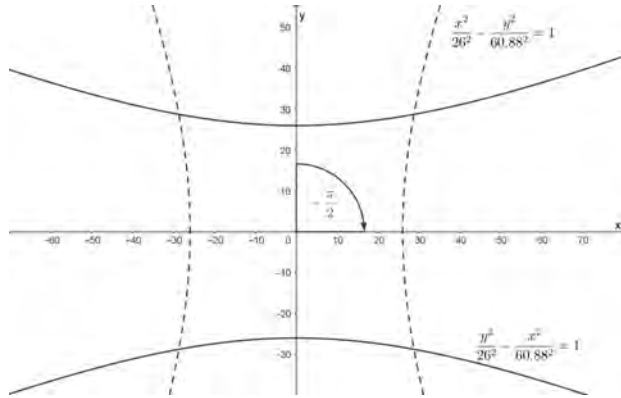


Figure 3.9: Rotation of a hyperbola around a point  $(0,0)$  by an angle  $-\frac{\pi}{2}$ , by A. Tereszkiewicz

For the mathematical description of the rotation of a point with coordinates  $(x, y)$  around the origin of the coordinate system  $OXY$  by an angle  $\beta$  we use the so-called rotation matrix.

$$\begin{bmatrix} \cos \beta & -\sin \beta \\ \sin \beta & \cos \beta \end{bmatrix},$$

namely

$$\begin{bmatrix} x' \\ y' \end{bmatrix} = \begin{bmatrix} \cos \beta & -\sin \beta \\ \sin \beta & \cos \beta \end{bmatrix} \begin{bmatrix} x \\ y \end{bmatrix}, \text{ otherwise } \begin{cases} x' = x \cos \beta - y \sin \beta \\ y' = x \sin \beta + y \cos \beta \end{cases}.$$

For  $\beta = -\frac{\pi}{2}$  we get

$$\begin{cases} x' = x \cos\left(-\frac{\pi}{2}\right) - y \sin\left(-\frac{\pi}{2}\right) \\ y' = x \sin\left(-\frac{\pi}{2}\right) + y \cos\left(-\frac{\pi}{2}\right) \end{cases}, \text{ after simplification } \begin{cases} x' = y \\ y' = -x \end{cases}.$$

After substituting into the equation (3.3) and omitting ', we get the hyperbolic  $c$

$$\frac{y^2}{26^2} - \frac{x^2}{60.88^2} = 1. \quad (3.4)$$

We can now calculate the volume of the cooling tower using the formula for the volume of a solid obtained from rotation about the  $OX$  axis in the  $OXY$  coordinate system.

$$V = \pi \int_{x_1}^{x_2} f^2(x) dx \quad \text{or equivalently} \quad V = \pi \int_{x_1}^{x_2} y^2 dx.$$

From (3.4) we get  $y^2 = 26^2 \left(1 + \frac{x^2}{60.88^2}\right)$  for  $-100 \leq x \leq 20$ , so

$$\begin{aligned} V_c &= \pi \int_{-100}^{20} 26^2 \left(1 + \frac{x^2}{60.88^2}\right) dx = \\ &= \pi \cdot 26^2 \left[ x + \frac{1}{60.88^2} \cdot \frac{x^3}{3} \right]_{-100}^{20} \approx 447\,371 \text{ m}^3 \end{aligned} \quad (3.5)$$

- B) In order to calculate the volume of a wall (shell structure) with a thickness of 0.16 m, we can use the two curves obtained from the (3.4)

$$c_1 : y = 26 \sqrt{1 + \frac{x^2}{60.88^2}} - 0.16 \quad c_2 : \frac{y^2}{(26 - 0.16)^2} - \frac{x^2}{60.88^2} = 1.$$

And here is an interesting point. Both curves  $c_1$  and  $c_2$  are hyperboloids, but as a result of rotating these hyperboloids around the  $OX$  axis, we get a hyperboloid only in the case of hyperbola  $c_2$ . This is because the second surface is not a ruled surface. The consequence of this fact is, among other things, a more complex way of calculating the integral in the case of curve  $c_1$ .

Considering the curve  $c_1$  as the curve generating the inner surface of the shell, the volume  $V$  will be the difference of two integrals  $V_c - V_{c_1}$ , i.e.

$$V_c = \pi \int_{-100}^{20} 26^2 \left( 1 + \frac{x^2}{60.88^2} \right) dx,$$

$$V_{c_1} = \pi \int_{-100}^{20} \left( 26 \sqrt{1 + \frac{x^2}{60.88^2}} - 0.16 \right)^2 dx.$$

We have calculated the integral of  $V_c$  (see (3.5)), while to calculate the integral of  $V_{c_1}$  we will use the formula

$$\int \sqrt{x^2 + k} dx = \frac{k}{2} \ln \left| x + \sqrt{x^2 + k} \right| + \frac{x}{2} \sqrt{x^2 + k}.$$

We get  $V_{c_1} \approx 443\,324$ , that is  $V_{c-c_1} = V_c - V_{c_1} = 4\,047.11$ .

Considering the curve  $c_2$  as the curve generating the inner surface of the shell, the volume  $V^*$  will be the difference of two integrals  $V_c - V_{c_2}$

$$V_c = \pi \int_{-100}^{20} 26^2 \left( 1 + \frac{x^2}{60.88^2} \right) dx,$$

$$V_{c_2} = \pi \int_{-100}^{20} (26 - 0.16)^2 \left( 1 + \frac{x^2}{60.88^2} \right) dx$$

we get  $V^* \approx 5489.16$  The difference we get between  $V$  and  $V^*$  is  $|V - V^*| = 1442.05$ . What will be the difference in the technology of making the shell wall of the cooling tower after adopting the  $c_2$  curve? Which wall forming technology is simpler? (see Fig. 3.10)

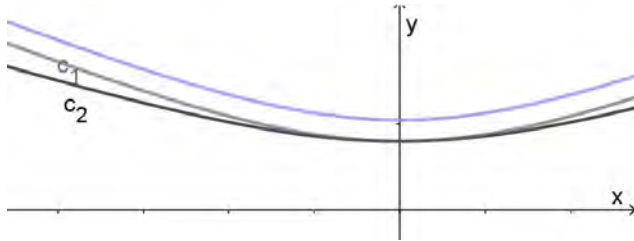


Figure 3.10: Curves  $c_1, c_2$  after shifting the branch of the hyperbola by 0.16, by A. Tereszkieicz



C) To calculate the area of the cooling tower, we will use the formula

$$A = 2\pi \int_{x_1}^{x_2} y \sqrt{1 + (y')^2} dx. \quad (3.6)$$

From (3.4) we calculate  $y = 26\sqrt{1 + \frac{x^2}{60.88^2}}$  and then  $y' = 26 \frac{\frac{1}{60.88^2} 2x}{2\sqrt{1 + \frac{x^2}{60.88^2}}}$ . After calculating, transforming, and substituting into (3.6) we obtain

$$A_c = 2\pi \cdot 26 \int_{-100}^{20} \sqrt{1 + \frac{x^2}{60.88^2}} \left(1 + \frac{26^2}{60.88^2}\right) dx. \quad (3.7)$$

Using  $\int \sqrt{1 + a^2 x^2} dx = \frac{1}{2}x\sqrt{1 + ax^2} + \frac{1}{2\sqrt{a}} \operatorname{arsinh}(\sqrt{a}x)$ , we have  $A_c \approx 26200.4 \text{ m}^2$ .

### 3.3. About curves and revolving surfaces

An *arc* is a continuous and mutually unambiguous image of a segment. For example, a semicircle is the image of the line segment  $[-r, r]$  in the transformation  $y = -\sqrt{r^2 - x^2}$ . This semicircle can be written in a different way, in a parametric form

$$\begin{cases} x = r \cos t \\ y = r \sin t \end{cases}, \quad t \in [0, 2\pi). \quad (3.8)$$

On the other hand, a circle cannot be represented by one function  $y = f(x)$ , but is still an arc. The parametric equations of the circle  $x^2 + y^2 = r^2$  can be written in the form (3.8)). How can we write the parametric equations of an ellipse  $\frac{x^2}{a^2} + \frac{y^2}{b^2} = 1$  and a hyperbola  $\frac{x^2}{a^2} - \frac{y^2}{b^2} = 1$ ?

A *curve* is a geometric object that can be represented as a sum of arcs. So the arc is a curve. A curve in three-dimensional space is represented by a system of three equations

$$\begin{cases} x = x(t) \\ y = y(t) \\ z = z(t) \end{cases}, \quad t \in [0, 2\pi), \quad (3.9)$$

where functions  $x(t)$ ,  $y(t)$ ,  $z(t)$  are sufficiently regular (continuous, differentiable). For example, using the system

$$\begin{cases} x = r \cos t \\ y = r \sin t \\ z = ht \end{cases}, \quad t \in [0, 2\pi), \quad (3.10)$$

we present a helical curve (line) with a pitch  $2\pi h$  (Fig. 3.11).

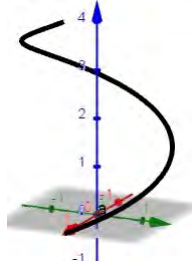


Figure 3.11: A helical curve, by A. Tereszkievich

### 3.3.1. Equation of the rotational surface

Consider the curve given by the equation (3.10). Let's fix its arbitrary point  $P_0 = (x(t_0), y(t_0), z(t_0))$ , assuming  $t = t_0$ , we fix the point  $\begin{cases} x = x(t_0) \\ y = y(t_0) \\ z = z(t_0) \end{cases}$  on the curve. Let's rotate this point around the  $OZ$ -axis (Fig. 3.12). We will write the parametric equations of such a circle in the form

$$\begin{cases} x = \sqrt{x^2(t_0) + y^2(t_0)} \cos u \\ y = \sqrt{x^2(t_0) + y^2(t_0)} \sin u \\ z = z(t_0) \end{cases}.$$

By changing the parameter  $t$ , we get the equations of the rotational surface

$$\begin{cases} x = \sqrt{x^2(t) + y^2(t)} \cos u \\ y = \sqrt{x^2(t) + y^2(t)} \sin u \\ z = z(t) \end{cases} \quad t \in [\alpha, \beta], u \in [0, 2\pi). \quad (3.11)$$

Note that this surface can also be written in the form of two equations

$$x^2 + y^2 = x^2(t) + y^2(t), \quad z = z(t) \text{ and one parameter } t \in [\alpha, \beta]. \quad (3.12)$$

By eliminating (i.e., determining  $t = t^{-1}(z)$  from  $z = z(t)$ ) the parameter  $t \in [\alpha, \beta]$  in (3.12) allows us to obtain the equation of the rotational surface in the form of a single equation

$$x^2 + y^2 = x^2(t^{-1}(z)) + y^2(t^{-1}(z)) \quad (3.13)$$

described by three variables  $x, y, z$ .

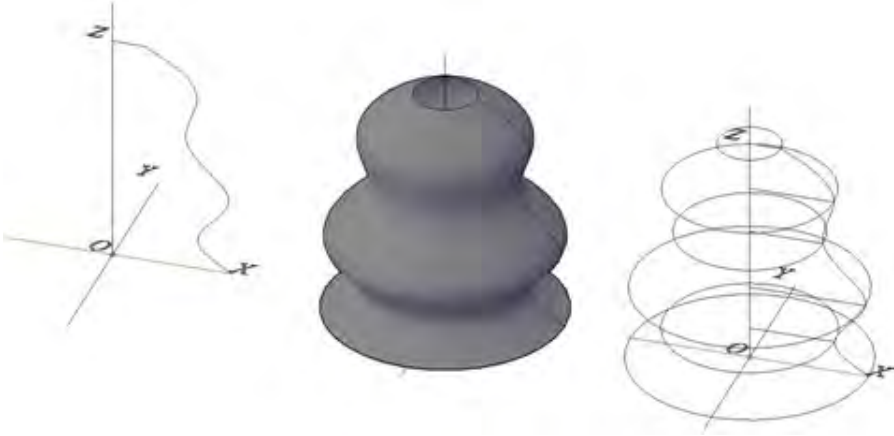


Figure 3.12: Creation of a revolved surface: an axis of revolution  $OZ$  and path curve; the resulting rotational surface; rotation circles of selected points, prep E. Koźniewski

A *rotational hyperboloid* (as a surface) can be obtained by rotating a straight line around another straight line (axis), with the straight line and the axis of rotation being skew.

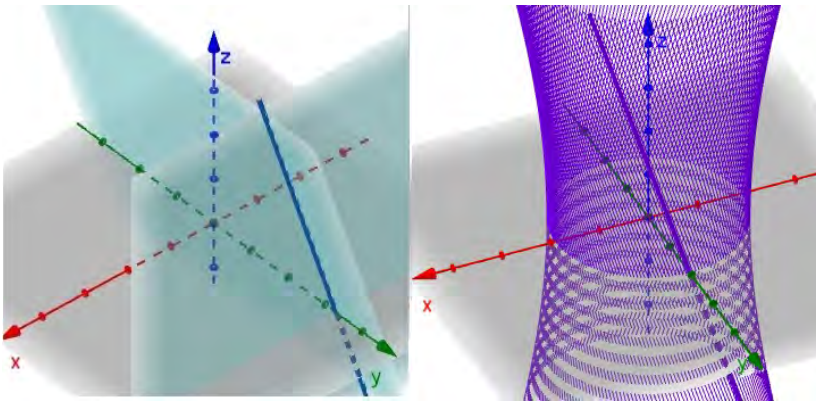


Figure 3.13: The line skewed to the  $z$ -axis, by A. Tereszkievich

Consider a line  $l$  as an edge of two planes  $z = px$  and  $y = a$  (Fig. 3.13). Assuming  $x = t, t \in R$ , the line  $l$  is written in the form

$$\begin{cases} x = t \\ y = a \\ z = pt \end{cases}, t \in R. \quad (3.14)$$

Thus, we obtain the hyperboloid

$$\begin{cases} x^2 + y^2 = t^2 + a^2 \\ z = pt \end{cases}, \quad t \in R, \quad \text{that is,} \quad x^2 + y^2 = \left(\frac{z}{p}\right)^2 + a^2. \quad (3.15)$$

The last equation can be written in the form

$$\left(\frac{x}{a}\right)^2 + \left(\frac{y}{a}\right)^2 - \left(\frac{z}{ap}\right)^2 = 1, \quad \text{i.e.} \quad \frac{x^2}{a^2} + \frac{y^2}{a^2} - \frac{z^2}{(ap)^2} = 1. \quad (3.16)$$

If, on the other hand, we take the line  $l^*$  as the edge of the two planes  $z = px + z_0$  and  $y = a$ , then we get the equation

$$\frac{x^2}{a^2} + \frac{y^2}{a^2} - \frac{(z - z_0)^2}{(pa)^2} = 1. \quad (3.17)$$

The conversion from the form (3.17) to (3.15) can be realized by

$$\begin{cases} x' = x \\ y' = y \\ z' = z - z_0 \end{cases}, \quad (3.18)$$

and from the form (3.15) to (3.17) by transforming (shifting) of the coordinate system

$$\begin{cases} x' = x \\ y' = y \\ z' = z + z_0 \end{cases}. \quad (3.19)$$

**Problem 3.2.** Determine the position (height) of the hyperboloid constriction circle (taper circle) for Ciechanów water tower model; find the equations of the rotational surface describing the support structure model and determine the cubature of the object.

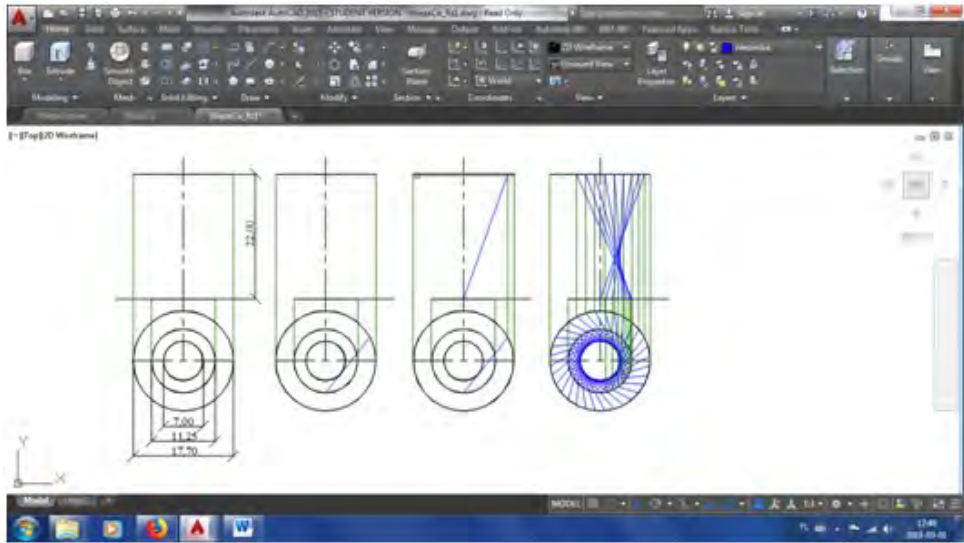


Figure 3.14: Assumptions made to create a model of a water tower in the program AutoCAD environment, by E. Koźniewski

### Solution.

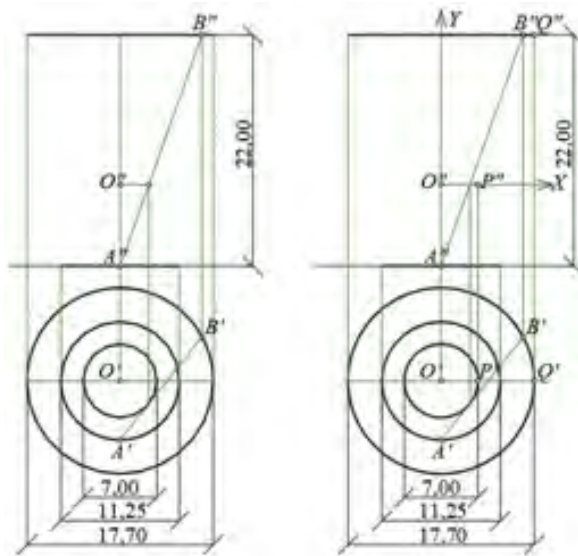


Figure 3.15: Constructions of geometric objects needed to determine the equations of the rotated line  $l(AB)$  in the program AutoCAD environment, by E. Koźniewski

To determine the equation of the rotational surface describing the model of the Ciechanów water tower, we will first find the equations of the rotated line (rotated curve) (Fig. 3.12). The equations of the line passing through the points  $A = (x_0, y_0, z_0)$ ,  $B = (x_1, y_1, z_1)$ , i.e.

$$\begin{cases} x = x_0 + (x_1 - x_0)t \\ y = y_0 + (y_1 - y_0)t \\ z = z_0 + (z_1 - z_0)t \end{cases} \quad t \in R, \quad (3.20)$$

the numbers  $x_1 - x_0$ ,  $y_1 - y_0$ ,  $z_1 - z_0$  are the coordinates of the vector  $\vec{AB} = [x_1 - x_0, y_1 - y_0, z_1 - z_0]$ .

```
Command: DIST
Specify first point:
Specify second point or [Multiple points]:
Distance = 7.7303, Angle in XY Plane = 270, Angle from XY Plane = 0
Delta X = 0.0000, Delta Y = -7.7303, Delta Z = 0.0000
```

(a) DIST  $O''A''$

```
Command: DIST
Specify first point:
Specify second point or [Multiple points]:
Distance = 8.8500, Angle in XY Plane = 28, Angle from XY Plane = 0
Delta X = 7.7977, Delta Y = 4.1855, Delta Z = 0.0000
```

(b) DIST  $O'B' \rightarrow B = (7.7977; 4.1855; 22.0000 - 7.7303) \rightarrow B = (7.7977; 4.1855; 14.2697)$

```
Command: DIST
Specify first point:
Specify second point or [Multiple points]:
Distance = 5.6250, Angle in XY Plane = 270, Angle from XY Plane = 0
Delta X = 0.0000, Delta Y = -5.6250, Delta Z = 0.0000
```

(c) DIST  $O'A' \rightarrow A = (-5.6250; 0.0000; -7.7303)$

Figure 3.16: Measuring distances resulting in the determination of coordinates of points  $A$ ,  $B$ ,  $P$ ,  $Q$ , by E. Koźniewski

Figure 3.15 shows the rectangular projections of three circles defining the hyperboloid. Assuming the center of the  $OXY$  coordinate system at point  $O$  (Fig. 3.15), the  $OY$  parallel to projection axes (Fig. 3.15), axis  $OX$  vertically down the horizontal projection, axis  $OZ$  vertically

(parallel to the vertical viewport), we determine the coordinates of point  $A, B$ . The coordinates are read out using the DIST command (Fig. 3.16).

Thus  $\overrightarrow{AB}$  has coordinates:

$$\overrightarrow{AB} = [7.7977 - 5.6250; 4.1855 - 0.0000; 14.2697 - (-7.7303)],$$

which means  $\overrightarrow{AB} = [13.4227; 4.1855; 22.0000]$ . Thus, the parametric equation of the line  $l(AB)$  is as follows

$$\begin{cases} x = -5.6250 + 13.4227t \\ y = 0.0000 + 4.1855t \\ z = -7.7303 + 22.0000t \end{cases} \quad t \in R. \quad (3.21)$$

Continuing according to the scheme (3.11)  $\rightarrow$  (3.12)  $\rightarrow$  (3.13).

We take the  $OXYZ$  coordinate system so that the circle of constriction of the hyperboloid lies in the  $OXY$  plane. Treating the vertical projection as the plane in which we define the  $OXY$  coordinate system, we take  $P'' = P$  i  $Q'' = Q$ :  $P = (3.5; 0)$ ,  $Q = (8.8500; 14.2697)$ . Then we can write the equation of the hyperbola

$$\frac{x^2}{a^2} - \frac{y^2}{b^2} = 1, \quad (3.22)$$

where  $a = 3.5$ ,  $b$ , on the other hand, is determined from the formula (3.2). Thus, after substituting in (3.2) the coordinates of the point  $Q$ ,

we get the following  $b = |14.2697| \cdot \left( \sqrt{\frac{8.8500^2}{3.5^2} - 1} \right)^{-1}$ .

### 3.4. Problems

1. Determine the equation of the surface area resulting from the rotation of the line  $OZ$  around the axis  $OZ$ . What surface area will be obtained?

**Hint.** Check whether the line is parallel, skew, or intersects the  $OZ$  axis.

2. Determine the equation of the surface area formed from the rotation of the straight line  $k$  around the axis  $OZ$ . What surface area will be obtained?

a)  $k : [x, y, z] = [1, 2, 3] + t[0, 0, 2], \quad t \in R;$

b)  $k : [x, y, z] = [1, 2, 3] + t[0, 1, 2], \quad t \in R;$

- c)  $k : [x, y, z] = [1, 2, 3] + t[-4, 0, 2], \quad t \in R;$   
 d)  $k : [x, y, z] = [-1, 2, 3] + t[0, 0, -2], \quad t \in R;$   
 e)  $k : [x, y, z] = [1, 2, 3] + t[-2, 1, 3], \quad t \in R.$
3. Show that the intersection of the hyperboloid  $\frac{x^2}{a^2} + \frac{y^2}{b^2} - \frac{z^2}{c^2} = 1$  with the planes  $x = k$  and  $y = k$  yields a hyperbola or two intersecting lines.
  4. Write the equations of the straight lines for selected  $p$  and  $q$  for the hyperboloid - cooling tower model.
  5. Describe the cross sections of a parabolic hyperboloid with the planes  $OXZ, OYZ, OXY$ .
  6. Treating a sphere of radius  $a$  as a solid formed by the rotation of a circle (or rather, a semicircle) of radius  $a$ , derive (using the appropriate integral) the formula for the volume and area of the sphere.
  7. Reasoning similarly to the previous task, check the formula for the volume of a cone of dimension  $a, h$ .
  8. A tank in the shape of a rotating paraboloid (the surface obtained by rotating a parabola) with a height of 8 m and a radius of 4 m (Fig. 3.17) is filled with liquid to a height of 3.5 m. What is the volume of liquid that is in the tank?

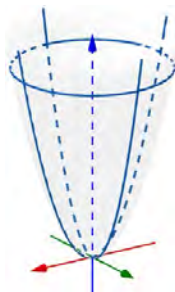


Figure 3.17: Task 8,  
by A. Tereszkievicz

9. Write the equation of the rotating hyperboloid formed by rotating the line  $\{y = a, z = c_1x\}$  around the  $OZ$  axis. In the resulting equation, assume  $c := ac_1$ .
10. Write the equation of the torus formed by rotating the circle  $(x - R)^2 + z^2 = r^2$  ( $r \leq R$ ) around the  $OZ$  axis.
11. Calculate the volume of the ellipsoid formed from the rotation of the ellipsoid around the  $OX, OY$  axis [43].
12. Calculate the volume of the open/closed container formed from the rotation of the function  $f(x) = e^x$  for  $x \in [0, 2]$  around the  $OY$  axis.
13. Calculate the volume of the open/closed container formed from the rotation of the function  $f(x) = 1 - e^{-2x}$  around the  $OY$  and  $OX$  axes.
14. Calculate the vacuum volume in a two-shell fuel tank with a height of 2 m. The cross-section of the outer and inner shells are described by the following functions:  $f(x) = \frac{1}{2}x^2$  and  $f(x) = x^2 + 1$ .





## Chapter 4

# Cubature

### 4.1. Cubature Ochota Railway Station Warszawa Ochota in Warsaw

#### Problem 4.1.

1. Calculate the *cubature* of the object with a covering in the form of a saddle surface. The station building is built on a square plan with a side:  $a = 17.25$  m; at two vertices it has a height of  $h_{1,3} = 8.34$  m; the other tops are at a height of  $h_{2,4} = 0.00$  m.
2. Calculate the amount of thermal insulation material to insulate the roof if the layer height is equal to  $q = 35$  cm.



Figure 4.1: Warszawa Ochota railway station in Warsaw, designed by Arseniusz Romanowicz, Piotr Szymaniak, realization 1960 – 1962, [17] photo by M. Czechowicz

**Hint.** The canonical equation of the saddle surface is of the form  $z = kxy + p$ , where  $k$  and  $p$  are parameters to be determined from the data. Assume that the points  $(\frac{a}{2}, \frac{a}{2}, h)$ ,  $(-\frac{a}{2}, \frac{a}{2}, 0)$  belong to the surface.

## 4.2. The construction of the saddle surface panel as a ruled surface

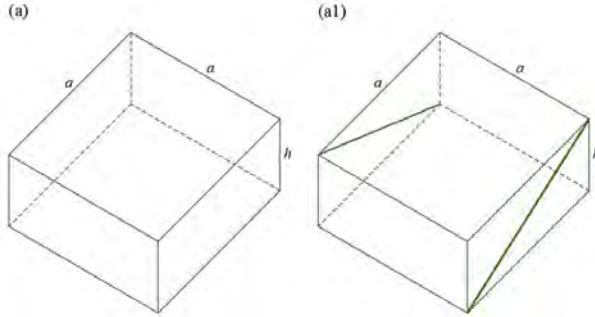


Figure 4.2: (a) We choose a cuboid with a square base of side length  $a$  and height  $h$ ; (a1) we construct the diagonals of opposite lateral faces, which are mutually skew (green), and serve as the basis for creating the ruled surface (AutoCAD), by E. Koźniewski

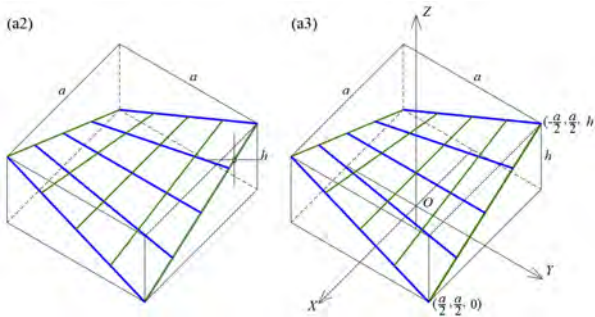


Figure 4.3: (a2) we connect the points of these diagonals with segments parallel to the other side walls (in practical implementation, we divide the diagonals into the same number of equal segments and connect the points obtained in this way with each other - blue segments). We obtain the generatrices, all of which are skew to each other (in blue), and two of them are diagonals of the remaining lateral faces. These two diagonals can be the basis for constructing the second family of generatrices (green); a3) in order to move from geometric to analytical characterization, we introduce the coordinate system  $OXYZ$  for the form of the canonical equation of the saddle surface (AutoCAD), by E. Koźniewski

Using the figure 4.3a3, we can write down the equation of the saddle surface  $z = kxy + p$ . After substituting the coordinates of the points  $(\frac{a}{2}, \frac{a}{2}, 0)$ ,  $(-\frac{a}{2}, \frac{a}{2}, h)$  we get  $k = -\frac{2h}{a^2}$ ,  $p = \frac{h}{2}$ . Thus, we have the surface equation

$$z = -\frac{2h}{a^2}xy + \frac{h}{2}. \quad (4.1)$$

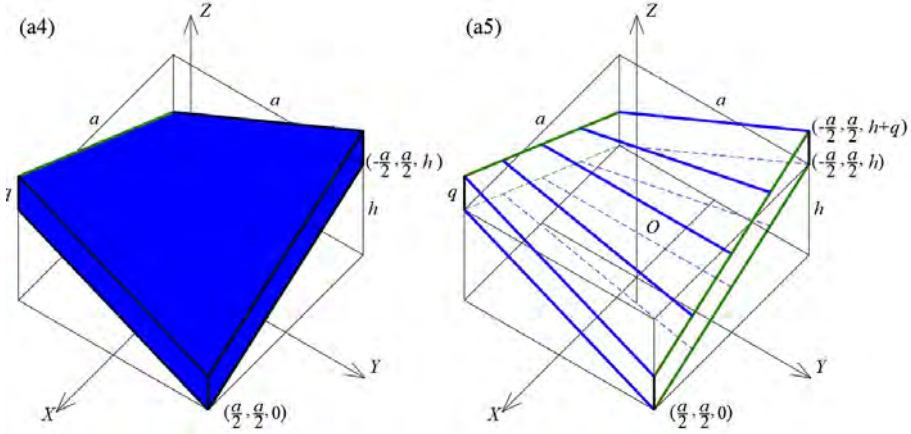


Figure 4.4: (a4) in order to obtain the roofing model, we give thickness by shifting the created surface by the vector  $[0, 0, q]$ ; (a5) the original skeleton form of the roofing model (AutoCAD), by E. Koźniewski

We give the thickness of the surface (4.1), by shifting this surface by vector  $[0, 0, q]$ , and we get the layer

$$\left( z = -\frac{2h}{a^2}xy + \frac{h}{2}, z = -\frac{2h}{a^2}xy + \frac{h}{2} + q \right) \quad (4.2)$$

as a set of

$$\left\{ (x, y, z) : -\frac{a}{2} \leq x \leq \frac{a}{2}, -\frac{a}{2} \leq y \leq \frac{a}{2}, \right. \\ \left. -\frac{2h}{a^2}xy + \frac{h}{2} \leq z \leq -\frac{2h}{a^2}xy + \frac{h}{2} + q \right\}. \quad (4.3)$$

We will now calculate the cubic volume of the object. For this, we will use the concept of the double integral of the function  $f(x, y) = -\frac{2h}{a^2}xy + \frac{h}{2}$  in square  $K = \{(x, y) : -\frac{a}{2} \leq x \leq \frac{a}{2}, -\frac{a}{2} \leq y \leq \frac{a}{2}\}$ . So

$$V = \iint_K \left( -\frac{2h}{a^2}xy + \frac{h}{2} \right) dx dy. \quad (4.4)$$

Let's calculate this integral

$$\begin{aligned}
 V &= \int_{-\frac{a}{2}}^{\frac{a}{2}} \left( \int_{-\frac{a}{2}}^{\frac{a}{2}} \left( -\frac{2h}{a^2}xy + \frac{h}{2} \right) dy \right) dx = \int_{-\frac{a}{2}}^{\frac{a}{2}} \left( -\frac{2hy^2}{2a^2}x + \frac{h}{2}y \Big|_{-\frac{a}{2}}^{\frac{a}{2}} \right) dx = \\
 &= \int_{-\frac{a}{2}}^{\frac{a}{2}} \frac{ah}{2} dx = \frac{ah}{2} x \Big|_{-\frac{a}{2}}^{\frac{a}{2}} = \frac{a^2h}{2}.
 \end{aligned}$$

Note that the cubature of the object is equal to half the volume of the cuboid on the basis of which the solid was created. Anyway, a careful analysis of the drawing of the (4.3) shows this result; because the created surface "divides" the cuboid into two congruent parts.

Now let's calculate the cubature of a saddle-shaped roofed surface of height  $h$ . Let us note that it is enough to subtract the solid part without the covering from the volume of the object containing the covering, i.e.

$$\begin{aligned}
 V_q - V &= \iint_K \left( -\frac{2h}{a^2}xy + \frac{h}{2} + q \right) dx dy - \iint_K \left( -\frac{2h}{a^2}xy + \frac{h}{2} \right) dx dy = \\
 &= \iint_K \left( -\frac{2h}{a^2}xy + \frac{h}{2} + q - \left( -\frac{2h}{a^2}xy + \frac{h}{2} \right) \right) dx dy = \iint_K q dx dy = \\
 &= q \iint_K dx dy = qa^2.
 \end{aligned}$$

The last equality (without calculating the integral) results directly from the geometric interpretation of the double integral because it is known that  $\iint_D dx dy = |D|$ ,  $|D|$  – area of the region  $D$ .

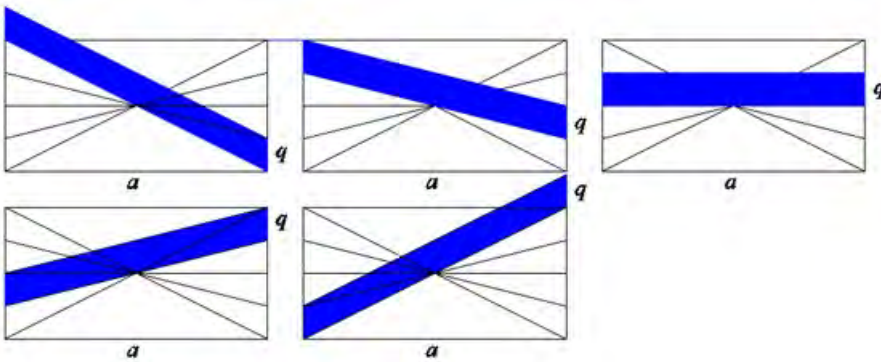


Figure 4.5: Illustration of cross-sections, a model of a roof covering with a thickness of  $q$ , parallel to the planes of the walls (planes of the base cuboid) of the object; these are parallelograms with the same area  $aq$  – it can be assumed that these are cuboid sections with a square base  $a \times a$  and height  $q$ , which can be considered a flat roof model (AutoCAD), by E. Koźniewski

### 4.3. Cavalieri's Theorem

Note that the cubature of the insulation layer of the covering is equal to that of a flat roof with the same layer thickness. This result is unexpected, but mathematically not surprising. That is because the *Cavalieri theorem* is known:

**Theorem 4.1.** If two solids have the property that their cross-sections with all planes parallel to one predetermined plane have the same area, then these solids have equal volumes.

### 4.4. Slice-based transformations

This observation allows us to notice another property of architectural objects, which is a consequence of the properties of the family of *slice-based transformations*. *Twist* and *shear* belong to such a class of transformations.

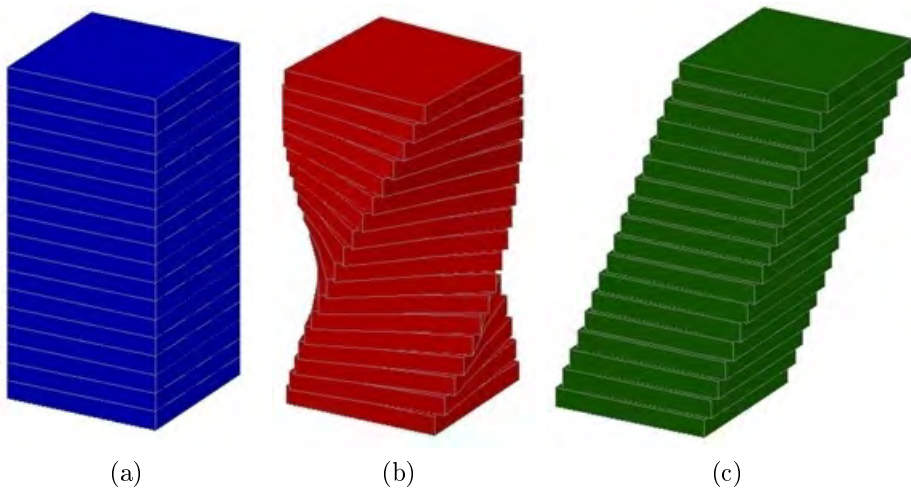


Figure 4.6: Illustration of the family of slice-based transformations: (a) existing perpendicular, (b) twist, (c) shear (AutoCAD), by E. Koźniewski based on [51]

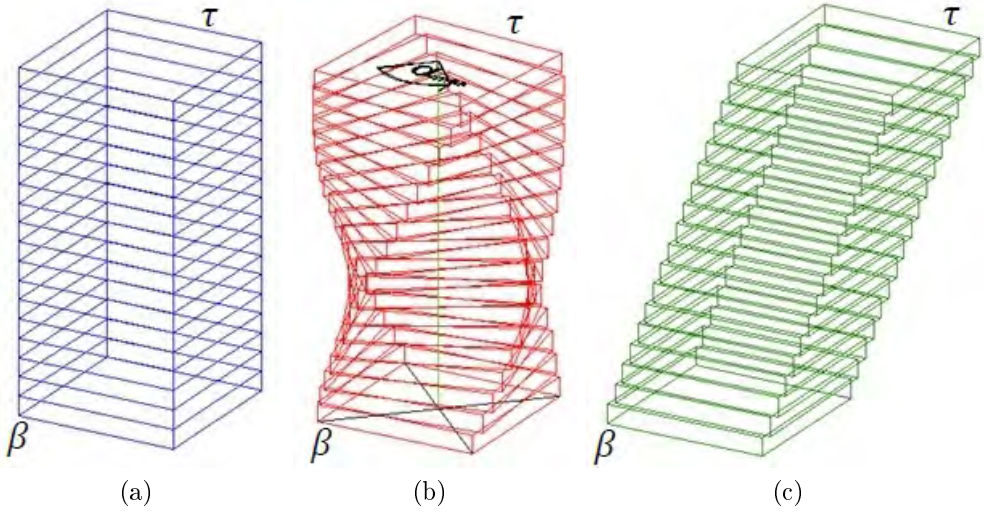


Figure 4.7: Illustration of slice-based transformations: twist (maximum angle  $\alpha_{\max}$ ), shear (AutoCAD), by E. Koźniewski based on [51]

To define the *twist* transformation, we choose any ground plane  $\beta$ , and the top plane  $\tau$  parallel to  $\beta$  distant by  $h$  (the twisted object has height  $h$  and is located between the planes  $\beta$  and  $\gamma$ ) and straight line  $l$  (called *twist axis*) perpendicular to the plane  $\beta$  (Fig. 4.6b, 4.7b). Object layers that lie in planes perpendicular to the axis of rotation (i.e. parallel to  $\beta$ ) rotate at an angle  $\alpha(z)$  around  $l$  in the manner (4.5)

$$\alpha(z) = \frac{z}{h} \alpha_{\max}. \quad (4.5)$$

The plane of the base  $\beta$  remains constant and the plane  $\tau$  rotates by the angle  $\alpha_{\max}$  predetermined. Points lying off-axis transform in a spiral manner. Any line parallel to the  $l$ -axis transforms into a helical line (Fig. 4.8). An important property of this transformation is that the volume of the object is preserved.



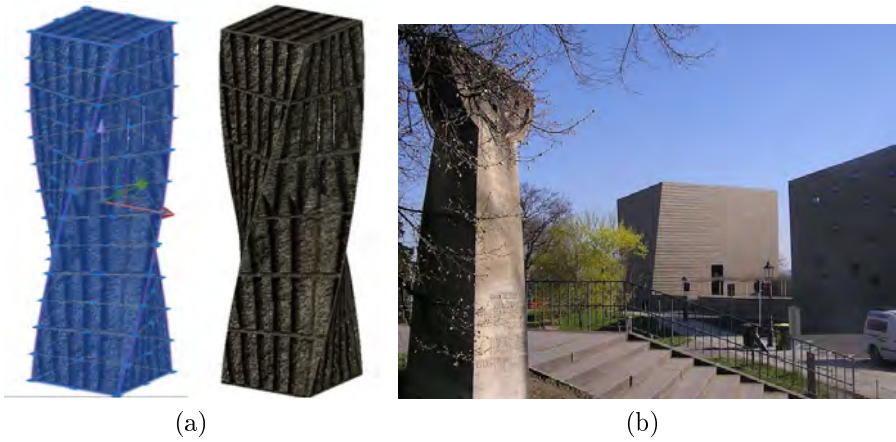


Figure 4.8: (a) Cuboid twist, vertical edges as helix lines (AutoCAD models), by E. Koźniewski based on [51]; (b) Dresden synagogue (2001, architects Rena Wandel-Hoefer and Wolfgang Lorch) – an example of the use of twist transformation in architecture [18]



Figure 4.9: Turning Torso in Malmö, Sweden (2005, architect Santiago Calatrava) – another example of the application of the twist transformation in modern architecture [19]



Another example of a section slice-based transformation is *shear*. This is an affine transformation, which is written in the form

$$\begin{cases} x' = x + a \cdot z \\ y' = y + b \cdot z \\ z' = z \end{cases}, \quad (4.6)$$

where  $a, b$  denote constant parameters.

As you can see, this is a shift by a vector that depends on the height ( $z$ ) of the object. This transformation also preserves the volume of the object (Fig. 4.6c i 4.7c). There are well-known architectural realizations of the transformation *shear* (Fig. 4.10).



Figure 4.10: "Puerta de Europa" in Madrid – An example of the use of the shear transformation in modern architecture, photo by D. Gawryluk

And finally, phenomenal examples of the use of transformation through cross-sections, present especially in Baroque architecture - a *twisted pillar*.

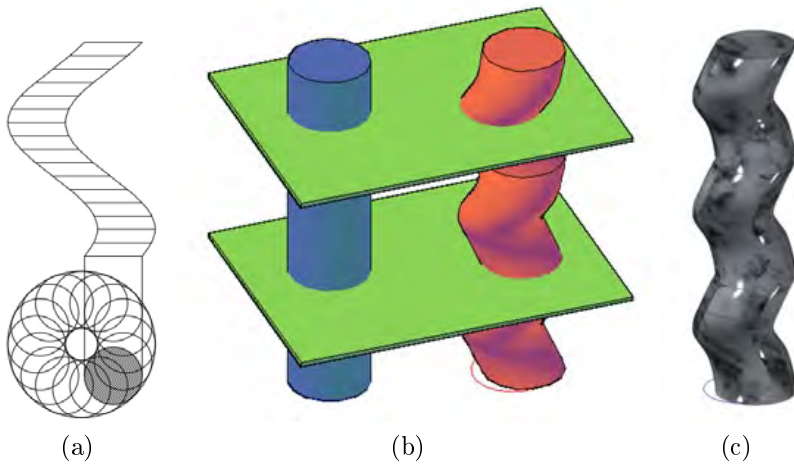


Figure 4.11: (a) sketch views of creating a spiral column ; (b) the volume of the spiraled column is the same as the cylinder - Cavalieri theorem (model realized in AutoCAD environment); (c) the model from the middle figure after rendering, by E. Koźniewski

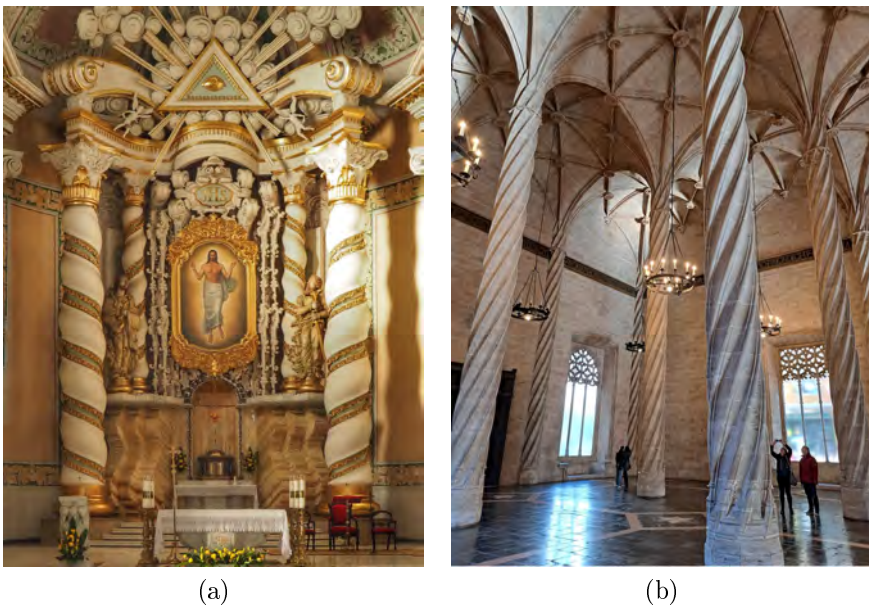


Figure 4.12: (a) the spiral columns in the Church of the Resurrection in Białystok, by M. Koźniewski; (b) twisted columns of a hall in the Valencia silk exchange (Spain), photo by D. Gawryluk



Figure 4.13: Contemporary ideas in single-family housing, left [20], right [21]

## 4.5. Problems

1. a) Show analytically that on the saddle surface (hyperbolic paraboloid)  $z = -\frac{2h}{a^2}xy$  (for  $a = 17.25$  m,  $h = 8.34$  m);  $z = -\frac{2 \cdot 8.34}{17.25^2}xy$ , i.e.,  $z = -0.0561xy$  lie two families of lines, as can be seen in Fig. 4.3 a2) – a3).
- b) Show that the lines of one family (let's call it  $ROXZ$ ) are parallel to the  $OXZ$  plane and are mutually skewed, the lines of the other family (let's call it  $ROYZ$ ) are parallel to  $OYZ$  and are mutually skewed.
- c) Show that the straight lines of the  $ROXZ$  and  $ROYZ$  families intersect each other. Determine the coordinates of the intersection of this point.
- d) To which plane of the system  $OXYZ$  is the plane  $y = \alpha$  parallel?
- e) Another form of saddle surface can be written in the form:  $z = \frac{x^2}{a^2} - \frac{y^2}{b^2}$ . Analogously, as above describe with lines.
- f) Calculate the cubature of the building with a saddle surface covering. The station building is built on the plan of a square with side  $a = 17.25$  m; it has a height of  $h_{1,3} = 8.34$  m at two vertices; the other vertices are at height  $h_{2,4} = 0.00$  m.

- g) Calculate the amount of thermal insulation material to insulate the roof, if the height of the layer is  $q = 35$  cm.

**Hint.** The saddle surface can be written in the simplest form  $z = kxy$  ( $k \neq 0$ ). This equation can be written in the equivalent manner

$$z = kxy \Leftrightarrow z = \alpha x \text{ i } \alpha = y.$$

Multiplying the last two equations by sides, and they are simple equations, we get equation one. But the system of  $z = \alpha x$  and  $\alpha = y$  represents a family of lines. What form does the second family take? To which plane of the system  $OXYZ$  is the plane  $y = \alpha$  parallel? A more complicated, but also simple, form of the saddle surface is  $\frac{x^2}{a^2} - \frac{y^2}{b^2} = z \Leftrightarrow \left(\frac{x}{a} - \frac{y}{b}\right) \left(\frac{x}{a} + \frac{y}{b}\right) = z$ .

- Consider a 2.96 m high twisted column with a base of a square with a side of about 370 mm, made of clinker bricks of  $250 \times 120 \times 65$  mm (assume a joint thickness of 15 mm). How many bricks were used? What should be the  $\alpha(z)$ , so that the effect is like the one in the photo 4.13?
- With the angle  $\alpha(z) = 2^\circ$  calculate the angle of twist of the column from the previous task.
- What should be  $\alpha(z)$  so that  $\alpha_{\max}$  is  $90^\circ$ ? (parameters of clinker brick  $250 \times 120 \times 65$  mm, assuming joint thickness 15 mm, , column height 2.88 m).
- What height of the column will be obtained if you build it with clinker bricks of  $250 \times 120 \times 65$  mm and a joint thickness of 15 mm with a base as shown in the figure 4.14, for  $\alpha_{\max} = 45^\circ$  ( $90^\circ$ ,  $180^\circ$ ) and  $\alpha(z) = 3^\circ$  ( $1^\circ$ ,  $2^\circ$ )? How many clinker bricks will be used?

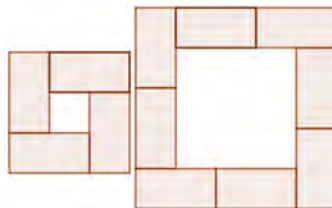


Figure 4.14: task 5, prep. A. Tereszkievich

- Describe the parameters of a twisted column from a selected implementation in architecture.

7. Describe the transformation (4.6) for the Puerta de Europa (Fig. 4.10).
8. Describe the transformation (4.5) for the Turning Torso (Fig. 4.9).
9. Identify other architectural structures that use similar geometric solutions.
10. Using the notation of the equation of the saddle surface in task 1e, describe the equations of the cross-section model of a building with a rectangular projection  $a \times b$  and height  $h$ . Perform the calculations from the tasks 1f, 1g assuming that  $a = 16$  m,  $b = 12$  m,  $h = 8$  m,  $q = 0.35$  m.

## Chapter 5

# Curves and offset surfaces in civil engineering

**Problem 5.1.** Make a study of the roadway width distribution in a roundabout designed using an ellipsoidal shape (Fig. 5.1).

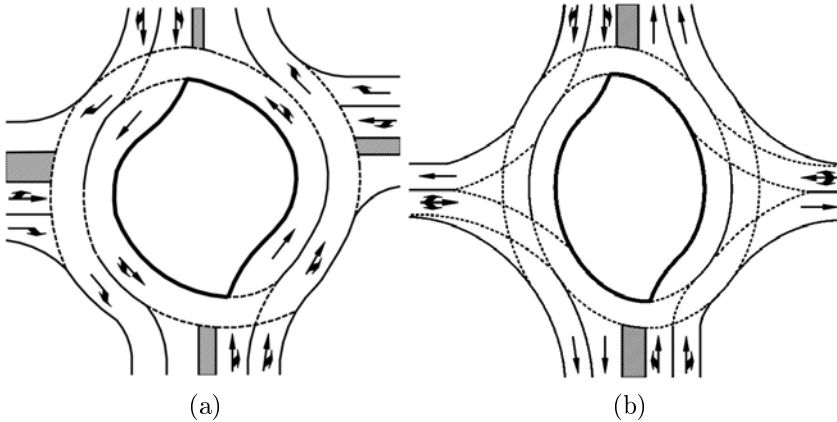


Figure 5.1: Sketch of a turbine roundabout shaped using: (a) two half-circles, by E. Koźniewski based on [9]; (b) ellipse, by E. Koźniewski based on [9]

When designing a road lane, for example, where the edge is an arc of a circle or a rectilinear segment, determining the width of the roadway is fairly straightforward. It is more difficult to determine the width of the road when there is an arbitrary curve. Then we have to deal with a more complicated process of constructing two distant edges. This will be the case when determining the edge of a turbine roundabout shaped with an ellipse [9]. The need to determine the second edge of the roadway leads to the introduction of the concept of an offset curve.

## 5.1. Offset curves

### 5.1.1. Definition of the offset curve

For any smooth curve  $c$ , we define *offset (parallel copy) curve*  $c_d = c'_d \cup c''_d$  at a distance  $d$  (shorter *offset*) as follows: on each normal to the curve  $c$  we choose two points at a distance  $d$  from the curve  $c$  ([51], p. 335). We obtain two families of  $c'_d, c''_d$  points (Fig. 5.2a), which will form the *offset*  $c_d$ , individual while we will call the  $c'_d, c''_d$  curves half-offsets.

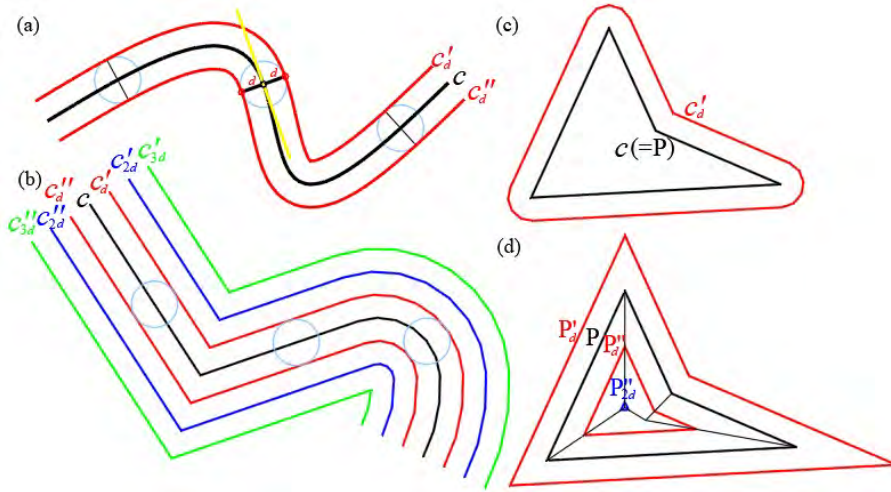


Figure 5.2: Offsets: (a) spline curve; (b) polyline; (c) polygon half-offset (obtained using AutoCAD with the constant *Offsetgapttype* = 1); (d) discrete polygon half-offset (obtained using AutoCAD with the constant *Offsetgapttype* = 0), by E. Koźniewski

AutoCAD allows multiple possibilities for creating offsets of a plane polygon. The system variable *Offsetgapttype* is responsible for this. For a  $P$  polygon, at a value of 0 of this variable, the line segments are extended and the polygon  $P_d$  is still a polygon (Fig. 5.2d), at a value of 1 the copy is rounded (Fig. 5.2c), in the case of a value of 2 the copy remains a polygon, but has beveled corners. In the first case,  $P_d$  is again a polygon and we call it the discrete offset of polygon  $P$ . In the figure 5.2d we have the discrete half-offsets of  $P'_d, P''_d, P'''_d$ . Note that the offset curve of a straight line is a straight line (more precisely: a pair of straights), while that of a circle is a circle (more precisely: a pair of circles). In contrast, the offset curve of an ellipse is no longer an ellipse (Fig. 5.3). When using ellipses to design turbine roundabouts, in order to accurately maintain a



constant road (roadway) width, the edges of the traffic circle cannot be ellipses at the same time (cf. [3, 9]).

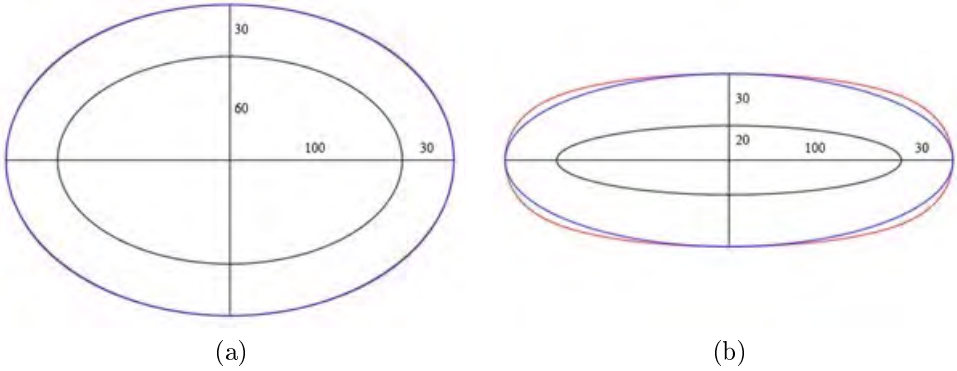


Figure 5.3: Offset  $e'_d$  ellipses  $e(a, b)$  with half-axes  $a, b$  and ellipse with half-axes  $a + d, b + d$ : (a)  $a = 100, b = 60, d = 30$ ; (b)  $a = 100, b = 20, d = 30$ . The difference between the offset  $e'_d$  of the ellipse  $e(a, b)$  and the ellipse  $e(a + d, b + d)$  is the greater the smaller the ratio  $b/a$ ; in the case of (a)  $b/a = 3/5$  visually the curves coincide, in the case of (b)  $b/a = 1/5$  there is a clear difference between the curves (offset  $e'_d$  of the ellipse with half-axes  $a, b$  [red] and the ellipse with half-axes  $a + d, b + d$  [blue], by E. Koźniewski

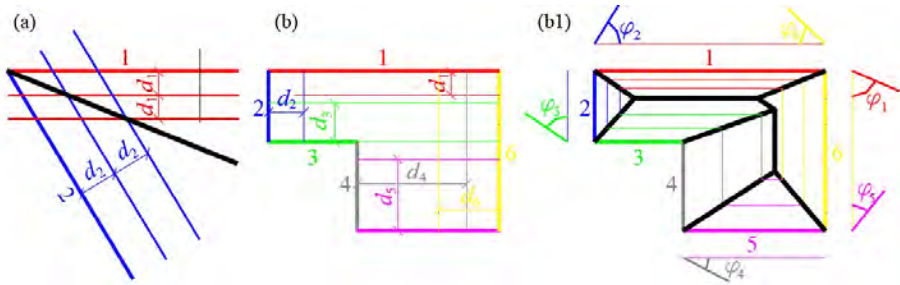


Figure 5.4: Generalized discrete offsets: (a) angle with parameters  $d_1, d_2$ ; (b) given distances  $d_1, d_2, d_3, d_4, d_5, d_6$  for the discrete offsets of the polygon; (b1) sequence of half-offsets of the discrete polygon  $(1, d_1; 2, d_2; 3, d_3; 4, d_4; 5, d_5; 6, d_6)$  ([3, 9, 34], by E. Koźniewski)

Just as for a polygon, we can construct a discrete offset for an angle, and here we come to the so-called  $(d_1, d_2)$ -secant (Fig. 5.4a). For a given  $n$ -angled polygon  $P_n$  and a sequence of positive real numbers  $d_1, d_2, \dots, d_n$  we can construct the skeleton of a roof [31, 34] spanning



over polygon  $P_n$ . Such a construction allows us to design roofs with variable slopes (Fig. 5.2 – 5.6). The equality  $d_i \operatorname{tg} \varphi_i = d_j \operatorname{tg} \varphi_j$  for any  $i, j = 1, 2, \dots, n$ .

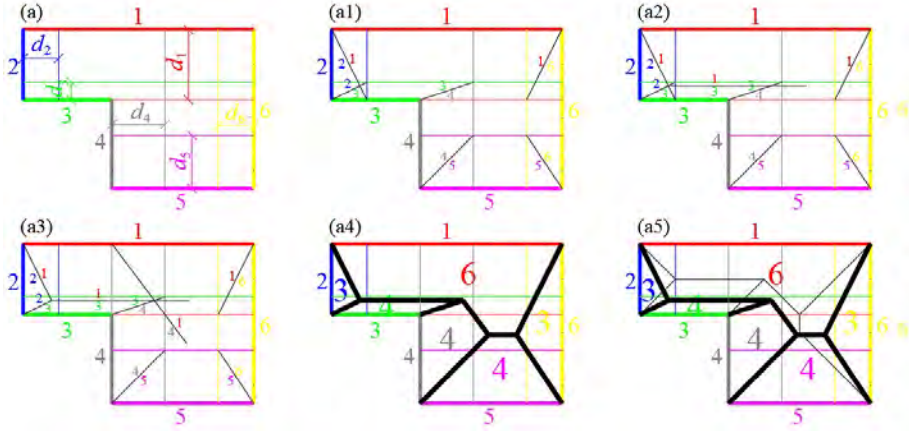


Figure 5.5: The structure of the roof skeleton generated by the hexagon  $(1, d_1; 2, d_2; 3, d_3; 4, d_4; 5, d_5; 6, d_6)$ , (cf. [33]), by E. Koźniewski

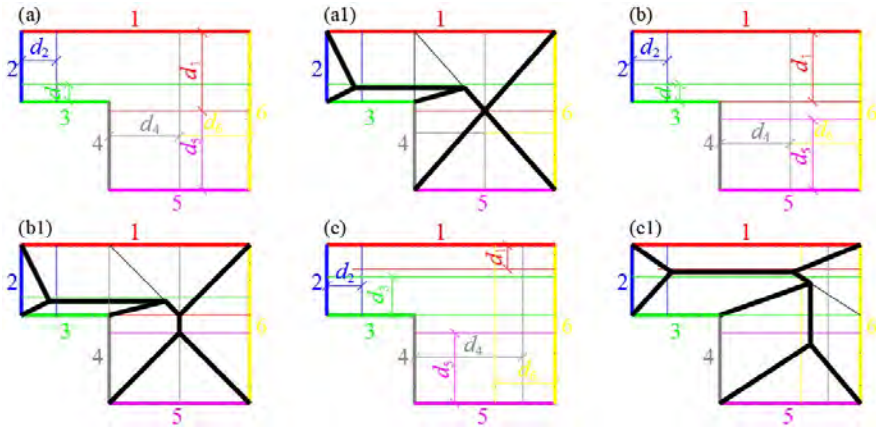


Figure 5.6: Topological types of roofs with a variable slope over the same hexagon  $(1, d_1; 2, d_2; 3, d_3; 4, d_4; 5, d_5; 6, d_6)$  (cf. [33]), by E. Koźniewski

It turns out that over any polygon it is possible to obtain all types of topological skeletons of roofs depending on a sequence of positive numbers  $d_1, d_2, \dots, d_n$  (Fig. 5.6). A shape similar to a roof over a polygon is assumed by an embankment formed as a result of the natural

arrangement (spreading) of the soil. As is well known, as a result of free-flowing soil, a cone is formed with an angle of natural repose [38]. Hence, when describing earthworks, the shape of contour lines, or offset curves, will be rounded. Using the principle of rounded lines (the variable *Offsetgap* type takes the value 1), we can geometrically describe and then calculate the size of the earthwork soil masses (cf. [33]). In the figures 5.7 – 5.10 The intersection line between the horizontal construction site at the 120 m ordinate and the 120-level will be the boundary line between the excavation and embankment areas (Fig. 5.7). The intersections of the 120-meter contour with the edges of the construction site mark the boundary points of the change from excavation to embankment. The demarcated points divide the construction site polygon into two parts (Fig. 5.7). On the left side of the area (Fig. 5.8, the "bottom" part of the polygon), the contours are arranged at a distance of 1 m to get a slope of 1. On the right side of the area (Fig. 5.9, the "top" part of the polygon), the contours are spaced at  $1\frac{1}{2}$  m, to get a ratio of  $1\frac{1}{2}$  to 1, that is, a slope of  $1\frac{1}{2}$ .

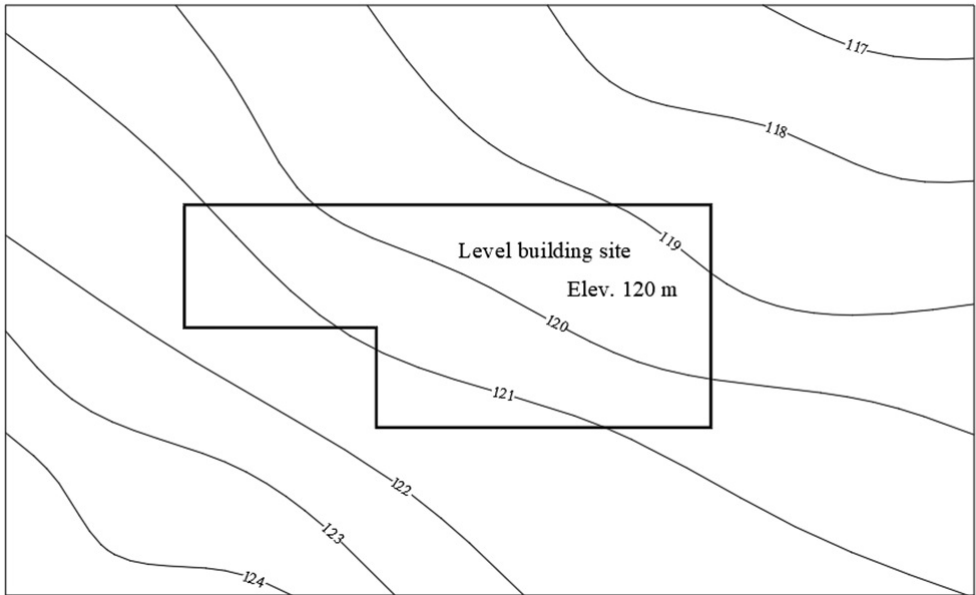


Figure 5.7: The intersections of the 120 m contour with the edges of the construction site will determine the change points from the excavation to the embankment (cf. [33])

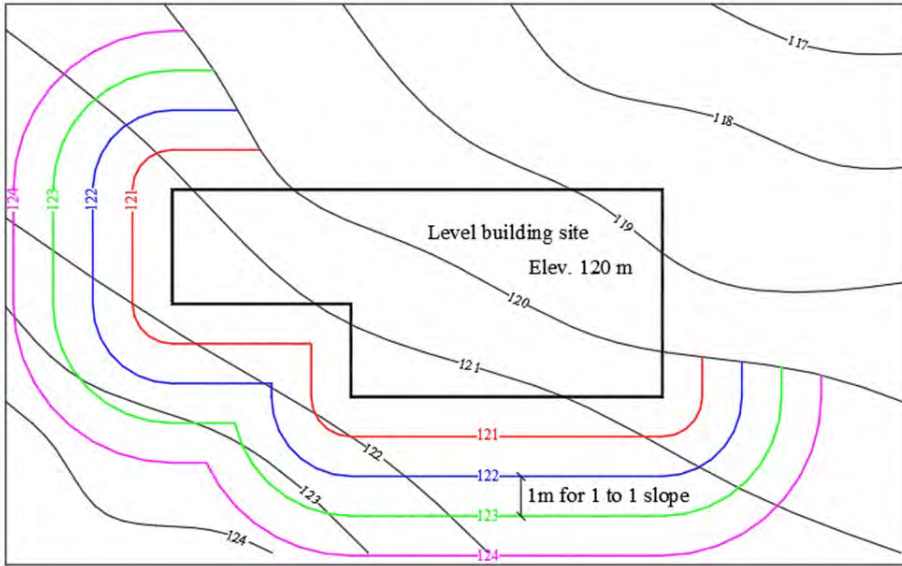


Figure 5.8: To the left and at the bottom of the area, the proposed contours of the contour lines (for the excavation) at a distance of  $d = 1$  m, to make the slope equal to 1 (cf. [33])

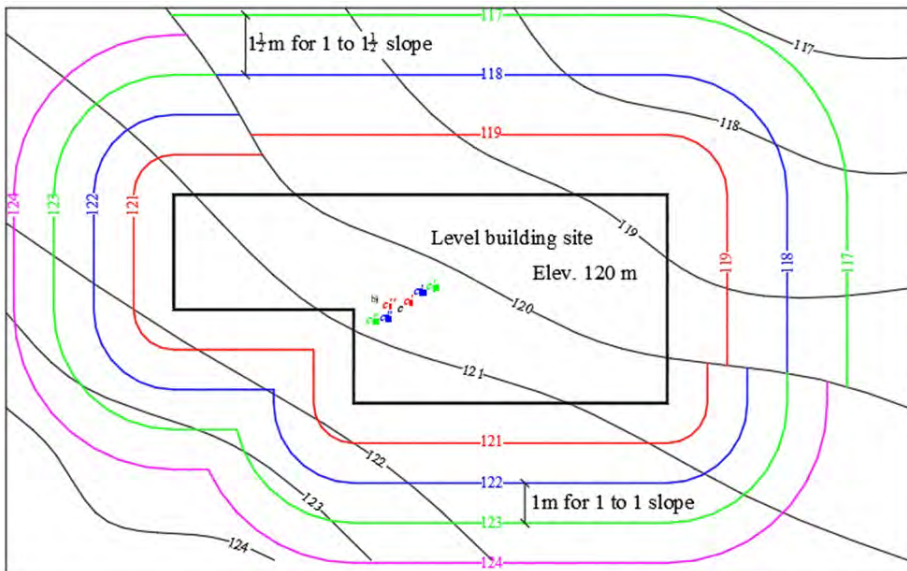


Figure 5.9: To the right and at the top of the area, the proposed contours of the layered areas (for the embankment) at intervals  $d = 1\frac{1}{2}$  m, to get a slope in the ratio of  $1\frac{1}{2}$  to 1 (cf. [33])

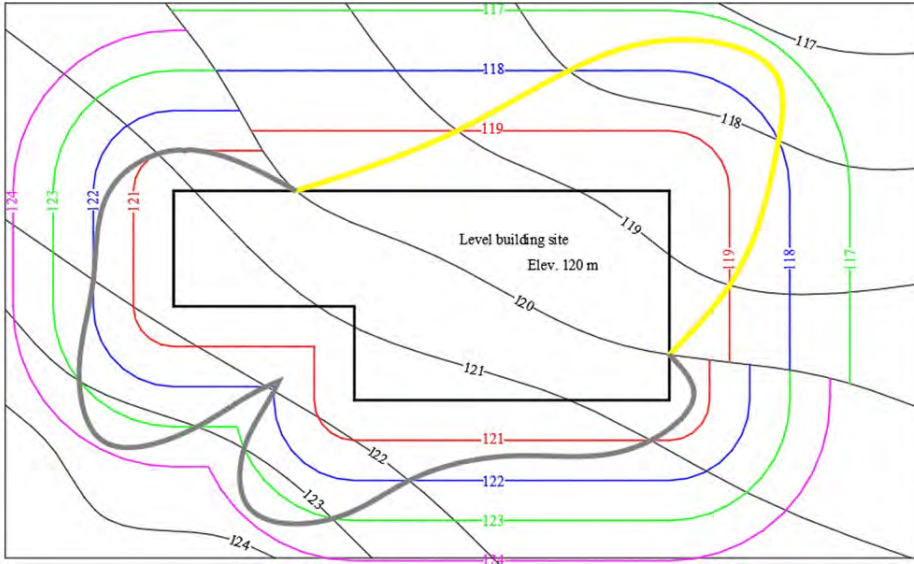


Figure 5.10: Edge of embankment and excavation line (cf. [33])

### 5.1.2. Analytical form of the offset curve

Consider a curve  $c : \begin{cases} x = x(t) \\ y = y(t) \end{cases}$  of class  $C^1$ ,  $t \in [\alpha, \beta]$ . At any point, let's find the tangent vector  $[x'(t), y'(t)]$ , then the normal  $\pm[y'(t), -x'(t)]$ . The versor normal (normal vector of length 1) takes the form  $\frac{[y'(t), -x'(t)]}{\sqrt{x'^2(t) + y'^2(t)}}$ . Then the equations of the offset curves  $c'_{off}(d)$ ,  $c''_{off}(d)$  of the  $c$  curve are of the form

$$c'_{off}(d) : \begin{cases} X = x(t) + \frac{y'(t)d}{\sqrt{x'^2(t) + y'^2(t)}} \\ Y = y(t) + \frac{-x'(t)d}{\sqrt{x'^2(t) + y'^2(t)}} \end{cases}, \quad c''_{off}(d) : \begin{cases} X = x(t) + \frac{-y'(t)d}{\sqrt{x'^2(t) + y'^2(t)}} \\ Y = y(t) + \frac{x'(t)d}{\sqrt{x'^2(t) + y'^2(t)}} \end{cases},$$

where  $t \in [\alpha, \beta]$ .

**Example 5.1.** Write down the equations of offset curves for hyperbolas

$$\frac{x^2}{a^2} - \frac{y^2}{b^2} = 1$$

with parameterization of hyperbolic functions (hyperbolic cosine:  $\cosh(x) = \frac{e^x + e^{-x}}{2}$ , hyperbolic sine:  $\sinh(x) = \frac{e^x - e^{-x}}{2}$ , in particular, the “hyperbolic identity” is true:  $\cosh^2(x) - \sinh^2(x) = 1$ ). The parameterization can be as follows:  $x = a \cosh(t)$ ,  $y = b \sinh(t)$ . Then the parametric

equations of the offset curves  $c'_{off}(d), c''_{off}(d)$  of the hyperbola  $\frac{x^2}{a^2} - \frac{y^2}{b^2} = 1$  are of the form

$$c'_{off}(d) : \begin{cases} X = a \cosh(t) + \frac{b \cosh(t)d}{\sqrt{a^2 \sinh^2(t) + b^2 \cosh^2(t)}} \\ Y = b \sinh(t) - \frac{a \sinh(t)d}{\sqrt{a^2 \sinh^2(t) + b^2 \cosh^2(t)}} \end{cases}, \text{ where } t \in R,$$

$$c''_{off}(d) : \begin{cases} X = a \cosh(t) - \frac{b \cosh(t)d}{\sqrt{a^2 \sinh^2(t) + b^2 \cosh^2(t)}} \\ Y = b \sinh(t) + \frac{a \sinh(t)d}{\sqrt{a^2 \sinh^2(t) + b^2 \cosh^2(t)}} \end{cases}, \text{ where } t \in R.$$

**Example 5.2.** Consider the hyperbola  $\frac{y^2}{26^2} - \frac{x^2}{0.83^2} = 1$  describing the cooling tower from chapter 3. Its parametric form is as follows

$$\begin{cases} x = 60.83 \sinh(t) \\ y = 26.00 \cosh(t) \end{cases},$$

where  $t \in [\operatorname{arsinh}(\frac{-93}{60.83}); \operatorname{arsinh}(\frac{20}{60.83})] = [-1.21066; 0.323132]$ . Visual realization of offset curves can be obtained after implementation in a suitable program (for example Geogebra Fig. 5.11, Matlab).

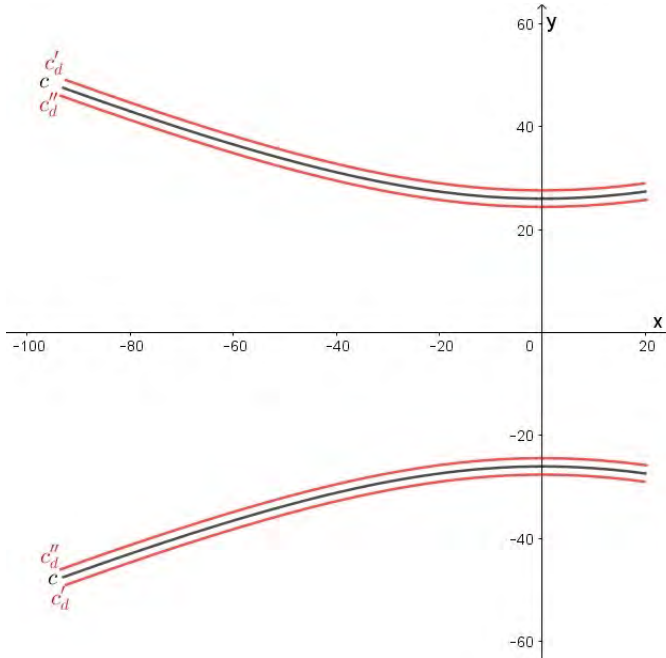


Figure 5.11: Illustration of the example (due to scale, instead of  $d = 0.16$  it was taken as  $d = 1.6$ ), by A. Tereszkieicz

### 5.1.3. About the thickness of the cooling tower in the aspect of offset curves

**Problem 5.2.** Determine the thickness function (distribution) in terms of the offset curve of the cooling tower shell, assuming that the shell wall is bounded by the surfaces formed from the rotation of the curves  $c : y = 26\sqrt{1 + \left(\frac{x}{60.83}\right)^2}$ ,  $x \in [-93.20]$ ;  $c_1 : y = 26\sqrt{1 + \left(\frac{x}{60.83}\right)^2} - 0.16$ ,  $x \in [-93.20]$ . We create an offset curve  $c'_{off}(0.16)$  for the curve  $c$  in the direction of the curve  $c_1$  and compare  $c'_{off}(0.16)$  with the curve  $c_1$ .

**Solution.** (sketch)

First way: The curve  $c$  parametrically given by the formula

$$\begin{cases} x = 60.83 \sinh(t) \\ y = 26.00 \cosh(t) \end{cases},$$

where  $t \in [\operatorname{arsinh}\left(\frac{-93}{60.83}\right); \operatorname{arsinh}\left(\frac{20}{60.83}\right)] = [-1.21066; 0.323132]$ .

For any but a fixed point of the curve  $c$ , that is, for a fixed parameter  $t$ , we find the equations of the perpendicular (normal) line. The normal vector has coordinates  $[26 \sinh(t), -60.83 \cosh(t)]$ , while the equations of the normal line have the form:

$$\begin{cases} x = 60.83 \sinh(t) + 26.00 \sinh(t)u \\ y = 26.00 \cosh(t) - 60.83 \cosh(t)u \end{cases}$$

where  $u \in R$ .

After substituting the  $c_1$  curve into the equation, we get:

$26 \cosh(t) - 60.83 \cosh(t)u = 26\sqrt{1 + \left(\frac{60.83 \sinh(t) + 26 \sinh(t)u}{60.83}\right)^2} - 0.16$ . Thus, solving the quadratic equation, we determine two values of  $u_1$ . From the conditions of the task, it follows that the value of  $u_1$  should be taken positive. We get  $(x_{u_1}, y_{u_1})$ , where

$$\begin{cases} x_{u_1} = 60.83 \sinh(t) + 26 \sinh(t)u_1 \\ y_{u_1} = 26 \cosh(t) - 60.83 \cosh(t)u_1 \end{cases}.$$

The distance of the points  $d(t)$ :

$(60.83 \sinh(t), 26 \cosh(t))$ ;

$(60.83 \sinh(t) + 26 \sinh(t)u_1, 26 \cosh(t) - 60.83 \cosh(t)u_1)$

is the thickness of the shell for the value of the parameter  $t$  and is given by the following formula

$$\begin{aligned} d(t) &= \sqrt{(26 \sinh(t)u_1)^2 + (-60.83 \cosh(t)u_1)^2} = \\ &= |u_1| \sqrt{(26 \sinh(t))^2 + (-60.83 \cosh(t))^2}. \end{aligned}$$

The value  $roz(t) = |0.16 - d(t)|$  is the difference in distance between the points on the curve  $c_1$  and  $c'_{off}(0.16)$ .

Second way: Let  $c : y = f(x)$ , that is,  $f(x) = 26\sqrt{1 + \left(\frac{x}{60.83}\right)^2}$  and  $c_1 : y = f_1(x)$ , where  $f_1(x) = 26\sqrt{1 + \left(\frac{x}{60.83}\right)^2} - 0.16$ . Let  $x = u$ , then the point of the curve has coordinates  $(u, f(u))$ , the tangent at that point has equation:  $t_c : y - f(u) = f'(u)(x - u)$ , normal  $n_c : y - f(u) = \frac{-1}{f'(u)}(x - u)$ . Solving the system of equations

$$\begin{cases} y - f(u) = \frac{-1}{f'(u)}(x - u) \\ y = f_1(x) \end{cases}$$

due to  $x$  and  $y$  we find the point  $(x_u, f_1(x_u))$ , depending on the parameter  $u$ , i.e.  $x_u = x(u)$ . Remembering that  $f(x) = 26\sqrt{1 + \left(\frac{x}{60.83}\right)^2}$  and  $f_1(x) = 26\sqrt{1 + \left(\frac{x}{60.83}\right)^2} - 0.16$ . The distance  $d(u)$  of the points  $(u, f(u))$ ,  $(x_u, f_1(x_u))$  is the thickness of the shell for the value  $x = u$ . Analyzing the function  $d(u)$  (or the function  $\Delta d(u) = d(u) - 0.16$ ), we obtain a description of the variation of cooling tower thickness in the context of the curves  $c, c_1$ .

## 5.2. Offset surfaces

### 5.2.1. Analytical description

Consider the surface

$$P : \begin{cases} x_1 = x(u, v) \\ y_1 = y(u, v) \\ z_1 = z(u, v) \end{cases} \quad (u, v) \in D,$$

where  $D$  is a flat area, and the functions  $x(u, v)$ ,  $y(u, v)$ ,  $z(u, v)$  are of class  $C^1$  (in the case of a rectangle  $D = \{(u, v) : u \in [u_1, u_2], v \in [v_1, v_2]\}$ ).

This surface can also be written in terms of the vector function  $\mathbf{r}(u, v) = [x(u, v), y(u, v), z(u, v)]$ . For a selected point  $(u_0, v_0)$  of the surface  $P$  the partial derivatives of the vector function have the form

$$\mathbf{r}_u(u_0, v_0) = \left[ \frac{\partial x}{\partial u}(u_0, v_0), \frac{\partial y}{\partial u}(u_0, v_0), \frac{\partial z}{\partial u}(u_0, v_0) \right]$$

and

$$\mathbf{r}_v(u_0, v_0) = \left[ \frac{\partial x}{\partial v}(u_0, v_0), \frac{\partial y}{\partial v}(u_0, v_0), \frac{\partial z}{\partial v}(u_0, v_0) \right].$$

If  $P_0 = (x_0, y_0, z_0)$  is a fixed point of the surface of  $P$ , and  $P = (x, y, z)$  – any point of the plane  $\tau$  tangent to the surface of  $P$  at the point  $P_0$ ,  $P_0P$  is a vector  $[x - x_0, y - y_0, z - z_0]$ , then the equation of this plane tangent  $\tau$  to the surface of  $P$  has the form

$$\tau : \mathbf{r}_u(u_0, v_0) \times \mathbf{r}_v(u_0, v_0) \cdot P_0P = 0,$$

where the symbol  $\times$  denotes the vector product of vectors,  $\cdot$  denotes the scalar product of vectors. The vector  $\mathbf{n}(u_0, v_0) = \mathbf{r}_u(u_0, v_0) \times \mathbf{r}_v(u_0, v_0)$  is the vector normal to the surface  $P$ . In coordinates, the vector product  $\mathbf{r}_u(u_0, v_0) \times \mathbf{r}_v(u_0, v_0)$  is expressed by the formula

$$\begin{aligned} \mathbf{r}_u(u_0, v_0) \times \mathbf{r}_v(u_0, v_0) &= \\ &= \left[ \begin{vmatrix} \frac{\partial y}{\partial u}(u_0, v_0) & \frac{\partial z}{\partial u}(u_0, v_0) \\ \frac{\partial y}{\partial v}(u_0, v_0) & \frac{\partial z}{\partial v}(u_0, v_0) \end{vmatrix}, \begin{vmatrix} \frac{\partial z}{\partial u}(u_0, v_0) & \frac{\partial x}{\partial u}(u_0, v_0) \\ \frac{\partial z}{\partial v}(u_0, v_0) & \frac{\partial x}{\partial v}(u_0, v_0) \end{vmatrix}, \begin{vmatrix} \frac{\partial x}{\partial u}(u_0, v_0) & \frac{\partial y}{\partial u}(u_0, v_0) \\ \frac{\partial x}{\partial v}(u_0, v_0) & \frac{\partial y}{\partial v}(u_0, v_0) \end{vmatrix} \right]. \end{aligned}$$

The length of the vector then is equal to

$$\begin{aligned} |\mathbf{r}_u(u_0, v_0) \times \mathbf{r}_v(u_0, v_0)| &= \\ &= \sqrt{\left| \begin{vmatrix} \frac{\partial y}{\partial u}(u_0, v_0) & \frac{\partial z}{\partial u}(u_0, v_0) \\ \frac{\partial y}{\partial v}(u_0, v_0) & \frac{\partial z}{\partial v}(u_0, v_0) \end{vmatrix} \right|^2 + \left| \begin{vmatrix} \frac{\partial z}{\partial u}(u_0, v_0) & \frac{\partial x}{\partial u}(u_0, v_0) \\ \frac{\partial z}{\partial v}(u_0, v_0) & \frac{\partial x}{\partial v}(u_0, v_0) \end{vmatrix} \right|^2 + \left| \begin{vmatrix} \frac{\partial x}{\partial u}(u_0, v_0) & \frac{\partial y}{\partial u}(u_0, v_0) \\ \frac{\partial x}{\partial v}(u_0, v_0) & \frac{\partial y}{\partial v}(u_0, v_0) \end{vmatrix} \right|^2}. \end{aligned}$$

The normal vector is expressed by  $\mathbf{n}_{ver}(u_0, v_0) = \frac{\mathbf{r}_u(u_0, v_0) \times \mathbf{r}_v(u_0, v_0)}{|\mathbf{r}_u(u_0, v_0) \times \mathbf{r}_v(u_0, v_0)|}$ . Thus, we will write the equation of the offset surface in the form

$$P_{off}(d) : \mathbf{r}(u, v) = [x(u, v), y(u, v), z(u, v)] + d \mathbf{n}_{ver}(u, v).$$

Using the formulas presented here, an analysis of the thickness of the saddle surface was carried out in the work of [42]. The analysis is a generalization of the reasoning used in solving the first problem in the section 5.1.3.



### 5.2.2. Thickness of the saddle surface

**Problem 5.3.** Analyze the thickness of the covering of the Warsaw Ochota railway station building (dimensions  $a = 17.35$  m,  $h = 8.34$  m, height of covering  $q = 0.35$  m).

**Hint.** In the case of a saddle surface, we can geometrically perform the thickness analysis much more simply. All we need to do is to analyze figure 4.5 from the chapter 4. There is a maximum (and minimum) height of the cross-section, which is a parallelogram.

### 5.3. Problems

1. Analyze the thickness of a saddle surface shaped cross-section spanning over a rectangular plan building with dimensions  $a = 16$  m,  $b = 12$  m,  $h = 8$  m,  $q = 0.4$  m. Draw the corresponding graphs.
2. The fragments of the edges of the inner and outer roadway of the designed roundabout are ellipses  $e_1$ ,  $e_2$  inscribed in rectangles of  $53 \times 43$  m,  $59 \times 49$  m. Compare the ellipse  $e_2$  with the offset curve of this ellipse  $e_1$  moved off by 6 m (compare to fig. 5.2). Calculate the value of the maximum deviation of the roadway width from the assumed value of 6 m. Analyze the problem with respect to the entire ellipse [9].
3. Find the offset curves of the parabola  $y = ax^2$ .
4. Determine the curvature of a straight line, circle, or ellipse.

**Hint.** The curvature  $k(t)$  in  $t \in [\alpha, \beta]$  of a curve  $c : \begin{cases} x = x(t) \\ y = y(t) \end{cases}$ ,  $t \in [\alpha, \beta]$  in  $R^2$  is given by the formula  $k(t) = \frac{|x'(t)y''(t) - x''(t)y'(t)|}{(x'^2(t) + y'^2(t))^{3/2}}$ .

5. Determine the curvature and twist of the helical line.

**Hint.** The parametric equation of the helical line is given by formula  $\mathbf{r}(t) = [a \cos t, a \sin t, kt]$  where  $a$ -the radius of the cylinder,  $k$ -the quotient of the velocity of motion of the point along the forming and the angular velocity of rotation of the cylinder. If  $k > 0$ , the line is clockwise; if  $k < 0$  the line is counterclockwise.

Curvature  $k(t)$  of the curve  $\mathbf{r}(t) = [x = x(t), y = y(t), z = z(t)]$ ,  $t \in [\alpha, \beta]$  in other words, in  $R^3$  is given by  $k(t) = \frac{|\mathbf{r}'(t_0) \times \mathbf{r}''(t_0)|}{|\mathbf{r}'(t_0)|^3}$ .

The twist  $\tau(t)$  of the curve  $\mathbf{r}(t)$  (the curve belongs to  $C^3$ ) in  $R^3$  is given by formula  $\tau(t) = \frac{(\mathbf{r}'(t_0), \mathbf{r}''(t_0), \mathbf{r}'''(t_0))}{|\mathbf{r}'(t_0) \times \mathbf{r}''(t_0)|^2}$ .

6. Determine the curvature and twist for  $t$  of the curve: a)  $\mathbf{r}(t) = [t, 5t^3, t^4 + 5]$ , b)  $\mathbf{r}(t) = [t, 5t^2, t^3]$ .
7. Perpendicular sections of the path are connected by a sinusoid  $y = 25 \sin \frac{x}{25}$  (Fig. 5.12). Show that the change in curvature is smooth (from zero to zero). Where (give the coordinates of the point) is this curvature maximum and how much is it? What is the radius of curvature at this point? Determine the offset curves.
8. Perpendicular sections of the path are connected by a parabola  $y = -0.01x^2 + x$  (Fig. 5.12). Show that the change in curvature is smooth (from zero to zero). Where (give the coordinates of the point) is this curvature maximum and how much is it? What is the radius of curvature at this point? Determine the offset curves.

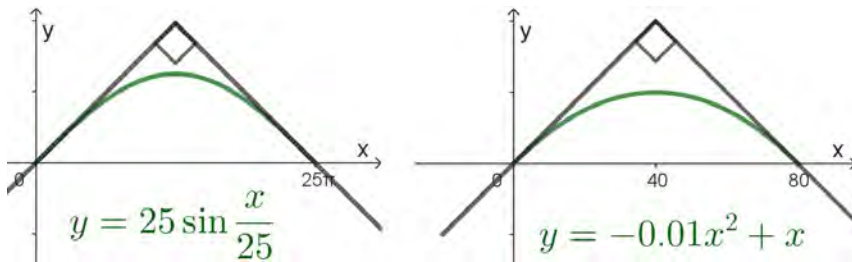


Figure 5.12: Task 7, 8, by A. Tereszkievich



## Chapter 6

# Chain curve in civil engineering and architecture

### 6.1. Chain curve (catenary curve)

**Problem 6.1.** Describe the shape of an inextensible homogeneous chain (rope) suspended at two points.

**Solution.** A chain suspended at points  $A$  and  $B$  is hanging – we assume that it is inextensible and flexible (Fig. 6.1). The chain hangs only under the influence of its own weight. By  $q$  let us denote the constant value representing the weight of the rope per unit of its length [kG/m]. It is necessary to determine the shape of the sag curve as the graph of a certain function  $y(x)$ . For the  $OX$  axis, we take a certain horizontal line below the horizontal segment  $AB$ , and for the  $OY$  axis we take a vertical line passing through the lowest point  $P$  of the hanging curve. Let's denote by  $T$  the length of the tension vector  $\mathbf{T}$  at the point  $M(x, y)$  hang curve, and by  $T_0$  the length of the tension vector  $\mathbf{T}_0$  at the point  $P$ . These vectors are tangent to the curve, and due to the symmetry of the curve, the vector  $\mathbf{T}_0$  is parallel to the  $OX$  axis. Let's consider the  $PM$  arc of the curve. Note that due to the equilibrium state of the chain, the sum formed from the forces  $\mathbf{T}_0$ ,  $\mathbf{T}$  and from the sum of the gravity of the individual elementary sections of the  $PM$  curve equals zero. The same is true for the sum of their components relative to the  $OX$  axis of the  $OY$  axis, respectively. So, still taking into account the formula for the length  $\int_0^x \sqrt{1 + (y')^2} dx$  of the arc  $y = y(x)$  in the interval  $[0, x]$  we obtain

$$-T_0 + T \cos \alpha = 0, \quad T \sin \alpha - \int_0^x q \sqrt{1 + (y')^2} dx = 0, \quad (6.1)$$

where  $\alpha$  is the angle formed by the vector  $\mathbf{T}$  with the axis  $OX$ .

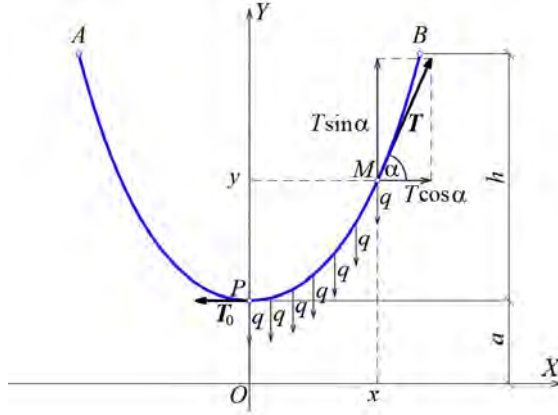


Figure 6.1: Chain curve, by A. Tereszkievicz

Hence

$$T \cos \alpha = T_0 = \text{const}, \quad \text{and} \quad T_0 \operatorname{tg} \alpha - \int_0^x q \sqrt{1 + (y')^2} dx = 0. \quad (6.2)$$

Differentiating with respect to  $x$  both sides of the last formula and noting that  $\operatorname{tg} \alpha = y'(x)$ , we get

$$y'' = \frac{1}{a} \sqrt{1 + (y')^2} \quad (6.3)$$

as the equation of the curve of hanging. We denoted this by  $\frac{T_0}{q} = a$ . This is an equation of the type  $F(x, y', y'') = 0$ . By substituting  $y' = u$  in the equation (6.3), we have

$$\frac{du}{\sqrt{1 + u^2}} = \frac{dx}{a}. \quad (6.4)$$

Integrating both sides, we get

$$\ln \left( u + \sqrt{1 + u^2} \right) = \frac{x}{a} + C_1. \quad (6.5)$$

Equation (6.5) can be transformed using the concept of hyperbolic sine function. Since we have  $\ln \left( w + \sqrt{1 + w^2} \right) = v \Leftrightarrow w + \sqrt{1 + w^2} = e^v \Leftrightarrow e^v - w = \sqrt{1 + w^2} \Leftrightarrow (e^v - w)^2 = 1 + w^2 \Leftrightarrow e^{2v} - 2e^v w + w^2 =$

$= 1 + w^2 \Leftrightarrow e^{2v} - 1 = 2e^v w \Leftrightarrow w = \frac{e^{2v}-1}{2e^v} \Leftrightarrow w = \frac{e^v - e^{-v}}{2}$ , that is,  $w = \sinh(v)$ . Thus, transforming (6.5), we get

$$u = \sinh\left(\frac{x}{a} + C_1\right), \quad \text{i.e.} \quad y' = \sinh\left(\frac{x}{a} + C_1\right). \quad (6.6)$$

Integrating again ( $\cosh(x) = \frac{e^x + e^{-x}}{2}$ ) we get the general integral of the equation (6.3):

$$y = a \cosh\left(\frac{x}{a} + C_1\right) + C_2. \quad (6.7)$$

To determine the initial conditions, we peel the  $OX$  axis so that the ordinate of the point  $P$  equals  $a$  (6.1). Thus, assume  $y'(0) = 0, y(0) = a$ . Hence  $C_1 = 0, C_2 = 0$  and the equation of the resulting curve called *chain curve* is of the form

$$y = a \cosh \frac{x}{a}. \quad (6.8)$$

After considering the designations in figure 6.1 we get

$$y = \frac{T_0}{q} \cosh\left(\frac{qx}{T_0}\right). \quad (6.9)$$

**Problem 6.2.** Determine the  $a$  parameter of the arc of the chain curve  $y = a \cosh\left(\frac{x}{a}\right)$  of the Gateway Arch, an architectural structure that is located in Saint Louis, USA. The span of the arch at the base is 192 m (the same as its height) and is shaped like a chain curve. Each part from which the arch is constructed is an equilateral triangle with a side of 16.5 m at the base, to 5.2 m at the highest point. The construction is made of double-walled steel modules with a triangular cross-section. An inner shell of carbon steel 0.01 m thick forms the construction, while an outer shell of stainless steel is the finishing touch to the arch. The innovative design has no internal supporting skeleton; the modules are self-supporting.



(a)



(b)



(c)



(d)



(e)



(f)



(g)

Figure 6.2: Architectural realizations based on the chain curve: (a) the chain barriers at Legionowa Street in Białystok, photo by E. Koźniewski; (b) Grunwald Bridge in Wrocław, photo by F. Sadowski; (c) viaduct over Piastowska Street in Białystok, photo by E. Koźniewski; (d) covering of Keleti Station in Budapest, photo by E. Koźniewski; (e) Gateway Arch in Saint Louis in USA, [22]; (f) Chain Bridge in Budapest, photo by E. Omieljańczuk; (g) the viaduct over the General Route in Białystok, photo by M. Koźniewski

**Solution.** In order to determine the parameter  $a$  for the chain curve describing Gateway Arch (and any curve describing any chain of this type), we first make a sketch (Fig. 6.3, right). After initially determining the value of the  $a$  parameter, this drawing can be made in the AutoCAD environment, using an Excel sheet. For a given span and height of the arc of the curve, we create two columns of data. The first column is the values of the independent variable in the interval  $[0, 96]$ , i.e. 0 and half of the span of the curve (at 6.3 is equal to 96 m), the second column is  $a$  plus the height of the curve (at 6.3 is equal to 192 m). Thus, to the curve  $y = a \cosh\left(\frac{x}{a}\right)$  belongs a point with coordinates  $(96, 192)$ . Substituting in (6.8) for  $x = 96$  and for  $y = a + 192$ , we get the equation  $a + 192 = a \cosh\left(\frac{96}{a}\right)$ . Equivalently, we write this in the form

$$a \cosh\left(\frac{96}{a}\right) - a - 192 = 0. \quad (6.10)$$

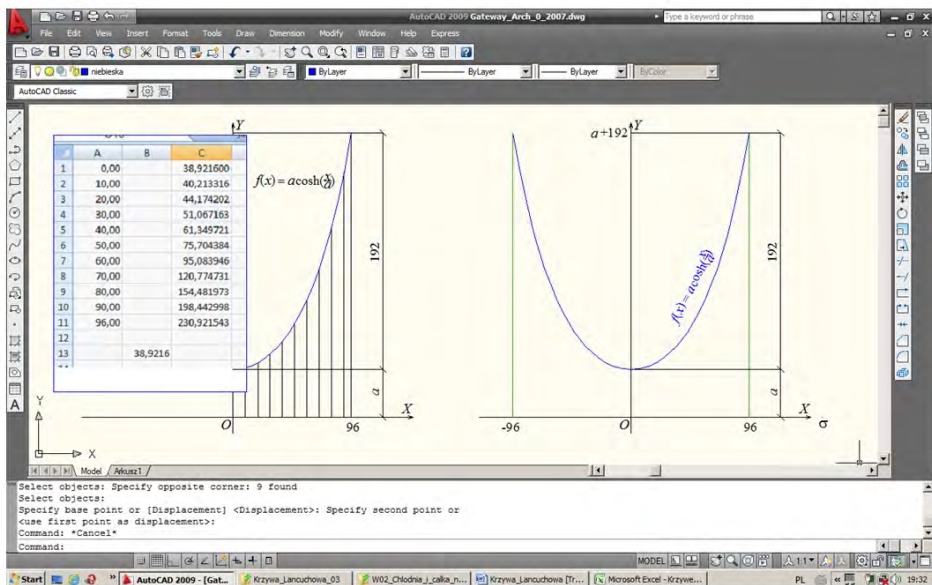


Figure 6.3: Generation of chain curve profile in AutoCAD: points were determined for chain curve (6.8) for  $a = 38.9216$ , for the values of 10, 20, ..., 80, 90, 96 (the first column of numbers), calculating in Excel the values of the function (6.8) (the second column) and measuring them on the vertical lines projected at points with abscissa 10, 20, ..., by E. Koźniewski



To find  $a$ , we solve the equation using, for example, the bisection method or any method or most simply in the Wolfram Alpha (solve) program. In our case  $a = 38.9216$ . Let's go back to making a drawing of a chain curve with a given parameter  $a$ . Well, the first thing is to solve the equation (6.10), or in the general case of equation

$$a \cosh \left( \frac{b}{2a} \right) - a - h = 0, \quad (6.11)$$

where  $b$  is the span of the arc and  $h$  is the height (in Gateway Arch  $b = 192$  m,  $h = 192$  m).

**Problem 6.3.** A 100-meter long wire weighing 20 kG hangs 5 m from a horizontal line drawn through suspension points  $A, B$  (Fig. 6.1). Find the tension  $T$  at the suspension points. Before that, we find the (somewhat simple) formula for calculating the tension  $T$ . From the first relation with (6.1) we get the following  $T = \frac{T_0}{\cos \alpha} =$

$$= \left| \begin{array}{l} \cos \alpha = \frac{1}{\sqrt{1+\tan^2 \alpha}}, \\ y' = \tan \alpha \end{array} \right| = T_0 \sqrt{1+(y')^2}, \text{ i.e. } T = T_0 \sqrt{1+(y')^2}.$$

From the (6.8) we have  $T = T_0 \sqrt{1 + \sinh^2 \frac{x}{a}}$ . And further from fact that  $\cosh^2 u - \sinh^2 u = 1$ , we get  $T = T_0 \cosh \frac{x}{a}$ . Since  $\frac{T_0}{q} = a$ , in view of (6.8) we have

$$T = qy. \quad (6.12)$$

Let us now turn to the solution of the task:  $y = h + a$  is the ordinate of point  $B$  (Fig. 6.1). To use the formula (6.12), let's determine  $a$ . We know  $h = 5$  m,  $q = 0.2$  kG/m. The length of the arc of the chain curve (6.8) equals

$$\begin{aligned} s &= \int_0^x \sqrt{1+(y')^2} dx = \left| \begin{array}{l} y = a \cosh \left( \frac{x}{a} \right) \\ y' = \sinh \left( \frac{x}{a} \right) \end{array} \right| = \int_0^x \sqrt{1 + \left( \sinh \left( \frac{x}{a} \right) \right)^2} dx = \\ &= \int_0^x \sqrt{\left( \cosh \left( \frac{x}{a} \right) \right)^2} dx = \int_0^x \cosh \left( \frac{x}{a} \right) dx = a \sinh \left( \frac{x}{a} \right) = \\ &= a \sqrt{\left( \cosh \left( \frac{x}{a} \right) \right)^2 - 1} = \sqrt{\left( a \cosh \left( \frac{x}{a} \right) \right)^2 - a^2} = \\ &= \sqrt{y^2 - a^2} = \sqrt{(h+a)^2 - a^2} = \sqrt{h^2 + 2ah}. \end{aligned}$$

Thus  $s^2 = h^2 + 2ah$ , and hence  $a = \frac{s^2 - h^2}{2h}$ . So,  $a = \frac{50^2 - 5^2}{2 \cdot 5} = 247.5$  m. Returning to determine the tension of the wire against (6.12), we have the following

$$T = q(h + a) = 0.2 \cdot (5 + 247.5) \text{ kG} = 0.2 \cdot 252.5 \text{ kG} = 52.5 \text{ kG}.$$

Having the vertical segments drawn, we draw a spline curve, connecting the upper ends of the segments one by one.

## 6.2. Problems

1. Find the value of the parameter  $a$  of the shape of the Golden Gate Bridge chain curve (Fig. 6.4). The construction has a length of 2700 m. The distance between the two pylons is 1280 m. The height of the pylons is 230 m, while the height of the pylons, measured from the roadway (pavement), is 152 m.

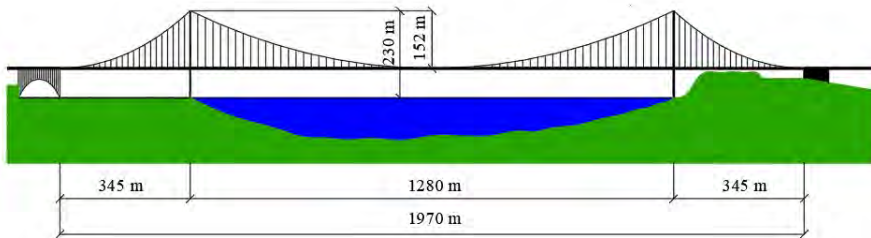


Figure 6.4: Basic dimensions of the Golden Gate Bridge suspension bridge connecting San Francisco and Marin County, California, USA, by E. Koźniewski based on [23]

2. How many meters of rope/chain should be bought to make a sidewalk chain barrier (on both sides) with a length of 10.4 m, and the rope/chain is to hang freely about 55 cm above the ground? How many posts (70 cm high) should be bought and how far apart should they be placed?
3. Consider a heavy rope of length  $l$ [m], its meter weighs  $k$ [kg]. One end is fixed at a point  $M$ , while the other end touches  $A$  with the horizontal surface of the ground. The height of point  $M$  above the horizontal is  $h$ . Determine the tension of the string at the points  $M$ ,  $A$  [57].

4. A heavy chain, whose weight per unit length is  $q$ , is hanging from two pegs  $A$  and  $B$ . The difference in height between point  $B$  and the lowest point of the chain  $W$  is  $b$ , between  $A$  and  $W$  is  $a$ , the length of the chain from  $B$  to  $W$  is equal to  $\beta$ , in contrast, from  $A$  to  $W$  is  $\alpha$ . Calculate the tensions (reactions) of the chain on the pegs, and the angles that these tensions form with the level (Fig. 6.5) [60].

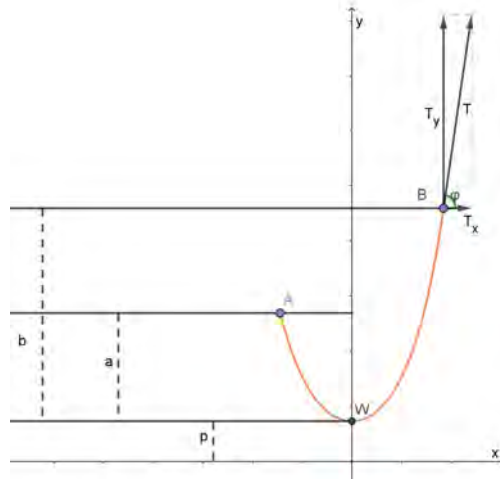


Figure 6.5: Illustration for task 4, by A. Tereszkieicz

5. The tangents at the hanging points of a heavy chain of length  $s$  form angles  $\alpha, \beta$  with the vertical. Calculate the height of one of the hanging points above the other (Fig. 6.6) [60].

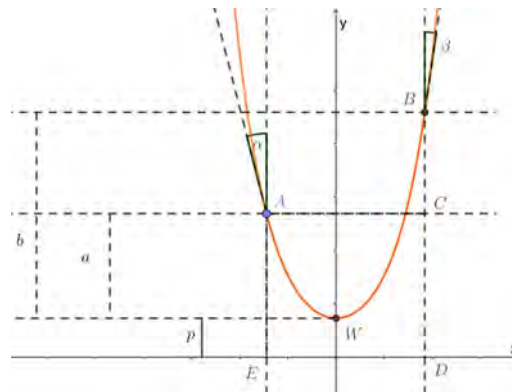


Figure 6.6: Illustration for task 5, by A. Tereszkieicz

6. Two rings  $M$  and  $N$  were threaded onto a stationary horizontal bar, completely smooth, to which the ends of a  $2l$  heavy chain were attached. If the system were left alone, the rings  $M$  and  $N$  would come together and the chain would assume a vertical position. To prevent this, we apply two equal and outwardly directed forces – each of these forces is equal to the weight of half the chain. Determine the distances of the rings in balance [57].

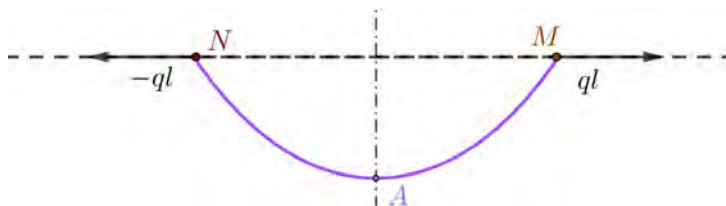


Figure 6.7: Illustration for task 6, by A. Tereszkieicz

7. Two smooth pegs  $M$  and  $N$  lie on one level. The distance between them is equal to  $2c$ . We hang a heavy rope on these pegs (Fig. 6.8). What should be the minimum length of the rope for balance to be possible? (If the rope is too short, it will slide off the pegs into the center) [57].

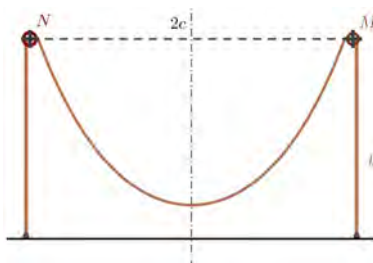


Figure 6.8: Illustration for task 7, by A. Tereszkieicz

8. Find the dimensions of two selected structures based on the shape of chain curves: bridges, vaults, arches; determine the parameter of the chain curve and draw the curve in both cases.



## Chapter 7

# Surfaces with fast run-up – brachistochrone in skateparks, aquaparks and ski jumps

### 7.1. The problem of brachistochrone – an example of an extremum of a function

**Problem 7.1.** Let the material point slip without friction under the influence of gravity along the curve connecting points  $A$ ,  $B$  (Fig. 7.1a). The *brachistochrone problem* (gr. *brachys* – short, *chronos* – time) consists in determining, among all the curves connecting points  $A$  and  $B$ , the point at which the material point slips in the shortest possible time.

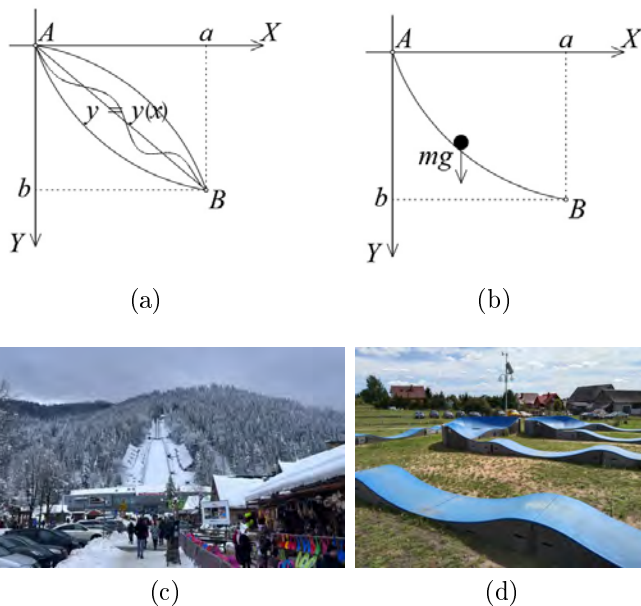


Figure 7.1: Illustration of the brachistochrone problem: (a) assumptions about the issue, by E. Koźniewski; (b) material point slipping without any friction, by E. Koźniewski; (c) the inrun of the Wielka Krokiew in Zakopane, photo by S. Kudźma; (d) skatepark in Sobolewo, photo by E. Koźniewski. Are high-speed descents desirable here?

This is historically the first issue of *variational calculus* (1696, Johann Bernoulli).

**Solution.** Let  $y = y(x)$  be the equation of the curve after which the material point slides (Fig. 7.1b). In the  $OXY$  system, according to the law of gravity, we can write  $y = \frac{gt^2}{2}$ , where  $g$  denotes gravity acceleration,  $t$  time. Multiply both sides by  $g$  and we get  $gy = \frac{g^2 t^2}{2}$ . After taking into account  $v = gt$ , we get  $v = \sqrt{2gy}$ . At the same time, after denoting by  $l$  the distance traveled by the point, the instantaneous velocity  $v$  is expressed by  $v = \frac{dl}{dt} = \frac{\sqrt{1+(y')^2}dx}{dt}$  (after all,  $dl = \sqrt{1+(y')^2}dx$ ). We get

$$dt = \frac{\sqrt{1+(y')^2}}{\sqrt{2gy}} dx. \quad (7.1)$$

The slip time of the point is equal to the integral of the

$$T = \frac{1}{\sqrt{2g}} \int_0^a \sqrt{\frac{1+(y')^2}{y}} dx. \quad (7.2)$$

We get time  $T$  as a functional  $J[y] = \int_0^a F(x, y, y') dx = \int_0^a \frac{\sqrt{1+(y')^2}}{\sqrt{2gy}} dx$ .

According to Euler's theorem, the extreme point of the function space  $C_{[0,a]}$  (i.e. a function) should satisfy the condition

$$\frac{\partial F}{\partial y} - \frac{d}{dx} \frac{\partial F}{\partial y'} = 0. \quad (7.3)$$

We calculate the derivative of the function  $F(x, y, y') = \frac{\sqrt{1+(y')^2}}{\sqrt{2gy}}$  with respect to  $y$  ( $y'$  and  $g$  are constants, the function  $F(x, y, y') = \frac{\sqrt{1+(y')^2}}{\sqrt{2gy}}$  can be written in the form  $F(x, y, y') = \frac{\sqrt{1+(y')^2}}{\sqrt{2g}} \cdot \frac{1}{\sqrt{y}}$ )

$$\begin{aligned} \frac{\partial F}{\partial y} &= \frac{\sqrt{1+(y')^2}}{\sqrt{2g}} \left( \frac{1}{\sqrt{y}} \right)'_y = \frac{\sqrt{1+(y')^2}}{\sqrt{2g}} \left( y^{-\frac{1}{2}} \right)'_y = \\ &= \frac{\sqrt{1+(y')^2}}{\sqrt{2g}} \left( -\frac{1}{2} y^{-\frac{3}{2}} \right) = -\frac{\sqrt{1+(y')^2}}{\sqrt{2g}} \frac{1}{y\sqrt{y}}. \end{aligned}$$

We compute the derivative of the function  $F(x, y, y') = \frac{\sqrt{1+(y')^2}}{\sqrt{2gy}}$  with respect to  $y'$  ( $y$  and  $g$  are constants, the function  $F(x, y, y') = \frac{\sqrt{1+(y')^2}}{\sqrt{2gy}}$  can be written in the form  $F(x, y, y') = \frac{1}{\sqrt{2g\sqrt{y}}} \sqrt{1+(y')^2}$  )

$$\begin{aligned}\frac{\partial F}{\partial y'} &= \frac{1}{\sqrt{2g\sqrt{y}}} \left( \sqrt{1+(y')^2} \right)'_{y'} = \\ &= \frac{1}{\sqrt{2g\sqrt{y}}} \frac{1}{2\sqrt{1+(y')^2}} \cdot 2y' = \frac{1}{\sqrt{2g\sqrt{y}}} \frac{y'}{\sqrt{1+(y')^2}}.\end{aligned}$$

After calculating the derivatives of  $\frac{\partial F}{\partial y} = -\frac{\sqrt{1+(y')^2}}{2y\sqrt{2gy}}$ ,  $\frac{\partial F}{\partial y'} = \frac{y'}{\sqrt{2gy(1+(y')^2)}}$  and substituting into (7.3) we get the equation

$$\frac{\sqrt{1+(y')^2}}{2y\sqrt{2gy}} - \frac{d}{dx} \frac{y'}{\sqrt{2gy(1+(y')^2)}} = 0, \quad (7.4)$$

which we can multiply both sides by  $\sqrt{2g}$  and we get (earlier we factor out  $\frac{1}{\sqrt{2g}}$  before the derivative).

$$\frac{\sqrt{1+(y')^2}}{2y\sqrt{y}} - \frac{d}{dx} \frac{y'}{\sqrt{y(1+(y')^2)}} = 0. \quad (7.5)$$

Left to calculate is the derivative of  $\frac{d}{dx} \frac{y'}{\sqrt{y(1+(y')^2)}}$ . Here it is important to remember that  $y$  and  $y'$  are functions of the variable  $x$ . So, using the quotient derivative formula (taking into account the derivative of the product of the inner function)

$$(y(1+(y')^2))' = y'(1+(y')^2) + y \cdot 2y' \cdot y'',$$

we get

$$\frac{d}{dx} \frac{y'}{\sqrt{y(1+(y')^2)}} = \frac{y'' \sqrt{y(1+(y')^2)} - \frac{y'(y'(1+(y')^2) + y \cdot 2y' \cdot y'')}{2\sqrt{y(1+(y')^2)}}}{y(1+(y')^2)}. \quad (7.6)$$

We take the numerator to the common denominator

$$\frac{d}{dx} \frac{y'}{\sqrt{y(1+(y')^2)}} = \frac{\frac{2y''(y(1+(y')^2) - y'(y'(1+(y')^2) + 2yy'y''))}{2\sqrt{y(1+(y')^2)}}}{y(1+(y')^2)}. \quad (7.7)$$



We sort out the numerator of the numerator of the fraction and write with one fractional bar

$$\frac{d}{dx} \frac{y'}{\sqrt{y(1+(y')^2)}} = \frac{2y''y + 2yy'(y')^2 - (y')^2 - (y')^4 - 2y(y')^2y''}{2\sqrt{y(1+(y')^2)}y(1+(y')^2)}. \quad (7.8)$$

After reducing the two products  $2y(y')2y''$  in the numerator, the result obtained is

$$\frac{d}{dx} \frac{y'}{\sqrt{y(1+(y')^2)}} = \frac{2y''y - (y')^2 - (y')^4}{2\sqrt{y(1+(y')^2)}y(1+(y')^2)} \quad (7.9)$$

we insert into (7.5)

$$\frac{\sqrt{1+(y')^2}}{2y\sqrt{y}} - \frac{2y''y - (y')^2 - (y')^4}{2\sqrt{y(1+(y')^2)}y(1+(y')^2)} = 0. \quad (7.10)$$

When both sides of the equation are multiplied by  $2\sqrt{y(1+(y')^2)}y$  we get

$$-(1+(y')^2) - \frac{2y''y - (y')^2 - (y')^4}{1+(y')^2} = 0. \quad (7.11)$$

After writing on the common fractional bar, we get

$$\frac{-(1+(y')^2)(1+(y')^2) - 2y''y + (y')^2 + (y')^4}{1+(y')^2} = 0. \quad (7.12)$$

A fraction is equal to zero if and only if the numerator is equal to zero. Thus, after reducing the expression  $(y')^4$  we have

$$-1 - (y')^2 - 2y''y = 0. \quad (7.13)$$

After converting, we finally get a differential equation of order two in the form of

$$\frac{y''}{1+(y')^2} = -\frac{1}{2y}. \quad (7.14)$$

In order to solve the equation (7.14) we introduce a new variable  $y' = u(y)$ . After calculating the derivative, we have  $y'' = u'y' = uu'$ . When substituted, we get

$$\begin{aligned} \frac{uu'}{1+u^2} &= -\frac{1}{2y} \Leftrightarrow \frac{u}{1+u^2} \frac{du}{dy} = -\frac{1}{2y} \Leftrightarrow \frac{2u}{1+u^2} du = -\frac{1}{y} dy \\ &\Leftrightarrow \ln(1+u^2) = -\ln y + C^* \Leftrightarrow \ln y = \ln C - \ln(1+u^2) \Leftrightarrow y = \frac{C}{1+u^2}. \end{aligned}$$

In the last equation, we substitute  $u = \operatorname{ctg} \frac{\varphi}{2}$ , where  $\varphi(x)$  is the unknown function. We have  $y = \frac{C}{2} (1 - \cos \varphi)$ . Since  $y' = \frac{dy}{dx}$  and  $y' = \operatorname{ctg} \frac{\varphi}{2}$ , i.e.  $\frac{dx}{d\varphi} = \frac{C}{2} (1 - \cos \varphi)$ . After integration, we get  $x = \frac{C}{2} (\varphi - \sin \varphi) + C_1$ . From the equality  $y(0) = 0$  we get  $C_1 = 0$ , in turn from  $y(a) = b$  it follows that there is a constant  $C$ , at which the cycloid (Fig. 7.2)

$$\begin{cases} x = \frac{C}{2} (\varphi - \sin \varphi) \\ y = \frac{C}{2} (1 - \cos \varphi) \end{cases}$$

is the solution to the issue of brachistochrone ([10] Fig. 7.3).

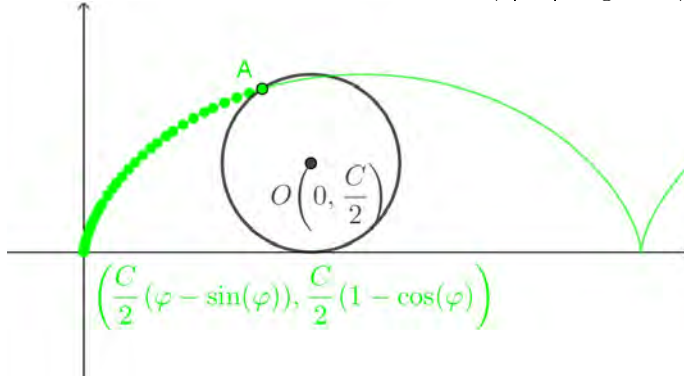


Figure 7.2: Cycloid, by A. Tereszkievicz

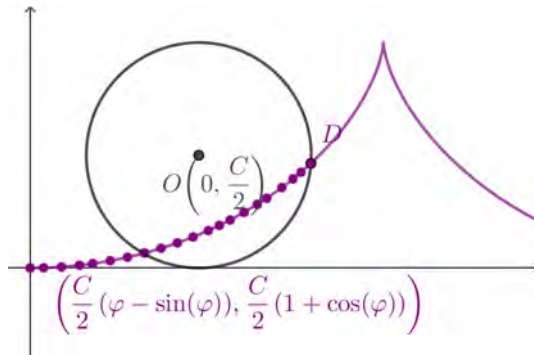


Figure 7.3: Brachistochrone, by A. Tereszkievicz

Brachistochrone is simultaneously *tautochrone*, [27] i.e., a curve along which a material point under the influence of gravity rolls to the lowest point of the curve in the same amount of time, regardless of the starting point on the curve.

## 7.2. Problems

1. Calculate the area and perimeter of a window opening, the edge of which is a cycloid having a height of 4 m at its highest point. If we want to install a window sill, how long should it be?

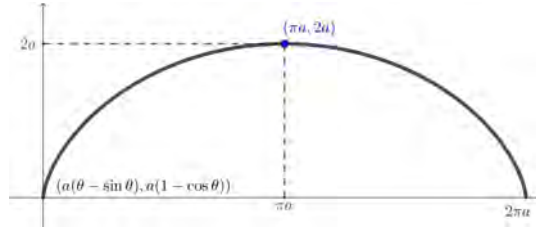


Figure 7.4: Illustration for task 1, by A. Tereszkievicz

2. For covering narrow rectangles, we usually use cylindrical shells. Their cross-section can be a circle, ellipse, parabola, cycloid, chain curve. Lighting can be obtained by making skylights along the length of the shell or by using barrel vault skylights. Calculate the area of the roof of a building with dimensions  $4 \times 10$  m, the cross-section of which is:
  - a) chain curve for  $a = -6$ ,
  - b) cycloid for  $a = \frac{2}{\pi}$ .

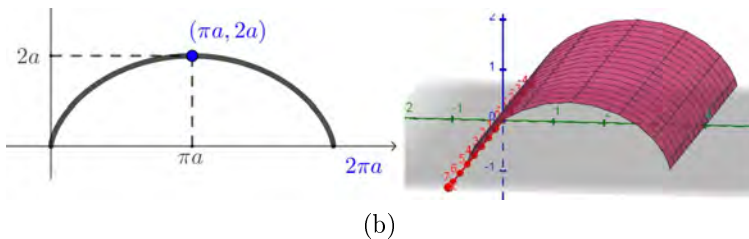
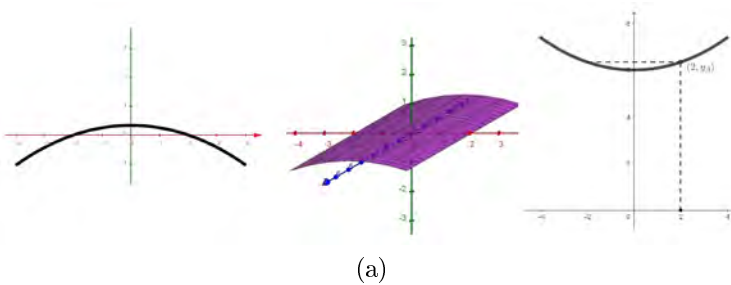


Figure 7.5: Illustration for task 2, by A. Tereszkievicz

3. Calculate the volume of a building with a height of 5 m from task 2.
4. The arc of the cycloid rotates around its axis of symmetry. Find the area of the resulting surface. (Such an inverted cycloid can be a starting point when planning skateparks, especially jump boxes, with the profile of the bump being a slice of the cycloid, i.e. the curve that puts the least drag on the rolling wheel, so that such a jump box kicks out impressively despite its not very high height).
5. Using the equation of the brachistochrone and parabola, describe the model of a ski jump.
6. Determine the  $\varphi$  i  $C$  parameters for cycloidal run-up curves (solution of the brachistochrone problem) of two selected ski jumps.

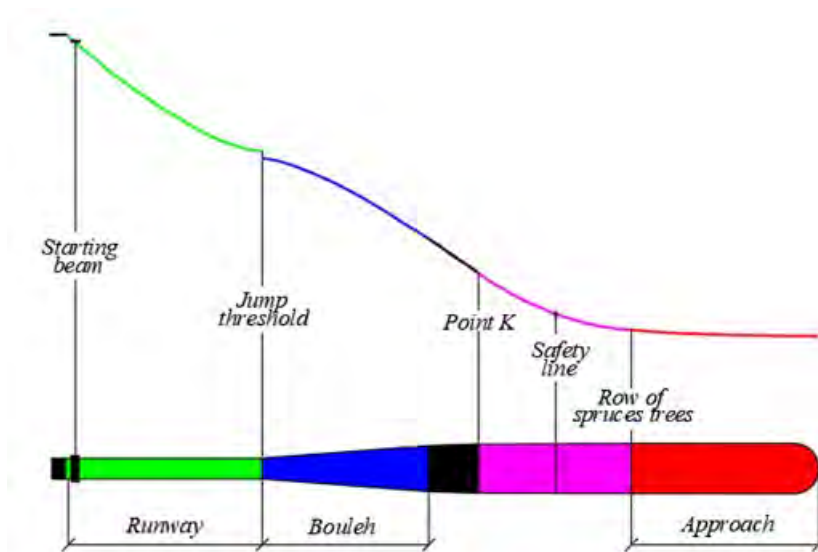


Figure 7.6: Scheme of a ski jump, by E. Koźniewski based on [24]

7. Given a window with the dimensions shown in figure 7.7a with four variants of the lintel.
  - a) cycloid:  $\begin{cases} x = r(t - \sin t) \\ y = r(1 - \cos t) \end{cases}, t \in [0, 2\pi];$
  - b) arc of the ellipse:  $\begin{cases} x = a \cos t \\ y = b \sin t \end{cases}, t \in [0, \pi];$
  - c) catenary (chain curve):  $y = a \cosh\left(\frac{x}{a}\right);$
  - d) bow, Fig. 7.7b.

The parameter  $b$  in items b)-d) determine from item a). Investigate which curve will provide the most daylight (i.e., for which curve, the area marked in the figure is the largest)? Give the difference in percentage points (%) in each variant with respect to the smallest area. We assume the data:

$$a = 0,70 + 0,01 \cdot (\text{student number on attendance list}),$$

$$h = 2,60 + 0,01 \cdot (\text{student number on attendance list}).$$

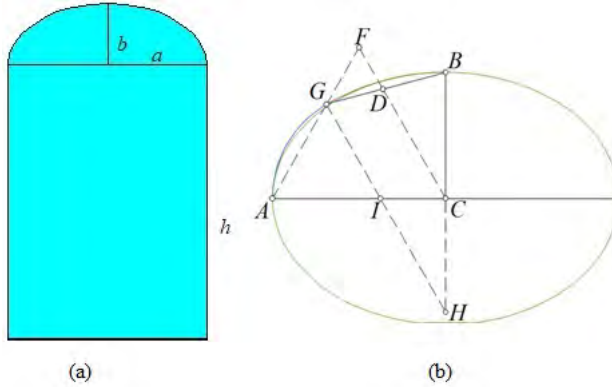


Figure 7.7: Design window: (a) window dimensions; (b) construction of a bowline with half-axes  $a = AC$ ,  $b = BC$ . Successive designs 1: equilateral triangle  $AFC$ ; 2: circle  $o(C, BC)$ ; 3: point  $D$  as intersection of line  $CF$  and circle  $o(C, BC)$ ; 4: point  $G$  as intersection of lines  $BD$  and  $AF$ ; 5: point  $I$  as the intersection of the line passing through point  $G$  and parallel to line  $CF$  with line  $AC$  and the point  $H$  as the intersection of the line passing through the point  $G$  and parallel to the line  $CF$  with the line  $BC$ ; 6: gluing the arcs of the circles  $o(H, HB)$  and  $o(I, IG)$ , illustration for task 7, by E. Koźniewski

**Hint.** The area of the bail (i.e., the area bounded by the bail and the longer axis) with half-axes  $a$ ,  $b$  is expressed as follows

$$P_{kab} = 2 \left( \frac{\pi}{6} \left( \left( \frac{b - a(2 - \sqrt{3})}{\sqrt{3} - 1} \right)^2 + \frac{1}{2} \left( \frac{a\sqrt{3} - b}{\sqrt{3} - 1} \right)^2 \right) - \frac{(a - b)^2 \sqrt{3}}{2(\sqrt{3} - 1)^2} \right).$$

## Chapter 8

# Vibrations in structural mechanics

### 8.1. Eigenvalues and eigenvectors of the operator and diagonalization of the matrix

For the linear operator (*endomorphism*)  $A : X \rightarrow X$  we define the eigenvalue and eigenvector of the operator. If  $I$  is an identity operator (unitary  $x = Ix$ ) and there exists such a number  $\lambda$  and a non-zero vector  $x \in X$  that, for the operator  $A$ , there occurs

$$Ax = \lambda x, \quad (8.1)$$

then the number  $\lambda$  is called *eigenvalue* of operator  $A$ , while  $x$  is called *eigenvector* of operator  $A$ . In  $n$ -dimensional space over a body of real (complex) numbers, the linear operator has a matrix representation. Then the notation  $Ax$  means the product of the matrix  $A$  and vector  $x$ .

**Theorem 8.1.** For the matrix  $A$ , the following conditions are equivalent:

- 1)  $\lambda$  is an eigenvalue  $A$ ,
  - 2) the system  $(A - \lambda I)x = 0$  has a non-zero solution,
  - 3)  $\det(A - \lambda I) = 0$ .
- (8.2)

The polynomial  $\varphi_A(\lambda) = \det(A - \lambda I)$  is called the *characteristic polynomial* of the matrix  $A$ . In the field of complex numbers, the polynomial has  $n$  elements (calculated with multiples). For the matrix

$$\begin{bmatrix} 1 & 2 & 0 \\ 0 & 2 & 0 \\ -2 & -2 & -1 \end{bmatrix} \quad (8.3)$$

$$\varphi_A(\lambda) = \det(A - \lambda I) = -(1 - \lambda)(2 - \lambda)(1 + \lambda).$$

A linear operator is *diagonalizable*, if there is a basis in the space where its matrix is diagonal.

We say that matrix  $A$  is similar to matrix  $B$  ( $A \sim B$ ), if there exists a non-singular matrix  $P$  such that  $A = PBP^{-1}$ . The similarity  $\sim$  of a matrix is an equivalence relation, i.e., reflexive ( $A \sim A$ ), symmetric ( $A \sim B \rightarrow B \sim A$ ) and transitive ( $A \sim B \wedge B \sim C \rightarrow A \sim C$ ).

Similar matrices have the same characteristic polynomial. Indeed, let  $A = PBP^{-1}$ , then  $\varphi(\lambda) = \det(A - \lambda I) = \det(PBP^{-1} - \lambda I) = \det(PBP^{-1} - \lambda PIP^{-1}) = \det P(B - \lambda I)P^{-1} = \det P \det(B - \lambda I) \det P^{-1} = \det(B - \lambda I) = \varphi_B(\lambda)$ .

We say that matrix  $A = \begin{bmatrix} a_{11} & \cdots & a_{1n} \\ \vdots & \ddots & \vdots \\ a_{n1} & \cdots & a_{nn} \end{bmatrix}$  is *diagonalizable*,

if it is similar to diagonal matrix  $B = \begin{bmatrix} b_{11} & \cdots & 0 \\ \vdots & \ddots & \vdots \\ 0 & \cdots & b_{nn} \end{bmatrix} = \text{diag}(b_{11}, b_{22}, \dots, b_{nn})$ .

From the identity of the characteristic polynomials of two matrices does not follow the diagonalizability of both of them. As an example, take the

matrices  $I = \begin{bmatrix} 1 & 0 & 0 \\ 0 & 1 & 0 \\ 0 & 0 & 1 \end{bmatrix}$ ,  $A = \begin{bmatrix} 1 & 1 & 1 \\ 0 & 1 & 1 \\ 0 & 0 & 1 \end{bmatrix}$ .

True is

**Theorem 8.2.** The matrix  $An \times n$  ( $A \in R^{n \times n}$ ) is diagonalizable if and only if:

- (a) its characteristic polynomial has  $n$  elements (calculated with multiplicities);
- (b) for each eigenvalue of the matrix  $A$  can be chosen as many eigenvectors as the multiplicity of that eigenvalue as a root of the characteristic polynomial.

Moreover, if  $v_1, v_2, \dots, v_n$  are linearly independent eigenvectors of a diagonalizable matrix  $A$  corresponding to its eigenvalues  $\lambda_1, \lambda_2, \dots, \lambda_n$  (not necessarily different), then matrix  $P = [v_1 v_2 \dots v_n]$  is the matrix fixing the similarity between matrices  $A$  and  $\text{diag}(\lambda_1, \lambda_2, \dots, \lambda_n)$ , such as  $P^{-1}AP = \text{diag}(\lambda_1, \lambda_2, \dots, \lambda_n)$  (or  $A = P \text{diag}(\lambda_1, \lambda_2, \dots, \lambda_n) P^{-1}$ ).

**Example 8.1.** Diagonalize the matrix  $A = \begin{bmatrix} 5 & 4 & 2 \\ 4 & 5 & 2 \\ 2 & 2 & 2 \end{bmatrix}$ .

**Solution.** First, we find the eigenvalues of the matrix, i.e., we look for non-zero solutions of the equation  $(A - \lambda I)x = 0$ . It has to be  $\det(A - \lambda I) = 0$ .

We calculate the determinant of the matrix  $\begin{bmatrix} 5 - \lambda & 4 & 2 \\ 4 & 5 - \lambda & 2 \\ 2 & 2 & 2 - \lambda \end{bmatrix}$

$$\begin{vmatrix} 5 - \lambda & 4 & 2 \\ 4 & 5 - \lambda & 2 \\ 2 & 2 & 2 - \lambda \end{vmatrix} = -(\lambda - 1)^2(\lambda - 10) = 0.$$

We obtain the eigenvalues and their algebraic multiplicities  $\lambda_1 = 1, k_1 = 2$ ;  $\lambda_2 = 10, k_2 = 1$ .

Let  $\lambda_1 = 1$ . For  $\lambda$  in the equation  $(A - \lambda I)x = 0$  substitute 1 and solve the system  $\begin{bmatrix} 5 - 1 & 4 & 2 \\ 4 & 5 - 1 & 2 \\ 2 & 2 & 2 - 1 \end{bmatrix} \begin{bmatrix} x_1 \\ x_2 \\ x_3 \end{bmatrix} = \begin{bmatrix} 0 \\ 0 \\ 0 \end{bmatrix}$ .

We transform the expanded matrix (by operating on rows)  $\begin{bmatrix} 4 & 4 & 2 & | & 0 \\ 4 & 4 & 2 & | & 0 \\ 2 & 2 & 1 & | & 0 \end{bmatrix} \xleftrightarrow[w_3 - \frac{1}{2}w_1 \rightarrow w_3]{w_2 - w_1 \rightarrow w_2} \begin{bmatrix} 4 & 4 & 2 & | & 0 \\ 0 & 0 & 0 & | & 0 \\ 0 & 0 & 0 & | & 0 \end{bmatrix} \xleftrightarrow{\frac{1}{4}w_1 \rightarrow w_1} \begin{bmatrix} 1 & 1 & \frac{1}{2} & | & 0 \\ 0 & 0 & 0 & | & 0 \\ 0 & 0 & 0 & | & 0 \end{bmatrix}$ .

We obtain the equation  $x_1 + x_2 + \frac{1}{2}x_3 = 0$ . Substituting  $x_3 := \alpha, x_2 := \beta$  we have  $x_1 = -\beta - \frac{1}{2}\alpha, x_2 := \beta, x_3 := \alpha$ , that is,

$\begin{bmatrix} -\beta - \frac{1}{2}\alpha \\ \beta \\ \alpha \end{bmatrix} = \beta \begin{bmatrix} -1 \\ 1 \\ 0 \end{bmatrix} + \frac{\alpha}{2} \begin{bmatrix} -1 \\ 0 \\ 2 \end{bmatrix}$ . We have two linearly independent vectors  $v_1 = \begin{bmatrix} -1 \\ 1 \\ 0 \end{bmatrix}, v_2 = \begin{bmatrix} -1 \\ 0 \\ 2 \end{bmatrix}$ . They span a two-dimensional space,

so the geometric multiplicity is equal to  $n_1 = 2$ .

Let  $\lambda_2 = 10$ . For  $\lambda$  in the equation  $(A - \lambda)x = 0$  we substitute 10 and solve the system  $\begin{bmatrix} 5 - 10 & 4 & 2 \\ 4 & 5 - 10 & 2 \\ 2 & 2 & 2 - 10 \end{bmatrix} \begin{bmatrix} x_1 \\ x_2 \\ x_3 \end{bmatrix} = \begin{bmatrix} 0 \\ 0 \\ 0 \end{bmatrix}$ .



We transform the expanded matrix (by operating on rows)

$$\begin{aligned}
 & \left[ \begin{array}{ccc|c} -5 & 4 & 2 & 0 \\ 4 & -5 & 2 & 0 \\ 2 & 2 & -8 & 0 \end{array} \right] \xleftrightarrow{w_1+w_2 \rightarrow w_1} \left[ \begin{array}{ccc|c} -1 & -1 & 4 & 0 \\ 4 & -5 & 2 & 0 \\ 2 & 2 & -8 & 0 \end{array} \right] \xleftrightarrow{w_3+2w_1 \rightarrow w_3, w_2+w_1 \rightarrow w_2} \\
 & \left[ \begin{array}{ccc|c} -1 & -1 & 4 & 0 \\ 3 & -6 & 6 & 0 \\ 0 & 0 & 0 & 0 \end{array} \right] \xleftrightarrow{\frac{1}{3}w_2 \rightarrow w_2} \left[ \begin{array}{ccc|c} -1 & -1 & 4 & 0 \\ 1 & -2 & 2 & 0 \\ 0 & 0 & 0 & 0 \end{array} \right] \xleftrightarrow{w_2+w_1 \rightarrow w_2} \\
 & \left[ \begin{array}{ccc|c} -1 & -1 & 4 & 0 \\ 0 & -3 & 6 & 0 \\ 0 & 0 & 0 & 0 \end{array} \right] \xleftrightarrow{\frac{1}{3}w_2 \rightarrow w_2} \left[ \begin{array}{ccc|c} -1 & -1 & 4 & 0 \\ 0 & -1 & 2 & 0 \\ 0 & 0 & 0 & 0 \end{array} \right] \xleftrightarrow{-w_1 \rightarrow w_1, -w_2 \rightarrow w_2} \left[ \begin{array}{ccc|c} 1 & 1 & -4 & 0 \\ 0 & 1 & -2 & 0 \\ 0 & 0 & 0 & 0 \end{array} \right].
 \end{aligned}$$

We obtain the system of linear equations 
$$\begin{cases} x_1 + x_2 - 4x_3 = 0 \\ x_2 - 2x_3 = 0 \end{cases}.$$

After substituting for  $x_3 := \alpha$  and solving, we get  $x_1 := 2\alpha$ ,  $x_2 := 2\alpha$  and  $x_3 := \alpha$ . We have one linearly independent vector  $\alpha \begin{bmatrix} 2 \\ 2 \\ 1 \end{bmatrix}$ . Thus,

we have  $v_3 = \begin{bmatrix} 2 \\ 2 \\ 1 \end{bmatrix}$ . Hence the geometric multiplicity  $n_2 = 1$ . Matrix

$P = [v_1 v_2 v_3] = \begin{bmatrix} -1 & -1 & 2 \\ 1 & 0 & 2 \\ 0 & 2 & 1 \end{bmatrix}$  diagonalizes the matrix  $A$ . To

check this, we will first determine the inverse matrix of the matrix

$$\begin{bmatrix} -1 & -1 & 2 \\ 1 & 0 & 2 \\ 0 & 2 & 1 \end{bmatrix}.$$

We will use the Gaussian elimination method:

$$\begin{aligned}
 & \left[ \begin{array}{ccc|ccc} -1 & -1 & 2 & 1 & 0 & 0 \\ 1 & 0 & 2 & 0 & 1 & 0 \\ 0 & 2 & 1 & 0 & 0 & 1 \end{array} \right] \xleftrightarrow{-w_1 \rightarrow w_1, w_2+w_1 \rightarrow w_2} \left[ \begin{array}{ccc|ccc} 1 & 1 & -2 & -1 & 0 & 0 \\ 0 & -1 & 4 & 1 & 1 & 0 \\ 0 & 2 & 1 & 0 & 0 & 1 \end{array} \right] \xleftrightarrow{w_1+w_2 \rightarrow w_1} \\
 & \left[ \begin{array}{ccc|ccc} 1 & 0 & 2 & 0 & 1 & 0 \\ 0 & -1 & 4 & 1 & 1 & 0 \\ 0 & 2 & 1 & 0 & 0 & 1 \end{array} \right] \xleftrightarrow{w_3+2w_2 \rightarrow w_3} \left[ \begin{array}{ccc|ccc} 1 & 0 & 2 & 0 & 1 & 0 \\ 0 & -1 & 4 & 1 & 1 & 0 \\ 0 & 0 & 9 & 2 & 2 & 1 \end{array} \right] \\
 & \xleftrightarrow{w_1 - \frac{2}{9}w_3 \rightarrow w_1, -w_2 + \frac{4}{9}w_3 \rightarrow w_2, \frac{1}{9}w_3 \rightarrow w_3} \left[ \begin{array}{ccc|ccc} 1 & 0 & 0 & -\frac{4}{9} & -\frac{5}{9} & -\frac{2}{9} \\ 0 & 1 & 0 & -\frac{1}{9} & -\frac{1}{9} & \frac{4}{9} \\ 0 & 0 & 1 & \frac{2}{9} & \frac{2}{9} & \frac{1}{9} \end{array} \right].
 \end{aligned}$$

We get the matrix  $P^{-1} = \begin{bmatrix} -\frac{4}{9} & \frac{5}{9} & -\frac{2}{9} \\ -\frac{1}{9} & -\frac{1}{9} & \frac{4}{9} \\ \frac{2}{9} & \frac{2}{9} & \frac{1}{9} \end{bmatrix}$ .

We check the correctness of the determination of the inverse of the matrix by multiplication:

$$\begin{bmatrix} -\frac{4}{9} & \frac{5}{9} & -\frac{2}{9} \\ -\frac{1}{9} & -\frac{1}{9} & \frac{4}{9} \\ \frac{2}{9} & \frac{2}{9} & \frac{1}{9} \end{bmatrix} \begin{bmatrix} -1 & -1 & 2 \\ 1 & 0 & 2 \\ 0 & 2 & 1 \end{bmatrix} = \begin{bmatrix} 1 & 0 & 0 \\ 0 & 1 & 0 \\ 0 & 0 & 1 \end{bmatrix}.$$

Finally, we verify that indeed the matrix  $P$  diagonalizes  $A$ . We realize this by multiplying

$$\begin{aligned} & \begin{bmatrix} -\frac{4}{9} & \frac{5}{9} & -\frac{2}{9} \\ -\frac{1}{9} & -\frac{1}{9} & \frac{4}{9} \\ \frac{2}{9} & \frac{2}{9} & \frac{1}{9} \end{bmatrix} \begin{bmatrix} 5 & 4 & 2 \\ 4 & 5 & 2 \\ 2 & 2 & 2 \end{bmatrix} \begin{bmatrix} -1 & -1 & 2 \\ 1 & 0 & 2 \\ 0 & 2 & 1 \end{bmatrix} = \\ & = \begin{bmatrix} -\frac{4}{9} & \frac{5}{9} & -\frac{2}{9} \\ -\frac{1}{9} & -\frac{1}{9} & \frac{4}{9} \\ \frac{20}{9} & \frac{20}{9} & \frac{10}{9} \end{bmatrix} \begin{bmatrix} -1 & -1 & 2 \\ 1 & 0 & 2 \\ 0 & 2 & 1 \end{bmatrix} = \begin{bmatrix} 1 & 0 & 0 \\ 0 & 1 & 0 \\ 0 & 0 & 10 \end{bmatrix} = \begin{bmatrix} \lambda_1 & 0 & 0 \\ 0 & \lambda_1 & 0 \\ 0 & 0 & \lambda_2 \end{bmatrix}. \end{aligned}$$

## 8.2. Second-order ordinary differential equation

- a) **Free mechanical vibrations.** May a material point of mass  $m$  ( $m > 0$ ) be subjected to an elastic force proportional to the deflection  $x$  ( $x(t)$  is a function of time  $t$ ) and directed always toward the balance point  $O$ . Denoting the coefficient of proportionality by  $k$ , based on the laws of mechanics we write

$$m \frac{d^2 x}{dt^2} = -kx. \quad (8.4)$$

Equivalently, we can write

$$m \frac{d^2 x}{dt^2} + kx = 0. \quad (8.5)$$

In other notations for representing derivatives, we have equivalent notations for the equation

$$m\ddot{x} + kx = 0 \quad \text{or} \quad mx'' + kx = 0. \quad (8.6)$$

We can also represent the equation in the form

$$x'' + \frac{k}{m}x = 0. \quad (8.7)$$

This is a *linear differential equation of second order homogeneous* with constant coefficients.

- b) **Damped mechanical vibration.** Now suppose that on a material point of mass  $m$ , in addition to the elastic force, there is a resistive force of the medium proportional to the velocity of  $-\lambda \frac{dx}{dt}$ , where  $\lambda$  is the coefficient of resistivity. We then obtain

$$m \frac{d^2x}{dt^2} = -kx - \lambda \frac{dx}{dt}, \quad (8.8)$$

i.e.

$$x'' + \frac{\lambda}{m}x' + \frac{k}{m}x = 0. \quad (8.9)$$

- c) **Forced mechanical vibration.** We can also consider the situation in which there is an additional force  $f(t)$  forcing the vibration. We then obtain an inhomogeneous equation

$$x'' + \frac{\lambda}{m}x' + \frac{k}{m}x = f(t). \quad (8.10)$$

### 8.3. Linear differential equations of order two with constant coefficients

To solve problems of oscillatory motion, we will recall how to solve a linear differential equation of the second order with constant coefficients and an unknown function  $y(x)$ , which we write in the form

$$y'' + py' + qy = f(x), \quad (8.11)$$

where  $p, q$  are given real numbers (constants),  $f(x)$  is a given continuous function. The homogeneous equation (8.11) is then of the form

$$y'' + py' + qy = 0. \quad (8.12)$$

We will first determine the so-called basic system of integrals of the equation (8.12), which is the base of the linear space that is the solution of (8.12). We will look for these integrals in the form of an exponential function

$$y = e^{rx}. \quad (8.13)$$

Let's calculate  $y' = re^{rx}$ ,  $y'' = r^2e^{rx}$ . After substitution, we have

$$r^2 + pr + q = 0. \quad (8.14)$$

The quadratic equation (8.14) is called the characteristic equation for the equation (8.12). Then,  $\Delta = p^2 - 4q$ . We have three cases:

- The case of  $\Delta > 0$ . The equation then has two different real roots  $r_1$  and  $r_2$ . It is easy to check that the functions  $y_1(x) = e^{r_1x}$  and  $y_2(x) = e^{r_2x}$  are the system of fundamental integrals (we calculate the Wronskian  $W(x) = \begin{vmatrix} y_1(x) & y_2(x) \\ y_1'(x) & y_2'(x) \end{vmatrix}$ , which should be different from zero). Indeed,  $W(x) = \begin{vmatrix} e^{r_1x} & e^{r_2x} \\ r_1e^{r_1x} & r_2e^{r_2x} \end{vmatrix} = e^{r_1x}e^{r_2x} \begin{vmatrix} 1 & 1 \\ r_1 & r_2 \end{vmatrix} = e^{r_1x}e^{r_2x}(r_1 - r_2) \neq 0$ , after all  $r_1 \neq r_2$ .

We can find the particular integrals of the equation (8.11) by using the prediction method or by using the method of invariance of constants.

**Example 8.2.** Find the general solution of the equation  $y'' + 3y' + 2y = 0$ .

- The case of  $\Delta = 0$ . The equation then has one real double root  $r_0$ . It is easy to check that the functions  $y_1(x) = e^{r_0x}$  and  $y_2(x) = xe^{r_0x}$  are a system of fundamental integrals (we check that  $y_2(x) = xe^{r_0x}$  is a special integral and compute the Wronskian).

**Example 8.3.** Find the general solution of the equation  $y'' + 2y' + y = 0$ .

- The case of  $\Delta < 0$ . The equation then has two different conjugate complex roots  $r_1 = \alpha + \beta i$  i  $r_2 = \alpha - \beta i$ . Then it turns out that functions of the form  $y_1(x) = e^{\alpha x} \sin \beta x$  and  $y_2(x) = e^{\alpha x} \cos \beta x$  constitute a system of fundamental integrals (we check that they are special integrals and calculate the Wronskian).

**Example 8.4.** Find the general solution of the equation  $y'' + 4y = 0$ .

**Example 8.5.** (formulation of the task: Prof. C. Miedziałowski on the basis of [52]) A horizontally loaded building is considered. The static system is composed of two strips conventionally cut along the vertical section (Fig. 8.1). Let  $T(z)$  denote the sum of shear forces (cutting force) acting along the cross-section (Fig. 8.1). The force  $T(z)$  satisfies the following differential equation [52]

$$T''(z) - \alpha^2 T(z) = -\beta(z), \quad (8.15)$$

where  $\alpha^2 = \left( \frac{p_2}{E_2 F_2} - \frac{p_1}{E_1 F_1} \right)$ ,  $\beta(z) = \left( \frac{p_2}{E_2 F_2} - \frac{p_1}{E_1 F_1} \right) z = pz$ ,  $p = \frac{p_2}{E_2 F_2} - \frac{p_1}{E_1 F_1}$ , with  $E_i$  – Young's modulus,  $F_i$  – cross section,  $p_i$  – load,  $i = 1, 2$ . The initial conditions are of the form  $T(0) = 0$ ,  $T'(H) = 0$ .

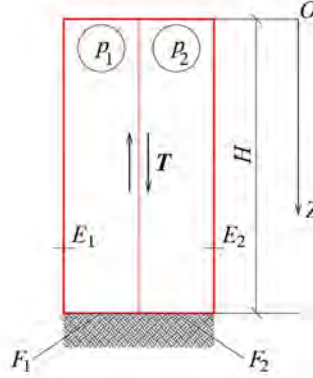


Figure 8.1: Static system composed of two bands (by E. Koźniewski based on [52])

The solution begins by writing the equation according to (8.12)

$$T''(z) - \alpha^2 T(z) = 0. \quad (8.16)$$

The general solution of the equation (8.16) is of the form

$$T^*(z) = c_1 e^{\alpha z} + c_2 e^{-\alpha z}. \quad (8.17)$$

Let's find the particular solution of (8.11), taking  $T_s(z) = az$ . Hence  $T'_s(z) = a$ ,  $T''_s(z) = 0$ . After substituting into (8.15) we get  $-\alpha^2 az = -pz \leftrightarrow -\alpha^2 a = -p \leftrightarrow a = \frac{p}{\alpha^2}$ . Thus, the general solution of the inhomogeneous equation is of the form

$$T(z) = c_1 e^{\alpha z} + c_2 e^{-\alpha z} = \frac{p}{\alpha^2} z. \quad (8.18)$$

After taking into account the initial conditions, we have  $c_1 + c_2 = 0$ ,  $c_1 \alpha e^{\alpha H} - c_2 \alpha e^{-\alpha H} + \frac{p}{\alpha^2} = 0$ . Solving the system of equations, we get:  $c_2 = -c_1$ ,  $c_1 = \frac{-\frac{p}{\alpha^2}}{\alpha^3(e^{\alpha H} + e^{-\alpha H})} \leftrightarrow c_1 = \frac{-\frac{p}{\alpha^2}}{\alpha^3(e^{\alpha H} + e^{-\alpha H})}$ ,  $c_2 = \frac{\frac{p}{\alpha^2}}{\alpha^3(e^{\alpha H} + e^{-\alpha H})}$ . Given that  $\cosh(x) = \frac{e^x + e^{-x}}{2}$  (the definition of hyperbolic cosine), the values

of  $c_1$  and  $c_2$  we can write  $c_1 = \frac{-p}{2\alpha^3 \cosh(\alpha H)}$ ,  $c_2 = \frac{p}{2\alpha^3 \cosh(\alpha H)}$ . Therefore,  $T(z) = \frac{-p}{\alpha^3 \cosh(\alpha H)} \frac{1}{2} (e^{\alpha z} - e^{-\alpha z}) + \frac{p}{\alpha^2} z$ , so (as a final solution)

$$\begin{aligned} T(z) &= \frac{-p}{\alpha^3 \cosh(\alpha H)} \sinh(\alpha z) + \frac{p}{\alpha^2} z = \\ &= \frac{p}{\alpha^2} \left( z - \frac{1}{\alpha \cosh(\alpha H)} \sinh(\alpha z) \right). \end{aligned} \quad (8.19)$$

## 8.4. The problem of vibrations in structural mechanics issues

The vibration of a structure with  $n$  degrees of freedom is described by an equation of motion of the form [53]

$$Mq''(t) + Cq'(t) + Kq(t) = F(t), \quad (8.20)$$

with initial conditions  $q(0) = q_0$ ,  $q'(0) = q'_0$ , where:

$M, C, K$  – mass, damping and stiffness matrices, respectively,

$q''(t), q'(t), q(t)$  – vectors of acceleration, velocity and generalized displacement, respectively,

$F(t)$  – external loads.

Taking the zero vector on the right side, we get the damped free vibration of the system (structure):

$$Mq''(t) + Cq'(t) + Kq(t) = 0. \quad (8.21)$$

We predict solutions in the form

$$q(t) = ue^{\lambda t}, \quad (8.22)$$

where  $u$  and  $\lambda$  are constants (in general, complex). According to (8.21) we obtain an equation of the form

$$M\lambda^2 + C\lambda + K = 0. \quad (8.23)$$

After zeroing the damping matrix  $C$ , we get the undamped free vibration of the system

$$Mq''(t) + Kq(t) = 0. \quad (8.24)$$

This is a system of homogeneous differential equations with constant coefficients. The solution is predicted in the form

$$q(t) = q_a \sin(\omega t), \quad (8.25)$$

where:

$q_a$  – vector of amplitudes also known as the vector of vibration form,

$\omega$  – angular frequency [rad],

$f = \frac{\omega}{2\pi}$  – frequency [Hz],

$T = \frac{1}{f}$  – period [s].

After differentiating twice

$$q''(t) = -\omega^2 q_a \sin(\omega t), \quad (8.26)$$

and substituting into (8.24) we get

$$(K - \omega^2 M)q_a = 0. \quad (8.27)$$

Substituting  $\lambda = \omega^2$ , we have a linear generalized eigenproblem (non-standard)

$$(K - \lambda M)q_a = 0. \quad (8.28)$$

It is solved by determining the characteristic polynomial, calculating the determinant of  $\det |K - \lambda M| = 0$  and solving the equation. However, this is inconvenient and worth using only for small systems. The generalized eigenproblem is solved by first reducing it to a standard eigenproblem of the form

$$(H - \Lambda I)Y = 0, \quad (8.29)$$

where:

$H$  – symmetric matrix,

$I$  – unit matrix,

$Y$  – eigenvector,

$\Lambda$  – eigenvalues of matrix  $H$ .

Multiplying the equation (8.28) by  $M^{-1}$ , we get the following

$$(M^{-1}K - \lambda I)q_a = 0. \quad (8.30)$$

After substituting  $q_a = (L^T)^{-1}Y$  in the equation (8.30) we get the following

$$(M^{-1}K - \lambda I)(L^T)^{-1}Y = 0. \quad (8.31)$$

Taking  $M = LL^T$  and considering the equality  $M^{-1} = (LL^T)^{-1} = (L^T)^{-1}L^{-1}$ , we have

$$\left( (L^T)^{-1}L^{-1}K(L^T)^{-1} - \lambda I(L^T)^{-1} \right) Y = 0. \quad (8.32)$$

Multiply again (8.32) by  $L^T$  from the right and you get

$$\left( L^T (L^T)^{-1} L^{-1} K (L^T)^{-1} - \lambda L^T I (L^T)^{-1} \right) Y = 0. \quad (8.33)$$

After simplifying the transformations, we have  $L^T (L^T)^{-1} = I$ ,  $IL^{-1} = L^{-1}$

$$\left( L^{-1} K (L^T)^{-1} - \lambda I \right) Y = 0, \quad (8.34)$$

and after substituting  $H = L^{-1} K (L^T)^{-1}$  we have (8.29), where  $H$  is a symmetric matrix, after all  $H^T = H$ .

## 8.5. Banachiewicz – Cholesky decomposition

Since the matrix  $M^{-1}K$  discussed in chapter 8.4 is not symmetric, although  $M$  is symmetric, the symmetrization of the matrix is done by *Banachiewicz – Cholesky decomposition*. If a matrix  $A$  is symmetric and positively definite ( $X^T A X > 0$  for every  $X$  such that  $X \neq 0$ ), then there exists a lower triangular matrix  $L$  such that  $A = LL^T$ .

Banachiewicz – Cholesky's method involves replacing a single system of equations with  $n$  unknowns described by a full matrix

$$AX = B \Leftrightarrow (LL^T)X = B \Leftrightarrow L(L^T X) = B \Leftrightarrow L^T X = Y \text{ i } LY = B \quad (8.35)$$

two systems of equations also with  $n$  unknowns, but described by triangular matrices

$$L^T X = Y, \quad (8.36)$$

$$LY = B. \quad (8.37)$$

The matrix  $L$  is determined according to the formulas

$$\begin{aligned} l_{ii} &= \sqrt{a_{ii} - \sum_{k=1}^{i-1} l_{ik}^2}, & i &= 1, 2, \dots, n, \\ l_{ji} &= \left( a_{ji} - \sum_{k=1}^{i-1} l_{jk} l_{ik} \right) \frac{1}{l_{ii}}, & j &= 1, 2, \dots, i-1. \end{aligned} \quad (8.38)$$

**Example 8.6.** Solve the equation  $AX = B$ , where

$$A = \begin{bmatrix} 4 & 2 & 2 \\ 2 & 5 & 3 \\ 2 & 3 & 6 \end{bmatrix}, B = \begin{bmatrix} 4 \\ 3 \\ 2 \end{bmatrix}. \quad (8.39)$$



**Solution.** We present  $A = LL^T$ . Using the formulas (8.38)

$$\begin{aligned} i = 1 : \quad l_{11} &= \sqrt{4} = 2, & l_{21} &= \frac{2}{2} = 1, & l_{31} &= \frac{2}{2} = 1, \\ i = 2 : \quad l_{22} &= \sqrt{5 - 1^2} = 2, & l_{32} &= \frac{3 - 1 \cdot 1}{2} = 1, \\ i = 3 : \quad l_{33} &= \sqrt{6 - 1 \cdot 1 - 1 \cdot 1} = 2 \end{aligned} \quad (8.40)$$

we finally get the distribution  $\begin{bmatrix} 4 & 2 & 2 \\ 2 & 5 & 3 \\ 2 & 3 & 6 \end{bmatrix} = \begin{bmatrix} 2 & 0 & 0 \\ 1 & 2 & 0 \\ 1 & 1 & 2 \end{bmatrix} \begin{bmatrix} 2 & 1 & 1 \\ 0 & 2 & 1 \\ 0 & 0 & 2 \end{bmatrix}$ . For a small system of equations, it is possible to do the decomposition without using the formulas (8.38) (of course, then we can not talk about the use of this scheme in computer algorithms). We multiply the matrices

$$\begin{array}{c|c} & \begin{bmatrix} l_{11} & l_{12} & l_{13} \\ 0 & l_{22} & l_{23} \\ 0 & 0 & l_{33} \end{bmatrix} \\ \hline \begin{bmatrix} l_{11} & 0 & 0 \\ l_{21} & l_{22} & 0 \\ l_{31} & l_{32} & l_{33} \end{bmatrix} & \begin{bmatrix} 4 & 2 & 2 \\ 2 & 5 & 3 \\ 2 & 3 & 6 \end{bmatrix} \end{array}$$

$$\begin{aligned} l_{11}^2 &= 4 \rightarrow l_{11} = 2; \\ l_{11} \cdot l_{12} &= 2 \rightarrow l_{12} = 1; \\ l_{11} \cdot l_{13} &= 2 \rightarrow l_{13} = 1; \\ l_{21} \cdot l_{11} &= 2 \rightarrow l_{21} = 1; \\ l_{21} \cdot l_{12} + l_{22}^2 &= 5 \rightarrow 1 \cdot 1 + l_{22}^2 = 5 \rightarrow l_{22} = 2; \\ l_{21} \cdot l_{13} + l_{22} \cdot l_{23} &= 3 \rightarrow 1 \cdot 1 + 2 \cdot l_{23} = 3 \rightarrow l_{23} = 1; \\ l_{31} \cdot l_{11} &= 2 \rightarrow l_{31} = 1; \\ l_{31} \cdot l_{12} + l_{32} \cdot l_{22} &= 3 \rightarrow 1 \cdot 1 + l_{32} \cdot 2 = 3 \rightarrow l_{32} = 1; \\ l_{31} \cdot l_{13} + l_{32} \cdot l_{23} + l_{33}^2 &= 6 \rightarrow 1 \cdot 1 + 1 \cdot 1 + l_{33}^2 = 6 \rightarrow l_{33} = 2, \end{aligned}$$

that is, we have

$$\begin{aligned} \begin{bmatrix} 4 & 2 & 2 \\ 2 & 5 & 3 \\ 2 & 3 & 6 \end{bmatrix} \begin{bmatrix} x_1 \\ x_2 \\ x_3 \end{bmatrix} &= \begin{bmatrix} 4 \\ 3 \\ 2 \end{bmatrix} \leftrightarrow \left( \begin{bmatrix} 2 & 0 & 0 \\ 1 & 2 & 0 \\ 1 & 1 & 2 \end{bmatrix} \begin{bmatrix} 2 & 1 & 1 \\ 0 & 2 & 1 \\ 0 & 0 & 2 \end{bmatrix} \right) \begin{bmatrix} x_1 \\ x_2 \\ x_3 \end{bmatrix} = \begin{bmatrix} 4 \\ 3 \\ 2 \end{bmatrix} \leftrightarrow \\ \leftrightarrow \begin{bmatrix} 2 & 0 & 0 \\ 1 & 2 & 0 \\ 1 & 1 & 2 \end{bmatrix} \left( \begin{bmatrix} 2 & 1 & 1 \\ 0 & 2 & 1 \\ 0 & 0 & 2 \end{bmatrix} \begin{bmatrix} x_1 \\ x_2 \\ x_3 \end{bmatrix} \right) &= \begin{bmatrix} 4 \\ 3 \\ 2 \end{bmatrix} \leftrightarrow \begin{bmatrix} 2 & 1 & 1 \\ 0 & 2 & 1 \\ 0 & 0 & 2 \end{bmatrix} \begin{bmatrix} x_1 \\ x_2 \\ x_3 \end{bmatrix} = \begin{bmatrix} y_1 \\ y_2 \\ y_3 \end{bmatrix}, \\ \begin{bmatrix} 2 & 0 & 0 \\ 1 & 2 & 0 \\ 1 & 1 & 2 \end{bmatrix} \begin{bmatrix} y_1 \\ y_2 \\ y_3 \end{bmatrix} &= \begin{bmatrix} 4 \\ 3 \\ 2 \end{bmatrix}. \end{aligned}$$

Thus, we obtained two systems of equations

$$\begin{bmatrix} 2 & 1 & 1 \\ 0 & 2 & 1 \\ 0 & 0 & 2 \end{bmatrix} \begin{bmatrix} x_1 \\ x_2 \\ x_3 \end{bmatrix} = \begin{bmatrix} y_1 \\ y_2 \\ y_3 \end{bmatrix}, \quad (8.41)$$

$$\begin{bmatrix} 2 & 0 & 0 \\ 1 & 2 & 0 \\ 1 & 1 & 2 \end{bmatrix} \begin{bmatrix} y_1 \\ y_2 \\ y_3 \end{bmatrix} = \begin{bmatrix} 4 \\ 3 \\ 2 \end{bmatrix}. \quad (8.42)$$

First we will solve the second system, we find  $y_1 = 2$  from the first equation,  $y_2 = \frac{1}{2}$  from the second equation, substituting for  $y_1 = 2$ ,  $y_3 = \frac{1}{4}$  from the third equation, substituting for  $y_1 = 2$ ,  $y_2 = \frac{1}{2}$ , finally we have:

$$\begin{cases} 2y_1 = 4 \\ y_1 + 2y_2 = 3 \\ y_1 + y_2 + 2y_3 = 2 \end{cases} \leftrightarrow \begin{bmatrix} y_1 \\ y_2 \\ y_3 \end{bmatrix} = \begin{bmatrix} 2 \\ \frac{1}{2} \\ -\frac{1}{4} \end{bmatrix}. \quad (8.43)$$

Then, after substituting for  $Y = \begin{bmatrix} y_1 \\ y_2 \\ y_3 \end{bmatrix} = \begin{bmatrix} 2 \\ \frac{1}{2} \\ -\frac{1}{4} \end{bmatrix}$ , we solve the first system, ie.  $\begin{bmatrix} 2 & 1 & 1 \\ 0 & 2 & 1 \\ 0 & 0 & 2 \end{bmatrix} \begin{bmatrix} x_1 \\ x_2 \\ x_3 \end{bmatrix} = \begin{bmatrix} 2 \\ \frac{1}{2} \\ -\frac{1}{4} \end{bmatrix}$ , i.e.  $\begin{cases} x_2 + x_3 = 2 \\ x_2 + x_3 = \frac{1}{2} \\ 2x_3 = -\frac{1}{4} \end{cases}$ .

Now we start with the last equation  $2x_3 = -\frac{1}{4} \leftrightarrow x_3 = -\frac{1}{8}$ , substituting for  $x_3 = -\frac{1}{8}$  in the second equation we get  $2x_2 - \frac{1}{8} = \frac{1}{2} \leftrightarrow x_2 = \frac{5}{16}$ , substituting for  $x_3 = -\frac{1}{8}$  and for  $x_2 = \frac{5}{16}$  we get  $2x_1 + \frac{5}{16} - \frac{1}{8} = 2 \leftrightarrow x_1 = \frac{29}{32}$ . Thus, the solution of the system (8.39) is of the form  $x_1 = \frac{29}{32}$ ,  $x_2 = \frac{5}{16}$ ,  $x_3 = -\frac{1}{8}$ .

When the matrices  $M$  and  $K$  are symmetric, we can use just the Banachiewicz method. After decomposing  $M = LL^T$ , this is possible because usually in applications, especially in the finite element method, the matrix  $M$  is symmetric and positively defined. We write down first

$$M^{-1} = (LL^T)^{-1} = (L^T)^{-1}L^{-1}. \quad (8.44)$$

We can find  $H$  a matrix similar to  $M^{-1}K$

$$\begin{aligned} L^T M^{-1} K (L^T)^{-1} &= L^T (L^T)^{-1} L^{-1} K (L^T)^{-1} = \\ &= L^{-1} K (L^T)^{-1} = L^{-1} K (L^{-1})^T = H. \end{aligned} \quad (8.45)$$

The matrix  $H$  thus has the same spectrum (set of eigenvalues) as  $M^{-1}K$ .

It is worth noting that for any matrix  $B$  the matrix  $BB^T$  is symmetric and if  $B$  is nonsingular, then  $BB^T$  is positively definite. Let's check this:

1. Is  $(BB^T)^T = BB^T$ ? Since  $(UV)^T = V^T U^T$ , we have  $(BB^T)^T = (B^T)^T B^T = BB^T$ . So the matrix  $BB^T$  is symmetric.
2.  $X^T(B^T B)X = (BX)^T BX = \|BX\|^2 > 0$  for  $X > 0$ . The matrix  $B^T B$  is thus positively defined.

This note allows us to obtain examples of decomposable matrices by the Banachiewicz – Cholesky method.

## 8.6. Problems

1. Diagonalize the matrix or show that the matrix is not diagonalizable:

$$\text{a) } \begin{bmatrix} 3 & 2 \\ 4 & 1 \end{bmatrix}; \quad \text{f) } \begin{bmatrix} 2 & 1 & 0 \\ -6 & 1 & -6 \\ -3 & 1 & -1 \end{bmatrix}; \quad \text{j) } \begin{bmatrix} 1 & 0 & 4 \\ 0 & 3 & 0 \\ 1 & 0 & 1 \end{bmatrix};$$

$$\text{b) } \begin{bmatrix} 3 & 2 \\ 10 & 2 \end{bmatrix}; \quad \text{g) } \begin{bmatrix} 3 & 4 \\ 2 & 1 \end{bmatrix}; \quad \text{k) } \begin{bmatrix} 1 & 1 \\ 4 & 1 \end{bmatrix};$$

$$\text{c) } \begin{bmatrix} 2 & 1 & 0 \\ 0 & 3 & 1 \\ 0 & 0 & 2 \end{bmatrix} \quad \text{h) } \begin{bmatrix} 1 & 0 & 0 \\ 0 & 2 & 1 \\ 0 & 0 & 2 \end{bmatrix}; \quad \text{l) } \begin{bmatrix} -1 & 0 & -1 \\ 3 & 2 & 3 \\ -3 & 0 & 1 \end{bmatrix};$$

$$\text{d) } \begin{bmatrix} 2 & -1 & 1 \\ 3 & -2 & -3 \\ -1 & 1 & 2 \end{bmatrix}; \quad \text{i) } \begin{bmatrix} 1 & 5 \\ 0 & 3 \end{bmatrix}; \quad \text{m) } \begin{bmatrix} 1 & 2 & 0 \\ 0 & 2 & 0 \\ -2 & -2 & -1 \end{bmatrix};$$

$$\text{e) } \begin{bmatrix} 1 & -1 & -1 \\ 1 & 1 & 0 \\ 3 & 0 & 1 \end{bmatrix}.$$

2. Check that  $\begin{bmatrix} 1 & 0 & 0 \\ 0 & 1 & 0 \\ 0 & 0 & 1 \end{bmatrix}$ ,  $\begin{bmatrix} 1 & 1 & 1 \\ 0 & 1 & 1 \\ 0 & 0 & 1 \end{bmatrix}$  are not similar even though they have the same eigenvalues.

3. Let  $A$  and  $B$  be the matrices of rotation  $\begin{cases} x' = x \cos \alpha - y \sin \alpha \\ y' = x \sin \alpha + y \cos \alpha \end{cases}$  for  $\alpha = \frac{\pi}{2}$  and  $\alpha = \frac{\pi}{4}$ , respectively. Are these matrices similar?
4. Do the triangularization by the Banachiewicz – Cholesky method of the matrices:

$$\text{a) } \begin{bmatrix} 4 & -2 & 2 \\ -2 & 2 & 2 \\ 2 & 2 & 14 \end{bmatrix}; \quad \text{b) } \begin{bmatrix} 2 & 1 \\ 1 & 2 \end{bmatrix}; \quad \text{c) } \begin{bmatrix} 3 & 1 \\ 1 & 2 \end{bmatrix}$$

and solve the corresponding systems of equations:

$$\text{a')} \quad \begin{bmatrix} 4 & -2 & 2 \\ -2 & 2 & 2 \\ 2 & 2 & 14 \end{bmatrix} \begin{bmatrix} x_1 \\ x_2 \\ x_3 \end{bmatrix} = \begin{bmatrix} -6 \\ 4 \\ 0 \end{bmatrix};$$

$$\text{b')} \quad \begin{bmatrix} 2 & 1 \\ 1 & 2 \end{bmatrix} \begin{bmatrix} x_1 \\ x_2 \end{bmatrix} = \begin{bmatrix} 3 \\ 3 \end{bmatrix};$$

$$\text{c')} \quad \begin{bmatrix} 3 & 1 \\ 1 & 2 \end{bmatrix} \begin{bmatrix} x_1 \\ x_2 \end{bmatrix} = \begin{bmatrix} 4 \\ 3 \end{bmatrix}.$$

5. Find solutions to the equations:

$$\text{a) } x'' + \frac{k}{m}x = 0;$$

$$\text{b) } x'' + \frac{\lambda}{m}x' + \frac{k}{m}x = 0.$$

6. Solve the differential equations:

$$\text{a) } y'' - 3y' + 2y = 0;$$

$$\text{d) } y'' - 4y = 0;$$

$$\text{b) } y'' + 3y' = 0;$$

$$\text{e) } y'' + 4y' + 4y = 0;$$

$$\text{c) } y'' - 2y' + 2y = 0;$$

$$\text{f) } y'' - 6y' + 9y = 0.$$

7. Solve differential equations with initial condition:

$$\text{a) } y'' - 3y' + 2y = 0, \quad y(0) = 1, y'(0) = 3;$$

$$\text{b) } y'' - 3y' + 2y = 3x, \quad y(0) = 1, y'(0) = 3;$$

$$\text{c) } y'' + 3y' = 0, \quad y(1) = 1, y'(1) = -3;$$

$$\text{d) } y'' + 3y' = e^{2x}, \quad y(1) = 1, y'(1) = -3;$$

$$\text{e) } y'' - 2y' + 2y = 0, \quad y(\pi/4) = 1, y'(\pi/4) = -2;$$

$$\text{f) } y'' - 2y' + 2y = 1, \quad y(\pi/4) = 1, y'(\pi/4) = -2;$$

$$\text{g) } y'' - 4y = 0, \quad y(\pi/4) = 1, y'(\pi/4) = -2;$$

$$\text{h) } y'' - 4y = 8x + 4, \quad y(\pi/4) = 1, y'(\pi/4) = -2;$$

$$\text{i) } y'' + 4y' + 4y = 0, \quad y(0) = 1, y'(0) = 2;$$

$$\text{j) } y'' + 4y' + 4y = e^{3x}, \quad y(0) = 1, y'(0) = 2;$$

- k)  $y'' - 6y' + 9y = 0, \quad y(0) = 1, y'(0) = 2;$
  - l)  $y'' - 6y' + 9y = \cos x, \quad y(0) = 1, y'(0) = 2.$
8. Solve differential equations with boundary condition:
- a)  $y'' - 3y' + 2y = 0, \quad y(0) = 1, y(1) = 3;$
  - b)  $y'' - 3y' + 2y = 3x, \quad y(0) = 1, y(1) = 3;$
  - c)  $y'' + 3y' = 0, \quad y(0) = 1, y(1) = -3;$
  - d)  $y'' + 3y' = e^{2x}, \quad y(0) = 1, y(1) = -3;$
  - e)  $y'' - 2y' + 2y = 0, \quad y(0) = 1, y(\pi/4) = -2;$
  - f)  $y'' - 2y' + 2y = 1, \quad y(0) = 1, y(\pi/4) = -2;$
  - g)  $y'' - 4y = 0, \quad y(0) = 1, y(\pi/4) = -2;$
  - h)  $y'' - 4y = 8x + 4, \quad y(0) = 1, y(\pi/4) = -2;$
  - i)  $y'' + 4y' + 4y = 0, \quad y(0) = 1, y(1) = 2;$
  - j)  $y'' + 4y' + 4y = e^{3x}, \quad y(0) = 1, y(1) = 2;$
  - k)  $y'' - 6y' + 9y = 0, \quad y(0) = 1, y(1) = 2;$
  - l)  $y'' - 6y' + 9y = \cos x, \quad y(0) = 1, y(1) = 2.$

**Hint.** About the equations of oscillatory motion you can read, for example, at: [http://www.ftj.agh.edu.pl/~wierzbanowski/R\\_Harm\(7\).pdf](http://www.ftj.agh.edu.pl/~wierzbanowski/R_Harm(7).pdf) [59].

## Chapter 9

# Moisture field and membrane shape description – the boundary value problem solved by Ritz method

### 9.1. About approximate methods for solving partial differential equations [29]

Partial differential equations can be solved by the following methods: characteristics, separation of variables, integral transformations, conformal transformations, potentials, Green's function, differential, as well as the methods of: Ritz, Kantorovich, Galerkin [29] etc.

#### 9.1.1. Ritz method

Let  $\varphi_1, \varphi_2, \varphi_3, \dots$  be a sequence of linearly independent functions, and  $\Phi$  the  $m$ -dimensional space defined as the set of all linear combinations of

$$\psi_m = \sum_{k=1}^m \lambda_k \varphi_k, \quad (9.1)$$

where  $\lambda_k$  are any real (complex) numbers. Let's note that the sequence of  $\varphi_1, \varphi_2, \dots, \varphi_m$  is the base of the space  $\Phi$ .

Determining the approximate solution of a boundary problem with homogeneous conditions for a differential equation using the Ritz method involves finding the minimum of the function  $J[u]$  for which the given differential equation (Euler's condition) is a necessary condition for optimality. The Euler condition for the functional

$$J[u] = \iiint_{\Omega} F(x, y, z, u, u_x, u_y, u_z) dx dy dz$$

is of the form  $\frac{\partial F}{\partial u} - \frac{\partial}{\partial x} \frac{\partial F}{\partial u_x} - \frac{\partial}{\partial y} \frac{\partial F}{\partial u_y} - \frac{\partial}{\partial z} \frac{\partial F}{\partial u_z} = 0$ , and for the the functional

$$J[u] = \iint_D F(x, y, u, u_x, u_y) dx dy,$$

is of the form  $\frac{\partial F}{\partial u} - \frac{\partial}{\partial x} \frac{\partial F}{\partial u_x} - \frac{\partial}{\partial y} \frac{\partial F}{\partial u_y} = 0$ .

We look for this minimum in the  $m$ -dimensional space  $\Phi$ , i.e.  $\min_{(\lambda_k)} J[\psi_m]$ .

Depending on the order of the differential equation and the boundary conditions, the functions will satisfy:

a) for the Dirichlet problem

$$\forall_{P \in S} \forall_k \varphi_k|_P = 0, \quad (9.2)$$

b) for the von Neumann problem

$$\forall_{P \in S} \forall_k \left. \frac{\partial \varphi_k}{\partial n} \right|_P = 0, \quad (9.3)$$

where  $S$  is the surface bounding the area  $\omega$ , in which we are looking for a solution,  $P$  is the point of the surface of  $S$ .

For inhomogeneous Dirichlet and Neumann problems, the approximate solution is represented as follows:

$$\psi_m^* = \varphi_0 + \psi_m,$$

where  $\psi_m$  is a function of the form (9.2) composed of elements of  $\varphi_k$ , with  $\varphi_k$  satisfying the corresponding homogeneous boundary conditions, while  $\varphi_0$  satisfies the heterogeneous condition.

When solving boundary problems, it is convenient to introduce a multivariate notation of the elements of the base of the space  $\Phi$  ((for two variables – two-variable, for three variables – three-variable etc.).

**Example 9.1.** (The problem of mass and heat exchange)

We will determine the stationary moisture field  $w(x, y)$  in a porous body with the shape of an infinitely long prism with a square cross section with sidewall moisture constant over time.

The function  $w(x, y)$  satisfies the Laplace equation in the region  $Q = (0, a) \times (0, a)$

$$\frac{\partial^2 w}{\partial x^2} + \frac{\partial^2 w}{\partial y^2} = 0 \quad (9.4)$$

and the boundary conditions

$$w(0, y) = 0, \quad w(a, y) = \frac{W_0}{a}y, \quad \text{for } y \in (0, a), \quad (9.5)$$

$$w(x, 0) = 0, \quad w(x, a) = \frac{W_0}{a}x, \quad \text{for } x \in (0, a), \quad (9.6)$$

where  $W_0 > 0$ . For a functional of the following form

$$J[w] = \int_0^a \int_0^a \left[ \left( \frac{\partial w}{\partial x} \right)^2 + \left( \frac{\partial w}{\partial y} \right)^2 \right] dx dy \quad (9.7)$$

the equation (9.4) is a necessary condition for optimality. Solving the formulated boundary problem by the Ritz method, we approximate the function by an expression of the form

$$w_{MN}(x, y) = \varphi_0(x, y) + \sum_{m=1}^M \sum_{n=1}^N A_{mn} \varphi_{mn}(x, y). \quad (9.8)$$

The function  $\varphi_0(x, y)$  must satisfy the boundary conditions (9.5) and (9.6), while  $\varphi_{mn}(x, y)$  satisfies the zero boundary conditions. We assume

$$\varphi_0(x, y) = \frac{W_0}{a^2} xy, \quad (9.9)$$

$$\varphi_{mn}(x, y) = x^m y^n (x - a)(y - a), \quad (9.10)$$

the coefficients of  $A_{nm}$  are selected so that the functional

$$J[w_{MN}] = \int_0^a \int_0^a \left[ \left( \frac{\partial w_{MN}}{\partial x} \right)^2 + \left( \frac{\partial w_{MN}}{\partial y} \right)^2 \right] dx dy \quad (9.11)$$

reaches a minimum.

In further calculations, we are limited to the solution of the form ( $M = 1$ ,  $N = 1$ ).

$$w_{11}(x, y) = \frac{W_0}{a^2} xy + A_{11} xy(x - a)(y - a), \quad (9.12)$$

and thus to the determination of the coefficient  $A_{11}$ . In the calculations you can use the Wolfram Alpha program, where we can calculate the partial derivatives (Fig. 9.1).



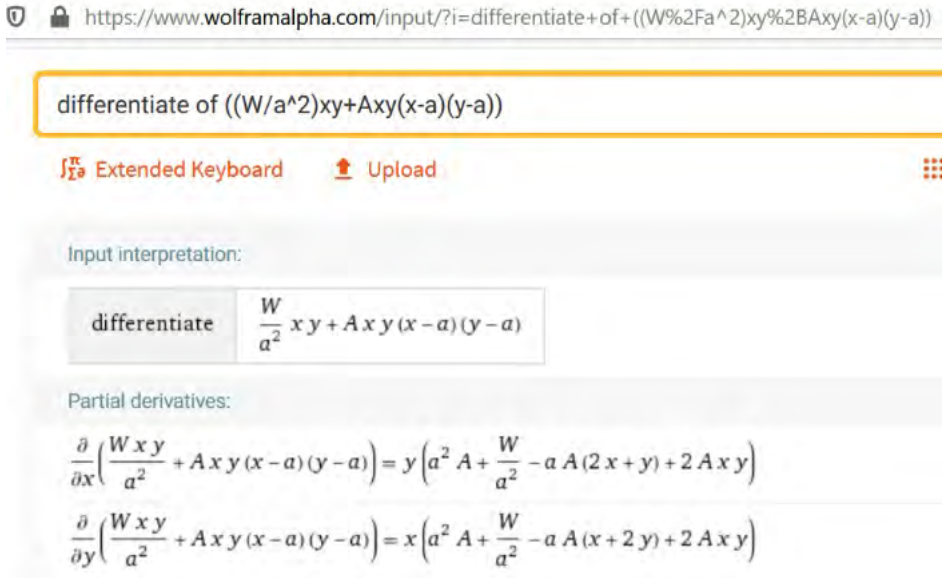


Figure 9.1: Calculation of partial derivatives, by E. Koźniewski

We square the calculated partial derivatives, sum and expand (Fig. 9.2).

expand	$\left( y \left( a^2 A + \frac{W}{a^2} + 2 A x y - a A (2 x + y) \right) \right)^2 +$ $\left( x \left( a^2 A + \frac{W}{a^2} + 2 A x y - a A (x + 2 y) \right) \right)^2$
--------	---

Result

$$\begin{aligned}
 & a^4 A^2 x^2 + a^4 A^2 y^2 + \frac{W^2 x^2}{a^4} + \frac{W^2 y^2}{a^4} - 2 a^3 A^2 x^3 - 4 a^3 A^2 x^2 y - \\
 & 4 a^3 A^2 x y^2 - 2 a^3 A^2 y^3 + a^2 A^2 x^4 + 8 a^2 A^2 x^3 y + 8 a^2 A^2 x^2 y^2 + \\
 & 8 a^2 A^2 x y^3 + a^2 A^2 y^4 + \frac{4 A W x^3 y}{a^2} + \frac{4 A W x y^3}{a^2} - 4 a A^2 x^4 y - \\
 & 8 a A^2 x^3 y^2 - 8 a A^2 x^2 y^3 - 4 a A^2 x y^4 - \frac{2 A W x^3}{a} - \frac{4 A W x^2 y}{a} - \\
 & \frac{4 A W x y^2}{a} - \frac{2 A W y^3}{a} + 4 A^2 x^4 y^2 + 4 A^2 x^2 y^4 + 2 A W x^2 + 2 A W y^2
 \end{aligned}$$

Figure 9.2: The expansion of the squares of partial derivatives, by E. Koźniewski

As a result of calculating the integral of (9.7) for  $w_{11}$ , we obtain a function  $F$  of the variable  $A_{11}$  of the form

$$J[w_{11}] = F(A_{11}) = B + CA_{11}^2. \quad (9.13)$$

This function gets to an extremum for  $A_{11} = 0$ . Therefore,  $w_{11}(x, y) = \frac{W_0}{a^2}xy$  is the solution of the boundary problem. Hence, the function  $w(x, y) = \frac{W_0}{a^2}xy$  describes the stationary moisture field.

**Example 9.2.** (The problem of mechanics – PM)

The membrane in the shape of a regular triangle with height  $a > 0$  is uniformly loaded. It is in a static state, with its edge located in the plane  $z = 0$ .

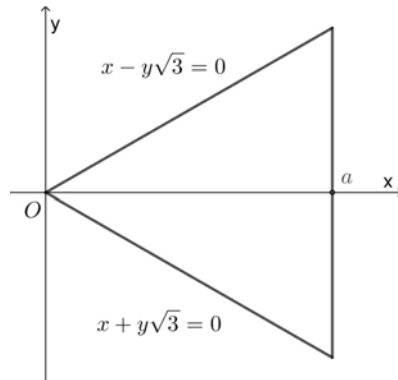


Figure 9.3: PM, by E. Koźniewski

The deformation of the membrane  $z(x, y)$  satisfies in the area

$$D = \left\{ (x, y) : x \in (0, a), y \in \left( -\frac{x}{\sqrt{3}}, \frac{x}{\sqrt{3}} \right) \right\} \quad (9.14)$$

Poisson's equation

$$\frac{\partial^2 z}{\partial x^2} + \frac{\partial^2 z}{\partial y^2} = -\frac{p}{T}, \quad (9.15)$$

where  $p > 0$  is the pressure exerted by the membrane load,  $T$  – membrane tension, with the function  $z(x, y)$  taking a value of zero at the edge of the area  $D$ .

For the functional

$$J[z] = \int_0^a \left\{ \int_{-\frac{x}{\sqrt{3}}}^{\frac{x}{\sqrt{3}}} \left[ \left( \frac{\partial z}{\partial x} \right)^2 + \left( \frac{\partial z}{\partial y} \right)^2 - 2 \frac{p}{T} z \right] dy \right\} dx \quad (9.16)$$

the equation (9.15) is a necessary condition for optimality. Solving the formulated boundary problem by the Ritz method, we approximate the function by an expression of the form

$$z_{MN}(x, y) = \sum_{m=1}^M \sum_{n=1}^N A_{mn} \varphi_{mn}(x, y). \quad (9.17)$$

The function  $\varphi_{mn}(x, y)$  must satisfy the boundary conditions (9.14). Thus, we assume the following polynomial form of the function

$$\varphi_{mn}(x, y) = (x^2 - 3y^2)(x - a)^m y^{2n-2}. \quad (9.18)$$

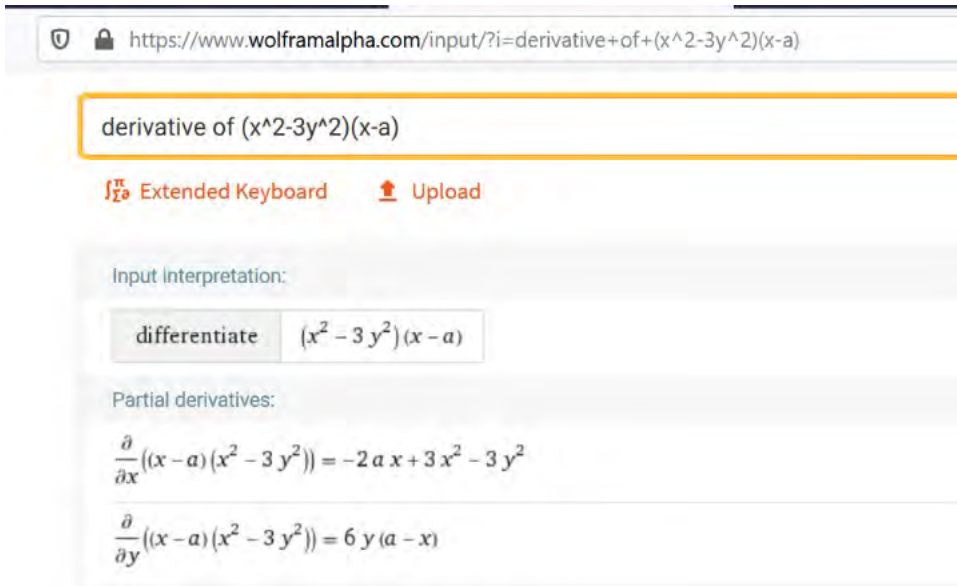
The coefficients  $A_{nm}$  are chosen so that the functional

$$J[z_{MN}] = \int_0^a \left\{ \int_{-\frac{x}{\sqrt{3}}}^{\frac{x}{\sqrt{3}}} \left[ \left( \frac{\partial z_{MN}}{\partial x} \right)^2 + \left( \frac{\partial z_{MN}}{\partial y} \right)^2 - 2 \frac{p}{T} z_{MN} \right] dy \right\} dx \quad (9.19)$$

reaches a minimum in the given class of functions. In further calculations, we restrict ourselves to an approximate solution of the form (for  $M = 1, N = 1$ )

$$z_{11}(x, y) = A_{11}(x^2 - 3y^2)(x - a), \quad (9.20)$$

and thus finding only one coefficient  $A_{11}$ , in which we can skip indices and write it as  $A$ . The derivatives of the function (9.20) will be determined in the Wolfram Alpha environment. For simplicity, we temporarily omit the coefficient  $A$ , which is a constant.



https://www.wolframalpha.com/input/?i=derivative+of+(x^2-3y^2)(x-a)

derivative of  $(x^2 - 3y^2)(x - a)$

Extended Keyboard Upload

Input interpretation:

differentiate  $(x^2 - 3y^2)(x - a)$

Partial derivatives:

$$\frac{\partial}{\partial x}((x - a)(x^2 - 3y^2)) = -2ax + 3x^2 - 3y^2$$

$$\frac{\partial}{\partial y}((x - a)(x^2 - 3y^2)) = 6y(a - x)$$

Figure 9.4: Calculation of partial derivatives in the Wolfram Alpha environment, by E. Koźniewski

By squaring the partial derivatives of the function, we get (Fig. 9.5)



https://www.wolframalpha.com/input/?i=expand+(-2ax%2B3x^2-3y^2)^2+(6y(a-x))^2

WolframAlpha computational intelligence.

expand  $(-2ax + 3x^2 - 3y^2)^2 + (6y(a - x))^2$

Extended Keyboard Upload Examples

Input interpretation:

expand  $(-2ax + 3x^2 - 3y^2)^2 + (6y(a - x))^2$

Result:

$$4a^2x^2 + 36a^2y^2 - 12ax^3 - 60axy^2 + 9x^4 + 18x^2y^2 + 9y^4$$

Figure 9.5: Expanding the sum of squares of partial derivatives in the Wolfram Alpha environment, by E. Koźniewski

Taking into account additionally the difference (the minuend of  $\frac{2p}{T}A(x^3 - 3xy^2 - ax^2 + 3y^2a)$ ), the expression under the integral will take the form

$$A^2(4a^2x^2 + 36a^2y^2 - 12ax^3 - 60axy^2 + 9x^4 + 18x^2y^2 + 9y^4) - 2\frac{p}{T}A(x^3 - 3xy^2 - ax^2 + 3y^2a).$$

Then the integral is calculated as follows

$$\begin{aligned} J[z_{MN}] &= \int_0^a \left\{ \int_{-\frac{x}{\sqrt{3}}}^{\frac{x}{\sqrt{3}}} \left[ \left( \frac{\partial z_{MN}}{\partial x} \right)^2 + \left( \frac{\partial z_{MN}}{\partial y} \right)^2 - 2\frac{p}{T}z_{MN} \right] dy \right\} dx = \\ &= \int_0^a \left\{ \int_{-\frac{x}{\sqrt{3}}}^{\frac{x}{\sqrt{3}}} [A^2(4a^2x^2 + 36a^2y^2 - 12ax^3 - 60axy^2 + 9x^4 + 18x^2y^2 + 9y^4) - \right. \\ &\quad \left. - 2\frac{p}{T}A(x^3 - 3xy^2 - ax^2 + 3y^2a)] dy \right\} dx. \end{aligned}$$

After calculating the integral of (9.19) we get the following

$$J[z_{11}] = F(A_{11}) = \frac{8a^6}{15\sqrt{3}}A_{11}^2 + \frac{4a^5p}{15\sqrt{3}T}A_{11}. \quad (9.21)$$

The coefficient  $A_{11}$  is the root of the equation

$$F'(A_{11}) = \frac{16a^6}{15\sqrt{3}}A_{11} + \frac{4a^5p}{15\sqrt{3}T} = 0, \quad (9.22)$$

hence

$$A_{11} = -\frac{p}{4aT}. \quad (9.23)$$

In view of (9.20) we have the final solution

$$z_{11}(x, y) = -\frac{p}{4aT}(x^2 - 3y^2)(x - a). \quad (9.24)$$

The obtained function satisfies both the equation (9.15), and the zero conditions at the edge, so it is a solution to the formulated boundary problem for the triangular-shaped membrane.

## 9.2. Difference method [53]

This is the most widely used numerical method. In this method, derivatives are replaced by difference quotients and the resulting equations are called difference equations. These equations relate the values of functions to each other at isolated points, which are chosen to form a regular grid (rectangular or cuboid).

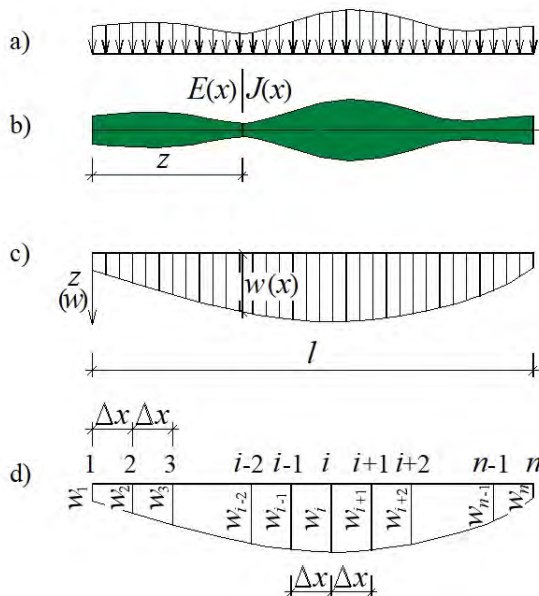


Figure 9.6: Difference method. A model of a bent rod, by E. Koźniewski based on [53]

### Example 9.3.

In the figure 9.6 the physical model of the rod bending in the plane  $OXZ$  (Fig. 9.6a,b). The searched field is the deflections  $w(x)$  ( $z(x)$ ) in the system  $OXZ$ , Fig. 9.6c). The mathematical description is expressed by the formula

$$\frac{d^2}{dx^2} \left( E(x)J(x) \frac{d^2 w}{dx^2} \right) = q(x). \quad (9.25)$$

The discretization will consist in replacing the differential operators (derivatives) with difference operators (i.e. difference quotients). In the interval  $(0, l)$  we set a finite number of points, nodes at intervals  $\Delta x$

and assign parameters to each of them ( $w$ -deflection,  $E$ -Young's modulus,  $J$ -moment of inertia,  $q_i$ -load),  $i = 1, 2, \dots, n$  (Fig. 9.6d). Then we expand the function into a Taylor series around the point  $i$  and consider its three terms.

$$w(x) = w_i + x \left. \frac{dw}{dx} \right|_i + \frac{x^2}{2} \left. \frac{d^2w}{dx^2} \right|_i. \quad (9.26)$$

This means that in the interval  $(0, l)$  we assume an interpolation function in the form of a second order polynomial. The three parameters  $w_{i-1}, w_i, w_{i+1}$  uniquely define this polynomial. In a system that starts at point  $i$  we can write

$$\begin{aligned} \text{for } x = -\Delta x, \quad w_{i-1} &= w_i - \Delta x \left. \frac{dw}{dx} \right|_i + \frac{\Delta x^2}{2} \left. \frac{d^2w}{dx^2} \right|_i, \\ \text{for } x = \Delta x, \quad w_{i+1} &= w_i + \Delta x \left. \frac{dw}{dx} \right|_i + \frac{\Delta x^2}{2} \left. \frac{d^2w}{dx^2} \right|_i, \end{aligned} \quad (9.27)$$

where  $w(-\Delta x) = w_{i-1}$ ,  $w(0) = w_i$ ,  $w(\Delta x) = w_{i+1}$ .

By adding sides (9.27), ) we get

$$w_{i-1} + w_{i+1} = 2w_i + \Delta x^2 \left. \frac{d^2w}{dx^2} \right|_i,$$

i.e.

$$\left. \frac{d^2w}{dx^2} \right|_i \approx \frac{w_{i-1} - 2w_i + w_{i+1}}{\Delta x^2} = \frac{\Delta^2 w}{\Delta x^2}, \quad (9.28)$$

while subtracting sides ((9.27); the first from the second), we get the following

$$w_{i+1} - w_{i-1} = 2\Delta x \left. \frac{dw}{dx} \right|_i, \quad (9.29)$$

that is

$$\left. \frac{dw}{dx} \right|_i \approx \frac{-w_{i-1} + w_{i+1}}{2\Delta x} = \frac{\Delta w}{\Delta x}. \quad (9.30)$$

We determine the operator of the third derivative using (9.30) and (9.28)

$$\begin{aligned} \left. \frac{d^3w}{dx^3} \right|_i &= \frac{d}{dx} \left. \frac{d^2w}{dx^2} \right|_i \approx \frac{1}{2\Delta x} \left( \left. \frac{d^2w}{dx^2} \right|_{i+1} - \left. \frac{d^2w}{dx^2} \right|_{i-1} \right) = \\ &= \frac{1}{2\Delta x} \left( \frac{w_i - 2w_{i+1} + w_{i+2}}{\Delta x^2} - \frac{w_{i-2} - 2w_{i-1} + w_i}{\Delta x^2} \right) = \\ &= \frac{1}{2\Delta x^3} (-w_{i-2} + 2w_{i-1} - 2w_{i+1} + w_{i+2}) = \frac{\Delta^3 w}{\Delta x^3}, \end{aligned} \quad (9.31)$$

while the operator of the fourth derivative is determined by using twice (9.28)

$$\begin{aligned} \left. \frac{d^4 w}{dx^4} \right|_i &= \left. \frac{d^2}{dx^2} \frac{d^2 w}{dx^2} \right|_i \approx \frac{1}{\Delta x^2} \left( \left. \frac{d^2 w}{dx^2} \right|_{i-1} - 2 \left. \frac{d^2 w}{dx^2} \right|_i + \left. \frac{d^2 w}{dx^2} \right|_{i+1} \right) = \\ &= \frac{1}{\Delta x^2} \left( \frac{w_{i-2} - 2w_{i-1} + w_i}{\Delta x^2} - 2 \frac{w_{i-1} - 2w_i + w_{i+1}}{\Delta x^2} + \frac{w_i - 2w_{i+1} + w_{i+2}}{\Delta x^2} \right) = \\ &= \frac{1}{\Delta x^4} (w_{i-2} - 4w_{i-1} + 6w_i - 4w_{i+1} + w_{i+2}) = \frac{\Delta^4 w}{\Delta x^4}. \end{aligned} \quad (9.32)$$

We will now write the equation (9.25) for  $i$ th point, i.e.  $\frac{d^2}{dx^2} \left( E(x)J(x) \frac{d^2 w}{dx^2} \right) = q(x)$  using differential operators

$$\begin{aligned} \frac{1}{\Delta x^2} \left( E_{i-1}J_{i-1} \left. \frac{d^2 w}{dx^2} \right|_{i-1} - 2E_iJ_i \left. \frac{d^2 w}{dx^2} \right|_i + E_{i+1}J_{i+1} \left. \frac{d^2 w}{dx^2} \right|_{i+1} \right) = \\ = \frac{1}{\Delta x^2} \left( E_{i-1}J_{i-1} \frac{w_{i-2} - 2w_{i-1} + w_i}{\Delta x^2} - 2E_iJ_i \frac{w_{i-1} - 2w_i + w_{i+1}}{\Delta x^2} + \right. \\ \left. + E_{i+1}J_{i+1} \frac{w_i - 2w_{i+1} + w_{i+2}}{\Delta x^2} \right) = q_i. \end{aligned}$$

By transforming we get

$$\begin{aligned} E_{i-1}J_{i-1} (w_{i-2} - 2w_{i-1} + w_i) - 2E_iJ_i (w_{i-1} - 2w_i + w_{i+1}) + \\ + E_{i+1}J_{i+1} (w_i - 2w_{i+1} + w_{i+2}) = q_i \Delta x^4. \end{aligned}$$

After sorting out, we get

$$\begin{aligned} E_{i-1}J_{i-1}w_{i-2} - 2(E_{i-1}J_{i-1} + E_iJ_i)w_{i-1} + (E_{i-1}J_{i-1} + 4E_iJ_i + \\ + E_{i+1}J_{i+1})w_i - 2(E_iJ_i + E_{i+1}J_{i+1})w_{i+1} + E_{i+1}J_{i+1}w_{i+2} = q_i \Delta x^4. \end{aligned} \quad (9.33)$$

We compose equations (9.33) for each node in the interval  $(0, l)$ .

For  $n = 5$  taking sequentially for  $i = 1, 2, 3, 4, 5$ , considering only the nodes located in the interval (we take only those components containing  $E_k, J_0, w_s$  whose indices satisfy the condition  $1 \leq k, o, s \leq n = 5, \Delta x = \frac{l}{n-1}$ ) we have

for  $i = 1$ :

$$(4E_1J_1 + E_2J_2)w_1 - 2(E_1J_1 + E_2J_2)w_2 + E_2J_2w_3 = q_1 \left( \frac{l}{4} \right)^4,$$



for  $i = 2$ :

$$-2(E_1 J_1 + E_2 J_2)w_1 + (E_1 J_1 + 4E_2 J_2 + E_3 J_3)w_2 - 2(E_2 J_2 + E_3 J_3)w_3 + E_3 J_3 w_4 = q_2 \left(\frac{l}{4}\right)^4,$$

for  $i = 3$ :

$$E_2 J_2 w_1 - 2(E_2 J_2 + E_3 J_3)w_2 + (E_2 J_2 + 4E_3 J_3 + E_4 J_4)w_3 - 2(E_3 J_3 + E_4 J_4)w_4 + E_4 J_4 w_5 = q_3 \left(\frac{l}{4}\right)^4,$$

for  $i = 4$ :

$$E_3 J_3 w_2 - 2(E_3 J_3 + E_4 J_4)w_3 + (E_3 J_3 + 4E_4 J_4 + E_5 J_5)w_4 - (E_4 J_4 + E_5 J_5)w_5 = q_4 \left(\frac{l}{4}\right)^4,$$

for  $i = 5$ :

$$E_4 J_4 w_3 - 2(E_4 J_4 + E_5 J_5)w_4 + (E_4 J_4 + 4E_5 J_5)w_5 = q_5 \left(\frac{l}{4}\right)^4.$$

We get a system of equations with a matrix (symmetric - (9.32)):

$$\begin{bmatrix} 4E_1 J_1 + E_2 J_2 & -2(E_1 J_1 + E_2 J_2) & E_2 J_2 & 0 & 0 \\ -2(E_1 J_1 + E_2 J_2) & E_1 J_1 + 4E_2 J_2 + E_3 J_3 & E_2 J_2 + E_3 J_3 & E_3 J_3 & 0 \\ E_2 J_2 & E_2 J_2 + E_3 J_3 & E_2 J_2 + 4E_3 J_3 + E_4 J_4 & -2(E_3 J_3 + E_4 J_4) & E_4 J_4 \\ 0 & E_3 J_3 & -2(E_3 J_3 + E_4 J_4) & E_3 J_3 + 4E_4 J_4 + E_5 J_5 & -2(E_4 J_4 + E_5 J_5) \\ 0 & 0 & E_4 J_4 & -2(E_4 J_4 + E_5 J_5) & E_4 J_4 + 4E_5 J_5 \end{bmatrix} \quad (9.34)$$

with a vector of unknowns  $[w_1, w_2, w_3, w_4, w_5]^T$  and a vector of free expressions.

After solving the system, we obtain as a discrete approximation the deflection function  $w(x)$  at the nodes of the vector values  $[w_1, w_2, w_3, w_4, w_5]^T$ .

#### Example 9.4. [29]

We will illustrate this using the Laplace equation as an example. We are looking for a function  $u(x, y)$  that satisfies the equation

$$\frac{\partial^2 u}{\partial x^2} + \frac{\partial^2 u}{\partial y^2} = 0 \quad (9.35)$$

in the flat region  $D$  bounded by the line  $L$  and satisfying the boundary condition

$$u(P) = f(P) \text{ for } P \in L, \quad (9.36)$$

where  $f$  is a given function (Dirichlet's problem).

We assume  $\Delta x = \Delta y = h > 0$  and determine  $x_i, y_j$  coordinates of the points for which we will calculate the approximate values of the function  $u$ . These are numbers

$$x_i = x_0 + ih, \quad y_j = y_0 + jh, \quad (9.37)$$

where  $x_0, y_0$  are the coordinates of the selected point. We assume the notation

$$u_{ij} = u(x_i, y_j). \quad (9.38)$$

In order to reduce the equation (9.35) to difference form, we replace the derivatives by the appropriate difference quotients

$$\frac{\Delta^2 u}{\Delta x^2} = \frac{u_{i+1,j} - 2u_{i,j} + u_{i-1,j}}{h^2}, \quad (9.39)$$

$$\frac{\Delta^2 u}{\Delta y^2} = \frac{u_{i,j+1} - 2u_{i,j} + u_{i,j-1}}{h^2}. \quad (9.40)$$

After substituting into (9.35) and transforming the quotients, we get the following

$$u_{ij} = \frac{u_{i+1,j} + u_{i-1,j} + u_{i,j+1} + u_{i,j-1}}{4}. \quad (9.41)$$

The value of the function  $u$  at any node is equal to the arithmetic mean value of the function  $u$  at neighboring nodes. The nodes lying on the contour  $L$  of the region  $D$  are assigned numbers determined by the boundary condition (9.36). Thus, we can write as many equations (9.41) with the same number of unknowns  $u_{nm}$  as there are nodes lying inside the region  $D$ . The resulting system is a system of linear equations. Problems may arise here:

- the nodal points do not lie on the edge of the region, in which case we do interpolation or extrapolation;
- we have a large number of unknowns in the notation.

We then use the so-called relaxation method, according to which:

- 1) we create a square mesh with distances between adjacent nodes equal to  $h > 0$ , spanning the entire region under consideration, and, based on the given condition, we assign the values of the function  $u$  to the edge nodes, while we assign arbitrary numbers to the interior nodes;
- 2) we draw up an analogous grid again and assign to its nodes the function values calculated according to the formula (9.41), i.e., the arithmetic mean function values corresponding to the neighboring nodes on the previous grid. It is shown that the sequences of function values  $u$  obtained by the relaxation method for the grid nodes converge to the roots of the mentioned system of equations.

### 9.3. Problems

1. Write the function  $w_{MN}(x, y) = \varphi_0(x, y) + \sum_{m=1}^M \sum_{n=1}^N A_{mn} \varphi_{mn}$  for  $M = 2$ ,  $N = 3$ .
2. Write the system of equations (9.33) for  $n = 6$ .
3. The membrane in the shape of an isosceles triangle with height  $a = 3$  m, and base length  $2a\sqrt{\frac{q}{r}}$  m (no – number of student in the list, table 9.1) is uniformly loaded. The membrane is in a static state, with its edge located in the  $z = 0$  plane, the vertex of the membrane triangle is located in the origin of the coordinate system, the axis  $OX$  is the axis of symmetry of the membrane. Find the solution of the boundary value problem given in this way, i.e., describe the area  $D$ , check the fulfillment of the boundary conditions, check the correctness of the description of the functional for the assumed form of the polynomial  $\varphi_{mn}(x, y)$ , assuming  $M = 1$  and  $N = 1$ . Leave the values of  $p$  and  $T$  general. In solving the problem, assume:  
 $\varphi_{mn}(x, y) = (qx^2 - ry^2)(x - a)^m y^{2n-2}$ .

Table 9.1: Data for task 3, by E. Koźniewski

nr	q	r	nr	q	r	nr	q	r	nr	q	r
1	2	3	23	4	7	45	5	7	67	8	15
2	2	4	24	4	8	46	5	8	68	8	17
3	2	5	25	4	9	47	5	9	69	9	4
4	2	6	26	4	10	48	6	5	70	9	5
5	2	7	27	4	11	49	6	7	71	9	7
6	2	8	28	4	12	50	6	9	72	9	8
7	2	9	29	4	13	51	6	11	73	9	11
8	4	11	30	4	14	52	7	2	74	9	13
9	4	13	31	4	2	53	7	3	75	9	14
10	5	14	32	4	3	54	7	4	76	9	15
11	6	15	33	4	5	55	7	5	77	9	16
12	7	15	34	4	7	56	7	6	78	10	7
13	3	2	35	4	9	57	7	8	79	10	9
14	3	4	36	4	11	58	7	9	80	10	11
15	3	5	37	4	5	59	7	10	81	10	13
16	3	6	38	4	7	60	7	11	82	10	17
17	3	7	39	4	9	61	8	7	83	10	19
18	3	8	40	4	11	62	8	3	84	11	6
19	3	2	41	5	2	63	8	5	85	11	7
20	3	4	42	5	3	64	8	9	86	11	8
21	3	5	43	5	4	65	8	11	87	11	9
22	3	6	44	5	6	66	8	13	88	11	10

## Chapter 10

# Demand for ready-mix concrete – attempt to describe the problem in the form of a linear model

### 10.1. Econometric model [48]

*Econometrics* is the science of methods for studying the quantitative relationships that exist between economic phenomena. The basic tool of econometric analysis is an econometric model. A *descriptive econometric model* is a description of the stochastic dependence of the phenomenon under study (*response variable*) on the factors (phenomena) shaping it (*explanatory variables*), expressed in the form of an equation or system of equations. We denote the response variable by  $Y$ , the explanatory variables by  $X_1, X_2, \dots, X_m$ . There are many factors that influence the formation of the response variable, but it is impossible to take into account all of them. The explanatory variables include the most important facts. Their selection is not an easy thing. A descriptive econometric model representing the dependence of the variable  $Y$  on the variables  $X_1, X_2, \dots, X_m$  can be written in analytical form using the function

$$Y = f(X_1, X_2, \dots, X_m, \varepsilon), \quad (10.1)$$

where  $\varepsilon$  stands for the so-called *random deviation*.

If the dependence of the response variable  $Y$  on the explanatory variables  $X_1, X_2, \dots, X_m$  is linear, then we are dealing with a descriptive econometric model of the form

$$Y = \alpha_0 + \alpha_1 X_1 + \alpha_2 X_2 + \dots + \alpha_m X_m + \varepsilon. \quad (10.2)$$

After rejecting random deviations  $\varepsilon$  we get the equation

$$\hat{Y} = \alpha_0 + \alpha_1 X_1 + \alpha_2 X_2 + \dots + \alpha_m X_m, \quad (10.3)$$

where  $\hat{Y}$  is the expectation value of the response variable  $Y$ . In an econometric model there are some unknown quantities that must be estimated,

these are the parameters of the model. We have two types: *structural parameters* and *stochastic structure parameters* of the model. In the model (10.2) the first ones are  $\alpha_0, \alpha_1, \alpha_2, \dots, \alpha_m$ , while the stochastic structure parameters of the model are the parameters of the distribution of random deviations, such as the expectation value and variance of random deviations and the autocorrelation coefficients of deviations.

Testing an econometric model is a multi-step process.

**Preliminary step:** It is determined what phenomenon will be studied, and therefore what is the response variable.

**First step:** Selection of explanatory variables from among a number of factors.

**Second step:** Selection of analytical form of the model (function (10.1)).

**Third step:** Parameter estimation of the model.

**Fourth step:** Model verification.

**Fifth step:** Making conclusions based on the model, that is, putting it to practical use in the form of economic analysis or forecasting.

### 10.1.1. Selection of explanatory variables

**Eliminating almost constant variables.** Explanatory variables in a linear econometric model from a formal point of view should have the following properties: high variability, strong correlation with the response variable, weak cross-correlation, strong correlation with variables that did not enter into the explanatory variables. We select variables using statistical methods.

#### Example 10.1.

Table 10.1: Values of variables in the model in 1991 – 2000 [48]

Years	$Y$	$X_1$	$X_2$	$X_3$	$X_4$
1991	10	6	8	14	12
1992	10	6	8	14	12
1993	16	10	12	18	12
1994	16	10	12	18	14
1995	12	8	8	18	10
1996	14	10	8	18	12
1997	20	12	14	24	14
1998	20	12	16	24	12
1999	20	12	16	26	12
2000	22	14	18	26	10

To describe the production of an enterprise ( $Y$ ) expressed in millions of zlotys, four quantities are preliminarily assumed:  $X_1$  – employment [thousand people],  $X_2$  – value of machines and equipment [million zloty],  $X_3$  – machine downtime [days],  $X_4$  – capital investments [million zloty]. The values of the variables in 1991 – 2000 are given in the table 10.1.

Model construction:

1. On the basis of substantive reconnaissance, we compile a set of potential (primary) variables  $X_1, X_2, \dots, X_m$ , that we believe (on first viewing) interact with the response variable ( $Y$ ).
2. Statistical data that are realizations of the response variable and potential explanatory variables are collected, i.e., a vector  $\mathbf{y}$  of observations of the variable  $Y$  and a matrix of observations  $\mathbf{X}$  of the variables  $X_1, X_2, \dots, X_m$  in the form

$$\mathbf{y} = \begin{bmatrix} y_1 \\ y_2 \\ \dots \\ y_n \end{bmatrix}, \quad \mathbf{X} = \begin{bmatrix} x_{11} & x_{12} & \dots & x_{1m} \\ x_{21} & x_{22} & \dots & x_{2m} \\ \dots & \dots & \dots & \dots \\ x_{n1} & x_{n2} & \dots & x_{nm} \end{bmatrix}. \quad (10.4)$$

3. Eliminate potential explanatory variables characterized by too low a level of variability.
4. Correlation coefficients between all variables under consideration are calculated.
5. Reduction of the set of potential explanatory variables is carried out using the selected statistical procedure.

The precondition for declaring a quantity as an explanatory variable is high variability, the measure of the level of which is the coefficient of variability

$$\nu_i = \frac{S_i}{\bar{x}_i} \quad i = 1, 2, \dots, m, \quad (10.5)$$

where  $\bar{x}_i$  is the arithmetic mean of the variable  $X_i$

$$\bar{x}_i = \frac{1}{n} \sum_{l=1}^n x_{li} \quad i = 1, 2, \dots, m, \quad (10.6)$$

while  $S_i$  is the standard deviation of the variable  $X_i$

$$S_i = \left( \frac{1}{n} \sum_{l=1}^n (x_{li} - \bar{x}_i)^2 \right)^{\frac{1}{2}} \quad i = 1, 2, \dots, m. \quad (10.7)$$

The critical value of the coefficient of variation  $\nu^*$ , is chosen, e.g.  $\nu^* = 0.01$ . Variables that satisfy the inequality

$$\nu_i \leq \nu^* \quad (10.8)$$

are considered almost constant and are excluded from the set of explanatory variables. It is assumed that these variables do not add significant information in the analysis being conducted.

We check what the variability of the variables in the example (10.1) is, assuming that the critical value of the coefficient of variation is  $\nu^* = 0.15$ . The arithmetic averages of the variables  $X_1, X_2, X_3, X_4$  are as follows

$$\bar{x}_1 = 10, \bar{x}_2 = 12, \bar{x}_3 = 20, \bar{x}_4 = 12.$$

Table 10.2: Calculation of the mean and standard deviation for data from the table 10.1, by E. Koźniewski

l	$x_{11} - \bar{x}_1$	$x_{12} - \bar{x}_2$	$x_{13} - \bar{x}_3$	$x_{14} - \bar{x}_4$	$(x_{11} - \bar{x}_1)^2$	$(x_{12} - \bar{x}_2)^2$	$(x_{13} - \bar{x}_3)^2$	$(x_{14} - \bar{x}_4)^2$
1	-4	-4	-6	0	16	16	36	0
2	-4	-4	-6	0	16	16	36	0
3	0	0	-2	0	0	0	4	0
4	0	0	-2	2	0	0	4	4
5	-2	-4	-2	-2	4	16	4	4
6	0	-4	-2	0	0	16	4	0
7	2	2	4	2	4	4	16	4
8	2	4	4	0	4	16	16	0
9	2	4	6	0	4	16	36	0
10	4	6	6	-2	16	36	36	4
$\Sigma$	0	0	0	0	64	136	192	16

With the help of the table 10.2 we determine the standard deviations

$$S_1 = \sqrt{\frac{1}{10} \cdot 64} = 2.530, \quad S_2 = \sqrt{\frac{1}{10} \cdot 136} = 3.688,$$

$$S_3 = \sqrt{\frac{1}{10} \cdot 192} = 4.382, \quad S_4 = \sqrt{\frac{1}{10} \cdot 16} = 1.265$$

and then the coefficients of variation

$$\begin{aligned}\nu_1 &= \frac{2.530}{10} = 0.253, & \nu_2 &= \frac{3.688}{12} = 0.307, \\ \nu_3 &= \frac{4.382}{20} = 0.219, & \nu_4 &= \frac{1.265}{12} = 0.105.\end{aligned}$$

The coefficient of variation of  $\nu_4$  is smaller than the assumed critical value  $\nu^* = 0.15$ , so we consider the variable denoted by  $X_4$  to be not useful.

**Vector and matrix of correlation coefficients.** To the evaluation of the strength of the linear relationship between the response variable  $Y$  and the potential explanatory variables  $X_1, X_2, \dots, X_m$  correlation coefficients  $r_i$  are calculated

$$r_i = \frac{\sum_{l=1}^n (y_l - \bar{y})(x_{li} - \bar{x}_i)}{\sqrt{\sum_{l=1}^n (y_l - \bar{y})^2 \sum_{l=1}^n (x_{li} - \bar{x}_i)^2}}, \quad i = 1, 2, \dots, m. \quad (10.9)$$

These coefficients are represented in the form of a correlation vector

$$\mathbf{R}_0 = [r_1, r_2, \dots, r_m]^T. \quad (10.10)$$

Correlation coefficients between potential explanatory variables are calculated according to the formula

$$r_{ij} = \frac{\sum_{l=1}^n (x_{li} - \bar{x}_i)(x_{lj} - \bar{x}_j)}{\sqrt{\sum_{l=1}^n (x_{li} - \bar{x}_i)^2 \sum_{l=1}^n (x_{lj} - \bar{x}_j)^2}}, \quad i, j = 1, 2, \dots, m. \quad (10.11)$$

These coefficients form a correlation matrix

$$\mathbf{R} = \begin{bmatrix} 1 & r_{12} & \dots & r_{1n} \\ r_{21} & 1 & \dots & r_{2n} \\ \dots & \dots & \ddots & \dots \\ r_{m1} & r_{m2} & \dots & 1 \end{bmatrix}. \quad (10.12)$$

The matrix  $\mathbf{R}$  is symmetrical, i.e.  $r_{ij} = r_{ji}$ .



### Analysis method of correlation coefficient matrix.

The point of this method is that we choose those explanatory variables that are strongly correlated with the response variable and at the same time weakly correlated with each other. We analyze the vector  $\mathbf{R}_0$  and the matrix  $\mathbf{R}$ . For a given level of significance  $\gamma$  and for  $n - 2$  degrees of freedom, determines the so-called critical value of the correlation coefficient

$$r^* = \left( \frac{(l^*)^2}{(l^*)^2 + n - 2} \right)^{\frac{1}{2}}, \quad (10.13)$$

where:  $l^*$  is the value of the statistic read from Student's  $t$  test tables for a given  $\gamma$  and for  $n - 2$  degrees of freedom. The critical value of the correlation coefficient  $r^*$  can also be asked in advance by the researcher. The procedure is as follows:

1. From the set of potential explanatory variables are eliminated those for which holds the inequality

$$|r_i| \leq r^*; \quad (10.14)$$

these variables are insignificantly correlated with the response variable.

2. Among the other explanatory variables, the variable  $X_h$  is selected such that

$$|r_h| = \max_i \{|r_i|\}; \quad (10.15)$$

this variable carries the largest amount of information about the response variable.

3. From the set of potential explanatory variables are eliminated those for which holds the inequality

$$|r_{hi}| > r^*; \quad (10.16)$$

are variables that are too highly correlated with the explanatory variable  $X_h$ , and therefore duplicate the information it provides.

The procedure described in 1, 2, 3 continues until the set of potential explanatory variables is exhausted.

**Example 10.2.** A construction materials trading company interested in the sales volume of concrete ( $Y$ ) analyzed the sales overview of other materials as well, to examine their relationship to concrete sales. It initially

proposed 8 potential explanatory variables determining sales volume in the past 24 months: extruded polystyrene foam for foundations ( $X_1$ ), ceramic roof tiles ( $X_2$ ), metal roofing tiles ( $X_3$ ), lime ( $X_4$ ), porotherm ceramic blocks ( $X_5$ ), glaze ( $X_6$ ), clinker bricks ( $X_7$ ), reinforcing steel ( $X_8$ ).

Using the building materials sales data, a vector of correlation coefficients of the response variable with potential explanatory variables was determined as follows  $\mathbf{R}_0 = [-0.59; -0.06; 0.08; 0.013; 0.54; -0.15; -0.10; 0.72]^T$  and the correlation matrix between the potential explanatory variables

$$\mathbf{R} = \begin{bmatrix} 1 & -0.09 & 0.35 & -0.17 & -0.62 & -0.40 & -0.16 & -0.55 \\ -0.09 & 1 & -0.06 & -0.38 & 0.00 & 0.15 & 0.22 & 0.11 \\ 0.35 & -0.06 & 1 & 0.33 & -0.11 & -0.20 & -0.45 & -0.02 \\ -0.17 & -0.38 & 0.33 & 1 & 0.20 & -0.07 & -0.44 & 0.07 \\ -0.62 & 0.00 & -0.11 & 0.20 & 1 & 0.22 & 0.17 & -0.11 \\ -0.40 & 0.15 & -0.20 & -0.07 & 0.22 & 1 & -0.19 & 0.47 \\ -0.16 & 0.22 & -0.45 & -0.44 & 0.17 & -0.19 & 1 & 0.05 \\ -0.55 & 0.11 & -0.02 & 0.07 & -0.11 & 0.47 & 0.05 & 1 \end{bmatrix}.$$

We will select the explanatory variables for a significance level of  $\gamma = 0.10$  and for  $n - 2 = 22$  degrees of freedom. From  $t$  Student's tables, we read the value of the theoretical statistic  $l^* = 1.717$ , and then calculate the critical value of the correlation coefficient

$$r^* = \left( \frac{(1.717)^2}{(1.717)^2 + 24 - 2} \right)^{\frac{1}{2}} = 0.344.$$

First, we eliminate all variables that are less correlated with the response variable than at the level 0.344 (values of  $r_i$  less than 0.344). These are the variables  $X_2, X_3, X_4, X_6, X_7$ , for which  $r_2 = -0.06$ ;  $r_3 = 0.08$ ;  $r_4 = 0.13$ ;  $r_6 = -0.15$ ;  $r_7 = -0.10$ .

From the remaining primary variables, we choose the variable most strongly correlated with the response variable. This is  $X_8$  ( $= 0.72$ ) – the first explanatory variable. We then eliminate the remaining explanatory variables for which  $|r_{8i}| > 0.344$ . There is one such variable:  $X_1$ , after all  $|r_{81}| = 0.55$  (the last row or last column of the  $\mathbf{R}$  matrix), although there is another ( $X_6$ ,  $|r_{86}| = 0.47$ ), but this one we eliminated earlier. From such a reduced set, we choose another (worse than the best) explanatory variable, it is  $X_5$ . But since it is the only variable already, so we leave it.

In the end, two explanatory variables  $X_5, X_8$  (porotherm ceramic blocks and reinforcing steel) remain. So we have a model

$$Y = \alpha_0 + \alpha_1 X_5 + \alpha_2 X_8 + \varepsilon.$$

**The multiple correlation coefficient** is a measure of the strength of the linear relationship of the response variable  $Y$  with the explanatory variables  $X_1, X_2, \dots, X_m$  and is defined as follows:

$$R = \sqrt{1 - \frac{\det(\mathbf{W})}{\det(\mathbf{R})}}, \quad (10.17)$$

where  $\det(\mathbf{R})$  denotes the determinant of the matrix  $\mathbf{R}$  of the correlation coefficients of the explanatory variables, combined in pairs,  $\det(\mathbf{W})$  denotes the determinant of the matrix

$$\mathbf{W} = \begin{bmatrix} 1 & \mathbf{R}_0^T \\ \mathbf{R}_0 & \mathbf{R} \end{bmatrix}. \quad (10.18)$$

In expanded form, the  $\mathbf{W}$  matrix is written as follows

$$\mathbf{W} = \begin{bmatrix} 1 & r_1 & r_2 & \dots & r_m \\ r_1 & 1 & r_{12} & \dots & r_{1m} \\ r_2 & r_{21} & 1 & \dots & r_{2m} \\ \dots & \dots & \dots & \ddots & \dots \\ r_m & r_{m1} & r_{m2} & \dots & 1 \end{bmatrix}. \quad (10.19)$$

The multivariate correlation coefficient  $R$  takes values of  $0 \leq R \leq 1$ . It takes on higher values the stronger the relationship between the response variable and the explanatory variables.

## 10.2. Estimating parameters of linear models by the method of least squares

Estimating the parameters of an econometric model gets down to assigning specific numerical values to unspecified parameters. A frequently used method for estimating the parameters of linear econometric models

$$Y = \alpha_0 + \alpha_1 X_1 + \alpha_2 X_2 + \dots + \alpha_m X_m + \varepsilon \quad (10.20)$$

is the method of least squares. It consists in determining such values of ratings  $a_0, a_1, a_2, \dots, a_m$ , of the parameters  $\alpha_0, \alpha_1, \alpha_2, \dots, \alpha_m$ , that the sum of squares of deviations of the observed values of the explained variable from its theoretical values calculated from the model is the smallest, i.e.

$$\sum_{i=1}^n e_i^2 \rightarrow \min, \quad (10.21)$$

where  $e_i$  ( $i = 1, 2, \dots, n$ ) is the deviation of the empirical values of the explanatory variable from its theoretical values, also known as the residual of the model. By  $e_i$  we mean the difference

$$e_i = y_i - \hat{y}_i \quad (i = 1, 2, \dots, n), \quad (10.22)$$

with

$$\hat{y}_i = a_0 + a_1 x_{i1} + a_2 x_{i2} + \dots + a_m x_{im}, \quad i = 1, 2, \dots, n. \quad (10.23)$$

The use of the least squares method requires certain assumptions. The estimated model is: (1) linear model, (2) explanatory variables are non-random quantities with fixed elements, (3) explanatory variables are not collinear, (4) the random component has an expected value equal to zero and a constant finite variance, (5) there is no autocorrelation of the random component (random component over time).

### 10.2.1. Estimation of parameters of a model with one explanatory variable

The linear econometric model with one explanatory variable is of the form

$$Y = \beta + \alpha X + \varepsilon. \quad (10.24)$$

The evaluation values  $a$  and  $b$  of the structural parameters  $\alpha$  and  $\beta$  are obtained from the condition

$$S(a, b) = \sum_{i=1}^n (y_i - b - ax_i)^2 \rightarrow \min. \quad (10.25)$$

The function  $S(a, b)$  reaches a minimum, at the point  $(a, b)$  where the partial derivatives of this function are zeroed. The necessary condition for the existence of an extremum is, due to the inequality  $S(a, b) > 0$ , at the

same time a sufficient condition. After equating the partial derivatives to zero, we obtain a system of equations with unknowns  $a$  and  $b$

$$\begin{cases} b \cdot n + a \sum_{i=1}^n x_i = \sum_{i=1}^n y_i, \\ b \sum_{i=1}^n x_i + a \sum_{i=1}^n x_i^2 = \sum_{i=1}^n y_i x_i. \end{cases} \quad (10.26)$$

Solving the system (10.26), we get the formulas for the evaluation  $a$  and  $b$

$$a = \frac{\sum_{i=1}^n y_i x_i - n \bar{x} \bar{y}}{\sum_{i=1}^n x_i^2 - n(\bar{x})^2}, \quad (10.27)$$

$$b = \bar{y} - a\bar{x}, \quad (10.28)$$

where  $\bar{y}$  and  $\bar{x}$  denote the arithmetic averages of the variables  $Y$  and  $X$ . Equivalently, the formula (10.27) can be written in the form

$$a = \frac{\sum_{i=1}^n (y_i - \bar{y})(x_i - \bar{x})}{\sum_{i=1}^n (x_i - \bar{x})^2}. \quad (10.29)$$

The evaluation value  $a$  of the  $\alpha$  parameter tells how many units the response variable  $Y$  will change if the explanatory variable  $X$  changes by a unit.

In the case where  $t$  is a time variable, we get a linear model of development trend

$$Y = \beta + \alpha t + \varepsilon. \quad (10.30)$$

If the variable  $t$  takes the values  $t = 1, 2, \dots, n$ , then  $\sum_{t=1}^n (t - \bar{t})^2 = \frac{n(n^2-1)}{12}$

and then, due to  $\bar{t} = \frac{n(n+1)}{2}$ , we can determine the assessment  $a$  from the formula

$$a = \frac{12 \sum_{t=1}^n (y_t - \bar{y}) \left( t - \frac{n(n+1)}{2} \right)}{n(n^2 - 1)}. \quad (10.31)$$

Then the evaluation  $b = \bar{y} - a\bar{t}$ . The evaluation of the variance of random deviations of a linear model with one explanatory variable is obtained from the formula

$$S_e^2 = \frac{\sum_{i=1}^n e_i^2}{n - 2}. \quad (10.32)$$

The magnitude of  $S_e$  is the standard deviation of the residuals of the model, by how much the observed values of the response variable on average differ from the theoretical values of this variable determined from the model. The standard errors  $S(a)$  and  $S(b)$  of the estimates of the structural parameters  $\alpha$  and  $\beta$  are determined from the formulas

$$S(a) = \frac{S_e}{\sqrt{\sum_{i=1}^n x_i^2 - n(\bar{x})^2}} \quad (10.33)$$

or

$$S(a) = \frac{S_e}{\sqrt{\sum_{i=1}^n (x_i - \bar{x})^2}}, \quad (10.34)$$

$$S(b) = S_e \sqrt{\frac{\sum_{i=1}^n x_i^2}{n \left( \sum_{i=1}^n x_i^2 - n(\bar{x})^2 \right)}} \quad (10.35)$$

or

$$S(b) = S_e \sqrt{\frac{\sum_{i=1}^n x_i^2}{n \sum_{i=1}^n (x_i - \bar{x})^2}}. \quad (10.36)$$

### 10.2.2. Estimation of parameters of a model with multiple explanatory variables

To show the least squares method applied to a linear econometric model with multiple ( $m$ ) explanatory variables

$$Y = \alpha_0 + \alpha_1 X_1 + \alpha_2 X_2 + \dots + \alpha_m X_m + \varepsilon, \quad (10.37)$$

we will introduce matrix notation

$\mathbf{y}^T = [y_1, y_2, \dots, y_n]$  – the vector of observations of the response variable,

$$\mathbf{X} = \begin{bmatrix} 1 & x_{11} & x_{12} & \dots & x_{1m} \\ 1 & x_{21} & x_{22} & \dots & x_{2m} \\ \dots & \dots & \dots & \ddots & \dots \\ 1 & x_{n1} & x_{n2} & \dots & x_{nm} \end{bmatrix} \quad \text{– observation matrix of explanatory variables,}$$

$\mathbf{a}^T = [a_0, a_1, a_2, \dots, a_m]$  – vector of ratings of structural parameters,  
 $\mathbf{e}^T = [e_1, e_2, \dots, e_n]$  – the residual vector of the model.

The function – the criterion of the method of least squares – is written as follows

$$S(a_0, a_1, a_2, \dots, a_m) = \mathbf{e}^T \mathbf{e} \rightarrow \min, \quad (10.38)$$

where

$$\mathbf{e} = \mathbf{y} - \mathbf{X}\mathbf{a}. \quad (10.39)$$

The formula for the vector  $\mathbf{a}$  ratings of the structural parameters of the model is as follows

$$\mathbf{e} = (\mathbf{X}^T \mathbf{X})^{-1} \mathbf{X}^T \mathbf{y}. \quad (10.40)$$

The variance of random deviations is estimated using the formula

$$S_e^2 = \frac{\mathbf{e}^T \mathbf{e}}{n - m - 1} = \frac{\sum_{i=1}^n e_i^2}{n - m - 1}. \quad (10.41)$$

The variance and covariance matrix of the evaluations  $a_0, a_1, a_2, \dots, a_m$ , of the structural parameters  $\alpha_0, \alpha_1, \alpha_2, \dots, \alpha_m$  estimated from the formula

$$\mathbf{D}^2(\mathbf{a}) = S_e^2 (\mathbf{X}^T \mathbf{X})^{-1}. \quad (10.42)$$

In the matrix (10.42) the elements on the main diagonal are the variances of  $V(a_i)$  ( $i = 0, 1, 2, \dots, m$ ) estimates of the structural parameters  $\alpha_0, \alpha_1, \alpha_2, \dots, \alpha_m$ . The magnitudes

$$S(a_i) = \sqrt{V(a_i)} \quad (i = 0, 1, 2, \dots, m) \quad (10.43)$$

are the standard errors of structural parameter estimates.

### 10.2.3. Verification of linear models

After estimating the parameters of the model, it should be examined whether it well describes the relationships under study. If there is a large discrepancy between the model and the empirical data, it should be corrected. Verification proceeds by examining three properties:

- 1) the degree to which the model is consistent with the empirical data,
- 2) the quality of structural parameter evaluations,
- 3) the distribution of random deviations.

We will only deal with the first two.

### Evaluation of the model's fit to empirical data

The primary measures of this fit are the standard deviation of residuals  $S_e$  (discussed earlier), the coefficient of random variation, the coefficient of convergence and the coefficient of determination.

The coefficient of random variation  $W_e$  is defined as follows:

$$W_e = \frac{S_e}{\bar{y}} \cdot 100\% \quad (10.44)$$

and informs what percentage of the arithmetic mean of the explanatory variable of the model is the standard deviation of the residuals. A smaller value indicates a better fit of the model to the empirical data. It is possible to assume a critical value of  $W^*$  (e.g.  $W^* = 10\%$ ) and then the inequality

$$W_e \leq W^* \quad (10.45)$$

shows a good fit of the model to the empirical data.

The convergence coefficient  $\varphi^2$  is expressed by the formula

$$\varphi^2 = \frac{\sum_{i=1}^n e_i^2}{\sum_{i=1}^n (y_i - \bar{y})^2} \quad (10.46)$$

and informs how much of the total variation in the explanatory variable is not explained by the model. Note that  $0 \leq \varphi \leq 1$ . The fit of the model to the data is better the closer the coefficient of convergence is to zero.

The coefficient of determination  $R^2$  is expressed by the formula

$$R^2 = \frac{\sum_{i=1}^n (\hat{y}_i - \bar{y})^2}{\sum_{i=1}^n (y_i - \bar{y})^2} \quad (10.47)$$

and reports what proportion of the total variation in the response variable is accounted for by the variation in the theoretical values of that variable. Note that  $0 \leq R^2 \leq 1$ . Fitting the model to the data is better the closer the coefficient of convergence is to unity.

The following equality holds

$$\varphi^2 + R^2 = 1. \quad (10.48)$$



The square root of the determination coefficient  $R^2$ , i.e.  $R$ , is the multiple correlation coefficient discussed earlier.

To find out whether the fit of the model is large enough, the null hypothesis of the form  $H_0 : [R = 0]$  can be verified against the alternative hypothesis  $H_1 : [R \neq 0]$ . The test of this hypothesis is a statistic

$$F = \frac{R^2}{1 - R^2} \cdot \frac{n - m - 1}{m}, \quad (10.49)$$

which has a  $F$  Fisher – Snedecor distribution with  $\nu_1 = m$ ,  $\nu_2 = n - m - 1$  degrees of freedom. From the tables of the test  $F$  for a given level of significance  $\gamma$  and for  $\nu_1, \nu_2$  degrees of freedom, the critical value  $F^*$ . If  $F \leq F^*$ , then there is no reason to reject the hypothesis  $H_0$ , that is, the correlation coefficient is insignificantly different from zero, so the fit is too weak. On the other hand, if  $F > F^*$ , then hypothesis  $H_0$  should be rejected in favor of hypothesis  $H_1$ . The multiple correlation coefficient is significant, and the degree of fit of the model to the data is high enough.

### Testing the significance of structural parameters

Testing the significance of the parameters  $\alpha_0, \alpha_1, \alpha_2, \dots, \alpha_m$  aims to test whether the explanatory variables significantly interact with the response variable. For each  $i = 1, 2, \dots, m$  the null hypothesis  $H_0[\alpha_i = 0]$  is verified against the alternative hypothesis  $H_1[\alpha_i \neq 0]$ . The test of this hypothesis is a statistic

$$I_i = \frac{|a_i|}{S(a_i)}, \quad (10.50)$$

where  $a_i$  is the value of the estimate of the structural parameter  $\alpha_i$ ,  $S(a_i)$  the standard error of the estimate of this parameter for  $i = 1, 2, \dots, m$ . The statistic  $I_i$  has a  $t$  Student distribution with  $n - m - 1$  degrees of freedom. From the tables of the  $t$  Student test for a specified significance level  $\gamma$  and for  $n - m - 1$  degrees of freedom, the critical value  $I^*$  is read. If  $I_i \leq I^*$ , then there is no reason to reject the hypothesis  $H_0$ , that is, the structural parameter  $\alpha_i$  is insignificantly different from zero, so the explanatory variable  $X_i$  does not significantly affect the response variable  $Y$ . On the other hand, if  $I_i > I^*$ , then hypothesis  $H_0$  should be rejected in favor of hypothesis  $H_1$ . The coefficient of multiple correlation is significant, and the degree of fit of the model to the data is sufficiently high. The structural parameter  $\alpha_i$  is significantly different from zero, so the explanatory variable  $X_i$  interacts significantly with the response variable  $Y$ . Now we can fully solve the following problem.

**Example 10.3.** Study the dependence of the sales volume of concrete [ $\text{m}^3$ ] of the selected concrete company on the volume of building permits issued (in its area of influence), expressed in square meters of useable area [ $\text{m}^2$ ]. The individual data are stored in the tables 10.3 and 10.4.

Table 10.3: Concrete sales ( $[\text{m}^3]$ ) in 2000–2006 by selected concrete company, by E. Koźniewski

Years	2000	2001	2002	2003	2004	2005	2006
$[\text{m}^3]$	15 573	9 900	12 233	10 470	15 616	24 135	37 590

Given classes of building types, we number the following:

$1 \rightarrow (a) + (b)$ ,  $2 \rightarrow (c) + (d) + (h)$ ,  $3 \rightarrow (f) + (g)$ ,  $4 \rightarrow (e) + (i)$  and insert into the table 10.5.

Table 10.4: Building permits issued in 2000–2006 in usable area [ $\text{m}^2$ ] [2]

	Buildings/years	2000	2001	2002	2003	2004	2005	2006
	Residential (total)	193 652	165 108	120 100	105 366	162 736	188 075	221 861
$a$	single-family	100 870	105 004	78 696	78 325	114 789	160 566	128 367
$b$	with 2 and more apartments	92 782	60 104	41 404	27 096	47 947	81 141	93 494
	Non-residential (total)	192 355	207 763	141 270	157 724	184 707	120 263	92 638
$c$	hotels and accommod. buildings	1 814	4 707	4 180	327	492	1 469	4 883
$d$	office	29 613	36 641	4 205	143	783	9 347	2 039
$e$	commercial and service	36 724	28 039	27 336	32 772	52 102	22 155	11 505
$f$	transport and communication	3 083	2 508	1 287	1 968	3 815	5 593	3 150
$g$	industrial and storage	29 176	20 756	33 458	36 802	35 949	25 323	25 294
$h$	public objects	47 328	41 708	19 620	20 819	14 588	24 177	5 874
$i$	other non-residential	44 616	73 404	51 185	64 893	76 978	32 199	39 893

So we have a new table 10.5.

Table 10.5: Construction permits issued in 2000–2006 (aggregation), by E. Koźniewski

Years/classes	$(a) + (b)$	$(c) + (d) + (h)$	$(f) + (g)$	$(e) + (i)$
2000	193 652	78 755	32 260	81 340
2001	165 108	83 056	23 265	101 442
2002	120 100	28 005	34 745	78 521
2003	105 366	21 289	38 770	97 665
2004	162 736	15 863	39 764	129 080
2005	188 075	34 993	30 916	54 354
2006	221 861	12 796	28 444	51 398

We create an output array of data: the response variable ( $Y$ ) and the explanatory variables ( $X_1, X_2, X_3, X_4$ ) – table 10.6.

Table 10.6: Output data array for table 10.5

	$Y$	$X_1$	$X_2$	$X_3$	$X_4$
Years		$(a) + (b)$	$(c) + (d) + (h)$	$(f) + (g)$	$(e) + (i)$
2000	15 573	193 652	78 755	32 260	81 340
2001	9 900	165 108	83 056	23 265	101 442
2002	12 233	120 100	28 005	34 745	78 521
2003	10 470	105 366	21 289	38 770	97 665
2004	15 616	162 736	15 863	39 764	129 080
2005	24 135	188 075	34 993	30 916	54 354
2006	37 590	221 861	12 796	28 444	51 398

We create the table 10.7, counting the average  $\bar{y}$ ,  $\bar{x}_1$ ,  $\bar{x}_2$ ,  $\bar{x}_3$ ,  $\bar{x}_4$ .

Table 10.7: Averages for the table 10.6, by E. Koźniewski

	$Y$	$X_1$	$X_2$	$X_3$	$X_4$
Years		$(a) + (b)$	$(c) + (d) + (h)$	$(f) + (g)$	$(e) + (i)$
2000	15 573	193 652	78 755	32 260	81 340
2001	9 900	165 108	83 056	23 265	101 442
2002	12 233	120 100	28 005	34 745	78 521
2003	10 470	105 366	21 289	38 770	97 665
2004	15 616	162 736	15 863	39 764	129 080
2005	24 135	188 075	34 993	30 916	54 354
2006	37 590	221 861	12 796	28 444	51 398
Średnie	17 931.00	165 271.14	39 251.00	32 594.86	84 828.57

Further calculations are carried out in Excel.

First, we calculate the coefficients of variation from the formula (10.5) and respectively obtain  $\nu_1 = 0.230554568$ ;  $\nu_2 = 0.693956505$ ;

$\nu_3 = 0.063225748$ ;  $\nu_4 = 0.777632324$ . After taking the critical value of  $v^* = 0.05$  for all variables, we have the satisfied inequality  $v^* \leq v_i$ , for  $i = 1, 2, 3, 4$ . Thus, there are no quasi-constant variables. This test does not eliminate any explanatory variable.

We go on to analyze the matrices  $\mathbf{R}_0$  and  $\mathbf{R}$ . We calculate the vector of correlation coefficients  $\mathbf{R}_0$  between the response variable and the potential explanatory variables and the correlation coefficient matrix  $\mathbf{R}$  of correlation coefficients

$$\mathbf{R}_0 = \begin{bmatrix} 0.77629646 \\ 0.42281913 \\ 0.06376574 \\ 0.69689022 \end{bmatrix},$$

$$\mathbf{R} = \begin{bmatrix} 1 & 0.16009455 & -0.53572469 & -0.48585437 \\ 0.16009455 & 1 & -0.59428665 & 0.08473649 \\ -0.53572469 & -0.59428665 & 1 & 0.44035481 \\ -0.48585437 & 0.08473649 & 0.44035481 & 1 \end{bmatrix}.$$

To analyze the matrix of correlation coefficients, we will use the formula (10.13). Let's assume a significance level of  $\gamma = 0.10$ . For  $n - 2 = 5$  degrees of freedom, let's first read from  $t$  Student's tables the value  $l^* = 2.015$ , and then determine (in Excel) the so-called critical value of the correlation coefficient

$$r^* = \left( \frac{(2.015)^2}{(2.015)^2 + 7 - 2} \right)^{\frac{1}{2}} = 0.66943059.$$

Next, from the set of potential explanatory variables, we eliminate those variables that are less correlated with the response variable than at 0.70974357, i.e. such variables  $X_i$ , for which  $r_i \leq r^*$ . These are variables  $X_2, X_3$ , for which  $r_2 = 0.42281913$ ,  $r_3 = 0.06376574$ . After this elimination, the set of explanatory variables is reduced to two variables  $X_1, X_4$ . The relationship between the volume of building permits in residential (single-family and multi-family) and commercial and other construction and the volume of concrete production still holds. In the next steps, we will estimate and test the significance of the dependence parameters using the least squares method.

**Example 10.4.** Determine the linear trend of ready-mixed concrete sales in 2001 – 2006 for the data in example 10.3. For simplicity, we will assume  $t = 1, 2, 3, 4, 5, 6$ .

### 10.3. Problems

1. The following observations of the variables  $X_1, X_2, X_3$  are given:

Table 10.8: Observations of variables  $X_1, X_2, X_3$ , by E. Koźniewski

$l$	1	2	3	4	5	6
$x_{l1}$	18	22	25	27	30	34
$x_{l2}$	4.0	4.1	4.0	4.1	4.1	4.0
$x_{l3}$	8	3	7	4	9	11

With the critical value of the coefficient of variation  $\nu^* = 0.10$ , assess the suitability of individual variables to describe the response variable due to the level of variation in their values.

2. Analyze the dependence of the sales volume of concrete [m<sup>3</sup>] of the selected concrete company on the volume of construction permits issued (in its area of influence), expressed in square meters of usable area [m<sup>2</sup>] according to the following aggregation.

We number the classes of building types as follows:

1 : 1  $\rightarrow$  (a), 2  $\rightarrow$  (b), 3  $\rightarrow$  (c) + (d) + (h), 4  $\rightarrow$  (g), 5  $\rightarrow$  (f), 6  $\rightarrow$  (e) + (i),  
 2 : 1  $\rightarrow$  (a), 2  $\rightarrow$  (b), 3  $\rightarrow$  (c) + (d), 4  $\rightarrow$  (g) + (h), 5  $\rightarrow$  (f), 6  $\rightarrow$  (e) + (i),  
 3 : 1  $\rightarrow$  (a) + (b), 2  $\rightarrow$  (c), 3  $\rightarrow$  (d), 4  $\rightarrow$  (g) + (h), 5  $\rightarrow$  (f) + (i), 6  $\rightarrow$  (e),  
 4 : 1  $\rightarrow$  (a) + (b), 2  $\rightarrow$  (c), 3  $\rightarrow$  (d) + (h), 4  $\rightarrow$  (f) + (g), 5  $\rightarrow$  (e) + (i),  
 5 : 1  $\rightarrow$  (a) + (b), 2  $\rightarrow$  (c) + (d), 3  $\rightarrow$  (h), 4  $\rightarrow$  (f), 5  $\rightarrow$  (g) + (e) + (i),  
 6 : 1  $\rightarrow$  (a), 2  $\rightarrow$  (b), 3  $\rightarrow$  (c) + (d), 4  $\rightarrow$  (h), 5  $\rightarrow$  (f), 6  $\rightarrow$  (g),  
 7 : 1  $\rightarrow$  (a), 2  $\rightarrow$  (b), 3  $\rightarrow$  (c), 4  $\rightarrow$  (d) + (h), 5  $\rightarrow$  (f) + (g), 6  $\rightarrow$  (e),  
 8 : 1  $\rightarrow$  (a) + (b), 2  $\rightarrow$  (c), 3  $\rightarrow$  (d), 4  $\rightarrow$  (h), 5  $\rightarrow$  (f) + (e), 6  $\rightarrow$  (g) + (i),  
 9 : 1  $\rightarrow$  (a) + (b), 2  $\rightarrow$  (c) + (d), 3  $\rightarrow$  (h), 4  $\rightarrow$  (f), 5  $\rightarrow$  (g), 6  $\rightarrow$  (e),  
 10 : 1  $\rightarrow$  (a), 2  $\rightarrow$  (b) + (c), 3  $\rightarrow$  (d) + (h) + (f), 4  $\rightarrow$  (e) + (g), 5  $\rightarrow$  (i), 7  $\rightarrow$  (i),

Particular data are stored in tables 10.3 and 10.4.

## Chapter 11

# Optimization of earthmoving in road construction – linear programming

### 11.1. Linear programming

Let's consider the following pair of decision problems:

**Problem. (P)** It is necessary to plan the realization of the construction work so that with the existing limitations of the resources of construction implementation (materials, labor, equipment) to achieve the maximum effect, e.g. the number of  $\text{m}^3$  of the cubature of buildings, the number of  $\text{m}^2$  of the usable area of apartments, the profit of the contractor, etc.

**Problem. (D)** Minimize the use of materials and machine labor, so that the effect of the work done is not less than the assumed value.

**Example 11.1.** A prefabricated building factory produces two types of slabs of different sizes. Let us assume here that the limiting factors of production are only the capacity of the concrete mixer and the vibrator (the table 11.1 [49]).

Table 11.1: Time required for concreting and vibrating one slab, monthly working time limit and unit profits for two types of slabs, by E. Koźniewski

	Slab 1	Slab 2	Time [h]
Concrete mixer [h/1 sl]	0.50	0.25	300
Vibrator [h/1 sl]	0.40	0.50	300
Unit profit [PLN/1 sl]	60.00	45.00	

**Solution.** Mathematical model P:

Let the decision variables:  $x_1, x_2$  – the number of slabs of type 1 and 2,

determine  $\max f(x_1, x_2) = 60x_1 + 45x_2$  – total profit, with constraints

$$\begin{aligned} 0.5x_1 + 0.25x_2 &\leq 300, \\ 0.4x_1 + 0.5x_2 &\leq 300, \\ x_1 &\geq 0, \\ x_2 &\geq 0. \end{aligned} \tag{11.1}$$

We solve this problem in Excel as follows:

1. In cells  $A1 : D4$  (or any other – this note applies to the entire solution), we enter table 11.1.
2. In cells  $F1 : G2$ , respectively, the text " $x_1$ ", " $x_2$ " and the numbers 0.0. In cell  $F4$  enter the text "target function", in cell  $G4$  – the formula  $= B4 * F2 + C4 * G2$  (i.e.  $60x_1 + 45x_2$  from (11.1)).
3. In cell  $B7$  we write the formula  $= B2 * F2 + C2 * G2$  ( $0.5x_1 + 0.25x_2$ ), in cell  $B8$  we write the formula  $= B3 * F2 + C3 * G2$  ( $0.4x_1 + 0.5x_2$  from (11.1)). In order to visually emphasize the description of the problem, we add in cells  $A7 : A8$  the labels of the bounding conditions and in cells  $C7 : C8$  the values of the left sides of the bounding conditions (the latter addition is not necessary). This ends the preparation of the problem for the Solver procedure (make sure that the Solver add-on is installed, if not, add it). So we call Formula/Solver and the dialog box, "Solver Parameters" appears.
4. In the field "Set Target Cell" we enter our target function, that is, the address of cell  $G4$ .
5. In the field "By Changing Cells" we enter the addresses of the cells containing the values of the variables, i.e.  $F2 : G2$ .
6. Press the "Add" button and enter the constraints one by one.
7. In the "Cell Reference", the address of cell  $B7$  (i.e.  $0.5x_1 + 0.25x_2$  – the left side of the inequality (11.1)).
8. We leave as proposed by the system the character  $\leq$ ,
9. in "Constraint" enter the address of cell  $C7$  or  $D2$ ,
10. press the "Add" button and then similarly type
11. in the "Cell Reference" the address of cell  $B8$  (i.e.  $0.4x_1 + 0.5x_2$  – left side of inequality (11.1)).
12. we leave suggested by the system character  $\leq$ ,
13. In "Constraint" we enter the address of cell  $C8$  or  $D3$ .
14. We press "Add".
15. Then we write in "Cell Reference" the address of cell  $F2$ .
16. We replace the character  $\leq$  with character  $\geq$ .

17. We type in "Constraint" 0 (zero).
  18. We press "Add".
  19. We enter in the "Cell Reference" the address of cell  $G2$ .
  20. We replace the character  $\leq$  with character  $\geq$ .
  21. We enter in "Constraint" 0 (zero).
  22. We press "OK".
  23. We check the correctness of the entered constraints.
  24. Press the "Solve" button.
- Then in the table 11.2

Table 11.2: Values needed for calculation of linear programming, by E. Koźniewski

	A	B	C	D	E	F	G
1		Slab 1	Slab 2	Time		$x_1$	$x_2$
2	Concrete mixer	0.50	0.25	300		0	0
3	Vibrator	0.40	0.50	300			
4	Unit profit	60.00	45.00			target function	0
5							
6							
7	n1	0	300				
8	n2	0	300				

after the program has run, we get table 11.3.

Table 11.3: View of the Excel sheet after the actions for model, by E. Koźniewski

	A	B	C	D	E	F	G
1		Slab 1	Slab 2	Time		$x_1$	$x_2$
2	Concrete mixer	0.50	0.25	300		500	200
3	Vibrator	0.40	0.50	300			
4	Unit profit	60.00	45.00			target function	39 000
5							
6							
7	n1	300	300				
8	n2	300	300				

The solution was obtained in cells  $F2 : G2$ , cells  $B7 : B8$  show that the time was used to the maximum. In figure 11.1 the geometric interpretation of the above solution is given.



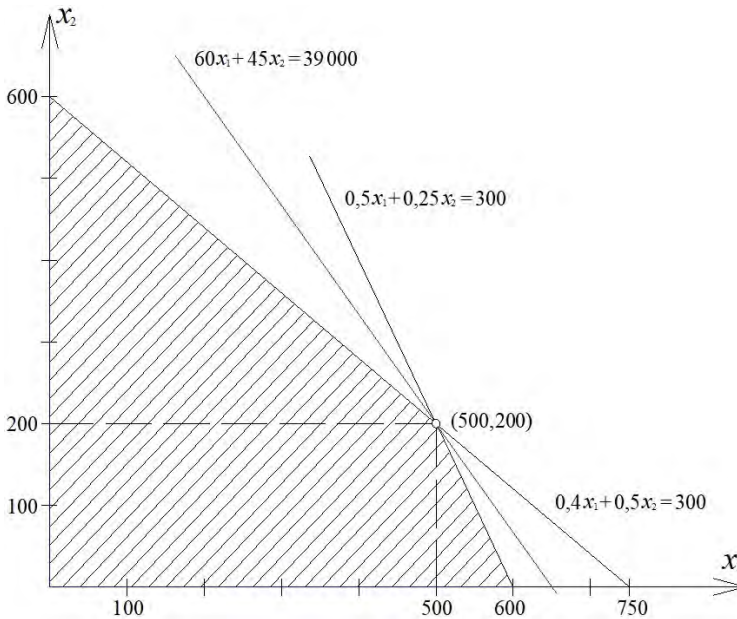


Figure 11.1: Geometric solution of the problem from example 11.1, by E. Koźniewski based on [49]

We will now formulate a dual task.

**Example 11.2.** Determine, for the task in the example 11.1, a cost-effective production plan that minimizes the cost of manufacturing. Thus, we have a model D. Let's denote the decision variables by  $w_1$ ,  $w_2$  – these are the one-hour values of the concrete mixer and vibrator [PLN/h], respectively. Determine the minimum of the function  $g(w_1, w_2) = 300w_1 + 300w_2$  – production cost, under the restrictions

$$\begin{aligned} 0.5w_1 + 0.4w_2 &\geq 60, \\ 0.25w_1 + 0.5w_2 &\geq 45, \\ w_1 &\geq 0, \\ w_2 &\geq 0. \end{aligned}$$

Example 11.1 is the inspiration for the general posing of the problem described in section 11.2.

## 11.2. General problem of linear programming

The matrix and two vectors (column and row) are given

$$\mathbf{A} = \begin{bmatrix} a_{11} & a_{12} & \dots & a_{1n} \\ a_{21} & a_{22} & \dots & a_{2n} \\ \dots & \dots & \dots & \dots \\ a_{m1} & a_{1m} & \dots & a_{mn} \end{bmatrix}, \quad \mathbf{b} = \begin{bmatrix} b_1 \\ b_2 \\ \vdots \\ b_m \end{bmatrix}, \quad \mathbf{c} = [c_1 \quad c_2 \quad \dots \quad c_n]. \quad (11.2)$$

Based on this data, two issues can be formulated.

- **Maximum problem:** find the column vector

$$\mathbf{x} = \begin{bmatrix} x_1 \\ x_2 \\ \vdots \\ x_n \end{bmatrix} \quad \left( \text{can be written } \mathbf{x} = [x_1 \quad x_2 \quad \dots \quad x_n]^T \right) \quad (11.3)$$

such that the linear function

$$\mathbf{c}\mathbf{x} = c_1x_1 + c_2x_2 + \dots + c_nx_n \quad (11.4)$$

has a maximum when the conditions are fulfilled

$$\mathbf{x} \geq 0, \mathbf{A}\mathbf{x} \leq \mathbf{b}. \quad (11.5)$$

- **Minimum problem:** find the row vector

$$\mathbf{w} = [w_1 \quad w_2 \quad \dots \quad w_m] \quad (11.6)$$

such that the linear function

$$\mathbf{w}\mathbf{b} = b_1w_1 + b_2w_2 + \dots + b_mw_m \quad (11.7)$$

has a minimum when the conditions are fulfilled

$$\mathbf{w} \geq 0, \mathbf{w}\mathbf{A} \geq \mathbf{c}. \quad (11.8)$$

We call these problems *dual* to each other.

### 11.3. Fundamental theorem of linear programming

Let the matrix and vectors (11.2) with non-negative elements be given. Let the vectors (11.3) and (11.6) satisfy the conditions (11.5) and (11.8). If the vectors

$$\mathbf{x}^o = [x_1^o \ x_2^o \ \dots \ x_n^o]^T, \quad \mathbf{w}^o = [w_1^o \ w_2^o \ \dots \ w_m^o] \quad (11.9)$$

satisfy the conditions (11.5), (11.8) and the equality holds

$$\mathbf{c}\mathbf{x}^o = \mathbf{w}^o\mathbf{b}, \quad (11.10)$$

then  $\mathbf{x}^o$  is the vector for which the linear function  $\mathbf{c}\mathbf{x} = c_1x_1 + c_2x_2 + \dots + c_nx_n$  reaches a maximum on the convex set defined by the inequality (11.5), and  $\mathbf{w}^o$  is the vector for which the linear function  $\mathbf{w}\mathbf{b} = b_1w_1 + b_2w_2 + \dots + b_mw_m$  reaches a minimum on the convex set defined by the inequality (11.8) [46].

*Proof.* To prove that  $\mathbf{x}^o$  is the optimal value for the maximum problem, it suffices to show that for any vector  $\mathbf{x}$  fulfilling the conditions (11.5) hold  $\mathbf{c}\mathbf{x} \leq \mathbf{c}\mathbf{x}^o$ . Thus, let  $\mathbf{x}$  satisfy the conditions (11.5). Since  $\mathbf{c} \leq \mathbf{w}^o\mathbf{A}$  (second condition of (11.8)), we get  $\mathbf{c}\mathbf{x} \leq (\mathbf{w}^o\mathbf{A})\mathbf{x}$  (the product of two non-negative matrices, i.e., with non-negative values). Applying the associativity of matrix multiplication, we get  $\mathbf{c}\mathbf{x} \leq \mathbf{w}^o(\mathbf{A}\mathbf{x})$ . Because  $\mathbf{x}$  satisfies the first condition  $\mathbf{A}\mathbf{x} \leq \mathbf{b}$ , so  $\mathbf{c}\mathbf{x} \leq \mathbf{w}^o\mathbf{b}$ . By assumption,  $\mathbf{w}^o\mathbf{b} = \mathbf{c}\mathbf{x}^o$ , so  $\mathbf{c}\mathbf{x} \leq \mathbf{c}\mathbf{x}^o$ , whence it follows that it is the largest value in the convex set defined by the inequality (11.5). Similarly, let  $\mathbf{w}$  be any vector satisfying the conditions (11.8). Reasoning similarly, and using the conditions  $\mathbf{A}\mathbf{x}^o \leq \mathbf{b}$  i  $\mathbf{c}\mathbf{x}^o = \mathbf{w}^o\mathbf{b}$ , we get  $\mathbf{w}\mathbf{b} \geq \mathbf{w}(\mathbf{A}\mathbf{x}^o) = (\mathbf{w}\mathbf{A})\mathbf{x}^o \geq \mathbf{c}\mathbf{x}^o = \mathbf{w}^o\mathbf{b}$ . Thus  $\mathbf{w}\mathbf{b} \geq \mathbf{w}^o\mathbf{b}$ . Hence,  $\mathbf{w}^o\mathbf{b}$  is the smallest value of the function  $\mathbf{w}\mathbf{b}$  in the convex set defined by the inequality (11.8).  $\square$

### 11.4. Transport problem [28, 55]

Among the numerous applications of linear programming, the transport problem deserves special attention. The problem involves planning the movement of homogeneous material from  $m$  suppliers to  $n$  customers so as to minimize the expenses incurred in transportation, assuming that they are proportional to the number of units transported. This simplification is acceptable when planning mass transportation. Often the criterion

taken is the minimization of costs or expenses expressed as the product of tons and kilometers. Let's denote for  $i = 1, \dots, m, j = 1, \dots, n$ :

$a_i$  – number of units of material at  $i$ th supplier,

$b_j$  – number of units of material needed by  $j$ th customer,

$c_{ij}$  – the connection distance between  $i$ th supplier and  $j$ th recipient [km] or the cost of transporting a unit of material along this route [PLN],

$x_{ij}$  – the number of units of material transported from  $i$ th supplier to  $j$ th recipient (decision variables).

The data can be stored in matrix form in a table:

Table 11.4: Data for a transport problem, by E. Koźniewski

$c_{11}$	$c_{12}$	$\dots$	$c_{1n}$	$a_1$	RESERVES
$c_{21}$	$c_{22}$	$\dots$	$c_{2n}$	$a_2$	
$\vdots$	$\vdots$	$\dots$	$\vdots$	$\vdots$	
$c_{m1}$	$c_{m2}$	$\dots$	$c_{mn}$	$a_m$	
$b_1$	$b_2$	$\dots$	$b_n$		
DEMANDS					

The mathematical model in terms of linear programming is as follows: Determine the minimum of the target function  $z = \sum_{i=1}^m \sum_{j=1}^n c_{ij}x_{ij}$  under the restrictions

$$\sum_{j=1}^n x_{ij} \leq a_i \quad \text{for } i = 1, 2, \dots, m, \quad (11.11)$$

$$\sum_{i=1}^m x_{ij} = b_j \quad \text{for } j = 1, 2, \dots, n, \quad (11.12)$$

and boundary conditions

$$x_{ij} \geq 0, i = 1, \dots, m, \quad j = 1, \dots, n. \quad (11.13)$$

A transport task is called *balanced*, if the following condition is met

$$\sum_{i=1}^m a_i = \sum_{j=1}^n b_j. \quad (11.14)$$

An *unbalanced* task, i.e. one in which demand (demands) does not equal

supply (reserves, resources), can be reduced to a balanced task, which will allow you to solve it with a typical computer program. To reduce it to a balanced form

- in the case of stocks over demand, we assume a fictitious customer with demand  $b_{n+1} = \sum_{i=1}^m a_i - \sum_{j=1}^n b_j$ ,
- in the opposite case, we assume a fictitious supplier with inventory  $a_{m+1} = \sum_{j=1}^n b_j - \sum_{i=1}^m a_i$  and define transportation costs as zero or give them values resulting from material deficit or surplus, respectively.

If the transportation task is **balanced**, the model is as follows:

Determine the minimum  $z = \sum_{i=1}^m \sum_{j=1}^n c_{ij}x_{ij}$ , given the constraints

$$\sum_{j=1}^n x_{ij} = a_i \quad (11.15)$$

(The entire reserve is exported from each supplier,  $i = 1, \dots, m$ ),

$$\sum_{i=1}^m x_{ij} = b_j \quad (11.16)$$

(demand of each customer will be satisfied,  $j = 1, \dots, n$ ) and boundary conditions

$$x_{ij} \geq 0, i = 1, \dots, m, \quad j = 1, \dots, n. \quad (11.17)$$

The transportation task is a special case of linear programming in standard form with  $mn$  variables and  $m + n$  constraints. Hence, the simplex algorithm can be used to solve transportation problems, which, however, in this case is not an efficient method (if only because a large number of variables appear). The essence of the simplex algorithm is to examine the base solutions successively for optimality. If a solution is not optimal, we look for a new base solution better than the previous one. Transport problems, due to a certain symmetry, can be solved by more concise methods than the simplex algorithm. Every balanced transportation task has a finite optimal solution in which there are at most  $m + n - 1$  non-zero variables.

It is worth noting that the solutions to the transportation task have the following properties.

**Theorem 11.1.** Every balanced transportation task has a finite optimal solution and it is integer if all elements  $a_i, b_j$  are integer.

Solving the transportation task has an interesting connection with graph theory. Before we formulate the relevant theorems, we will introduce three terms related to linear programming: admissible solution and base solution and cycle.

- An admissible solution of a linear programming task is called any solution of the constraint equations and inequalities satisfying the non-negativity condition, i.e., any point of the convex polyhedron associated with the linear problem.
- The base solution of a linear programming task is called any solution of the constraint equations assuming that the decision variables in  $n - m$  (when  $n > m$ ) are equal to zero.
- A cycle is called any rectangle in an table of graphs (Fig. 11.2).

**Theorem 11.2.** An admissible solution to a transportation task is a base solution if and only if the corresponding graph is a connected and cycle-free graph.

**Theorem 11.3.** For the solution graph of the transport task to be a connected and cycle-free graph, it is necessary and sufficient that it contains exactly  $m + n - 1$  vertices.

Coherent graph is one in which any two vertices (circles in the figure 11.2) can be connected by an alternating sequence of vertices and branches (branches are only horizontal and vertical).

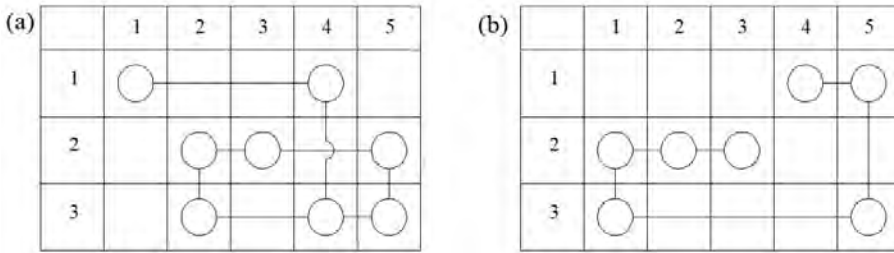


Figure 11.2: Graphs in the transport task matrix: (a) with cycles – is not a solution ( $8 > 3 + 5 - 1$ ); (b) without cycles – is a solution ( $3 + 5 - 1 = 7$ ), by E. Koźniewski

In figure 11.2 are shown the graphs in the solution matrix of the transportation task. The graph without cycles is the base solution ( $3+5-1=7$ ).

**Example 11.3.** Minimizing cut-and-fill haul costs of earth on constructions of section of highway by earthmoving method [56].

In the construction of the road, huge amounts of earth are moved, as illustrated in the road profile drawing (Fig. 11.3). The plan shows the location of the borrow pit and the haul costs are given by  $1 \text{ m}^3/\text{station}$ . The latter are a function of the profile (drawbar pull) and therefore depend on the location and direction of transport. It is assumed that unused land can be removed at no cost. In order to formulate the problem, we will take as starting (transport) points the borrow pits and stations where the earth is available for disposal, and as destination points those sections that require fill. Unit costs are obtained by calculating the unit cost of transportation from each starting point to each destination point. Approximate transportation costs for land lying between two stations are calculated as if the land being transported was at the lower station. For example, the transportation cost from station 2 to station 5 is  $2.0 + 1.7 + 1.5 = 5.2 (\$/\text{m}^3)$ ; from station 5 to station 3 is  $2.5 + 2.3 = 4.8 (\$/\text{m}^3)$ ; from borrow pit  $B$  to station 3 is  $12 + 2.3 = 14.3$ ; from borrow pit  $B$  to station 6 is  $12 + 1.5 + 2.8 = 16.3$ . Let  $x_{ij}$  be the number of cubic meters of earth to be transported from station  $i$  to station  $j$ , and let  $c_{ij}$  denote the unit cost. We will consider only a portion of the road, from station 3 to station 7. This section contains one borrow pit labeled  $B$ , so, for example,  $x_{Bj}$  denotes the amount of earth taken in borrow pit  $B$  that will be transported to station  $j$ .

The target function has the form

$$\begin{aligned}
 z = & 1.7x_{34} + 3.2x_{35} + 6.0x_{36} + 14.3x_{B3} + \\
 & + 12.0x_{B4} + 13.5x_{B5} + 16.3x_{B6} + 6.8x_{63} + \\
 & + 4.5x_{64} + 2.0x_{65} + 8.3x_{73} + 6.0x_{74} + 3.5x_{75} + 1.5x_{76}.
 \end{aligned}$$

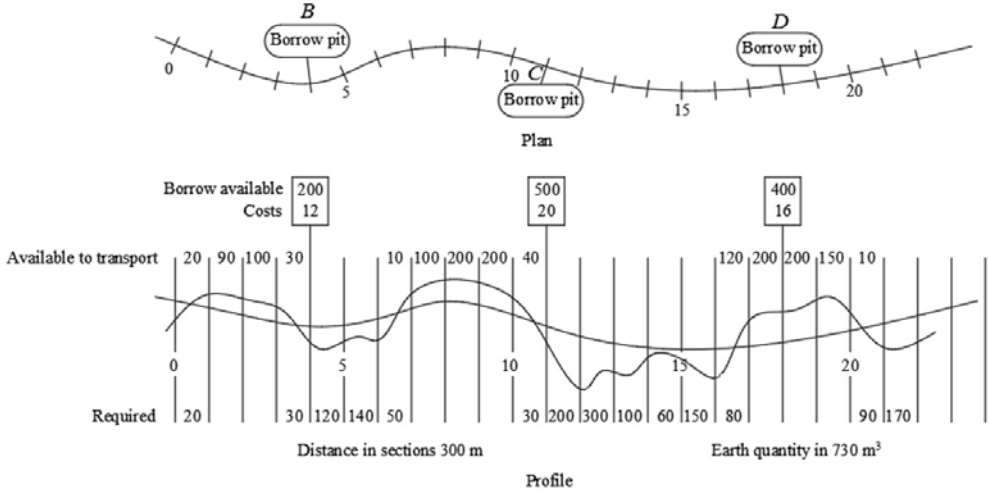


Figure 11.3: Cut and fill for highway [56], by E. Koźniewski

With restrictions

$$\begin{aligned}
 x_{33} + x_{34} + x_{35} + x_{36} &\leq 30, \\
 x_{B3} + x_{B4} + x_{B5} + x_{B6} &\leq 200, \\
 x_{63} + x_{64} + x_{65} + x_{66} &\leq 10, \\
 x_{73} + x_{74} + x_{75} + x_{76} &\leq 100,
 \end{aligned}
 \quad (\text{available earth quantity})$$

$$\begin{aligned}
 x_{33} + x_{B3} + x_{63} + x_{73} &\leq 30, \\
 x_{34} + x_{B4} + x_{64} + x_{74} &\leq 120, \\
 x_{35} + x_{B5} + x_{65} + x_{75} &\leq 140, \\
 x_{36} + x_{B6} + x_{66} + x_{76} &\leq 50,
 \end{aligned}
 \quad (\text{required earth quantity})$$

$x_{ij} \geq 0$  for all  $i, j$ .

The model is clearer in writing when we renumber the indexes of the variables: the first index according to the scheme  $(3, B, 6, 7) \rightarrow (1, 2, 3, 4)$ ;



the second index:  $(3, 4, 5, 6) \rightarrow (1, 2, 3, 4)$  This problem can be solved by the standard method, in which case you need to decompose a matrix of large size. It is much simpler to solve the problem using a special method.

## 11.5. Optimization of transportation of earth masses using various means of transport

We will formulate the task as follows [1]. Given the data

$a_i$  – volume of  $i$ -th earth reserve,  $i = 1, \dots, m$ ,

$b_j$  – volume of  $j$ -th section of embankment,  $j = 1, \dots, n$ ,

$k$  – type of transportation means,  $k = 1, \dots, l$ ,

$c_{ij}^k$  – unit cost of transporting a unit of goods from  $i$ th reserve to  $j$ th section of the embankment  $k$ th means of transportation,

it is necessary to find the quantities of earth  $x_{ij}^k$  transported from the  $i$ th reserve to the  $j$ th section of the embankment  $k$ th means of transport that minimize the function  $m \cdot n \cdot k$  variables

$$z = \sum_{i=1}^m \sum_{j=1}^n \sum_{k=1}^l c_{ij}^k x_{ij}^k, \quad (11.18)$$

under the conditions

$$\sum_{j=1}^n \sum_{k=1}^l x_{ij}^k = a_i, \quad i = 1, 2, \dots, m, \quad (11.19)$$

$$\sum_{i=1}^m \sum_{k=1}^l x_{ij}^k = b_j, \quad j = 1, 2, \dots, n, \quad (11.20)$$

$$x_{ij}^k \geq 0, \quad i = 1, 2, \dots, m, \quad j = 1, 2, \dots, n, \quad k = 1, 2, \dots, l. \quad (11.21)$$

**Example 11.4.** The technical-manpower design of the embankment provides for the construction of a linear embankment with the extraction of soil from point soil reserves. The contractor's company has the following data (table 11.5) [1]:

Table 11.5: Data needed for the linear embankment, by E. Koźniewski

	$b_1 = 47\,000\text{ m}^3$	$b_2 = 70\,500\text{ m}^3$	$b_3 = 58\,750\text{ m}^3$	$\sum_{j=1}^3 b_j = 476\,250\text{ m}^3$
	transport distances in meters			
$a_1 = 67\,500\text{ m}^3$	1820	2490	2746	
$a_2 = 96\,400\text{ m}^3$	2750	2430	2895	
$a_3 = 62\,300\text{ m}^3$	2540	2150	1240	
$\sum_{i=1}^3 a_i = 476\,250\text{ m}^3$	$\sum_{i=1}^3 a_i > \sum_{j=1}^3 b_j$			

For transporting the earth, the available transportation means are as follows:

Tractors with trailers 3 t (means of transportation  $k = 1$ ),  
 trailer scrapers 6 m<sup>3</sup> (means of transportation  $k = 2$ ),  
 dump trucks 3.5 t (means of transportation  $k = 3$ ).

The cost of transporting 1 m<sup>3</sup> of earth by individual means at distances from the table 11.5 is a matrix stored in the table 11.6.

Table 11.6: Unit transport costs for individual distances of embankment sections, by E. Koźniewski

		$b_1$	$b_2$	$b_3$
Earth reserves	$a_1$	$c_{11}^1 = 12.32$	$c_{12}^1 = 16.34$	$c_{13}^1 = 19.05$
		$c_{11}^2 = 8.87$	$c_{12}^2 = 36.19$	$c_{13}^2 = 61.56$
		$c_{11}^3 = 13.60$	$c_{12}^3 = 13.60$	$c_{13}^3 = 16.20$
	$a_2$	$c_{21}^1 = 12.32$	$c_{22}^1 = 19.05$	$c_{23}^1 = 10.05$
		$c_{21}^2 = 16.67$	$c_{22}^2 = 49.86$	$c_{23}^2 = 50.91$
		$c_{21}^3 = 13.60$	$c_{22}^3 = 16.20$	$c_{23}^3 = 16.20$
	$a_3$	$c_{31}^1 = 21.76$	$c_{32}^1 = 16.67$	$c_{33}^1 = 12.32$
		$c_{31}^2 = 71.32$	$c_{32}^2 = 16.67$	$c_{33}^2 = 20.58$
		$c_{31}^3 = 18.80$	$c_{32}^3 = 13.60$	$c_{33}^3 = 13.60$

Due to the inequality  $\sum_{i=1}^3 a_i > \sum_{j=1}^3 b_j$  we introduce additional fictional variables:  $y_1, y_2, y_3$  (volumes of earth transported from reserves  $a_1, a_2, a_3$ ) and write the conditions (11.19) – (11.21).

The conditions (11.19) are of the form

$$\begin{aligned}\sum_{j=1}^3 \sum_{k=1}^3 x_{1j}^k + y_1 &= a_1 (= 67\,500), \\ \sum_{j=1}^3 \sum_{k=1}^3 x_{2j}^k + y_2 &= a_2 (= 96\,400), \\ \sum_{j=1}^3 \sum_{k=1}^3 x_{3j}^k + y_3 &= a_3 (= 62\,300).\end{aligned}$$

The conditions (11.20) have the form

$$\begin{aligned}\sum_{i=1}^3 \sum_{k=1}^3 x_{i1}^k &= b_1 (= 47\,000), \\ \sum_{i=1}^3 \sum_{k=1}^3 x_{i2}^k &= b_2 (= 70\,500), \\ \sum_{i=1}^3 \sum_{k=1}^3 x_{i3}^k &= b_3 (= 58\,750).\end{aligned}$$

The target function is following

$$z = \sum_{i=1}^3 \sum_{j=1}^3 \sum_{k=1}^3 c_{ij}^k x_{ij}^k = 12.32x_{11}^1 + 16.34x_{12}^1 + 19.05x_{13}^1 + \dots$$

For the calculation, you need to transform the variables and formulate the conditions for the linear planning problem.

Solving the task, we get the results (table 11.7).

Table 11.7: Solving the problem of transportation of earth masses, by E. Koźniewski

		Embankment sections			Unused reserve volume
		$b_1 = 47\ 000$	$b_2 = 70\ 500$	$b_3 = 58\ 750$	
Earth reserves	$a_1 = 67\ 500$	$x_{11}^1 = 0$	$x_{12}^1 = 0$	$x_{13}^1 = 0$	$y_1 = 12\ 300$
		$x_{11}^2 = 47\ 000$	$x_{12}^2 = 0$	$x_{13}^2 = 0$	
		$x_{11}^3 = 0$	$x_{12}^3 = 8\ 200$	$x_{13}^3 = 0$	
	$a_2 = 96\ 400$	$x_{21}^1 = 0$	$x_{22}^1 = 0$	$x_{23}^1 = 58\ 750$	$y_2 = 37\ 650$
		$x_{21}^2 = 0$	$x_{22}^2 = 0$	$x_{23}^2 = 0$	
		$x_{21}^3 = 0$	$x_{22}^3 = 0$	$x_{23}^3 = 0$	
	$a_3 = 62\ 300$	$x_{31}^1 = 0$	$x_{32}^1 = 62\ 300$	$x_{33}^1 = 0$	$y_3 = 0$
		$x_{31}^2 = 0$	$x_{32}^2 = 0$	$x_{33}^2 = 0$	
		$x_{31}^3 = 0$	$x_{32}^3 = 0$	$x_{33}^3 = 0$	

## 11.6. Problems

1. Write the transport problem in terms of standard linear programming with  $mn$  variables and  $m+n$  constraints (appropriate matrices, vectors, and conditions).
2. Illustrate the solution of the dual problem from the example 11.1.
3. Design and solve the task of cost minimization with the earthmoving method of road construction:
  - a) from 3 to 17, b) from 4 to 20,
  - c) from 6 to 21, d) from station 8 to station 22.
 Draw the corresponding graphs.
4. Write down a transport problem for different modes of transport in the form of standard linear programming.
5. Formulate a transportation task in classical terms for different transportation means. Is it possible to do so?
6. Draw several variant graphs of solutions to the transport problem for  $m = 7$ ,  $n = 6$ . How many potential solutions theoretically exist?



## Chapter 12

# Mathematical methods of multi-criteria benchmarking analysis on the example of design solutions of selected roof coverings

### 12.1. Mathematical methods

Mathematical methods of multi-criteria comparative analysis here means the principle that the comparison algorithm is based on the construction of a *scalar*, whose numerical value is a synthetic scoring indicator. The construction of the scalar requires that the values of the criteria (nominated or unnominated) be given numerical values that are unnominated. Thus, in the algorithm of mathematical methods, the so-called *coding* is used, which involves reducing the values of nominated features to unnominated ones. Features can be "increasing" (*stimulants*) or "decreasing" (*destimulants*); depending on whether we want to maximize a given quantity (profit, efficiency, quality) or minimize it (cost, time, burden).

### 12.2. Method assumptions

We consider the set  $W$  of specified and acceptable solution variants

$$W = \{W_i : i = 1, 2, \dots, n\}. \quad (12.1)$$

We assume a set of *criteria*  $K$ ,

$$K = \{K_j : j = 1, 2, \dots, m\}, \quad (12.2)$$

for which we determine the set of *measures*

$$X = \{x_{ij} : i = 1, 2, \dots, n; j = 1, 2, \dots, m\}. \quad (12.3)$$

So we get *data matrix*

$$X = \begin{bmatrix} x_{11} & x_{12} & \dots & x_{1m} \\ x_{21} & x_{22} & \dots & x_{2m} \\ \dots & \dots & \dots & \dots \\ x_{n1} & x_{n2} & \dots & x_{nm} \end{bmatrix}. \quad (12.4)$$

The rows of the matrix represent the *partial measures* of individual variants, while the columns - the partial measures of all variants according to the specified partial criterion. The purpose of multi-criteria analysis is to find such a variant (or variants), which, according to the adopted criteria, has the most favorable arrangement of partial measures. These measures in practice are usually nominated quantities (if  $K_j$  means cost, the measures will be expressed in [zloty], if  $K_j$  means time, the measures will be expressed in [days]). Therefore, in order to carry out further considerations involving the comparison of numbers, it makes sense to replace the output data with their codes. By code, we will mean replacing the value of a partial measure with an unmandated numeric value from a specified interval, most often from the interval  $[0, 1]$ .

## 12.3. Coding types

### 12.3.1. Standardization [58]

The essence of this coding is to replace the value of the partial measure  $x_{ij}$  by  $z_{ij}$  based on the mean value and standard deviation for the criterion  $K_j$ . For *stimulant*, we have the following

$$z_{ij} = \frac{x_{ij} - \overline{x_j}}{s_j}, \quad (12.5)$$

and for *destimulant*

$$z_{ij} = (-1) \cdot \frac{x_{ij} - \overline{x_j}}{s_j}, \quad (12.6)$$

where

$$\overline{x_j} = \frac{\sum_{i=1}^n x_{ij}}{n} \quad (12.7)$$

is the average value of the measures of the analyzed variants according to criterion  $j$ ,

$$s_j = \sqrt{\frac{\sum_{i=1}^n (x_{ij} - \bar{x}_j)^2}{n}} \quad (12.8)$$

is the standard deviation of the measures of the analyzed variants according to the criterion  $j$ , and  $i = 1, 2, \dots, n$ ;  $j = 1, 2, \dots, m$ .

### 12.3.2. Normalization

The essence of this coding is to replace the value of the partial measure  $x_{ij}$  by  $z_{ij}$  based on the maximum value for the criterion  $K_j$ . For *stimulant*, we have the following

$$z_{ij} = \frac{x_{ij}}{x_{jmax}}, \quad (12.9)$$

and for *destimulant*

$$z_{ij} = \left( \frac{x_{ij}}{x_{jmin}} \right)^{-1}, \quad (12.10)$$

where  $x_{jmin}$  is the minimum value, and  $x_{jmax}$  is the maximum value of the measure according to the  $j$ -th criterion, for  $i = 1, 2, \dots, n$ ;  $j = 1, 2, \dots, m$ .

### 12.3.3. Coding by Neumann – Morgenstern [58]

The essence of this coding is to replace the value of the partial measure  $x_{ij}$  by  $z_{ij}$  expressed by the ratio of the difference of this measure and the measure of the worst of all variant measures according to the criterion  $K_j$  to the difference of the best and worst measure according to this criterion. For *stimulants* we have the following

$$z_{ij} = \frac{x_{ij} - x_{jmin}}{x_{jmax} - x_{jmin}}, \quad (12.11)$$

and for *destimulants*

$$z_{ij} = \frac{x_{jmax} - x_{ij}}{x_{jmax} - x_{jmin}}, \quad (12.12)$$

for  $i = 1, 2, \dots, n$ ;  $j = 1, 2, \dots, m$ .



### 12.3.4. Coding by Pattern method

The essence of this encoding is to replace the value of the partial measure  $x_{ij}$  by  $z_{ij}$  expressed as the quotient of the given measure and the sum of the measures of all variants according to the criterion  $K_j$ . For *stimulants* we have

$$z_{ij} = \frac{x_{ij}}{\sum_{i=1}^n x_{ij}} \quad (12.13)$$

and for *destimulants*

$$z_{ij} = \frac{1 - x'_{ij}}{n - 1}, \quad (12.14)$$

where  $x'_{ij} = \frac{x_{ij}}{\sum_{i=1}^n x_{ij}}$ , for  $i = 1, 2, \dots, n$ ;  $j = 1, 2, \dots, m$ .

The formula (12.14) represents a linear transformation of the *complement to unity*, which simultaneously preserves the *normalization to unity*, i.e.  $\sum_{i=1}^n z_{ij} = 1$ . Indeed, the last equality is proved by the following calculus

$$\sum_{i=1}^n z_{ij} = \sum_{i=1}^n \frac{1 - x'_{ij}}{n - 1} = \frac{\sum_{i=1}^n \left( 1 - \frac{x_{ij}}{\sum_{i=1}^n x_{ij}} \right)}{n - 1} = \frac{n - \frac{\sum_{i=1}^n x_{ij}}{\sum_{i=1}^n x_{ij}}}{n - 1} = \frac{n - 1}{n - 1} = 1.$$

It is worth noting that in the literature for distimulants, often instead of the formula (12.14) proposed is the nonlinear transformation  $z_{ij} = \frac{x'_{ij}}{\sum_{i=1}^n x'_{ij}}$ ,

where  $x'_{ij} = \frac{1}{x_{ij}}$ . Since the inverses of small numbers are large numbers, such a solution may be burdened with high instability.

## 12.4. Algorithm for applying mathematical methods [58]

Step 1: selection of features - criteria that will determine the solution is made.

Step 2: is determined, with expert input, the weights  $\nu_j$  of each criterion ( $j = 1, 2, \dots, m$ ), whereby  $\sum_{j=1}^m \nu_j = 1$ .

Step 3: numerical measures of variants of solutions are determined, that is, a data matrix is created; for non-measurable features, a scale of evaluations is introduced and, with the help of experts (judges), variants are evaluated. Statistically, the trustworthiness (compatibility) of the judges is evaluated.

Step 4: numerical measures of variances according to each partial criterion are subjected to coding by one of the methods described earlier.

Step 5: an evaluation of the variant solutions is carried out by calculating synthetic indicators. The most favorable solution is characterized by the lowest score if the coding of measure values used minimization, or the highest if the coding consisted of maximization.

## 12.5. Synthetic evaluation formulas [58]

If the formula for direct comparison of the analyzed variants fails, another parameter of comparison is taken for example, the corrected sum index

$$J_i = \sum_{j=1}^m \nu_j z_{ij}, \quad (12.15)$$

where  $\nu_j$  is the criterion weight,  $i = 1, 2, \dots, n$ ;  $j = 1, 2, \dots, m$ .

## 12.6. Hasse diagrams

These are drawings of partially ordered sets. Let us first consider as an example the set of all subsets of a finite set  $\{a, b, c\}$  :  $\{\{a, b, c\}, \{a, b\}, \{a, c\}, \{b, c\}, \{a\}, \{b\}, \{c\}, \emptyset\}$  with the inclusion relation  $\subseteq$ .

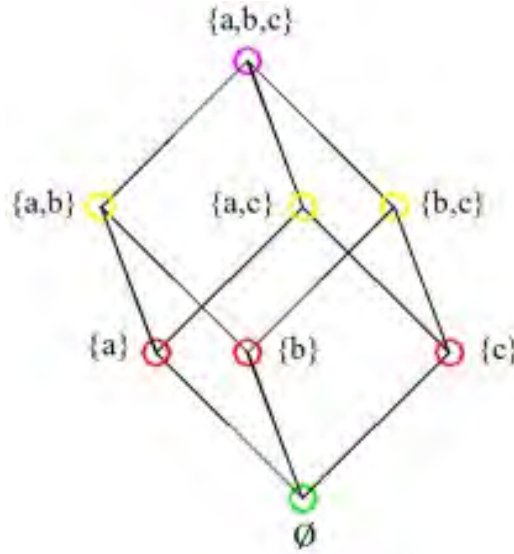


Figure 12.1: Illustration of the partial order dictated by inclusion, by E. Koźniewski

We will say that the element  $\{b, c\}$  "covers"  $\{c\}$  and "covers"  $\{b\}$ . Further  $\{a, b, c\}$  "covers"  $\{a, b\}$ ,  $\{a, c\}$  and  $\{b, c\}$ , while it does not "cover"  $\{a\}$ ,  $\{b\}$  or  $\{c\}$ . The partial order in the set  $S$  is the relation  $\subseteq$ :

- (refl) *reflexive*, i.e.  $s \subseteq s$  for each  $s$  of the set  $S$ ,
- (ants) *antisymmetric*, i.e.,  $s \subseteq t$  and  $t \subseteq s \Rightarrow s = t$ ,
- (trans) *transitive*, i.e.  $s \subseteq t$  and  $t \subseteq u \Rightarrow s \subseteq u$ .

Set  $S$ , in which such a relation  $\subseteq$  is defined, is called *partially ordered*.

We then introduce the relation  $\subset$  such that  $x \subset y$  if and only if  $x \subseteq y$  and  $x \neq y$ .

We say that an element  $t$  "covers" an element  $s$  when  $s \subset t$  and in  $S$  there is no element  $u$  such that  $s \subset u \subset t$ .

*Hasse diagram* of partially ordered set  $(S, \subseteq)$  is *drawing of directed graph*, whose vertices are elements of the set  $S$  and in which an edge runs from a vertex  $t$  to a vertex  $s$  if and only if  $t$  "covers"  $s$ .

The relation  $\subseteq$  – more generally also denoted by  $s \leq t$ , which indicates direction – we interpret:

$$s \leq t \Leftrightarrow t \text{ "is better than" } s.$$

Elements corresponding to points near the very top of the Hasse diagram are considered the best.

Hasse diagrams, like trees with a distinguished root, are usually drawn with edges pointing downward and (usually) without arrows.

## 12.7. Ordering set rules

**The first ordering set rule.** Ordering has a direct character. The term "better" is understood as defined:  $X = \{x_i\}$  ( $i \in \{1, \dots, n\}$ ) is evaluated from the point of view of  $m$  criteria  $K_s$  ( $s \in \{1, \dots, m\}$ ), for which the best values are their maximum values, then  $x_i$  is "better than"  $x_j$  if and only if there exists such  $r$  ( $r \in \{1, \dots, m\}$ )

$$K_r(x_i) > K_r(x_j)$$

and for the others  $K_p$ ,  $p \neq r$ ,

$$K_p(x_i) \geq K_p(x_j).$$

**The second ordering set rule.** Choice of elements is carried out taking into account the sum (average) of the criteria, based on the relationship

$$x_i \text{ "is better than" } x_j \Leftrightarrow \sum_{r=1}^m K_r(x_i) \geq \sum_{r=1}^m K_r(x_j).$$

**The third ordering set rule.** According to this rule, the selection of better elements is carried out taking into account the weighted sum (weighted average) of the adopted criteria. The individual criteria  $K_r$  ( $r = 1, 2, \dots, m$ ) should be assigned different numerical weights  $\nu_r$  ( $r = 1, 2, \dots, m$ ). The selection of "better" variants (elements) is carried out on the basis of the relationship

$$x_i \text{ "is better than" } x_j \Leftrightarrow \sum_{r=1}^m \nu_r K_r(x_i) \geq \sum_{r=1}^m \nu_r K_r(x_j).$$

**The fourth ordering set rule (ordering according to the desired parameters).** For a pair of elements  $i, j$  we determine for how many criteria is  $K_r(x_i) \geq K_r(x_j)$  and denote this number by  $l(i, j)$  ( $x_i$  "is better

than"  $x_j$ ), except that in at least one  $r'$  we demand  $K_{r'}(x_i) > K_{r'}(x_j)$ , then for the remaining  $g(i, j)$  criteria we have  $K_s(x_i) < K_s(x_j)$  ( $x_i$  "is worse than"  $x_j$ ). Obviously, we have  $l(i, j) + g(i, j) = m$ . Finally, we consider an element  $x_i$  as "better than"  $x_j$  if and only if  $l(i, j) > g(i, j)$ . In particular, we can apply this rule when we want to omit in the analysis (at a given moment) certain criteria.

## 12.8. Criteria for evaluation of features of selected roofing covers

- Total costs (materials, labor, equipment) [PLN] – criterion  $K_1$ ,
- Weight of coverage [ $\text{kN}/\text{m}^2$ ] – criterion  $K_2$ ,
- Durability of coverage [years] – criterion  $K_3$ ,
- Aesthetics of coverage (evaluation 1-6) – criterion  $K_4$ ,
- Simplicity of exploitation ( evaluation 1-6) – criterion  $K_5$ .

### 12.8.1. Total costs (materials, labor and equipment)

Costs for materials, labor and equipment, as well as total costs, were developed using Norma Pro based on cost estimations.

Table 12.1: Summary of costs of construction of selected roofing covers [PLN], by E. Koźniewski

	<b>Variant 1</b> Roof tile Ceramic Granat 13V	<b>Variant 2</b> Roof tile concrete Verona	<b>Variant 3</b> Roof tile metal Finnea	<b>Variant 4</b> Roof tile metal Monterrey Standard	<b>Variant 5</b> shingles bitumen	<b>Variant 6</b> shingles wooden
<b>MLE</b>	52 428.26	63 620.02	41 711.10	33 788.91	64 511.38	74 029.33
<b>Materials</b>	35 592.22	36 314.19	24 605.99	14 454.80	25 510.02	46 971.78
<b>Labor</b>	15 615.45	25 050.82	16 684.79	18 753.06	36 480.89	25 321.10
<b>Equipment</b>	1 220.59	2 255.01	420.32	581.05	2 520.47	1 736.45

### 12.8.2. Weight of coverage

By weight of roof covering we mean only the weight of the material used for it. Weights of formwork, battening, etc. are not included.

Table 12.2: Summary of the weight of the roofing [kN/m<sup>2</sup>], by E. Koźniewski

	Variant 1	Variant 2	Variant 3	Variant 4	Variant 5	Variant 6
Roofing weight [kN/m <sup>2</sup> ]	0.474	0.479	0.053	0.048	0.095	0.459

The lowest weight coverage has variant 4 – roof tile metal Monterrey Standard, while the heaviest coverage is Verona – variant 2.

### 12.8.3. Coverage durability

Durability is a difficult word to define. In construction, we want the materials used to be strong, reliable, durable and resistant to external factors. The term with which we often replace the word durability is, among other things, the product (material) warranty. The values of this criterion are determined on the basis of warranties from the catalogs of manufacturers of selected roofing materials.

Table 12.3: Summary of roofing warranties [years], by E. Koźniewski

	Variant 1	Variant 2	Variant 3	Variant 4	Variant 5	Variant 6
Durability [years]	20	30	40	30	15	40

Two coverings – Finnera modular metal roofing tile (3rd variant) and wooden shingles (6th variant) – have the highest warranties, while bitumen shingles (5th variant) have the lowest warranties.

### 12.8.4. Coverage aesthetics

Aesthetics is related to the sense of beauty and depends on a person's individual judgment. Therefore, its value was prepared by experts through a questionnaire. The authors of the publication, in order to verify the reliability of the experts (judges), subjected a specific aspect to statistical analysis, namely: what is the degree of correlation between  $k$  sets of evaluations (expert ratings) on  $n$  objects (roof evaluation criteria:  $K_1, K_2, K_3, K_4, K_5$ ). A measure of this interdependence is the *W-Kendall compatibility coefficient*, which takes values from "0" (no concordance) to "1" (complete concordance). It should be noted that the high  $W$  score we interpret as the fact that the judges agree on the criteria they used to evaluate the given objects. At the same time, it should be noted that a high value of coefficient  $W$  does not at all mean that the

evaluation of specific objects is correct. It may be that the judges, using a false criterion (from the point of view of the external criterion), came to consensual opinions.

Testing the  $W$  Kendall coefficient for evaluations of criterion  $K_4$  (aesthetics of coverage) is done according to the following procedure. The results of the questionnaires of ten experts (judges) for the six variants are compiled in a table (Table 12.4). To determine the ranks in each row of the table 12.4 we setup the results in descending order from left to right, thus creating table 12.5, calculate the ranks and insert into table 12.6.

Table 12.4: Summary of the results of the questionnaire for criterion  $K_4$  – aesthetics of coverage, by E. Koźniewski

AESTHETICS	$E1$	$E2$	$E3$	$E4$	$E5$	$E6$	$E7$	$E8$	$E9$	$E10$	Average
Variant 1	5	4	4	5	5	3	4	3	5	4	4.2
Variant 2	6	4	5	6	4	6	5	5	4	4	4.9
Variant 3	4	5	4	4	6	4	4	5	6	5	4.7
Variant 4	4	5	5	4	4	5	4	5	5	5	4.6
Variant 5	2	3	3	3	1	4	4	1	4	4	2.9
Variant 6	1	2	2	2	2	2	6	1	2	3	2.3

Table 12.5: Summary of questionnaire results for criterion  $K_4$  – aesthetics of coverage, arranged in descending order, by E. Koźniewski

AESTHETICS											
Variant 1	5	5	5	5	4	4	4	4	3	3	
Variant 2	6	6	6	5	5	5	4	4	4	4	
Variant 3	6	6	5	5	5	4	4	4	4	4	
Variant 4	5	5	5	5	5	5	4	4	4	4	
Variant 5	4	4	4	4	3	3	3	2	1	1	
Variant 6	6	3	2	2	2	2	2	2	1	1	

We will discuss in detail the determination of the ranks based on the first row of the table 12.4: evaluation 5 is in the four positions 1, 2, 3, 4; we calculate their average  $\frac{1+2+3+4}{4} = 2.5$  and insert it into the table in place of evaluations 5. Evaluation 4 is in positions 5, 6, 7, 8; we calculate the average  $\frac{5+6+7+8}{4} = 6.5$  and insert this number in place of evaluations

4. Evaluation 3 is at positions 9, 10; we calculate the average  $\frac{9+10}{2} = 9.5$  and insert this number in the table instead of evaluations 3. This gives us the first row of the table 12.6. We will repeat the determination of ranks based on the second row of the table 12.4: the ratings 6 are at three positions 1, 2, 3; we calculate their average  $\frac{1+2+3}{3} = 2$  and insert it into the table 12.6 in place of the ratings 6; evaluation 5 is on three items 4, 5, 6; we calculate the average of these positions 4, 5, 6; we calculate the average of these items  $\frac{4+5+6}{3} = 5$  and insert it into the table 12.6 in place of ratings 5; evaluation 4 is on items 7, 8, 9, 10; we calculate the average  $\frac{7+8+9+10}{4} = 8.5$  and insert it into the table 12.6 in place of grades 4.

Table 12.6: Summary of the results of the questionnaire for criterion  $K_4$  – aesthetics of coverage, by E. Koźniewski

AESTHETICS	E1	E2	E3	E4	E5	E6	E7	E8	E9	E10
Variant 1	2.5	6.5	6.5	2.5	2.5	9.5	6.5	9.5	2.5	6.5
Variant 2	2	8.5	5	2	8.5	2	5	5	8.5	8.5
Variant 3	8	4	8	8	1.5	8	8	4	1.5	4
Variant 4	8.5	3.5	3.5	8.5	8.5	3.5	8.5	3.5	3.5	3.5
Variant 5	8	6	6	6	9.5	2.5	2.5	9.5	2.5	2.5
Variant 6	9.5	5.5	5.5	5.5	5.5	5.5	1	9.5	5.5	2

Table 12.7: Table of ranks for criterion  $K_4$  – aesthetics of coverage ( $R_i = k \cdot \overline{EX}$ ), by E. Koźniewski

AESTHET.	E1	E2	E3	E4	E5	E6	E7	E8	E9	E10	Average $\overline{EX}$	$R_i$	$(R_i - R)^2$
Variant 1	2.5	6.5	6.5	2.5	2.5	9.5	6.5	9.5	2.5	6.5	5.5	55	492.84
Variant 2	2	8.5	5	2	8.5	2	5	5	8.5	8.5	5.5	55	492.84
Variant 3	8	4	8	8	1.5	8	8	4	1.5	4	5.5	55	492.84
Variant 4	8.5	3.5	3.5	8.5	8.5	3.5	8.5	3.5	3.5	3.5	5.5	55	492.84
Variant 5	8	6	6	6	9.5	2.5	2.5	9.5	2.5	2.5	5.5	55	492.84
Variant 6	9.5	5.5	5.5	5.5	5.5	5.5	1	9.5	5.5	2	5.5	55	492.84
											$R = 33$	$\text{Sum\_}R_i = 330$	$S = 2872.24$



When the evaluation results are repeated, we get the so-called tied ranks. For these ranks, we calculate the so-called corrections. First, in the columns of the table 12.7 we find repeated ranks – in  $E1$  there are two: 8, 8; in  $E2, E3$  and  $E4$  there are none; in  $E5$  there are two 8.5 and 8.5; in  $E6$  and  $E7$  there are none; in  $E8$  there are three times 9.5; 9.5; 9.5; in  $E10$  there are none. Denoting by  $t$  the number of rank repetitions, in columns  $E1, E5, E9$  we have  $t = 2$ , in column  $E8$   $t = 3$ , in the other columns  $E2, E3, E4, E6, E7, E10$   $t = 0$ . Calculating the corrections  $t^3 - t$ , we get the values 6 ( $2^3 - 2 = 6$ ) and 24 ( $3^3 - 3 = 24$ ) and 0 ( $0^3 - 0 = 0$ ), respectively, which we enter in the second column of the table 12.8, we add up (just rewrite here) and write in the third column of table 12.8, and after dividing by 12 we write in the fourth column of the table 12.8.

Table 12.8: Calculation of corrections for criterion  $K_4$  – aesthetics of coverage, by E. Koźniewski

	$t^3 - t$	SUM	$T_{EX} = \frac{\sum(t^3 - t)}{12}$
$T_{E1}$	6	6	0.5
$T_{E2}$	0	0	0
$T_{E3}$	0	0	0
$T_{E4}$	0	0	0
$T_{E5}$	6	6	0.5
$T_{E6}$	0	0	0
$T_{E7}$	0	0	0
$T_{E8}$	24	24	2
$T_{E9}$	6	6	0.5
$T_{E10}$	0	0	0
			$\sum T_{EX} = 3.50$

The  $W$  Kendall coefficient for  $k = 10$ ;  $n = 6$  we calculate from the formula

$$W = \frac{S}{\frac{1}{12} \cdot n^2 \cdot (k^3 - k) - n \cdot \sum_{i=1}^k T_i} \quad (12.16)$$

based on the results in the tables 12.7 and 12.8. We get  $W = 0.98$ . After taking into account the relationship  $\chi^2 = k(n - 1)W$  this is a general

method of checking the reliability of judges.

In the case when  $3 \leq k \leq 20$  and  $3 \leq n \leq 7$ , the relevance of the  $W$  factor is checked in a special table. Using it involves comparing  $S_{kr}$  ( $S$  critical) number from the table for  $k$  judges and  $n$  rated objects with the calculated  $S$  value from the rank table.

$S_{kr} = 376.7$  – the value from the table 12.9.

Because of the satisfied inequality  $S_{kr} = 376.7 < S = 2872.24$  there are no reasons to reject the judges' concordance hypothesis.

Table 12.9: Critical values for  $3 \leq k \leq 20$  and  $3 \leq n \leq 7$  (Siegel S., Nonparametric Statistics for the Behavioral Sciences, McGraw-Hill, NY 1956, 286p).

$\alpha = 0.05$	$n$				
$k$	3	4	5	6	7
3			64.4	103.9	157.3
4		49.5	84.4	143.3	217.0
5		62.6	112.3	182.4	276.2
6		75.7	136.1	221.4	335.2
8	48.1	101.7	183.7	299.0	453.1
9	54.0	—	—	—	—
10	60.0	127.8	231.2	376.7	571.0
12	71.9	—	—	—	—
14	83.8	—	—	—	—
15	89.8	192.9	349.8	570.5	864.9
16	95.8	—	—	—	—
18	107.7	—	—	—	—
20	119.7	258.0	468.5	764.4	1158.7

### 12.8.5. Simplicity of exploitation

The use of a roof involves conservation and various repairs of damaged roof fragments. Everyone has an individual opinion on the operation of a given roofing, so as with criterion 4 ( $K_4$  – aesthetics of the roofing) its value was determined by experts.

Testing  $W$  Kendall coefficient for evaluations of criterion  $K_5$  – simplicity of exploitation.

Table 12.10: Summary of questionnaire results for criterion  $K_5$  – simplicity of exploitation, by E. Koźniewski

EXPLOITATION	E1	E2	E3	E4	E5	E6	E7	E8	E9	E10	Średnia
Variant 1	6	5	5	4	5	4	6	3	5	6	4.9
Variant 2	6	5	5	5	4	5	6	3	3	5	4.7
Variant 3	5	4	4	5	5	5	4	4	5	4	4.5
Variant 4	5	4	4	5	5	5	4	4	5	4	4.5
Variant 5	3	3	3	3	3	4	3	3	4	5	3.4
Variant 6	1	2	3	2	3	3	5	3	2	4	2.8

Table 12.11: Rank table for criterion  $K_5$  – simplicity of exploitation, by E. Koźniewski

EXPLOITATION	E1	E2	E3	E4	E5	E6	E7	E8	E9	E10	AVERAGE	$R_i$	$(R_i - R)^2$
Variant 1	2	5.5	5.5	8.5	5.5	8.5	2	10	5.5	2	5.5	55	484
Variant 2	1.5	5	5	5	8	5	1.5	9.5	9.5	5	5.5	55	484
Variant 3	3	8	8	3	3	3	8	8	3	8	5.5	55	484
Variant 4	3	8	8	3	3	3	8	8	3	8	5.5	55	484
Variant 5	7	7	7	7	7	2.5	7	7	2.5	1	5.5	55	484
Variant 6	10	8	4.5	8	4.5	4.5	1	4.5	8	2	5.5	55	484
												$R = 33$	
												Sum $R_i = 330$	
													$S = 2904$

Determination of the coefficient  $W$ : for  $k = 10$ ;  $n = 6$  (based on calculations, analysis and (12.16) and the table 12.12) we find the value of  $W = 0.99$ . In the case when  $3 \leq k \leq$  and  $3 \leq n \leq 7$ , the significance of the coefficient  $W$  is checked in a special table 12.9. Using it involves comparing the number  $S_{kr}$  ( $S$  critical) from the table for  $k$  judges and  $n$  rated objects with the calculated  $S$  value from the rank table.

$S_{kr} = 376.70$  – value from the table.

Since  $S_{kr} = 376.70 < S = 2904$ , so there are no reasons to reject the judges' concordance hypothesis.

When the evaluation results are repeated, we get the so-called tied ranks,

for which we calculate the so-called corrections:

Table 12.12: Calculation of corrections for criterion  $K_5$  – simplicity of exploitation, by E. Koźniewski

	$t^3 - t$	SUM	$T_{EX} = \frac{\sum(t^3 - t)}{12}$
$T_{E1}$	6	6	0.5
$T_{E2}$	24	24	2
$T_{E3}$	6	6	0.5
$T_{E4}$	6	6	0.5
$T_{E5}$	6	6	0.5
$T_{E6}$	6	6	0.5
$T_{E7}$	6	6	0.5
$T_{E8}$	6	6	0.5
$T_{E9}$	6	6	0.5
$T_{E10}$	6	12	1
			$\sum T_i = 7$

## 12.9. Proposals of weights for synthetic evaluation

Weights, like evaluations of criteria, can be adopted using judges' evaluations and perform compliance analysis, but can be adopted arbitrarily. But also the weighting of individual criteria can be adopted by the investor, but also by the contractor or other decision-maker. In this example, we adopt the weights of individual criteria by the decision of the investor.

Table 12.13: Criteria for the weights proposed by the investor, by E. Koźniewski

	Weights
$K1$ – Total costs	0.30
$K2$ – Weight of coverage	0.10
$K3$ – Durability of coverage	0.25
$K4$ – Aesthetics of coverage	0.15
$K5$ – Simplicity of exploitation	0.20

Table 12.14: Inputs for synthetic evaluations, by E. Koźniewski

	<i>K1</i> Total costs [PLN]	<i>K2</i> Weight [kN/m <sup>2</sup> ]	<i>K3</i> Durability [yaers]	<i>K4</i> Aesthetics (points 1-6)	<i>K5</i> Exploitation simplicity (points 1-6)
<i>V</i> <sub>1</sub> : Ceram. Granat 13 V	52 428.26	0.474	20	4.2	4.9
<i>V</i> <sub>2</sub> : Concrete Verona	63 620.02	0.479	30	4.9	4.7
<i>V</i> <sub>3</sub> : Met. Finnera	41 711.10	0.053	40	4.7	4.5
<i>V</i> <sub>4</sub> : Met. Montenerrey	33 788.91	0.048	30	4.6	4.5
<i>V</i> <sub>5</sub> : Bitumen shingles	64 511.38	0.095	15	2.9	3.4
<i>V</i> <sub>6</sub> : Wooden shingles	74 029.33	0.459	40	2.3	2.8
Sum	330 089.00	1.61	175.00	23.60	24.80

## 12.10. Multi-criteria analysis of selected variants

We return to the analysis of the basic table 12.14. We will apply Pattern coding (12.13) to both stimulants (*K3*, *K4*, *K5*) and destimulants (*K1*, *K2*). As a result of this operation, we get table 12.15.

Table 12.15: Applied Pattern coding for all criteria, by E. Koźniewski

	<i>K1</i> Total costs [PLN]	<i>K2</i> Weight [kN/m <sup>2</sup> ]	<i>K3</i> Durability [yaers]	<i>K4</i> Aesthetics (points 1-6)	<i>K5</i> Exploitation simplicity (points 1-6)
<i>V</i> <sub>1</sub> : Ceram. Granat 13 V	0.158831	0.294776	0.114286	0.177966	0.197581
<i>V</i> <sub>2</sub> : Concrete Verona	0.192736	0.297886	0.171429	0.207627	0.189516
<i>V</i> <sub>3</sub> : Met. Finnera	0.126363	0.032960	0.228571	0.199153	0.181452
<i>V</i> <sub>4</sub> : Met. Montenerrey	0.102363	0.029851	0.171429	0.194915	0.181452
<i>V</i> <sub>5</sub> : Bitumen shingles	0.195436	0.059080	0.085714	0.122881	0.137097
<i>V</i> <sub>6</sub> : Wooden shingles	0.224271	0.285448	0.228571	0.097458	0.112903

After applying the Pattern recoding ((12.14) for  $n = 6$ ) to the destimulants (*K1*, *K2*), we get the final coded table 12.16.

Table 12.16: Applied Pattern recoding for destimulants ( $K1, K2$ ), by E. Koźniewski

	$K1$ Total costs [PLN]	$K2$ Weight [kN/m <sup>2</sup> ]	$K3$ Durability [yaers]	$K4$ Aesthetics (points 1-6)	$K5$ Exploitation simplicity (points 1-6)
$V_1$ : Ceram. Granat 13 V	0.168234	0.141045	0.114286	0.177966	0.197581
$V_2$ : Concrete Verona	0.161453	0.140423	0.171429	0.207627	0.189516
$V_3$ : Met. Finnera	0.174727	0.193408	0.228571	0.199153	0.181452
$V_4$ : Met. Montenerrey	0.179527	0.194030	0.171429	0.194915	0.181452
$V_5$ : Bitumen shingles	0.160913	0.188184	0.085714	0.122881	0.137097
$V_6$ : Wooden shingles	0.155146	0.142910	0.228571	0.097458	0.112903

The values of the codes shown in the table 12.16 do not allow a constructive indication of the diagram using the first rule (comparing the corresponding values of two rows, each with each). Such results of the analysis provide an incentive to use the third rule of comparison (the one with weights) or, otherwise, the corrected summation indicator.

Table 12.17: Results of the third rule of comparison (with weights), by E. Koźniewski

	$\sum_{r=1}^m \nu_r K_r(x_i)$
$V_1$ : Ceram. Granat 13 V	0.159357110
$V_2$ : Concrete Verona	0.174382567
$V_3$ : Met. Finnera	0.195065066
$V_4$ : Met. Montenerrey	0.181645957
$V_5$ : Bitumen shingles	0.134372358
$V_6$ : Wooden shingles	0.155176942

The results of comparison according to the third comparison rule lead to an ordering  $V_5 \leq V_6 \leq V_1 \leq V_2 \leq V_4 \leq V_3$ . Hence, the best option is variant 3. We can apply the second comparison rule, where no weights are used, or equivalently assume that all weights  $\nu_r$  are identical, i.e.  $\nu_r = \frac{1}{m}$  FOR  $r = 1, 2, \dots, m$ . Then we get the table 12.18 and ordering of  $V_5 \leq V_6 \leq V_1 \leq V_2 \leq V_4 \leq V_3$ .

Table 12.18: Results of the second comparison rule (without weights), by E. Koźniewski

	$\sum_{r=1}^m K_r(x_i)$
$V_1$ : Ceram. Granat 13 V	0.799111101
$V_2$ : Concrete Verona	0.870447513
$V_3$ : Met. Finnera	0.977310905
$V_4$ : Met. Monteneroy	0.921352683
$V_5$ : Bitumen shingles	0.694789231
$V_6$ : Wooden shingles	0.736988566

As can be seen, the result of comparison without weights does not differ and is the same as the result of comparison with weights.

Another issue is the obtained values in the tables 12.17 and 12.18. What is the difference between the two? We can evaluate it, for example, by rounding (approximations with precision) to two places or one place after the decimal.

Table 12.19: Results of the second comparison rule with assumed accuracy (with weights), by E. Koźniewski

	$\sum_{r=1}^m \nu_r K_r(x_{ij})$ accuracy to 1 decimal place	$\sum_{r=1}^m \nu_r K_r(x_{ij})$ accuracy to 2 decimal places	$\sum_{r=1}^m \nu_r K_r(x_{ij})$ accuracy to 3 decimal places
$V_1$ : Ceram. Granat 13 V	0.2	0.16	0.159
$V_2$ : Concrete Verona	0.2	0.17	0.174
$V_3$ : Met. Finnera	0.2	0.20	0.195
$V_4$ : Met. Monteneroy	0.2	0.18	0.182
$V_5$ : Bitumen shingles	0.1	0.13	0.134
$V_6$ : Wooden shingles	0.2	0.16	0.155

The result of the comparison according to the third comparison rule is illustrated in figure12.2.

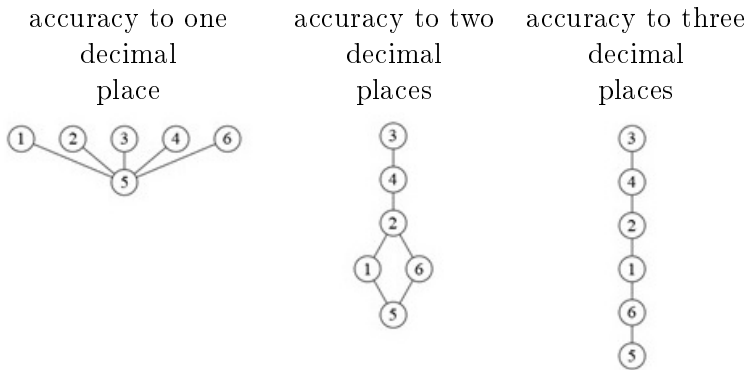


Figure 12.2: Hasse diagrams constructed for different accuracies according to the third rule of comparison, by E. Koźniewski

Table 12.20: The results of the second rule of comparison with assumed accuracy (without weights), by E. Koźniewski

	$\sum_{r=1}^m K_r(x_{ij})$ accuracy to 1 decimal place	$\sum_{r=1}^m K_r(x_{ij})$ accuracy to 2 decimal places	$\sum_{r=1}^m K_r(x_{ij})$ accuracy to 3 decimal places
$V_1$ : Ceram. Granat 13 V	0.8	0.80	0.799
$V_2$ : Concrete Verona	0.9	0.87	0.870
$V_3$ : Met. Finnera	1.0	0.98	0.977
$V_4$ : Met. Montenerrey	0.9	0.92	0.921
$V_5$ : Bitumen shingles	0.7	0.69	0.695
$V_6$ : Wooden shingles	0.7	0.74	0.737

The result of the comparison according to the second ordering rule is presented in the figure 12.3.

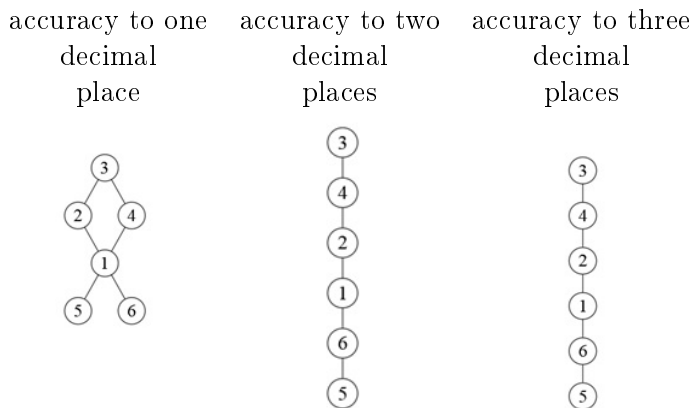


Figure 12.3: Hasse diagrams constructed for different accuracies according to the second ordering rule, by E. Koźniewski



The posted graphs (Fig. 12.2, 12.3) diagram of coded values indicate a good representation obtained with calculation accuracy to the third decimal place. But the results with accuracy to the second place indicate careful use of the ranking. It is worth checking the difference between the different values of the synthetic evaluations (12.15). The final decision should already be made in the context of the analysis of the real data (Table 12.14).

### **12.11. Summary**

As a result of the analysis, it was concluded that the best roof covering from the point of view of the discussed criteria is roofing tile Finnea (variant 3), while the worst covering in this evaluation is wooden spruce shingles (variant 6) or bitumen shingles (variant 5). The total cost of Finnea tile roofing was estimated at 41 711.10PLN. This is not the lowest cost among the analyzed coverings, but quite low. The durability of the selected covering is the longest. In terms of aesthetics, this covering was ranked the highest.

### **12.12. Problems**

1. Make a benchmarking analysis of the roofing presented in Chapter 12 using coding:
  - a) Neumann – Morgenstern,
  - b) normalization.Assume the values and weights specified in Chapter 12.
2. In the 1st task, make a benchmark analysis of 12 roofing, adopt the experts' own assessments and weight values.
3. Make a comparative analysis of single-family houses made with different technologies and materials with regard to cost.

# Bibliography

- [1] Bala W., Koźniewski E., Paczyński W., *Metoda optymalizacji transportu mas ziemnych przy budowie wałów przeciwpowodziowych*, referat wygłoszony podczas XIV sesji referatowo-dyskusyjnej „Technologia i organizacja budowy wałów przeciwpowodziowych”, Kraków 1973, 44–50.
- [2] „Biuletyn Statystyczny Województwa Podlaskiego”, lata 2000–2006.
- [3] Borowska A., *Approximation of the Ellipse Offset Curves in Turbo Roundabouts Design*, „The Journal Biuletyn of Polish Society for Geometry and Engineering Graphics” 2018, vol. 31, 43–51.
- [4] Bostancıoğlu E., *Effect of Building Shape on Residential Building's Construction, Energy and Life Cycle Costs*, „Architectural Science Review” 2010, vol. 53, 441–467.
- [5] Bribiesca E., *A Measure of Compactness for 3D Shapes*, „Computers and Mathematics with Applications” 2000, vol. 40, 1275–1284.
- [6] Brzeziński J., *Metodologia badań psychologicznych*, Wydawnictwo Naukowe PWN, Warszawa 1987, 500–505.
- [7] Coxeter H.S.M., *Introduction to Geometry*, John Wiley and Sons, Inc., New York 1961.
- [8] Górnicki J., *Własności ekstremalne figur izoperymetrycznych na płaszczyźnie*, „Matematyka – Społeczeństwo – Nauczanie” 1990, nr 5, 43–48.
- [9] Grabowski R.J., *Ellipse Offset Curves in the Formation of Turbo-Roundabouts*, „Roads and Bridges – Drogi i Mosty” 2015, vol. 14, 193–202.
- [10] *Brachistochrona*, <https://pl.wikipedia.org/wiki/Brachistochrona> [dostęp 22.08.2022].
- [11] *Patio*, <https://pl.wiktionary.org/wiki/patio> [dostęp 26.07.2022].
- [12] *Tessellation Creator*, <https://www.nctm.org/Classroom-Resources/Illuminations/Interactives/Tessellation-Creator/> [dostęp 16.09.2022].
- [13] *Art. hutnicze*, <https://semex.pl/art-hutnicze-czestochowa> [dostęp 24.08.2023].
- [14] *Grupa Azoty Zakłady Azotowe „PUŁAWY” S.A.*, <https://www.linked>

- in.com/posts/grupa-azoty-zak%C5%82ady-azotowe-pu%C5%82awy-s-a-\_grupaaazotypu%C5%82awy-takpracujemy-activity-7028680348410462209-jmXy?trk=public\_profile\_like\_view [dostęp 2.08.2023].
- [15] *Pojemnik IBC UN EX 1000L z odprowadzeniem ładunków elektrostatycznych*, [https://www.eco24.pl/Paletopojemnik-IBC-z-odprowadzenie-m-ladunkow-elektrostatycznych-1000-L?gclid=Cj0KCQjwoK2mBhDzARIsADGbjeq67G2WG3jI\\_Baj2kRzZejxStLZobUvrLyQHdUscweYBfsE5qeGVPMAruFEALw\\_wcB](https://www.eco24.pl/Paletopojemnik-IBC-z-odprowadzenie-m-ladunkow-elektrostatycznych-1000-L?gclid=Cj0KCQjwoK2mBhDzARIsADGbjeq67G2WG3jI_Baj2kRzZejxStLZobUvrLyQHdUscweYBfsE5qeGVPMAruFEALw_wcB) [dostęp 3.08.2023].
- [16] Brown J.C., *Arata Izosaki – wybrane realizacje w Japonii*, [https://architektura.info/architektura/polska\\_i\\_swiat/arata\\_izosaki\\_wybrane\\_realizacje\\_w\\_japonii](https://architektura.info/architektura/polska_i_swiat/arata_izosaki_wybrane_realizacje_w_japonii) [dostęp 3.08.2023].
- [17] Archirama, [https://archirama.smcloud.net/s/photos/t/114/stacja\\_warszawa\\_ochota\\_1846.jpg](https://archirama.smcloud.net/s/photos/t/114/stacja_warszawa_ochota_1846.jpg) [dostęp 20.04.2022].
- [18] Rögner K., *Jüdische Heimat in 3.000 Betonsteinen*, Der Sonntag, <https://www.sonntag-sachsen.de/juedische-heimat-3000-betonsteinen> [dostęp 31.08.2023].
- [19] *Turning Torso Malmo*, [https://commons.wikimedia.org/wiki/File:Turning\\_Torso\\_Malmo.jpg](https://commons.wikimedia.org/wiki/File:Turning_Torso_Malmo.jpg) [dostęp 2.08.2023].
- [20] <https://www.google.com/search?client=firefox-b-d&q=s%C5%82up+kr%C4%99cony+z+klinkieru#imgcr=x2oGbFdSV7fA4M&imgdii=qwI2na6LuXiLbM> [dostęp 2.08.2023].
- [21] Witlinek, <https://witlinek.mojabudowa.pl/galeria?current=8&page=26> [dostęp 20.04.2022].
- [22] James K., *We've lived under McNutt's persistent surveillance. Here's why St. Louis should say 'no'*, Missouri Independent, <https://missouriindependent.com/2021/01/05/weve-lived-under-mcnutts-persistent-surveillance-heres-why-st-louis-should-say-no/> [dostęp 2.08.2023].
- [23] *Golden Gate Bridge*, Wikipedia, [https://pl.wikipedia.org/wiki/Golden\\_Gate\\_Bridge](https://pl.wikipedia.org/wiki/Golden_Gate_Bridge) [dostęp 2.08.2023].
- [24] *Skocznia narciarska*, Wikipedia, [https://upload.wikimedia.org/wikipedia/commons/d/d8/Skocznia\\_narciarska\\_schemat.png](https://upload.wikimedia.org/wikipedia/commons/d/d8/Skocznia_narciarska_schemat.png) [dostęp 22.08.2022].
- [25] *Hinterzarten Adler-Skistadion*, <http://www.skisprungschanzen.com/PL/Skocznie/GER-Niemcy/BW-Badenia-Wirtembergia/Hinterzarten/0594-Adler-Skistadion/> [dostęp 22.08.2022].
- [26] Derewienko E., *Największa chłodnia w Europie stanęła w Kozienicach*, Rynek Infrastruktury, <https://www.rynekinfrastruktury.pl/wiadomosci/biznes-i-przemysl/najwieksza-chlodnia-w-europie-stanela-w-kozienicach-49052.html> [dostęp 2.08.2023].
- [27] *Wpis z mikrobloga*, Wykop.pl, <https://www.wykop.pl/wpis/21>

- 839319/brachistochrona-jest-jednoczesnie-tautochrona-brac/ [dostęp 22.08.2022].
- [28] Jaworski K.M., *Organizacja i planowanie w budownictwie*, t. 2, WPW, Warszawa 1992.
- [29] Kącki E., *Równania różniczkowe cząstkowe w zagadnieniach fizyki i techniki*, Wydawnictwa Naukowo-Techniczne, Warszawa 1989.
- [30] Kirkham R., *Ferry and Brandon's Cost Planning of Buildings*, wyd. 9, Wiley-Blackwell, Chichester 2015.
- [31] Koźniewski E., *Geometria dachów. Teoria i zastosowanie*, Wydawnictwo Politechniki Białostockiej, Białystok 2007.
- [32] Koźniewski E., *Monge Method in Creating Regular Polyhedrons Models*, „The Journal Biuletyn of Polish Society for Geometry and Engineering Graphics” 2014, vol. 26, 41–46.
- [33] Koźniewski E., *Offsets in Geometric Creation of Roof Skeletons with Varying Slope and Cut-and-Fill Problems in Topographic Projection*, „The Journal of Polish Society for Geometry and Engineering Graphics” 2010, vol. 21, 29–35.
- [34] Koźniewski E., *On the Existence of Shapes of Roofs*, „Journal for Geometry and Graphics” 2004, vol. 8(2), 185–198.
- [35] Koźniewski E., *Rectangular polygons and its shape parameters*, „The Journal Biuletyn of Polish Society for Geometry and Engineering Graphics” 2015, vol. 27, 9–15.
- [36] Koźniewski E., *Wykłady z geometrii w urządzaniu przestrzeni*, preskrypt w wersji elektronicznej, Białystok 2014.
- [37] Koźniewski E., Banaszak K., *Geometric Aspects of Assessing the Amount of Material Consumption in the Construction of a Designed Single-Family House*, „Energies” 2020, vol. 13, 5382.
- [38] Koźniewski E., Koźniewski M., Orłowski M., Owerczuk J., *Modeling an embankment with a natural slope*, „The Journal of Polish Society of Geometry and Engineering Graphics” 2016, vol. 28, 25–32.
- [39] Koźniewski E., Orłowski M., *The Implementation of the Slice-based Transformations in AutoCAD*, „The Journal of Polish Society for Geometry and Engineering Graphics” 2012, vol. 23, 51–56.
- [40] Koźniewski E., Sadowska B., Banaszak K., *Geometric Aspects of Assessing the Anticipated Energy Demand of Designed Single-Family House*, „Energies” 2022, vol. 15, 3308.
- [41] Koźniewski E., Żaba A., Dudzik P., *The Compactness Indicators of Solids Applied to Analysis of Geometric Efficiency of Buildings*, „Journal of Civil Engineering & Management” 2019, vol. 25, 742–756.
- [42] Koźniewski M., *Thickness Analysis of a Saddle*, „The Journal of Polish Society for Geometry and Engineering Graphics” 2016, vol. 28, 25–32.

- [43] Krynicki W., Włodarski L., *Analiza matematyczna w zadaniach*, Wydawnictwo Naukowe PWN, Warszawa 2008.
- [44] Kumaszką P., *O kilku rodzajach regularnych parkietów płaszczyzny*, praca lic., Uniwersytet Wrocławski, Wrocław 2015, [https://www.math.uni.wroc.pl/~swiatkow/\\_dydaktyka/parkiet/Patrycja\\_Kumaszk%C5%82a\\_praca\\_licencjacka.pdf](https://www.math.uni.wroc.pl/~swiatkow/_dydaktyka/parkiet/Patrycja_Kumaszk%C5%82a_praca_licencjacka.pdf) [dostęp 16.09.2022].
- [45] Mahdavi A., Gurtekin B., *Shapes, numbers, perception: Aspects and dimensions of the design-performance space*, w: *Proceedings of the 6th International Conference: Design and Decision Support Systems in Architecture*, Netherlands 2002, 291–300.
- [46] Maurin L., Mączyński M., Traczyk T., *Matematyka*, t. 1, PWN, Warszawa 1975.
- [47] Mickiewicz A., *Pan Tadeusz*, <https://wolnelektury.pl/media/book/pdf/pan-tadeusz.pdf> [dostęp 26.07.2022].
- [48] Nowak E., *Zarys metod ekonometrii. Zbiór zadań*, Wydawnictwo Naukowe PWN, Warszawa 2006.
- [49] Olędzka D., Witkowski M., Żmijewski K.H., *Metody komputerowe w inżynierii lądowej*, WPW, Warszawa 1992.
- [50] Owczarzy J., Kossowski J., *Nieklasyczne zachowanie się modelu hiperboloidalnej chłodni kominowej pod obciążeniem osiowo symetrycznym*, „Journal of Theoretical and Applied Mechanics” 1981, vol. 19(2), 225–238.
- [51] Pottmann H., Asperl A., Hofer M., Kilian A., *Architectural Geometry*, Bentley Institute Press, Exton 2007.
- [52] Rosman R., *Obliczanie ścian usztywniających osłabionych otworami*, Arkady, Warszawa 1971.
- [53] Rakowski G., Kacprzyk Z., *Metoda elementów skończonych w mechanice konstrukcji*, Oficyna Wydawnicza Politechniki Warszawskiej, Warszawa 2005.
- [54] Seręga S., Hojdys Ł., Krajewski P., Płachecki M., *Ocena bezpieczeństwa chłodni kominowej eksploatowanej od 35 lat*, „Inżynier Budownictwa” 2013, vol. 12, 96–102.
- [55] Siudak M., *Badania operacyjne*, WPW, Warszawa 1994.
- [56] Stark R.M., Nicholls R.L., *Mathematical foundations for design: Civil engineering systems*, Dover Publications, INC., Mineola, New York 2005.
- [57] Straszewicz Z., *Mechanika. Według wykładów Zygmunta Straszewicza*, cz. 1: *Statyka*, Skład Główny Komisji Wydawniczej, Politechnika, Warszawa 1923.
- [58] Szwabowski J., Deszcz J., *Metody wielokryterialnej analizy porów-*

- nawczej. Podstawy teoretyczne i przykłady zastosowań w budownictwie*, Wydawnictwo Politechniki Śląskiej, Gliwice 2001.
- [59] Wierzbanowski K., *Materialy do wykładów z fizyki*, [http://www.ftj.agh.edu.pl/~wierzbanowski/R\\_Harm\(7\).pdf](http://www.ftj.agh.edu.pl/~wierzbanowski/R_Harm(7).pdf) [dostęp 14.04.2021].
- [60] Zarankiewicz K., *Mechanika teoretyczna*, t. 1: *Statystyka*, PWN, Warszawa 1963.
- [61] Żak T., *Izoperymetria gaussowska*, Politechnika Wrocławska, Wrocław 2010, [http://prac.im.pwr.edu.pl/~zak/Izoperymetria\\_miar\\_gausso-wskich.pdf](http://prac.im.pwr.edu.pl/~zak/Izoperymetria_miar_gausso-wskich.pdf) [dostęp 26.07.2022].
- [62] Koźniewski E., Tereszkiewicz A., *Matematyka w przykładach z budownictwa i architektury*, Oficyna Wydawnicza Politechniki Białostockiej, Białystok 2023.



# Index

## A

anti-prism, 40  
 antisymmetric relationship, 178  
 arc, 56  
 Archimedean polyhedron, 39, 40  
 area defect of the rectangular polygon, 24  
 atrium, 22  
 axial symmetry, 29

## B

balanced transport task, 163  
 Banachiewicz – Cholesky decomposition, 119  
 brachistochrone problem, 101

## C

Cavalieri theorem, 69  
 central symmetry (half-rotation), 29  
 chain curve, 93  
 characteristic polynomial, 109  
 circular cylinder, 17  
 classical measure of compactness, 14  
 coding, 173  
 compactness, 14  
 compactness of a building, 14  
 compactness of a rigid solid, 14  
 complement to unity, 176  
 cone, 47  
 criteria, 173  
 cubature, 65  
 curve, 56  
 cylinder, 47  
 cylindrical surface, 47

## D

data matrix, 174  
 described, 23  
 descriptive econometric model, 139  
 destimulant, 174–176  
 destimulants, 173  
 diagonalizable matrix, 110  
 diagonalizable operator, 109  
 drawing of directed graph, 178  
 dual, 161  
 dual polyhedron, 39

## E

econometrics, 139  
 eigenvalue, 109  
 eigenvector, 109  
 endomorphism, 109  
 explanatory variables, 139  
 External Wall Area/Floor Area, 20

## F

form polyhedrons, 39

## G

generator, 29  
 geometric efficiency, 14  
 glide symmetry, 29, 36

## H

Hasse diagram, 178  
 height of covering, 88  
 hyperboloid of one sheet, 47

## I

inscribed in the rectangle, 23  
 isometries, 29  
 isoperimetric problem, 12

## L

Length/Breadth Index, 19  
 linear differential equation of second order  
     homogeneous, 114

## M

measure, 173  
 Miastoprojekt Mazowsze, 48  
 model (reference), 16

## N

normalization to unity, 176

## O

offset, 78  
 Offsetgatype, 78, 81

## P

partial measures, 174  
 partially ordered set, 178  
 patio, 22  
 perimeter defect, 24  
 Plan/Shape Index, 19

## R

random deviation, 139  
 ratio between the area of the solid and the volume,  
     14  
 rectangular polygon, 21  
 reference shape, 12  
 reflexive relation, 178  
 regular cuboid, 17  
 relative area defect, 25  
 relative compactness indicator, 16  
 relative compactness indicator of the solid relative  
     to the cube, 16  
 relative perimeter defect, 24  
 response variable, 139  
 rhombic dodecahedron, 38  
 rotaion, 36  
 rotation, 29, 36  
 rotational hyperboloid , 58  
 ruled surfaces, 47

## S

scalar, 173  
 secant, 79  
 self isometries, 30  
 self-dual tetrahedron, 39  
 semi-regular polyhedron, 39  
 semi-regular polyhedron, 40  
 shear, 69, 72  
 slice-based transformations, 69  
 span, 26  
 stimulant, 174–176  
 stimulants, 173, 175  
 structural parameters, stochastic structure  
     parameters, 140  
 symmetry, 36  
 symmetry of a hyperplane, 29  
 symmetry of a plane, 29  
 symmetry with respect to a straight line, 29



## T

tautochrone, 105  
tessellation/tiling, 31  
the absolute indicator of the compactness of the  
    solid relative to the sphere, 17  
Torus Science Park, 49  
transformation group, 29  
transitive relationship, 178  
translation, 29, 36  
twist, 69, 70  
twist axis, 70  
twisted pillar, 72

## U

unbalanced task, 163

## V

variational calculus, 102

## W

$W$ -Kendall compatibility coefficient, 181  
Wall/Floor ratio, 19

# List of Tables

1.1	Measures of compactness of $\frac{A_t}{V}$ platonic solids and spheres calculated under the assumption that $V=1$ (prep. by A.Tereszkiewicz)	13
1.2	Ideological illustration of the indicator $RC_{S_{pat}}(S)$ , prep. E. Koźniewski based on [41]	16
1.3	Determination of the indicators $RC_{cd}$ and $RC_{cyl}$ , prep. E. Koźniewski	18
1.4	Definition of indicators $RC_{cd}$ i $RC_{cyl}$ , prep. E. Koźniewski	18
2.1	Seventeen crystallographic two-dimensional space groups according to Coxeter [7] (*half-turn = rotation by $180^\circ$ or central symmetry, **reflection with glide = superposition of axial symmetry and translation with respect to the same straight line, ***quarter-turn = rotation by $90^\circ$ )	35
9.1	Data for task 3, by E. Koźniewski	138
10.1	Values of variables in the model in 1991 – 2000 [48]	140
10.2	Calculation of the mean and standard deviation for data from the table 10.1, by E. Koźniewski	142
10.3	Concrete sales ( $[m^3]$ ) in 2000–2006 by selected concrete company, by E. Koźniewski	153
10.4	Building permits issued in 2000–2006 in usable area $[m^2]$ [2]	153
10.5	Construction permits issued in 2000–2006 (aggregation), by E. Koźniewski	154
10.6	Output data array for table 10.5	154
10.7	Averages for the table 10.6, by E. Koźniewski	154
10.8	Observations of variables $X_1, X_2, X_3$ , by E. Koźniewski	156
11.1	Time required for concreting and vibrating one slab, monthly working time limit and unit profits for two types of slabs, by E. Koźniewski	157
11.2	Values needed for calculation of linear programming, by E. Koźniewski	159
11.3	View of the Excel sheet after the actions for model, by E. Koźniewski	159
11.4	Data for a transport problem, by E. Koźniewski	163
11.5	Data needed for the linear embankment, by E. Koźniewski	169
11.6	Unit transport costs for individual distances of embankment sections, by E. Koźniewski	169

11.7	Solving the problem of transportation of earth masses, by E. Koźniewski	171
12.1	Summary of costs of construction of selected roofing covers [PLN], by E. Koźniewski	180
12.2	Summary of the weight of the roofing [kN/m <sup>2</sup> ], by E. Koźniewski	181
12.3	Summary of roofing warranties [years], by E. Koźniewski	181
12.4	Summary of the results of the questionnaire for criterion $K_4$ – aesthetics of coverage, by E. Koźniewski	182
12.5	Summary of questionnaire results for criterion $K_4$ – aesthetics of coverage, arranged in descending order, by E. Koźniewski	182
12.6	Summary of the results of the questionnaire for criterion $K_4$ – aesthetics of coverage, by E. Koźniewski	183
12.7	Table of ranks for criterion $K_4$ – aesthetics of coverage ( $R_i = k \cdot \overline{EX}$ ), by E. Koźniewski	183
12.8	Calculation of corrections for criterion $K_4$ – aesthetics of coverage, by E. Koźniewski	184
12.9	Critical values for $3 \leq k \leq 20$ and $3 \leq n \leq 7$ (Siegel S., Nonparametric Statistics for the Behavioral Sciences, McGraw-Hill, NY 1956, 286p).	185
12.10	Summary of questionnaire results for criterion $K_5$ – simplicity of exploitation, by E. Koźniewski	186
12.11	Rank table for criterion $K_5$ – simplicity of exploitation, by E. Koźniewski	186
12.12	Calculation of corrections for criterion $K_5$ – simplicity of exploitation, by E. Koźniewski	187
12.13	Criteria for the weights proposed by the investor, by E. Koźniewski	187
12.14	Inputs for synthetic evaluations, by E. Koźniewski	188
12.15	Applied Pattern coding for all criteria, by E. Koźniewski	188
12.16	Applied Pattern recoding for destimulants ( $K1, K2$ ), by E. Koźniewski	189
12.17	Results of the third rule of comparison (with weights), by E. Koźniewski	189
12.18	Results of the second comparison rule (without weights), by E. Koźniewski	190
12.19	Results of the second comparison rule with assumed accuracy (with weights), by E. Koźniewski	190
12.20	The results of the second rule of comparison with assumed accuracy (without weights), by E. Koźniewski	191

# List of Figures

1.1	Steel profiles at SEMEX in Czestochowa [13]	11
1.2	Example tanks: (a) spherical tanks at Zakłady Azotowe "PUŁAWY" S.A. [14] (b) cubic tank [15];	12
1.3	(a) Fragment of a poster - "information board" of the new SONATA estate being built in Druskininkai, Lithuania. Buildings in the shape of cylinders with an oval base; (b) buildings (cylindrical, oval-shaped) of the new SONATA housing estate in Druskininkai, Lithuania, photo by Ł. Kolendo	14
1.4	(a) The Town Hall in Białystok - an example of a building on the plan of a rectangular polygon, photo by E. Koźniewski; (b) The Town Hall in Białystok – study of the solution of the roof shape, prep. E. Koźniewski	15
1.5	(a) rectangular polygons; (b) rectangular polygons: hexagon, octagon, decagon, dodecagon, tetradecagon, prep. E. Koźniewski	21
1.6	(a) patio [11]; (b) atrial buildings in Białystok on Warszawska street [31], photo by W. Wołkow	22
1.7	Rectangular polygons inscribed in a rectangle: (a) simple connected polygon monotonic (any line parallel to the axis but not containing a side intersects the edge at two points) with respect to both axes, i.e., normal; (b) simple connected polygon monotonic with respect to the $OY$ axis but non-monotonic with respect to the $OX$ axis; (c) 3-connected polygon non-monotonic with respect to both axes [35]	23
1.8	Rectangular polygons inscribed in a rectangle of $x \times y$ , $x = 9u$ , $y = 12u$ : (a) with large field defect ( $\Delta A = 88u^2$ ), $RDA = 0.81(81\%)$ and zero perimeter defect, $RDP = 0(0\%)$ ; (b) with positive perimeter defect ( $\Delta P = 24u$ , $RDP = 0.57(57\%)$ ), with area defect ( $\Delta A = 38u^2$ , $RDA = 0.35(35\%)$ ); (c) with a positive perimeter defect ( $\Delta P = 40u$ , $RDP = 0.95(95\%)$ ), with a area defect ( $\Delta A = 44u^2$ , $RDA = 0.41(41\%)$ ) [35]	24

1.9	Determining the span of a rectangular polygon: (a) after the first overview the span value of a polygon is not directly visible: $s_2$ or $s_3$ , or perhaps $s_4$ ?; (b) after constructing a simple skeleton the algorithm for determining the span is easy to formulate; c) a shape close to a rectangular polygon [35] . . . . .	25
1.10	Determining the span of a 3-connected rectangular polygon $RP^3$ : (a) a 3-connected rectangular polygon indicating the polygon $C_1$ and sub-polygons (holes) $C_2, C_3$ of the line segment defined in figure (b) defining the span; (b) the process of determining the span $s(RP^3)$ by the roof solution: $s(RP^3) = 2 \cdot s_{18}$ , $s(RP^3) = 2 \cdot s_{33}$ , as well as the sum of $s(RP^3) = s_{18} + s_{33}$ heights of hipped roof end adjacent to each other along the ridge [35] . .	26
1.11	Solid and projection of the base of the solid, prep. A. Tereszkievich . .	28
2.1	(a) the superposition $S_b S_a$ of axial symmetries $S_a, S_b$ with $a b$ -parallel axes is a translation $T_{2AB}$ ( $AB$ – a vector defined by the points $A, B$ lying on the lines $a$ and $b$ , respectively, with $AB \perp a$ and $AB \perp b$ ); (b) the superposition $S_b S_a$ of the axial symmetries $S_a, S_b$ with axes $a, b$ intersecting $a \cap b = \{O\}$ is a rotation of $R_{O, 2\varphi}$ by an angle of $2\varphi$ , prep. E. Koźniewski . . . . .	30
2.2	(a) the superposition $S_b S_a$ of axial symmetries $S_a, S_b$ with perpendicular axes $a, b$ is point symmetry $S_O$ , with point $O$ ; (b) the superposition $S_c S_b S_a$ of the three symmetries $S_a, S_b, S_c$ with respect to the straight lines $a, b, c$ transforms the triangle into a pre-given triangle congruent to it, prep. E. Koźniewski . . . . .	30
2.3	(a) regular tilings (from regular polygons of one kind), photo by E. Koźniewski; (b) semi-regular tilings (from regular polygons of different types), prep. E. Koźniewski; (c) monohedral tessellation of any shape, photo by E. Koźniewski . . . . .	31
2.4	Transformations on a parallelogram: (a) any two curves with ends at the vertices of the polygon; (a1) shift the curves by the vectors induced by the parallelogram; (a2) the resulting shape ("pigeon"), prepared by E. Koźniewski based on [51] . . . . .	32
2.5	Tessellations with two curves spanning a parallelogram ("pigeons"), prepared by E. Koźniewski based on [51] . . . . .	32
2.6	Transformations on an equilateral triangle - variations on Escher's three butterflies: (a) any curve; (a1) its central image of symmetry; (a2) two rotations; (a3) six (five) rotations, prepared by E. Koźniewski based on [51] . . . . .	33

2.7	(a) two rotations of the shape from the figure 2.6 [36]; (b) a few corresponding shifts of the shape from figure 2.7a in directions parallel to the sides of the triangles (hexagons), prepared by E. Koźniewski based on [51] . . . . .	33
2.8	Transformations on a square: (a) two curves; (a1) two rotations around the vertices by an angle of $90^\circ$ ; (a2) received elementary shape, prepared by E. Koźniewski based on [51] . . . . .	34
2.9	Transformations on a square: (a3) three selected vertices; (a4) configuration obtained by three rotations around the vertices with corresponding rotation angles $90^\circ$ , $180^\circ$ , $90^\circ$ ; (a5) obtained compound shape (prepared by E. Koźniewski based on [51]) . . . . .	34
2.10	(a) transformations on a square: – the obtained tessellations, prepared by E. Koźniewski based on [51]; (b) concrete paving texture designed on the basis of an equilateral triangle, photo by E. Koźniewski . . . . .	35
2.11	Modeling of the icosahedron: (a) finding (using Monge's method) the appropriate angle; (a1) five rotations (four rotations) of one wall; (a2) plane symmetry; (a3) one rotation and one translation, prep. E. Koźniewski based on [32] . . . . .	37
2.12	Creating an icosahedron model: (a) determining (by Monge method) the corresponding triangular pyramid with the edge in the vertical position; (a1) one reflection relative to the pyramid wall; (a2) three reflections about the corresponding planes or three rotations; (a3) three reflections about the corresponding walls; (a4) two consecutive reflections and one reflection about the plane determined by the five top vertices of the bottom solid and one corresponding rotation about the vertical line; (a5) one translation, prep. E. Koźniewski based on [32] . . . . .	37
2.13	Creating a model of the rhombic dodecahedron: (a) building a tetrahedral pyramid with a height equal to half the edge of the cube; (a1) one rotation; (a2) one reflection, three rotations and one translation; (a3) whole solid with visual decomposition; (a4) a solid obtained by a (Boolean) sum, prep. E. Koźniewski based on [36] . . . . .	38
2.14	The rhombic dodecahedron can be treated as a refined brick shape: (a) brick; (b) wall made of rhombic dodecahedrons, prep. E. Koźniewski . . . . .	38
2.15	Art Tower model creation: (a) Art Tower in Mito, designed by Arata Isozaki [51], [16]; (a1)–(a3) sequence of reflected tetrahedrons in different visualization styles [36], prep. E. Koźniewski . . . . .	39
2.16	(a) Construction of the Archimedean tetrahedron on the basis of an octahedron; (b) The Archimedean tetrahedron constructed on the basis of a regular octahedron, prep. E. Koźniewski . . . . .	40

- 2.17 (a) icosahedron regular, by E. Koźniewski; (b) construction of a truncated icosahedron, by E. Koźniewski; (c) the way of stitching the soccer ball (football) according to the structure of the truncated icosahedron, photo by E. Koźniewski . . . . . 40
- 2.18 Orthodox Church of the Resurrection in Białystok, designed by Jerzy Uścińowicz, 1991 – 1994. Shape of dome fragment resembling flat  $8 - 4 - 8$  semiformal tessellation (dome from left), shape of other domes resembling fragment of Archimedean tetrahedron (Fig. 2.16) – square bordered by four regular hexagons (four domes from right), photo by M. Koźniewski . . . . . 41
- 2.19 (a) fragment of tessellation  $8 - 8 - 4$  arranged over a ferny octagon (eight octagons), the squares "become" rhomboids with little deformation relative to the square and unexpectedly the possibility of completing a regular hexagon (AutoCAD) appears; (b) Space structure of tessellation  $8 - 8 - 4$  on octagon (AutoCAD), prep. E. Koźniewski . . . . . 41
- 2.20 (a) modeling of the dome based on  $8 - 8 - 4$  tessellation, construction of a regular hexagon as a complement to the space tessellation (AutoCAD); (b) rectangular projection of two rhombuses whose edges together with the edge of the regular octagon generate a regular hexagon (AutoCAD), prep. E. Koźniewski . . . . . 43
- 2.21 (a) modeling of the geometric structure of the dome – addition of the hexagon to the pentagon constituting the upper slope of the dome, prep. E. Koźniewski; (b) the space structure of the  $8 - 8 - 4$  tessellation (without the lower part) topologically equivalent to the solid of the orthodox church dome, prep. E. Koźniewski; (c) the dome over the chapel of the Orthodox Church of the Resurrection in Białystok, designed by Jerzy Uścińowicz, photo by M. Koźniewski . . . . . 43
- 2.22 Left: the main dome of the Orthodox Church of the Resurrection in Białystok, designed by Jerzy Uścińowicz, photo by M. Koźniewski; right: geometric model topologically equivalent to the structure of the main dome of the Orthodox Church, prep. E. Koźniewski . . . . . 44
- 2.23 Examples of practical solutions in floor and pavement design, photo by E. Koźniewski: (a) floor tiles– styling of semi-regular tessellation  $x - y - z$ ; (b) parking lot paving –paver blocks "mirror", sidewalk designed according to  $p - q - r$  semi-regular tessellation; (c) sidewalk paving – paver blocks designed according to tessellation based on transformations on the square (combining the schemes from examples 2.2, 2.3 and gluing the two patterns) . . . . . 45

3.1	Three surfaces resulting from the rotation of the straight line around a given straight line (axis) (three variants: the straight line intersects the axis, is parallel to it, is skew to it) , prep. E. Koźniewski . . . . .	47
3.2	Three surfaces resulting from the rotation of the straight line around a given straight line (top view), prep. E. Koźniewski . . . . .	47
3.3	Design of fuel tank canopy (cylindrical and conical surface structure). Design collaboration B. Koźniewski . . . . .	49
3.4	Hyperboloid-shaped structures: (a) water tower in Ciechanów – single-shell hyperboloid-shaped support structure and torus-shaped tank – condition before renovation; (b) The Ciechanów water tower after renovation as the main element of the science park, photo by B. Koźniewski . . . . .	49
3.5	Torus Science Park in Ciechanów, photo by B. Koźniewski . . . . .	50
3.6	(a) Kaszubskie Oko in Gniewino – geometry of construction solutions (cylinder, helical surface, single-shell hyperboloid); (b) Kaszubskie Oko in Gniewino has socio-cultural and tourist functions, photo by W. Reglińska . . . . .	50
3.7	3D model of Ciechanów water tower realized in AutoCAD environment; in the second line on the left is given an illustration of 2D structure forming hyperboloids in axonometry using axial affinity, made by E. Koźniewski . . . . .	51
3.8	Schema of cooling tower [50, 54] . . . . .	52
3.9	Rotation of a hyperbola around a point $(0, 0)$ by an angle $-\frac{\pi}{2}$ , by A. Tereszkiewicz . . . . .	53
3.10	Curves $c_1, c_2$ after shifting the branch of the hyperbola by 0.16, by A. Tereszkiewicz . . . . .	55
3.11	A helical curve, by A. Tereszkiewicz . . . . .	57
3.12	Creation of a revolved surface: an axis of revolution $OZ$ and path curve; the resulting rotational surface; rotation circles of selected points, prep E. Koźniewski . . . . .	58
3.13	The line skewed to the $z$ -axis, by A. Tereszkiewicz . . . . .	58
3.14	Assumptions made to create a model of a water tower in the program AutoCAD environment, by E. Koźniewski . . . . .	60
3.15	Constructions of geometric objects needed to determine the equations of the rotated line $l(AB)$ in the program AutoCAD environment, by E. Koźniewski . . . . .	60
3.16	Measuring distances resulting in the determination of coordinates of points $A, B, P, Q$ , by E. Koźniewski . . . . .	61
3.17	Task 8, by A. Tereszkiewicz . . . . .	63



4.1	Warszawa Ochota railway station in Warsaw, designed by Arseniusz Romanowicz, Piotr Szymaniak, realization 1960 – 1962, [17] photo by M. Czechowicz . . . . .	65
4.2	(a) We choose a cuboid with a square base of side length $a$ and height $h$ ; (a1) we construct the diagonals of opposite lateral faces, which are mutually skew (green), and serve as the basis for creating the ruled surface (AutoCAD), by E. Koźniewski . . . . .	66
4.3	(a2) we connect the points of these diagonals with segments parallel to the other side walls (in practical implementation, we divide the diagonals into the same number of equal segments and connect the points obtained in this way with each other - blue segments). We obtain the generatrices, all of which are skew to each other (in blue), and two of them are diagonals of the remaining lateral faces. These two diagonals can be the basis for constructing the second family of generatrices (green); a3) in order to move from geometric to analytical characterization, we introduce the coordinate system $OXYZ$ for the form of the canonical equation of the saddle surface (AutoCAD), by E. Koźniewski . . . . .	66
4.4	(a4) in order to obtain the roofing model, we give thickness by shifting the created surface by the vector $[0, 0, q]$ ; (a5) the original skeleton form of the roofing model (AutoCAD), by E. Koźniewski . . . . .	67
4.5	Illustration of cross-sections, a model of a roof covering with a thickness of $q$ , parallel to the planes of the walls (planes of the base cuboid) of the object; these are parallelograms with the same area $aq$ – it can be assumed that these are cuboid sections with a square base $a \times a$ and height $q$ , which can be considered a flat roof model (AutoCAD), by E. Koźniewski . . . . .	68
4.6	Illustration of the family of slice-based transformations: (a) existing perpendicular, (b) twist, (c) shear (AutoCAD), by E. Koźniewski based on [51] . . . . .	69
4.7	Illustration of slice-based transformations: twist (maximum angle $\alpha_{\max}$ ), shear (AutoCAD), by E. Koźniewski based on [51] . . . . .	70
4.8	(a) Cuboid twist, vertical edges as helix lines (AutoCAD models), by E. Koźniewski based on [51]; (b) Dresden synagogue (2001, architects Rena Wandel-Hoefer and Wolfgang Lorch) – an example of the use of twist transformation in architecture [18] . . . . .	71
4.9	Turning Torso in Malmö, Sweden (2005, architect Santiago Calatrava) – another example of the application of the twist transformation in modern architecture [19] . . . . .	71
4.10	"Puerta de Europa" in Madrid – An example of the use of the shear transformation in modern architecture, photo by D. Gawryluk . . . . .	72

4.11	(a) sketch views of creating a spiral column ; (b) the volume of the spiraled column is the same as the cylinder - Cavalieri theorem (model realized in AutoCAD environment); (c) the model from the middle figure after rendering, by E. Koźniewski . . . . .	73
4.12	(a) the spiral columns in the Church of the Resurrection in Białystok, by M. Koźniewski; (b) twisted columns of a hall in the Valencia silk exchange (Spain), photo by D. Gawryluk . . . . .	73
4.13	Contemporary ideas in single-family housing, left [20], right [21] . . . .	74
4.14	task 5, prep. A. Tereszkievicz . . . . .	75
5.1	Sketch of a turbine roundabout shaped using: (a) two half-circles, by E. Koźniewski based on [9]; (b) ellipse, by E. Koźniewski based on [9]	77
5.2	Offsets: (a) spline curve; (b) polyline; (c) polygon half-offset (obtained using AutoCAD with the constant <i>Offsetgaptype</i> = 1); (d) discrete polygon half-offset (obtained using AutoCAD with the constant <i>Offsetgaptype</i> = 0), by E. Koźniewski . . . . .	78
5.3	Offset $e'_d$ ellipses $e(a, b)$ with half-axes $a, b$ and ellipse with half-axes $a + d, b + d$ : (a) $a = 100, b = 60, d = 30$ ; (b) $a = 100, b = 20, d = 30$ . The difference between the offset $e'_d$ of the ellipse $e(a, b)$ and the ellipse $e(a + d, b + d)$ is the greater the smaller the ratio $b/a$ ; in the case of (a) $b/a = 3/5$ visually the curves coincide, in the case of (b) $b/a = 1/5$ there is a clear difference between the curves (offset $e'_d$ of the ellipse with half-axes $a, b$ [red] and the ellipse with half-axes $a + d, b + d$ [blue], by E. Koźniewski . . . . .	79
5.4	Generalized discrete offsets: (a) angle with parameters $d_1, d_2$ ; (b) given distances $d_1, d_2, d_3, d_4, d_5, d_6$ for the discrete offsets of the polygon; (b1) sequence of half-offsets of the discrete polygon (1, $d_1$ ; 2, $d_2$ ; 3, $d_3$ ; 4, $d_4$ ; 5, $d_5$ ; 6, $d_6$ ) ([3, 9, 34], by E. Koźniewski) . . . . .	79
5.5	The structure of the roof skeleton generated by the hexagon (1, $d_1$ ; 2, $d_2$ ; 3, $d_3$ ; 4, $d_4$ ; 5, $d_5$ ; 6, $d_6$ ), (cf. [33]), by E. Koźniewski . . . . .	80
5.6	Topological types of roofs with a variable slope over the same hexagon(1, $d_1$ ; 2, $d_2$ ; 3, $d_3$ ; 4, $d_4$ ; 5, $d_5$ ; 6, $d_6$ ) (cf. [33]), by E. Koźniewski . .	80
5.7	The intersections of the 120 m contour with the edges of the construction site will determine the change points from the excavation to the embankment (cf. [33]) . . . . .	81
5.8	To the left and at the bottom of the area, the proposed contours of the contour lines (for the excavation) at a distance of $d = 1$ m, to make the slope equal to 1 (cf. [33]) . . . . .	82
5.9	To the right and at the top of the area, the proposed contours of the layered areas (for the embankment) at intervals $d = 1\frac{1}{2}$ m, to get a slope in the ratio of $1\frac{1}{2}$ to 1 (cf. [33]) . . . . .	82

5.10	Edge of embankment and excavation line (cf. [33]) . . . . .	83
5.11	Illustration of the example (due to scale, instead of $d = 0.16$ it was taken as $d = 1.6$ ), by A. Tereszkiewicz . . . . .	84
5.12	Task 7, 8, by A. Tereszkiewicz . . . . .	89
6.1	Chain curve, by A. Tereszkiewicz . . . . .	92
6.2	Architectural realizations based on the chain curve: (a) the chain barriers at Legionowa Street in Białystok, photo by E. Koźniewski; (b) Grunwald Bridge in Wrocław, photo by F. Sadowski; (c) viaduct over Piastowska Street in Białystok, photo by E. Koźniewski; (d) covering of Keleti Station in Budapest, photo by E. Koźniewski; (e) Gateway Arch in Saint Louis in USA, [22]; (f) Chain Bridge in Budapest, photo by E. Omieljańczuk; (g) the viaduct over the General Route in Białystok, photo by M. Koźniewski . . . . .	94
6.3	Generation of chain curve profile in AutoCAD: points were determined for chain curve (6.8) for $a = 38.9216$ , for the values of 10, 20, . . . , 80, 90, 96 (the first column of numbers), calculating in Excel the values of the function (6.8) (the second column) and measuring them on the vertical lines projected at points with abscissa 10, 20, . . . , by E. Koźniewski . . . . .	95
6.4	Basic dimensions of the Golden Gate Bridge suspension bridge connecting San Francisco and Marin County, California, USA, by E. Koźniewski based on [23] . . . . .	97
6.5	Illustration for task 4, by A. Tereszkiewicz . . . . .	98
6.6	Illustration for task 5, by A. Tereszkiewicz . . . . .	98
6.7	Illustration for task 6, by A. Tereszkiewicz . . . . .	99
6.8	Illustration for task 7, by A. Tereszkiewicz . . . . .	99
7.1	Illustration of the brachistochrone problem: (a) assumptions about the issue, by E. Koźniewski; (b) material point slipping without any friction, by E. Koźniewski; (c) the inrun of the Wielka Krokiew in Zakopane, photo by S. Kudźma; (d) skatepark in Sobolewo, photo by E. Koźniewski. Are high-speed descents desirable here? . . . . .	101
7.2	Cycloid, by A. Tereszkiewicz . . . . .	105
7.3	Brachistochrone, by A. Tereszkiewicz . . . . .	105
7.4	Illustration for task 1, by A. Tereszkiewicz . . . . .	106
7.5	Illustration for task 2, by A. Tereszkiewicz . . . . .	106
7.6	Scheme of a ski jump, by E. Koźniewski based on [24] . . . . .	107

7.7	Design window: (a) window dimensions; (b) construction of a bowline with half-axes $a = AC$ , $b = BC$ . Successive designs 1: equilateral triangle $AFC$ ; 2: circle $o(C, BC)$ ; 3: point $D$ as intersection of line $CF$ and circle $o(C, BC)$ ; 4: point $G$ as intersection of lines $BD$ and $AF$ ; 5: point $I$ as the intersection of the line passing through point $G$ and parallel to line $CF$ with line $AC$ and the point $H$ as the intersection of the line passing through the point $G$ and parallel to the line $CF$ with the line $BC$ ; 6: gluing the arcs of the circles $o(H, HB)$ and $o(I, IG)$ , illustration for task 7, by E. Koźniewski . . . . .	108
8.1	Static system composed of two bands (by E. Koźniewski based on [52]) .	116
9.1	Calculation of partial derivatives, by E. Koźniewski . . . . .	128
9.2	The expansion of the squares of partial derivatives, by E. Koźniewski .	128
9.3	PM, by E. Koźniewski . . . . .	129
9.4	Calculation of partial derivatives in the Wolfram Alpha environment, by E. Koźniewski . . . . .	131
9.5	Expanding the sum of squares of partial derivatives in the Wolfram Alpha environment, by E. Koźniewski . . . . .	131
9.6	Difference method. A model of a bent rod, by E. Koźniewski based on [53]	133
11.1	Geometric solution of the problem from example 11.1, by E. Koźniewski based on [49] . . . . .	160
11.2	Graphs in the transport task matrix: (a) with cycles – is not a solution ( $8 > 3 + 5 - 1$ ); (b) without cycles – is a solution ( $3 + 5 - 1 = 7$ ), by E. Koźniewski . . . . .	166
11.3	Cut and fill for highway [56], by E. Koźniewski . . . . .	167
12.1	Illustration of the partial order dictated by inclusion, by E. Koźniewski .	178
12.2	Hasse diagrams constructed for different accuracies according to the third rule of comparison, by E. Koźniewski . . . . .	191
12.3	Hasse diagrams constructed for different accuracies according to the second ordering rule , by E. Koźniewski . . . . .	191

